Universidade de Lisboa

Faculdade de Medicina de Lisboa

Modulatory role of adenosine upon GABAergic transmission: consequences for excitability control

Diogo Miguel Santos Rombo

Doutoramento no Ramo de Ciências Biomédicas

Especialidade em Neurociências

Lisboa, 2015

Universidade de Lisboa

Faculdade de Medicina de Lisboa

Modulatory role of adenosine upon GABAergic transmission: consequences for excitability control

Diogo Miguel Santos Rombo

Tese orientada pela Professora Doutora Ana Maria Sebastião

Doutoramento no Ramo de Ciências Biomédicas
Especialidade em Neurociências

Júri: Prof. Doutor. J. Melo Cristino (Presidente), Faculdade de Medicina da Universidade de Lisboa; Prof. Doutor Alfonso Araque, University of Minnesota, USA; Prof. Doutora. Ana Luísa Carvalho, Faculdade de Ciências e Tecnologia da Universidade de Coimbra; Prof. Doutor. Joaquim Alexandre Ribeiro, Prof. Doutora. Ana Maria Sebastião, Prof. Doutor. Alexandre de Mendonça e Prof. Doutora. Raquel B. Dias, Faculdade de Medicina da Universidade de Lisboa.

Lisboa, 2015

A impressão desta dissertação foi aprovada pelo Conselho Científico da Faculdade de Medicina de Lisboa em reunião de 20 de Outubro de 2015

Todas as opiniões expressas nesta publicação são da exclusiva responsabilidade do seu autor, não cabendo qualquer responsabilidade à Faculdade de Medicina de Lisboa pelos conteúdos apresentados.

All opinions expressed in this document are of the sole responsibility of its author and Faculdade de Medicina de Lisboa is not liable in any way for its content.

O trabalho experimental constante da presente tese foi realizado no Instituto de Farmacologia e Neurociências, Faculdade de Medicina de Lisboa e Unidade de Neurociências, Instituto de Medicina Molecular, sob orientação da Professora Doutora Ana Maria Ferreira de Sousa Sebastião e no Department of Pharmacology, University of Oxford, Oxford, Reino Unido, sob a supervisão do Doutor Karri Lämsä.

The experimental work described in this thesis was performed at the Instituto de Farmacologia e Neurociências, Faculdade de Medicina de Lisboa e Unidade de Neurociências, Instituto de Medicina Molecular, under the orientation of Professor Ana Maria Sebastião and at the Department of Pharmacology, University of Oxford, Oxford, United Kingdom, under the supervision of Doctor Karri Lämsä.

À minha família.

Publications

The scientific content of this thesis was included in the publication of the following original articles:

- **Rombo DM**, Dias RB, Duarte ST, Ribeiro JA, Lamsa KP, Sebastião AM (2014). Adenosine A1 receptors suppress tonic GABAA receptor currents in hippocampal pyramidal cells and in a defined subpopulation of interneurons. *Cerebral Cortex*. (Epub ahead of print).

- **Rombo DM**, Newton K, Nissen W, Badurek S, Horn J, Minichiello L, Jefferys J, Sebastiao AM, Lamsa K (2015). Synaptic mechanims of adenosine A2A receptor mediated hyperexcitability in the hippocampus. *Hippocampus* 25, 566-80.

Other publications closely related to the content of this thesis:

- Dias RB, **Rombo DM**, Ribeiro JA, Henley JM, Sebastião AM (2013). Adenosine: setting the stage for plasticity. *Trends Neurosci* 36, 248-57.

- Sebastião AM, **Rombo DM**, Ribeiro JA. (2015). Adenosine Receptor Modulation of GABAergic Transmission. In Adenosine Signaling Mechanisms: Pharmacology, Functions and Therapeutic Aspects., eds. Vickram Ramkumar, Roberto Paes de Carvalho. New York: Nova Science Publishers

Other publications from the author:

- Diógenes MJ*, Dias RB*, **Rombo DM***, Vicente Miranda H, Maiolino F, Guerreiro P, Näsström T, Franquelim HG, Oliveira LM, Castanho MA, Lannfelt L, Bergström J, Ingelsson M, Quintas A, Sebastião AM, Lopes LV, Outeiro TF (2012). Extracellular alpha-synuclein oligomers modulate synaptic transmission and impair LTP via NMDA-receptor activation. *J Neurosci* 32, 11750-62. *Co-fist authors.

- Dias RB, **Rombo DM**, Ribeiro JA, Sebastião AM (2013). Ischemia-induced synaptic plasticity drives sustained expression of calcium-permeable AMPA receptors in the hippocampus. *Neuropharmacol* 65, 114-22.

- Félix-Oliveira A, Dias RB, Colino-Oliveira M, **Rombo DM**, Sebastião AM (2014). Homeostatic plasticity induced by brief activity deprivation enhances long-term potentiation in the mature rat hippocampus. *J Neurophysiol* 112, 3012-22.

- Santos AR, Mele M, Vaz SH, Kellermayer B, Grimaldi M, Colino-Oliveira M, **Rombo DM**, Comprido D, Sebastião AM, Duarte CB (2015). Differential role of the proteasome in the early and late phases of BDNF-induced facilitation of LTP. *J Neurosci* 35, 3319-29.

- Fernandes TG, Duarte ST, Ghazvini M, Gaspar C, Santos DC, Porteira AR, Rodrigues GM, Haupt S, **Rombo DM**, Armstrong J, Sebastião AM, Gribnau J, Garcia-Cazorla À, Brüstle O, Henrique D, Cabral JM, Diogo MM (2015). Neural commitment of human pluripotent stem cells under defined conditions recapitulates

neural development and generates patient-specific neural cells. *Biotechnol J* (Epub ahead of print).

Table of contents

Figure index

Table index

List of abbreviations

5-HT$_3$R – 5-hydroxytryptamin (serotonin) tupe 3 receptor

A$_1$R – A$_1$ receptor

A$_{2A}$R – A$_{2A}$ receptor

A$_{2B}$R – A$_{2B}$ receptor

A$_3$R – A$_3$ receptor

AA – arachidonic acid

AAV2/5 – adeno-associated vírus serotype 2 or 5

AAC – axo-axonic cell

ABC – ATP-binding cassete transporter

AC – adenylate cyclase

ACC - associational commissural connection

aCSF – artificial cerebrospinal fluid

ADA – adenosine deaminase

ADP – adenosine 5'-diphosphate

AK – adenosine kinase

AM-251 - N-(Piperidin-1-yl)-5-(4-iodophenyl)-1-(2,4-dichlorophenyl)-4-methyl-1H-pyrazole-3-carboxamide

AMP – adenosine 5'-monophosphate

AMPA - α-amino-3-hydroxy-5-methyl-4-isoxazolepropionic acid

AMPAR – AMPA receptor

ATP – adenosine 5'-triphosphate

BC – basket cell

BDNF – brain derived neurotrophic factor

BSC – bistratified cell

BSNP – burst-spiking non-pyramidal cell

CA – *cornu ammonis*

Ca^{2+} - calcium ion

CAM – calcium/calmodulin-dependent protein

CAMK – calcium/calmodulin-dependent protein kinase

cAMP – cyclic adenosine 5'-monophosphate

CB – cannabinoid

CB_1R – cannabinoid type 1 receptor

CB_2R – cannabinoid type 2 receptor

CCK – cholecystokinin

CGP55845 - (2S)-3-[[(1S)-1-(3,4-Dichlorophenyl)ethyl] amino-2-hydroxypropyl] (phenylmethyl) phosphinic acid hydrochloride

CGRP - calcitonin gene-related peptide

CGS21680 - 4-[2-[[6-Amino-9-(N- ethyl-β-D-ribofuranuronamidosyl)-9H-purin-2-yl] amino] ethyl] benzenepropanoic acid hydrochloride

ChR2 – channelrhodopsin-2

Cl^- - chloride ion

CNQX - 6-cyano-7-nitroquinoxaline-2,3-dione disodium salt

CNS – central nervous system

CPA - N6-cyclopentyladenosine

CREB – cAMP response element binding protein

D_2R – dopamine type 2 receptor

DAG - diacylglycerol

DG – dentate gyrus

DIO – doble-floxed inverted open reading frame

DIC-IR – differential interference contrast-infrared

dIPSC – disynaptic inhibitory postsynaptic current

DL-AP5 - DL-2-Amino-5-phosphonopentanoic acid sodium salt

DMSO – dimethyl sulfoxide

DPCPX - 1,3-dipropyl-8-cyclopentylxanthine

DR – dopamine receptor

DTT - dithiothreitol

EC – entorhinal cortex

eCB – endocannabinoid

ECL – enhanced chemiluminescence detection method

E_{Cl} – equilibrium potential for chloride ion

EDTA – ethylenediamine tetra-acetic acid

E_{GABA} – equilibrium potential for GABA

E_{HCO3} – equilibrium potential for bicarbonate ion

E_{Na} – equilibrium potential for sodium ion

ENT – equilibrative nucleoside transporter

EPSC – excitatory postsynaptic current

EPSP – excitatory postsynaptic potential

eYFP – enhanced yellow fluorescent protein

fEPSP – field excitatory postsynaptic potential

FSI – fast-spiking interneuron

GABA - gamma-aminobutyric acid

$GABA_AR$ – GABA type A receptor

$GABA_CR$ – GABA type C receptor

$GABA_BR$ – GABA type B receptor

GAD - glutamic acid decarboxylase

GAPDH – glyceraldehyde-3-phosphate dehydrogenase

G_{input} – membrane input conductance

GAT – GABA transporter

GAT-1 – GABA transporter 1

GAT-3 – GABA transporter 3

GF109203x - 2-[1-(3-Dimethyl aminopropyl)indol-3-yl]-3-(indol-3-yl) maleimide

GIRK – G-protein dependent inwardly rectifying potassium channel

Glu - glutamate

GPCR – G-protein coupled receptor

H-89 - N-[2-[[3-(4-Bromophenyl)-2-propenyl] amino]ethyl]-5-isoquinoline sulfonamide dihydrochloride

HCO_3^- - bicarbonate ion

HFS – high frequency stimulation

I – current

IN - interneuron

I_{peak} – current peak

I_{SS} – steady-state current

IP_3 – inositol 1,4,5-triphosphate

IPSC – inhibitory postsynaptic current

IPSP – inhibitory postsynaptic potential

IS-I - interneuron-selective interneuron

K^+ - potassium ion

KA - kainate

KCC2 – potassium-chloride co-transporter 2

kDa – kilo Dalton

KN-62 - 4-[(2S)-2-[(5-isoquinolinylsulfonyl) methylamino]-3-oxo-3-(4-phenyl-1-piperazinyl) propyl] phenyl isoquinoline sulfonic acid ester

LAC – Local axon collateral

MAPK – mitogen-activated protein kinase

MCPG - (RS)-α-Methyl-4-carboxyphenylglycine disodium salt

MF – mossy fibers

mGluR – metabotropic glutamate receptor

mIPSC – miniature inhibitory postsynaptic current

muscimol-PSC – muscimol-evoked postsynaptic current

Na^+ - sodium ion

nAChR – nicotinic acetylcholine receptor

NBQX - 2,3-Dioxo-6-nitro-1,2,3,4-tetrahydrobenzo[f] quinoxaline-7-sulfonamide disodium salt

NF-kB – nuclear factor-κB

NHS – normal horse serum

NKCC1 – sodium-potassium-2chloride co-transporter 1

NMDA - N-methyl-D-aspartate

NMDAR – NMDA receptor

NPY - neuropeptide Y

NR-RSNP – non-rebounding-regular spiking non-pyramidal cell

NTPDase - ecto-nucleoside triphosphate diphosphohydrolase

NT5 – cytosolic 5'-nucleotidase

NT5E – ecto-5'-nucleotidase

O-LM - *oriens-lacunosum moleculare*

PB – phosphate buffer

PC – pyramidal cell

P_{Cl} – permeability for chloride ion

PDD - Phorbol 12,13-didecanoate

PDE - phosphodiesterase

P_{HCO3} – permeability for bicarbonate ion

PI3K – phosphatidylinositol 3-kinase

PIP3 – phosphatidylinositol-4,5-biphosphate

PiTX – picrotoxin

PKA – protein kinase A

PKB/AKT – protein kinase B

PKC – protein kinase C

PLC – phospholipase C

PP – perforant path

PPR – paired-pulse ratio

PV – parvalbumin

PVDF – polyvinylidene fluoride

QX-314 - N-(2,6-Dimethylphenyl carbamoylmethyl) triethylammonium bromide

R – resistance

R-RSNP – rebounding-regular skipink non-pyramidal cell

RMP – resting membrane potential

Rm – membrane resistance

Rp-cAMPs - R)-Adenosine, cyclic 3',5'-(hydrogen phosphorothioate) triethylammonium

Rs – series resistance

R_{seal} – seal resistance

RSNP – regular-spiking non-pyramidal cell

s.l-m. – *stratum lacunosum-moleculare*

s.o. - *stratum oriens*

s.p. – *stratum pyramidale*

s.r. – *stratum radiatum*

SAH – S-adenosyl-L-homocysteine

SAHH – S-adenosyl-L-homocysteine hydrolase

SC - schaffer collaterals

SCA - schaffer-collateral associated interneuron

SCH58261 - 2-(2-Furanyl)-7-(2-phenylethyl)-7H-pyrazolo[4,3-e][1,2,4]triazolo[1,5-c]pyrimidin-5-amine

SDS – sodium dodecyl sulfate

SEM – standard error of the mean

SFK-89976A - 1-(4,4-Diphenyl-3-butenyl)-3-piperidinecarboxylic acid hydrochloride

SNAP5114 - 1-[2-[tris(4-methoxyphenyl) methoxy]ethyl]-(S)-3-piperidinecarboxylic acid

SOM – somatostatin

SR-95531 – gabazine (2-(3-Carboxypropyl)-3-amino-6-(4 methoxyphenyl) pyridazinium bromide)

Sub – subiculum

TAP - temporoammonic pathway

TBS – tris-buffered saline

TPS-Tx – tris-buffered saline with 0.3% Triton-X-100

Tonic-IC – tonic inhibitory current

TTX - tetrodotoxin

V – voltage / volts

VDCC – voltage-dependent calcium channel

Vh – holding voltage

VIP - vasoactive intestinal polypeptide

Vm – membrane potential

V_{step} – voltage-clamp step

WIN 55,212-2 - (R)-(+)-[2,3-Dihydro-5-methyl-3-(4-morpholinylmethyl) pyrrolo[1,2,3-de]-1,4-benzoxazin-6-yl]-1-naphthalenyl methanone mesylate

Resumo

A transmissão glutamatérgica no hipocampo é continuamente controlada por neurónios inibitórios, denominados interneurónios, que libertam o neurotransmissor ácido gama-aminobutírico (GABA). Estas células apresentam uma grande diversidade anatómica, fisiológica e bioquímica, estando descritos mais de vinte e um tipos diferentes de interneurónios no hipocampo. Estes são capazes de comunicar quer com células principais excitatórias (denominadas células piramidais), quer com outros interneurónios inibitórios, com resultados diferentes para a excitabilidade do sistema. A inibição de células piramidais leva a uma diminuição direta da sua excitabilidade; ao passo que a inibição de outros interneurónios pode resultar na desinibição das células principais e consequente aumento da excitabilidade. Desta grande variedade de interneurónios, destacam-se duas grandes classes que correspondem às duas populações de interneurónios mais importantes e abundantes no hipocampo - os neurónios que expressam colecistocinina (CCK) e os neurónios que expressam parvalbumina (PV). As funções de cada uma destas populações no hipocampo são únicas e complementares no controlo da atividade das redes neuronais. Desta forma, um controlo rigoroso destes circuitos inibitórios é de extrema importância na regulação das funções do hipocampo. A adenosina é um neuromodulador ubíquo do sistema nervoso central que atua através de dois grandes tipos de recetores de alta afinidade – os recetores A_1 (A_1R) e os recetores A_{2A} ($A_{2A}R$). Os primeiros têm ações principalmente inibitórias da excitabilidade neuronal, e portanto estão normalmente

associados a funções neuroprotetoras, enquanto os segundos atuam no sentido de aumentar a excitabilidade no hipocampo e induzir excitotoxicidade. Enquanto que a função da adenosina no controlo da transmissão excitatória glutamatérgica tem vindo a ser caracterizada há várias décadas, o papel da adenosina na modulação da transmissão inibitória tem sido muito menos explorada.

O trabalho apresentado nesta tese tem como objetivo a caracterização das ações dos A_1Rs (Capítulo 5.1, p99) e dos A_{2A}Rs (Capítulo 5.2, p143) na comunicação neuronal inibitória no hipocampo bem como tentar perceber quais as consequências que uma possível modulação a este nível tem na excitabilidade das células piramidais e no desenvolvimento de atividade do tipo epiléptica.

Para responder a estas questões foi planeado e executado um trabalho experimental que envolveu o registo da atividade elétrica neuronal no hipocampo de ratos e ratinhos através de técnicas eletrofisiológicas *ex vivo* (nomeadamente registos extracelulares e registos de *patch-clamp*).

Relativamente às ações dos A_1Rs, foi demonstrado que apenas um tipo de respostas inibitórias, denominadas por respostas tónicas, são afetadas pela ativação dos A_1Rs, levando à sua diminuição. Este tipo de resposta tónica tem caraterísticas lentas e prolongadas no tempo e é mediada principalmente por recetores ionotrópicos do GABA do tipo A ($GABA_AR$) que estão localizados em porções peri- e extrasináticas dos neurónios. Pelo contrário, as respostas habitualmente rápidas e concertadas no tempo, denominadas por respostas fásicas, e que são mediadas por recetores localizados nas sinapses, não parecem ser afetadas

pela ativação dos A_1Rs. Curiosamente, estas ações ocorrem seletivamente em neurónios excitatórios piramidais e numa subpopulação de interneurónios que expressam o neuropéptido CCK. O efeito dos A_1Rs na diminuição das respostas tónicas está associado a uma cascata de sinalização intracelular que envolve as proteínas cinase A (PKA) e C (PKC) e é acompanhado pela diminuição da expressão de $GABA_A$Rs que contêm a subunidade δ, habitualmente implicada nas respostas tónicas.

Neste trabalho foi também demonstrado que a adenosina, através dos A_{2A}Rs, também influencia a transmissão inibitória no hipocampo. De facto, os efeitos da ativação dos A_{2A}Rs levam a um aumento da excitabilidade das células piramidais, que pode ser explicado pela ação destes recetores em dois locais: (1) a ativação dos A_{2A}Rs aumentam diretamente as respostas glutamatérgicas sobre as células piramidais; (2) simultaneamente, os A_{2A}Rs vão desinibir as células principais através de um mecanismo que envolve o aumento da libertação de GABA dos terminais sinápticos de neurónios que expressam PV e que contactam com outros neurónios inibitórios. Estas ações moduladoras têm implicações importantes em modelos de hiperexcitabilidade neuronal induzida pelo aumento das concentrações extracelulares de potássio, na medida em que a ativação ou inibição dos A_{2A}Rs leva a um exacerbação ou diminuição, respetivamente, desta hiperatividade neuronal sincronizada.

No seu conjunto, os resultados apresentados nesta tese revelam, pela primeira vez, o envolvimento dos recetores de adenosina na modulação da transmissão neuronal inibitória no hipocampo. Estes resultados poderão abrir novas e promissoras perspetivas

relativamente ao envolvimento da adenosina no controlo das funções do hipocampo em condições fisiológicas e patológicas.

Hipocampo; adenosina; GABA; interneurónios; modulação;

Abstract

Glutamatergic principal cell excitability in the hippocampus is regulated by local circuit neurons that release the inhibitory neurotransmitter gamma-aminobutyric acid (GABA). These GABAergic interneurons exhibit vast structural, physiological and biochemical diversity, innervating both excitatory principal cells and other inhibitory interneurons. In the hippocampus, two classes of interneurons, the cholecystokinin (CCK)- and parvalbumin (PV)-containing neurons, are the most significant and abundant cell type displaying unique and complementary functions in the control of principal cells output. Hence a tuned modulation of inhibitory circuits is of great importance in the control of network hippocampal function. Adenosine, acting through high affinity A_1 receptor (A_1R) and A_{2A} receptor ($A_{2A}R$), is a well-recognized endogenous modulator of glutamatergic principal cells excitability. Actions mediated by A_1Rs are long-known to decrease hippocampal excitability with neuroprotective effects while actions through $A_{2A}Rs$ are associated with increased neuronal excitability and excitotoxicity. However, the role of adenosine to modulate inhibitory transmission is much less known.

This work aimed to evaluate and characterize the involvement of A_1Rs (Chapter 5.1, p99) and $A_{2A}Rs$ (Chapter 5.2, p143) on inhibitory neuronal communication in CA1 hippocampus and its impact on principal cells excitability and in the control of epileptiform discharges.

These main goals were achieved by performing *ex vivo* electrophysiology recordings (field and patch-clamp recordings) from rat and mice hippocampus.

Regarding A_1R-actions, it was found that tonic - mediated by GABA receptor type A ($GABA_AR$) localized peri- and extrasynaptically - but not phasic - mediated by $GABA_ARs$ located at synapses - inhibitory transmission in pyramidal cells and CCK-positive interneurons were diminished after A_1R activation. The effect was dependent on a signaling cascade involving both protein kinase A (PKA) and protein kinase C (PKC) and was accompanied by decreased $GABA_AR$ δ-subunit expression. On the other hand, it was also found that $A_{2A}R$-mediated increase in pyramidal cells excitability results from a direct increase of glutamatergic transmission in parallel with disinhibition of principal cells by a mechanism that involves increased GABA release from PV-positive cells to other interneurons. Also, $A_{2A}R$ activation or blockage respectively promotes or reduces synchronous pyramidal cell firing in hyperexcitable conditions induced by elevated extracellular potassium or following high-frequency electrical stimulation.

Together the results presented in this thesis show for the first time a direct involvement of adenosine receptors in the control of inhibitory network transmission in the hippocampus. This results open new promising perspectives for the involvement of adenosine in the control of physiological hippocampal operations and maladaptive conditions.

Hippocampus; adenosine; GABA; interneurons; modulation;

1 Introduction

The main goal of neuroscience is to “understand the biological mechanisms that account for mental activity” (Albright et al. 2000). This concept includes the understanding of how the complex neuronal circuits that are assembled during development allow individuals to perceive the world around them, how this perception is recalled from memory and how is translated into emotions, thinking and behavior. Historically, the first written record about the nervous system can be dated back to the 17th century BC, with the Edwin Smith Surgical Papyrus, an Ancient Egyptian medical text describing 48 case histories of trauma, with the first two cases being related to brain injuries (Gross 1987). This treatise shows already a vague recognition from Ancient Egyptians of the effect of brain trauma on the human body. Until the end of the 19th century, the history of neuroscience was made of a combination of breakthroughs and setbacks with great names of science, such as Hippocrates, Aristotle, Galen, Vesalius and Descartes. Most of the works were anatomical descriptions of brain and nerves, although several of its functions were already proposed. In fact, Hippocrates (in *On The Sacred Disease*, 400 BC) recognized already epilepsy as an abnormal functioning of the brain rather than a spiritual affliction and Galen (AD 129–199) considered the brain as the site of sensation and thought as well as the controller of movement.

Last century was incredibly enthusiastic for neuroscience, with many disciplines contributing for our current knowledge of brain’s structure and function. In anatomy, the microscopic era was

flourishing and the work made by the great Spanish anatomist Ramón y Cajal marked the beginning of modern neuroscience. Ramón y Cajal used Golgi's technique of neuronal staining to visualize individual cells in the brain and demonstrate that each nerve cell with axons and dendrites is an individual unit (Ramón y Cajal 1911). This finding extended Hook's cell theory (Hooke 1665) to the nervous system creating what is now known as the *neuron doctrine* (Gest 2004) - only completely confirmed with electron microscopy (Gray 1959a,b). In physiology, experimentation started with Galvani's pioneering work on animal electricity (see Piccolino, 1998). Galvani was followed by many others that were driven to understand the electrical nature of neuronal signaling: Émile du Boi-Reymond differentiated nerve currents from muscle currents (du Bois-Reymond 1848); his student Julius Bernstein introduced the modern membrane theory of action potential (Bernstein 1902); later, Alan Hodgkin and Andrew Huxley, together with Bernard Katz, uncovered its ionic basis (Hodgkin & Huxley 1939, 1947, 1952a; Hodgkin et al. 1952). The next great step in electrophysiology was made by Neher and Sakmann who developed the "patch-clamp" technique (Neher & Sakmann 1976), revolutionizing the recordings of neuronal activity. Pharmacological sciences gave an enormous contribution to the understanding of nervous system. Here, is worth mentioning the work of John Langley, who introduced the concept of "receptive substance" or "receptors" as we now call it (Langley 1905); Otto Loewi, that studied the chemical nature of neuronal communication (Loewi 1921); the identification of many neurotransmitters, as acetylcholine (Dale & Dudley 1929), adrenaline and noradrenaline (von Euler 1946, 1948), gamma-

aminobutyric acid (GABA) (Awapara et al. 1950, Roberts & Frankel 1950, Udenfriend 1950) or glutamate (Curtis et al. 1959) occurring right after Loewi's discoveries.

This brief historical perspective, although lacking many other important breakthroughs in the field, already shows the significance of multi-disciplinarity for the progress of neuroscience. In fact, neuroscience is one of the most inter-disciplinary areas of knowledge, influenced not only by anatomy, physiology and pharmacology, as already mentioned, but also with strong contributions from psychology, genetics, molecular biology, mathematics, computer science among many others.

In the work described in this thesis, I used some of these approaches to understand how hippocampal inhibitory network is regulated and modulated by adenosine. Many of the neuromodulatory capabilities of adenosine in the hippocampus are long known by the scientific community (see Chapter 1.3.1, p31 for details). However, regardless the fact that adenosine is released by all brain cells and its receptors are ubiquitously distributed in neurons including GABA-releasing interneurons (Rivkees et al. 1995, Ochiishi et al. 1999), the study of its role in hippocampal inhibitory neurotransmission has been mostly neglected. There is also strong evidence for adenosine influence on neuronal plasticity (de Mendonça et al. 1997, Izumi & Zorumski 2008, Fontinha et al. 2009, Dias et al. 2012), meta-plasticity (Dias et al. 2013), hippocampal rhythms (Schulz et al. 2012) and neuronal excitotoxicity (de Mendonça et al. 2000), all phenomena leaning on GABAergic regulation. All these evidences denote that the study of the modulatory role of adenosine on hippocampal inhibitory system should not be delayed.

1.1 The hippocampal formation

The term hippocampus (derived from the Greek word hippos meaning "horse" and kampos meaning "sea monster") was first used by the anatomist Giulio Cesare Arantius, in 1587, after linking the shape of the hippocampus to the tropical fish seahorse (Figure 1.1).

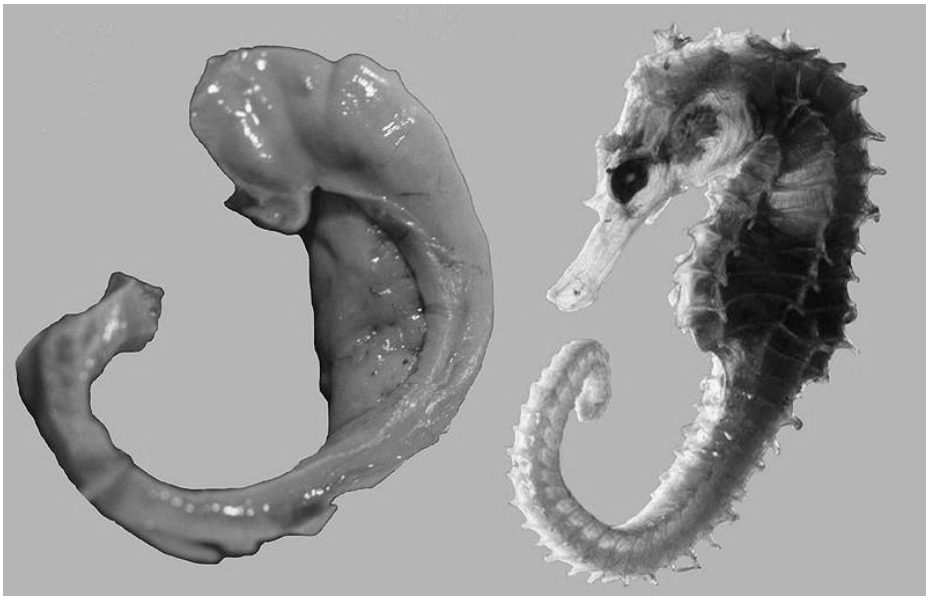

Figure 1.1. The human hippocampus compared with a seahorse
Preparation of the human hippocampus dissected free (left) alongside with a specimen of *Hippocampus leria* (right). Not in scale. Preparation by László Seress in 1980.

The hippocampal formation is a specialized cortical structure located in the medial temporal lobe, in the floor of the inferior horn of the lateral ventricle. During late nineteenth and early twentieth centuries, this part of the brain has been proposed to be responsible for many functions ranging from olfaction (Ferrier 1886, Jackson & Beevor 1890, Penfield & Erickson 1941), emotion (Papez 1995) and attention control (Jung & Kornmüller 1938, Green & Arduini 1954). Today it is largely accepted as

mostly involved in memory acquisition, spatial learning and navigation (Stark 2007).

The hippocampal formation is a group of distinct but related brain regions that together comprise one functional system. These regions include the dentate gyrus (DG), hippocampus proper, subiculum, presubiculum, parasubiculum, and entorhinal cortex (EC), which are linked, one to the next, by a largely unidirectional neuronal pathway (Amaral & Witter 1989) (Figure 1.2). Often, as in this thesis, the word hippocampus is used to refer to a structure comprising the hippocampus proper and DG.

The hippocampus proper can be further divided into three major subregions identified by the neuroanatomist Rafael Lorente de Nó (Lorente de Nó 1934) that comprise the C*ornu Ammonis* (CA) fields (CA1, CA2 and CA3). Early neuroanatomical studies together with electrophysiological recordings identified a powerful excitatory feedforward glutamatergic circuit known as the trisynaptic circuit (Andersen et al. 1971) [EC → DG (synapse 1); DG → CA3 (synapse 2); CA3 → CA1 (synapse 3); see Figure 1.2B].

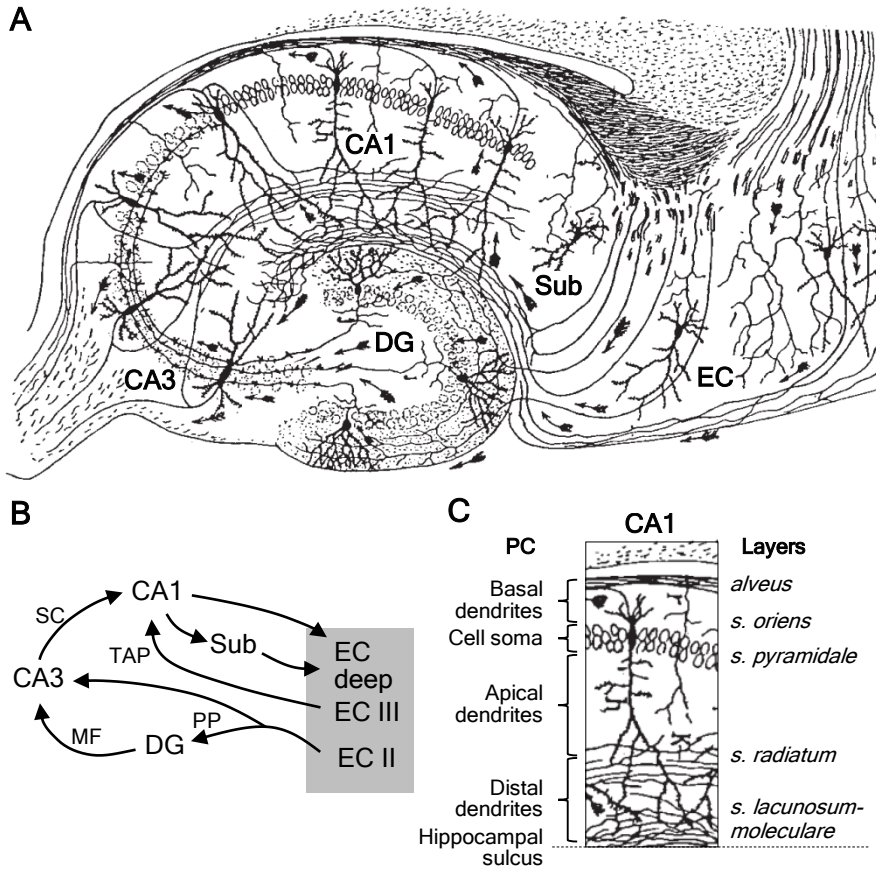

Figure 1.2. Illustration of the neuronal circuitry of the rodent hippocampus
(A) Original drawing by Ramón y Cajal of the rodent hippocampus, processed with Golgi and Weigert staining. Schematic in **(B)** shows the flow of information from the Entorhinal Cortex (EC) to Dentate Gyrus (DG) and CA3 pyramidal neurons via Perforant Path (PP) and to CA1 pyramidal neurons through Temporoammonic pathway (TAP) and from DG to CA3 neurons via the mossy fibers (MF). From CA3 region, cells project to CA1 pyramidal neurons via Schaffer Collateral Pathway (SC) which than project to Subiculum (Sub) and back to EC forming a uni-directional loop. **(C)** Magnification of CA1 region in (A) showing the different *strata* contained in a cross section of the hippocampus and the projection of basal and apical dendrites of pyramidal cells. The drawing in (A) and (C) is adapted from Ramón y Cajal 1911.

The first synaptic connections to form the intrinsic hippocampal circuit are axons from layer II of the EC. These will form the major hippocampal input pathway called the perforant path (PP) and project, among other destinations, to granule cells of DG (Steward 1976). From these cells, the information flows unidirectionally

through mossy fibers (MF) to CA3 pyramidal cells forming the second hippocampal synapse (Claiborne et al. 1986). The third connection in the trisynaptic loop brings the information from the CA3 cells via Schaffer collaterals (SC) to the CA1 pyramidal cells. Adding to this major trisynaptic loop, shorter monosynaptic pathways also occur. Thus, we can find monosynaptic connections from layer II of the EC directly to CA3 neurons through PP (Steward 1976), and from layer III of the EC to CA1 pyramidal cells through temporoammonic pathway (TAP) (Amaral 1993). At CA3 region, the information is further processed through auto-association fibers that connect CA3 pyramidal cells with one another (Schaffer 1892, Le Duigou et al. 2014). This recurrent network activity can also be observed in DG where granule cells excite mossy cells, another type of cell in DG (Scharfman & Schwartzkroin 1988), that project back to granule cells (Hetherington et al. 1994, Jackson & Scharfman 1996). The CA1 field of the hippocampus projects monosynaptically (Nakashiba et al. 2008) or disynaptically via subiculum pyramidal cells to deep layers of the EC. The monosynaptic pathway was suggested to be relatively weaker compared to the disynaptic one (Swanson et al. 1978, Amaral & Witter 1989). These connections close the hippocampal excitatory unidirectional loop (Figure 1.2B).

The detailed anatomical knowledge of hippocampal circuitry described above has been of great value to comprehend the functional contribution of each subregion for memory formation and navigation (Lisman 1999, van Strien et al. 2009). Indeed, the EC was found to work as an input-output structure that maintains information flow from and towards the cortex (Naber et al. 1997). Moreover, EC also integrates generic and contextual information

before entering the hippocampus (Selden et al. 1991, Mayeaux & Johnston 2004, Sargolini et al. 2006). The processed contextual patterns reach the DG where they are separated and contrasts are recognized and amplified (Bakker et al. 2010). At the CA3 field, the recurrent connections will work as an auto-associative network and have been proposed as essential for reconstructing already encoded patterns and retrieving previous experiences (Hasselmo et al. 1995, Nakazawa et al. 2002, Rolls 2007). Finally, the CA1 field operates as a match/mismatch decoder, switching from encoding new information arriving from direct EC inputs or feedforwarding retrieved information from CA3 inputs (Duncan et al. 2012). Importantly, the existence of place cells in CA1/CA3 fields (O'Keefe & Dostrovsky 1971, O'Keefe & Conway 1978) and grid cells in EC (Fyhn et al. 2004, Hafting et al. 2005) also confer to the hippocampus a fundamental role in navigation processes. Cells at the CA2 subregion (located between CA3 and CA1) have been subject of substantial controversy due to their less distinct anatomy. However, recent studies have begun to stablish a unique connectivity and physiology for these cells (Jones & McHugh 2011).

Hippocampal subregions are structured in a lamellar organization. Each lamella is called *stratum* and the CA1 field is composed of five clearly defined *strata* (Figure 1.2C). The most superficial layer is the *stratum alveus* that is virtually devoid of cell bodies but contains the bulk of axons from CA1 pyramidal cells; next to *alveus* is the *stratum oriens*, a layer that contains the cell bodies of GABAergic interneurons as well as collaterals from CA3 principal cells and basal dendrites of CA1 pyramidal neurons; the *stratum pyramidale* corresponds to a thin layer containing

neuronal cell bodies of principal pyramidal cells (making up 90% of total neurons in CA1 region) and disperse interneurons; the *stratum radiatum* is the largest CA1 layer, containing not only sparse interneuron cell bodies but mostly the SC fibers from CA3 cells that terminate in CA1 pyramidal cell dendrites; finally, the *stratum lacunosum-moleculare* is adjacent to the hippocampal fissure (sulcus) and contains the distal and apical dendritic ramifications of pyramidal cells together with fibers from TAP (EC → CA1) (Figure 1.2C).

1.1.1 Excitatory glutamatergic connections in CA1 region

Excitatory connective inputs into CA1 neurons can arise mainly from four different pathways (Figure 1.3): (1) SC fibers projecting from CA3 pyramidal cells. These will target both basal and apical dendrites of CA1 pyramidal neurons and interneurons from all CA1 layers (Ishizuka et al. 1990, Li et al. 1994). (2) Local axon collaterals (LAC) of CA1 pyramidal cells synapsing with CA1 pyramidal basal dendrites and *stratum oriens* interneurons (Deuchars & Thomson 1996). (3) TAP inputs from EC layer III that will predominantly target distal apical dendrites of principal cells and interneurons. (4) Associational Commissural connections (ACC) that project from contralateral CA3 region hippocampus to CA1 cells (Blackstad 1956, Fricke & Cowan 1978). These fibers are termed commissural fibers since they cross from one hemisphere of the brain to the other. These synapses (contralateral) differ from SC fibers (ipsilateral) in many molecular, anatomical and functional properties (Shinohara et al. 2008, Kohl et al. 2011) (Figure 1.3).

There are also two other less explored inputs to CA1 hippocampus from thalamic *nucleus reuniens* targeting distal dendritic tuffs (Dolleman-Van Der Weel & Witter 1996) and from amygdala terminating in *stratum oriens* (Pikkarainen et al. 1999).

As mentioned before, excitatory fibers project not only to principal glutamatergic cells but also to CA1 interneurons, resulting in feedforward and feedback inhibitory operations (Figure 1.3B). The direct recruitment of interneurons from afferent pathways originates feedforward inhibition and enforces the temporal fidelity of pyramidal cells discharges (Pouille & Scanziani 2001). Local CA1 pyramidal cell projections to interneurons results in feedback recurrent inhibition that sequentially recruits somatic-targeting or dendritic-targeting inhibitory circuits which synergistically restrain principal cell activity (Pouille & Scanziani 2004, Somogyi & Klausberger 2005).

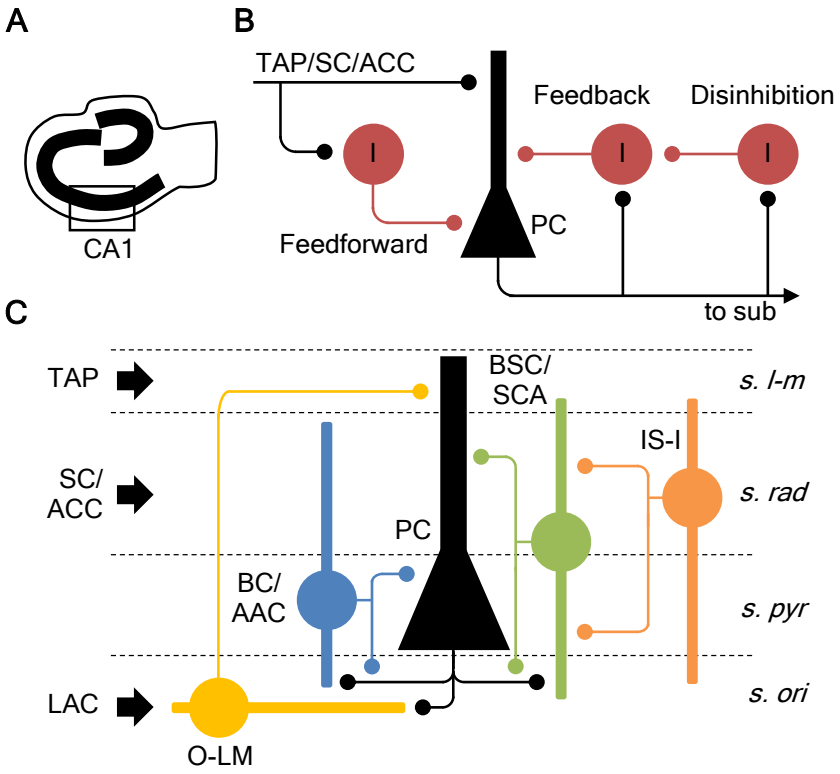

Figure 1.3. Hippocampal operations performed by distinct populations of CA1 interneurons

(A) Schematic representation of a coronal slice of the hippocampus highlighting the CA1 region. Orientation of the slice corresponds to orientation of schematic circuits represented in (B) and (C). Schematic in **(B)** shows a simplistic representation of forms of feedback and feedforward operations performed by interneurons. It is also shown interneurons that selectively innervate other interneurons disinhibiting principal cells. **(C)** Principal subtypes of interneurons in hippocampal CA1 area and their laminar distribution. The main glutamatergic inputs to CA1 region are indicated on the left. For (B) and (C), thick lines coming out from the soma correspond to neuronal dendrites; thin lines terminating in circles correspond to axonal projections; PC: pyramidal cell (black); I: interneuron (red); BC / AAC: Basket cell/Axo-axonic cell (blue); O-LM: *oriens-lacunosum moleculare* cell (yellow); BSC/SCA: bistratified cell/schaffer-collateral associated interneuron (green); IS-I: interneuron-selective interneuron (orange); ACC: associational commissural connection; LAC: Local axon collateral; TAP: temporoammonic pathway; SC: schaffer collaterals fibers; sub: subiculum; *s. l-m*: *stratum lacunosum-moleculare*; *s. rad*: *stratum radiatum*; *s. pyr*: *stratum pyramidale*; *s. ori*: *stratum oriens*. (Somogyi & Klausberger 2005).

1.1.2 Hippocampal interneurons

Contrary to what happens to pyramidal cells, GABAergic interneurons in the cortex are very diverse, which has hindered a satisfactory consensus in its classification (DeFelipe et al. 2013). This diversity is manifested in many aspects of their phenotype, such as their distinct anatomical, neurochemical and physiological features (Ascoli et al. 2008). These different characteristics confer to interneurons distinct roles in controlling pyramidal cell excitability and the overall hippocampal activity. The CA1 region, given its well-organized laminar structure and well-characterized oscillatory activity patterns is the most studied cortical structure with respect to interneuron diversity and function (Somogyi & Klausberger 2005).

1.1.2.1 Anatomical classification

From the earliest work of Ramon y Cajal (Ramón y Cajal 1911) and later from the work of Janos Szentágothai (Szentágothai 1975) it was hypothesized that different neuronal shapes could have distinct roles in cortical functions. Extensive morphological studies allow us today to discriminate more than twenty different types of interneurons (Somogyi & Klausberger 2005). The analysis of anatomical characteristics of interneurons provides intuitive insights about its contributions to network operations. In fact, the dendritic arborization and axonal projections of basket cells (BC) (Freund & Buzsáki 1996) and axo-axonic cells (AAC) (Szentágothai & Arbib 1974, Somogyi et al. 1983) places them in optimal position to contribute to both feedforward and feedback

network processes and to play a major role in controlling pyramidal cells final integration and output (Miles et al. 1996, Pouille & Scanziani 2001). BC axonal projections target the soma and proximal dendrites of pyramidal cells and AAC project selectively to axon initial segments of pyramidal cells (Figure 1.3C, Blue). Other neurons that are driven in feedback and feedforward manner are bistratified cells (BSC) (Buhl et al. 1994) and schaffer-collateral associated interneurons (SCA) (Vida et al. 1998). With some exceptions, these cells receive inputs from SC and ACC fibers and span their axons to the entire width of *stratum radiatum* and *stratum oriens* (Figure 1.3C, Green).

Although the majority of interneurons work in a feedback-feedforward dichotomy, there are GABAergic neurons exclusively operating feedback inhibition. These include *oriens-lacunosum moleculare* (O-LM) cells (Lacaille et al. 1987, McBain et al. 1994). The O-LM GABAergic interneurons receive most glutamatergic inputs from CA1 pyramidal cells (Blasco-Ibáñez & Freund 1995) and innervate the distal dendrites of the same pyramidal cells (Maccaferri et al. 2000) (Figure 1.3C, Yellow). There is another group of interneurons that selectively target other inhibitory cells, and are hence called interneuron-selective interneurons (IS-I) (Acsády et al. 1996, Gulyás et al. 1996). The IS-I are particularly relevant in synchronizing interneuron outputs and disinhibitory actions (inhibition of inhibitory cells culminating in increased excitability of principal cells) (Freund & Buzsáki 1996) (Figure 1.3B and Figure 1.3C, orange). It is noteworthy that interneurons such as BC, AAC or O-LM cells can also synapse with other interneurons at different layers of the hippocampus and also contribute to disinhibitory phenomena.

Other types of interneurons also occur in CA1 region such as neurogliaform cells, *lacunosum moleculare* neurons, trilaminar cells or back projecting cells (Somogyi & Klausberger 2005).

1.1.2.2 Neurochemical classification

Despite the usefulness of anatomical characterization, this is not always sufficient criteria to distinguish different types of interneurons. Also, the role of an interneuron is not only influenced by its morphology but also strongly shaped by its biochemical properties. The first evidence for biochemical differences in neurons that were translated in completely different functional outputs came from the distinction between glutamate and GABA-releasing neurons (Storm-Mathisen et al. 1983). However, some years earlier, Roberts' group had already described the GABA-synthesizing enzyme, glutamic acid decarboxylase (GAD), in neurons from cerebellum, spinal cord, substantia nigra and olfactory bulb (Saito et al. 1974, McLaughlin et al. 1975, Ribak et al. 1976, 1977), clearly identifying inhibitory cells. Many markers were later found to distinguish different types of interneurons which include peptides [e.g. somatostatin (SOM), cholecystokinin (CCK), neuropeptide Y (NPY) and vasoactive intestinal polypeptide (VIP)] or calcium-binding proteins [e.g. calbindin, parvalbumin (PV) and calretinin] (Somogyi & Klausberger 2005). For example, there are morphologically identified BC that can be further sub-divided into two groups based on their neurochemical content: one expressing the calcium-binding protein PV and the other containing the peptide CCK. These two BC differ markedly in their functional characteristics (Bartos & Elgueta 2012). The PV

BC are associated with fast, stable and time-controlled inhibition onto their target cells (Kraushaar & Jonas 2000, Bartos et al. 2002, Hefft & Jonas 2005, Doischer et al. 2008) and CCK BC are known to generate asynchronous, fluctuating and less timed inhibitory outputs (Hefft & Jonas 2005, Daw et al. 2009, Ali & Todorova 2010).

On the other hand, different types of morphological identified interneurons may express the same neurochemical marker. For example, PV can be found in four anatomical-identified interneurons (AAC, BC, BSC and O-LM cells) and CCK can be found in three types of neurons (BC, SCA and *lacunosum moleculare* neurons) (Somogyi & Klausberger 2005).

These examples show that a combination of anatomical and neurochemical evaluation is required to unambiguously distinguish interneurons operating in the hippocampus.

1.1.2.3 Functional classification

The morphological and neurochemical approaches have been combined with a physiological characterization of interneurons. These characteristics include, among others, passive and subthreshold properties of neurons, action potential measurements and firing pattern (Ascoli et al. 2008). The knowledge of the electrophysiological characteristics of a particular neuronal population is important to understand its role in circuit activity and computation. As an example, CCK-positive BC and PV-positive BC largely differ in their intrinsic functional properties. The first show slow and accommodating trains of action potentials when depolarized by suprathreshold current

injection (Lee et al. 2011) while PV cells show a high frequency and non-accommodating discharge pattern (Doischer et al. 2008). The fast time constants of PV-positive neurons make them temporally precise followers of pyramidal cell input and the less accurate CCK-positive BCs are better suited to integrate feedforward and feedback inputs (Klausberger et al. 2005, Glickfeld & Scanziani 2006, Freund & Katona 2007). However, we should bear in mind that although some of these features correlate well with anatomical and biochemical characteristics, others do not.

1.2 GABA and GABA receptors

Since the early 1950's that the amino acid GABA was found to be present in the mammalian brain (Awapara et al. 1950, Roberts & Frankel 1950, Udenfriend 1950). However, GABA was not readily acknowledged as a natural transmitter (Elliott & Van Gelder 1958, Hayashi 1958, Curtis 1959) and only in 1967, with the work of Krnjević and Schwartz on cerebral cortical neurons, GABA was unequivocal accepted as a neurotransmitter of the central nervous system (CNS) (Krnjević & Schwartz 1967) (Roberts 1986, Martin & Olsen 2000, Bowery & Smart 2006). Today, GABA is considered the main inhibitory neurotransmitter in the adult brain, being primary released by around 20% of brain neurons (Beaulieu et al. 1992, Somogyi et al. 1998). These GABA-releasing neurons are characterized by the presence of GAD, the enzyme which catalyzes the decarboxylation of glutamate to GABA (Roberts & Kuriyama 1968) beeing considered as the principal marker of GABA-releasing interneurons.

When first described in neurons, GABA was shown to produce inhibitory hyperpolarizing responses (Krnjević & Schwartz 1967) that were blocked by bicuculline (Curtis et al. 1970). These actions were later found to be mediated by the chloride (Cl^-) permeable ionotropic receptor called $GABA_A$ receptor ($GABA_AR$) (Schofield et al. 1987). However, attempts to identify GABA receptors on peripheral nerve terminals revealed that GABA application led to a reduction of noradrenaline release in the rat heart, an effect that was not blocked by bicuculline and was mimicked by baclofen (Bowery et al. 1980). These actions were later found to be mediated by a new GABA receptor called $GABA_B$ receptor ($GABA_BR$) (Bowery et al. 1981, Hill & Bowery 1981, Kerr & Ong 1995). This $GABA_BR$ does not increase Cl^- flux like $GABA_AR$, but is coupled *via* second messengers (Hill 1985) to potassium (K^+) channels at the postsynaptic site and to calcium (Ca^{2+}) channels at presynaptic terminals. The former produces the late inhibitory postsynaptic potential characteristic of a GABA response (Newberry & Nicoll 1985) and the later mainly decreases transmitter release (Dunlap & Fischbach 1981). A third type of GABA receptor, mostly localized in subpopulations of retinal neurons (Feigenspan et al. 1993, Qian & Dowling 1993), that is bicuculine- and baclofen-insensitive was identified (Johnston et al. 1975) and named $GABA_C$ receptor ($GABA_CR$) (Drew et al. 1984, Bormann & Feigenspan 1995). This receptor was, however, later included in the $GABA_AR$ class, on the recommendations of IUPHAR Nomenclature Committee (Barnard et al. 1998).

1.2.1 $GABA_A$ receptors

The $GABA_AR$ is a member of the "cys-loop" superfamily of ligand-gated ion channels to which nicotinic acetylcholine receptor (nAChR), glycine receptor and serotonin (5-hydroxytryptamine) 5-HT_3 receptor also belong (Unwin 1989, Barnard et al. 1998). All of these receptors are heteromeric pentamers composed of five subunits arranged around a central pore. When the ligand binds to the receptor it triggers a conformational change in the channel protein that results in the flow of ions through the transmembrane pore that will depend on the electrochemical gradient of the particular permeant ion. $GABA_AR$ is permeable to Cl^- and bicarbonate (HCO_3^-) ions (Bormann et al. 1987, Kaila 1994). The net flow response that results from the increasing membrane permeability to Cl^- and HCO_3^- caused by $GABA_AR$ activation will depend on the distribution of these two ions across the membrane and on the membrane potential of the cell. In most mature neurons of the CNS the expression of the K^+ - Cl^- co-transporter 2 (KCC2) (Payne et al. 2003, Rivera et al. 2005), a Cl^- extruder , will result in a Cl^- equilibrium potential (E_{Cl}) that is more negative than the resting membrane potential (RMP) of the neuron (Thompson & Gähwiler 1989a, Rivera et al. 1999). On the other hand, the equilibrium potential for HCO_3^- (E_{HCO3}) is more positive then the RMP (Roos & Boron 1981, Chesler 1990), but the $GABA_AR$ permeability to HCO_3^- is about fivefold less than that to Cl^- ions (Bormann et al. 1987, Kaila 1994). Thereby, $GABA_AR$ activation in these conditions will lead to the net entry of anions (outward current) that results in a hyperpolarizing inhibitory postsynaptic potential (IPSP).

The $GABA_AR$ action is, therefore, considered “inhibitory” for two main reasons (Figure 1.4): (1) there is a general increase in membrane input conductance that shunts the ability of excitatory potentials to depolarize the membrane (Figure 1.4A); (2) the Cl^--mediated hyperpolarization of the membrane will summate to any eventual depolarizing signal arriving to the neuron that reduces the probability of the cell to fire an action potential (Figure 1.4B) (see Kuffler 1960; McCormick 1989).

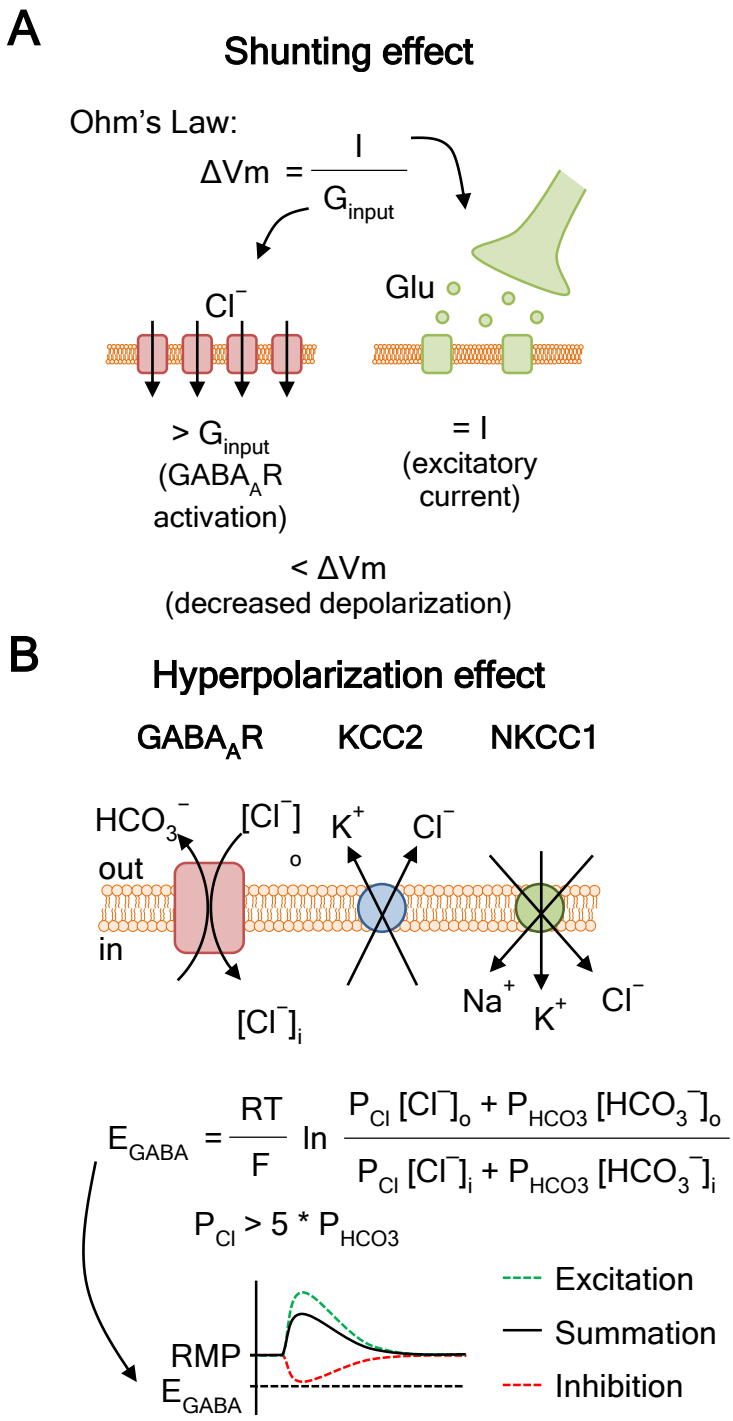

Figure 1.4. Neuronal inhibition mediated by $GABA_AR$
The inhibitory action mediated by $GABA_AR$s results from a combination of two main effects:

(A) Shunting effect, corresponds to an increase in membrane input conductance (G_{input}) due to activation of $GABA_AR$s. According to Ohm's law, $GABA_AR$-mediated increase in chloride permeability will lead to an overall increase in input conductance. This increased G_{input} will necessarily decrease membrane depolarization induced by any excitatory glutamatergic current (I) arriving to the neuron. The shunting effect does not result in a direct hyperpolarization of the neuron but it limits any changes in glutamate-induced membrane depolarization.
(B) Hyperpolarizing effect, contrary to the shunting effect, corresponds to a direct hyperpolarizing action of $GABA_AR$s. The $GABA_AR$s are primary permeable to chloride ions and, in a less extent, to bicarbonate ions (P_{Cl} is 5 times bigger than P_{HCO3}). The expression of chloride transporters (KKC2 and NKCC1) in the adult brain results in low concentration of chloride inside the cell compared to outside. Considering the relative permeability of $GABA_AR$s to chloride and bicarbonate and the concentration of the ions inside and outside the cell, the Goldmann equation calculates the equilibrium potential for GABA (E_{GABA}) in physiological conditions more negative than the resting membrane potential (RMP). When an inhibitory input arrives to the neuron, the RMP will get more negative, towards E_{GABA}, hyperpolarizing the cell. The inhibitory potential will propagate to the soma and summate to any excitatory potential arriving simultaneously to the neuron and restrain neuronal excitability. F: Faraday's constant (≈9.6 x 10^4 J/mol*V); I: current; R: ideal gas constant, (≈8.3 J/K*mol; T: temperature (37°C = 310 K); Vm: membrane potential.

In immature and developing neurons, however, the activation of $GABA_AR$ can lead to membrane depolarization and, in some cases, firing of action potential (Ben-Ari et al. 1989, Brickley et al. 1996, Chen et al. 1996, Owens et al. 1996, 1999; Dammerman et al. 2000, Gao & van den Pol 2001, Wang et al. 2001). This results from a higher intracellular concentration of Cl^- due to early developmental expression of Na^+ - K^+ - $2Cl^-$ co-transporter 1 (NKCC1) (Delpire 2000) pumping Cl^- inside the cell, and lack of expression of KCC2 (Rivera et al. 1999) involved in extruding Cl^- from the neuron. This intracellular accumulation of Cl^- in immature neurons leads to depolarized E_{Cl} compared to the resting membrane potential and excitatory actions of GABA during development. Also, neuronal activity, such as epileptiform discharges, can transiently change the reversal potential for GABA and turn $GABA_AR$ currents into depolarizing and excitatory (Alger & Nicoll 1982, Huguenard & Alger 1986, Perreault & Avoli 1988, 1992; Thompson & Gähwiler 1989b, Michelson & Wong

1991, Grover et al. 1993, Staley et al. 1995, Kaila et al. 1997). The shift in $GABA_AR$ response polarity results from an increased and prolonged receptor conductance that dissipates Cl^- (Thompson et al. 1988, Thompson & Gähwiler 1989a) and HCO_3^- (Kaila & Voipio 1987, Grover et al. 1993, Staley et al. 1995) gradient towards an equilibrium potential of $GABA_AR$ more positive then the RMS, explaining the depolarizing responses of GABA (Kaila 1994).

As mentioned before, the $GABA_AR$ is a heteropentameric glycoprotein of about 275kDa and composed of five subunits (Olsen & Tobin 1990). To date, there are seven subunit families described and some of them have multiple subtypes making a total of 19 different subunit isoforms: α1-6, β1-3, γ1-3, δ, ε, π, ρ1-3, and θ (Schofield et al. 1987, Macdonald & Olsen 1994, Mehta & Ticku 1999). In addition, further structural complexity exists due to alternative splicing of subunits such as γ2 subunit (Whiting et al. 1990, Kofuji et al. 1991). Within a subunit family there is about 70% sequence homology that drops to around 30% homology in between families (Schofield et al. 1987, Olsen & Tobin 1990, DeLorey & Olsen 1992). Despite the multiplicity of receptor subunits, there is a limited number of $GABA_AR$ subunit combinations *in vivo* (Olsen & Sieghart 2008). Current evidence shows that most $GABA_AR$ subtypes are formed from two copies of a single α, two copies of a single β, and one copy of another subunit, such as γ, δ, ε, π or θ (McKernan & Whiting 1996). The ρ subunit contribute to the assembly of $GABA_CR$ (Cutting et al. 1991).

The physiological significance of the structural heterogeneity of $GABA_AR$ may lie on the provision of functional diversity such as channel kinetics, affinity for GABA, rate of desensitization and

susceptibility for transient chemical modification (e.g. phosphorylation) (Macdonald & Olsen 1994). Also, given the differential subunit expression throughout brain regions, different $GABA_AR$ subunit compositions also distributes differently between cell-types and subcellular locations, where they can mediate distinct forms of $GABA_AR$ inhibition (phasic *vs* tonic inhibition) (Farrant & Nusser 2005, Glykys & Mody 2007a).

1.2.2 Phasic receptor activation

Phasic $GABA_AR$-mediated synaptic transmission allows a fast and precisely-timed communication between GABAergic presynaptic terminal and the postsynaptic target. With the arrival of an action potential at the interneuron axonal terminal, a pool of GABA-containing vesicles is synchronously released to the synaptic cleft in a calcium-dependent manner. This will transiently increase local GABA concentration up to about 1.5 to 3.0 mM that lasts between 10-100 ms (Mody et al. 1994, Nusser et al. 2001, Mozrzymas et al. 2003). Released GABA is rapidly removed from the synapse either by high affinity GABA transporters in presynaptic nerve terminals and surrounding astrocytes or, in a less extend, by passive diffusion (Iversen & Neal 1968, Conti et al. 2004). Ten to a few hundred $GABA_ARs$ clustered opposite to the releasing site are activated (Edwards et al. 1990, Mody et al. 1994, Nusser et al. 1997), producing an inhibitory postsynaptic current (IPSC). The kinetics of this inhibitory synaptic response will mainly depend on the properties and number of receptors and by the magnitude and duration of the GABA transient. Each $GABA_AR$ will transit between a closed state, a brief open state, a desensitized state (a closed

but still agonist-bound form) and finally deactivation state (with release of receptor ligand) (Maconochie et al. 1994, Jones & Westbrook 1995, Chang & Weiss 1999, Bianchi & Macdonald 2001). Besides the activation of $GABA_AR$ at the active zone of the synapse, there are also receptors adjacent to the synaptic button that can be recruited. Its activation results from GABA diffusion and consequent recruitment of $GABA_ARs$ located perisynaptically or located in the nearby synapses (Nusser et al. 1998, Wei et al. 2003). It is worth noting that this form of inhibition is also considerer phasic transmission since is time-locked to presynaptic GABA release that only transiently activates $GABA_ARs$. A schematic representation of phasic transmission is depicted in Figure 1.5.

1.2.3 Tonic receptor activation

In addition to the phasic GABAergic transmission explained above, other form of sustained and persistent $GABA_AR$-mediated activity can be found in the brain (Figure 1.5). The first experimental indication for the existence of this tonic GABA response arrived from anatomical studies showing the presence of $GABA_AR$ outside the synapse (Somogyi et al. 1989, Soltesz et al. 1990) together with physiological recordings of a perpetual form of $GABA_AR$-dependent inhibitory response (Otis et al. 1991). A few years later tonic GABA transmission was directly measured while recording from granule cells of rat cerebellar cortex (Kaneda et al. 1995, Brickley et al. 1996, Wall & Usowicz 1997). Much attention have been given to this topic in the following years and tonic conductances were also reported in several other areas of

the CNS such as mice dentate gyrus, hippocampus, neocortex, thalamus, striatum, hypothalamus, spinal cord and also in human brain.

Tonic inhibition results from the continuous activation of $GABA_A$Rs by low concentrations of ambient GABA. Receptors responsible for this form of transmission must fulfill some criteria. One of these characteristics is their extra- and perisynaptic location. By localizing outside the synapse they are in ideal position to sense ambient levels of GABA continuously present in the extracellular space and be less influenced by huge fluctuations of GABA concentrations that occur at the synaptic level (Wei et al. 2003). Other important property is their high affinity for GABA, conferring the ability to sense very low concentrations of ambient GABA that range from tens of nanomolar to a few micromolar (Lerma et al. 1986, Tossman et al. 1986, Attwell et al. 1993, Kennedy et al. 2002). There are also $GABA_A$Rs that can be activated even in the absence of any ligand and contributing to tonic currents (McCartney et al. 2007). A third important factor to be considered in tonic activation is $GABA_A$R slow desensitization (Bianchi et al. 2001), which reduces the period of ligand-bound closed state of the receptor (Farrant & Nusser 2005, Glykys & Mody 2007a).

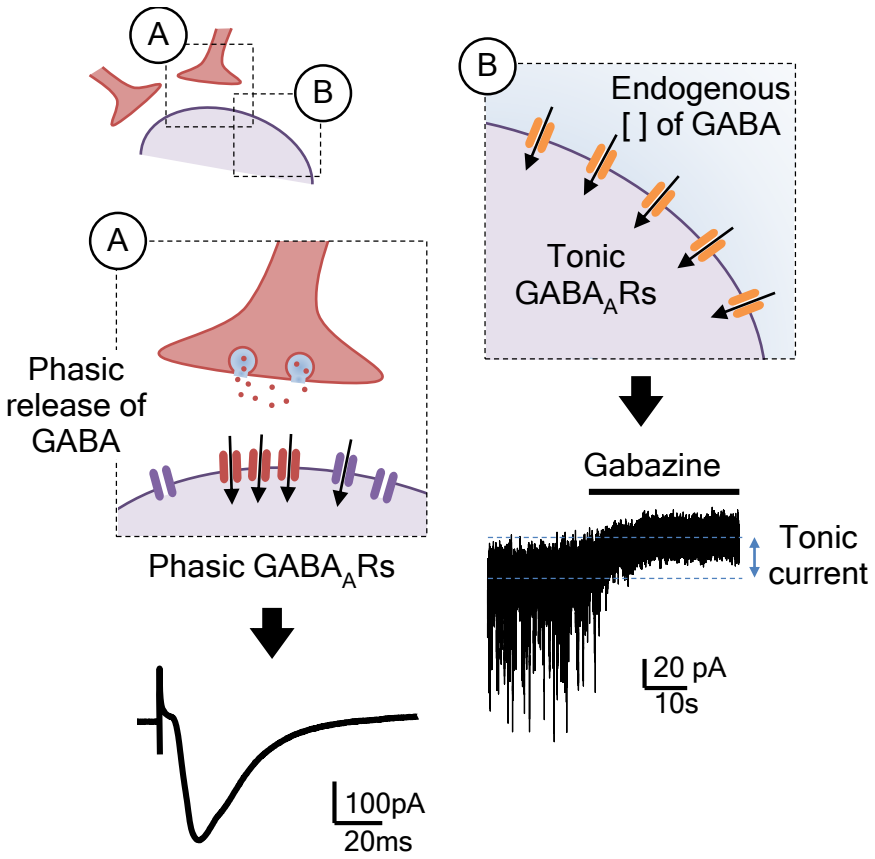

Figure 1.5. Phasic and tonic activation of $GABA_ARs$
GABAergic transmission is characterized by two forms of inhibition: (A) Phasic $GABA_AR$-mediated transmission; (B) Tonic $GABA_AR$ activation.
(A) Phasic responses result from spontaneous release of GABA-containing vesicle from the presynaptic terminal or action potential-mediated synchronized release of multiple vesicles that will activate postsynaptic $GABA_AR$ that are positioned inside the synapse, clustered beneath the releasing sites (red receptors). The transient increase in GABA concentration up to about 1.5 to 3.0 mM and consequent activation of synaptic $GABA_ARs$ will result in a fast and transient current that is called phasic-transmission. Synchronous release of GABA can promote neurotransmitter diffusion (spillover) and activation of receptors located perisynaptically (purple receptors). This will result in a larger and slower waveform IPSC that is still considered phasic transmission. A representative IPSC evoked by electrical stimulation is shown below.
(B) A low concentration of ambient GABA, which persists despite the activity of the neuronal and glial GABA transporters (GAT1 and GAT3), tonically activates high-affinity extrasynaptic receptors (orange receptors). The trace shows the 'noisy' tonic current that results from stochastic opening of these high-affinity $GABA_ARs$, with superimposed phasic currents (in this case, the synaptic events would be arising at sites not depicted in the schematic diagram, but already shown in A). A high concentration (10 μM) of the $GABA_AR$ antagonist gabazine (SR-95531) blocks the phasic IPSCs and tonic channel activity, causing a change in the 'holding' current and a reduction in current variance (see trace below) that corresponds to the tonic current. The currents shown in A and B are from whole-cell patch-clamp recordings (Vh = -70

mV) of CA1 pyramidal neurons in the continuous presence of glutamate receptor blockers (DL-AP5, 50μM and CNQX, 10μM). Both traces were recorded for the purpose of this thesis. Details on the procedure for its acquisition are described in Chapter 4.4.1.2, p76 and Chapter 4.4.1.4, p77. Original illustration, based on (Farrant & Nusser 2005).

These macroscopic properties of $GABA_AR$s depend strongly on their subunit composition. In fact, according to our current knowledge, the α_4, α_5, α_6 and δ subunits are the major candidates for $GABA_AR$ subunits with preferential extrasynaptic location. These receptors assemble with other subunits to form functional receptors composed by $\alpha_4\beta_3\delta$, $\alpha_5\beta_3\gamma_{2/3}$, $\alpha_6\beta_{2/3}\delta$ (McKernan & Whiting 1996). On the other hand, receptors containing the γ_2 subunit, responsible for incorporating the receptor at the synapse (Essrich et al. 1998, Wang et al. 1999), in association with α_1, α_2 or α_3 subunits, compose $\alpha_1\beta_{2/3}\gamma_2$, $\alpha_2\beta_{2/3}\gamma_2$ ad $\alpha_3\beta_{2/3}\gamma_2$ and are the predominant receptor subtypes mediating phasic synaptic transmission. Some exceptions, such as the $\alpha_5\beta_3\gamma_2$ subtype are predominantly responsible for tonic responses in CA1 pyramidal cells despite the presence of γ_2 subunit (Caraiscos et al. 2004a). In this case, the incorporation of the α_5 subunit seems to override the ability of the γ_2 subunit to promote synaptic localization (Brünig et al. 2002). The δ subunit-containing receptors seem to occur only extrasynaptically and its presence confers to $GABA_AR$s a increased sensitivity to the endogenous agonist GABA (measured by a reduction in EC_{50} value), when compared to γ_2-containing receptors (Fisher & Macdonald 1997, Brown et al. 2002). Also, αβδ receptors desensitize more slowly and less extensively than αβγ receptors (Haas & Macdonald 1999, Bianchi & Macdonald 2002), another important feature of receptors involved in a tonic form of transmission.Thus, the different biophysical properties of

the receptors together with their differential cell surface distributions contribute to their involvement in phasic and tonic signaling.

Another important aspect for tonic transmission is the source of ambient GABA, which can have different origins depending on the brain region, cell type or anatomy of the synapses. It has been suggested to originate from activity-dependent vesicular release of GABA that spills over from the synapse and escapes the existent reuptake mechanisms (Brickley et al. 2003). Non-vesicular sources also occur, including release from astrocytes (Kimelberg et al. 1990, Liu et al. 2000, Wang et al. 2002), reversed transport of GABA by its transporter (Attwell et al. 1993), non-vesicular GABA exocytosis (Rossi et al. 2003) and channel-mediated GABA release from glia (Lee et al. 2010a).

Experimentally, $GABA_AR$-mediated tonic transmission can be recorded by exogenously applying the $GABA_AR$ antagonists bicuculline or SR-95531 (gabazine) while monitoring the holding current required to voltage-clamp the cell at a given membrane potential. Blockage of $GABA_ARs$ will not only abolish miniature IPSCs (mIPSCs) that are involved in phasic transmission, but also will change neuron's input holding current that corresponds to $GABA_AR$-mediated tonic conductance. This is accompanied by a reduction of current variance associated with decreased number of open channels (Glykys & Mody 2007b).

1.2.4 Functional role of phasic and tonic transmission

There are clear physiological differences between phasic and tonic neurotransmission, albeit the fact that both control neuronal

excitability. In the adult CNS, phasic inhibition is mainly involved in suppressing principal glutamatergic cells and preventing over-excitation of neurons. Besides this classical role of synaptic GABA transmission, fast and precisely timed phasic responses mediated by GABA-releasing interneurons have other important and complex functions in neuronal communication. These include a key role in feedback and feedforward inhibition of principal cells with consequent synchronization of population activity and induction and maintenance of rhythmic network oscillations (e.g. gamma and theta frequency oscillations). Different types of cortical interneurons (already described above, see Chapter 1.1.2, p12) have distinct neuronal targets and distinct temporal precision of their IPSC (Spruston et al. 1995, Miles et al. 1996, Pouille & Scanziani 2001, Somogyi & Klausberger 2005) contributing in this way to variations in the network oscillatory behavior (Cobb et al. 1995, Jonas 2004, Somogyi & Klausberger 2005).

Tonic transmission, on the other hand, acts on a much larger time window when compared to phasic responses. A persistent increase in GABA input conductance in a particular neuron will significantly contribute to a phenomena called “shunting effect” (see chapter 1.2, p16 and Figure 1.4, p20) (Semyanov et al. 2004). This effect will result in a shift in neuronal input-output relationship and decrease in neuronal excitability (Brickley et al. 1996, Holt & Koch 1997, Mitchell & Silver 2003). The physiological significance of this shift is that the same excitatory input current arriving to a neuron (e.g. glutamatergic input) will lead to a decrease in the output firing rate of the same neuron and a decrease in its excitability. Also, there will be a reduction in the duration of the depolarizing voltage change that is induced by this excitatory input

current. The consequence will be that the temporal fidelity of the excitatory input will be narrowed, and there will be a decrease in the overall gain of the neuronal input-output (Chance et al. 2002, Mitchell & Silver 2003). One important aspect to bear in mind is that although tonic conductances are considered a constant and uninterrupted form of GABA transmission, changes in the concentration of ambient GABA or in the number and properties of extrasynaptic $GABA_AR$s can occur and contribute to change the magnitude of tonic transmission and consequently control and fine-tune neuronal excitability (Mody & Pearce 2004).

Because tonic and phasic inhibition display distinct functional roles in GABA-mediated actions, selectively modulating these different forms of inhibition also affect the network excitability differently.

1.3 Neuromodulation

According to Krames, neuromodulation emcompasses a huge area of knowledge that considers all “technologies that have an impact on neuronal interfaces” (Krames et al. 2009). This broad definition includes many fields of science, from medicine to bioengineering, that develop strategies and therapies to improve quality of life of humans by means of altering the function and performance of the nervous system.

In this thesis a much narrow definition of neuromodulation is used. Neuromodulation is herein considered only at the cellular level, as any alteration of the electrical or chemical properties of neurons as a consequence of synaptic changes and/or endogenous/exogenous drug action (Kaczmarek & Levitan 1987).

Defined this way, neuromodulation encompasses most changes that continuously occur during physiological functioning of neurons as well as in pathological situations. A neuromodulator is thus defined as any molecule that, although not directly involved in neuronal communication (as neurotransmitters are) can alter and influence electrical and chemical neuronal activity. One such neuromodulator of the CNS is adenosine (Dunwiddie & Masino 2001, Sebastião & Ribeiro 2009).

1.3.1 Adenosine

Adenosine is a naturally occurring purine nucleoside which plays modulatory roles in a variety of tissues and physiological circumstances. The first suggestion that adenosine and its precursor, adenosine 5´-triphosphate (ATP), might have physiological actions was advanced more than 80 years ago by Drury and Szent-Györgyi in heart and coronary blood vessels (Drury & Szent-Györgyi 1929). Central actions of purines were demonstrated only 40 years later with the findings that micro-iontophoretic application of adenosine and ATP directly into neurons induced biochemical and electrophysiological alterations (Phillis et al. 1974). This may have been indeed the first evidence of a neuromodulatory action of adenosine in the CNS. ATP, but not adenosine, can also behave as a neurotransmitter (Burnstock 1972, 2006) being classically stored and released from vesicles in nerve terminals (usually as a cotransmitter) and exerts its actions through specific ATP receptors - P2 receptors (Burnstock 1978, Ralevic & Burnstock 1998). Inactivation of ATP results from breakdown to adenosine by a cascade of ecto-enzymes

(Richardson et al. 1987, Terrian et al. 1989, White & MacDonald 1990, Zimmermann et al. 2012).

As a neuromodulatory substance, adenosine can influence neurotransmission by acting directly onto neurons, either pre-, post- or peri/extra-synaptically, or onto non-neuron cells by influencing glia function. Regulatory targets include neurotransmitter release machinery, ionotropic or metabotropic receptors, neuronal and glia transporters or control of function of other neuronal modulators (Ribeiro & Sebastião 2010) (Figure 1.6).

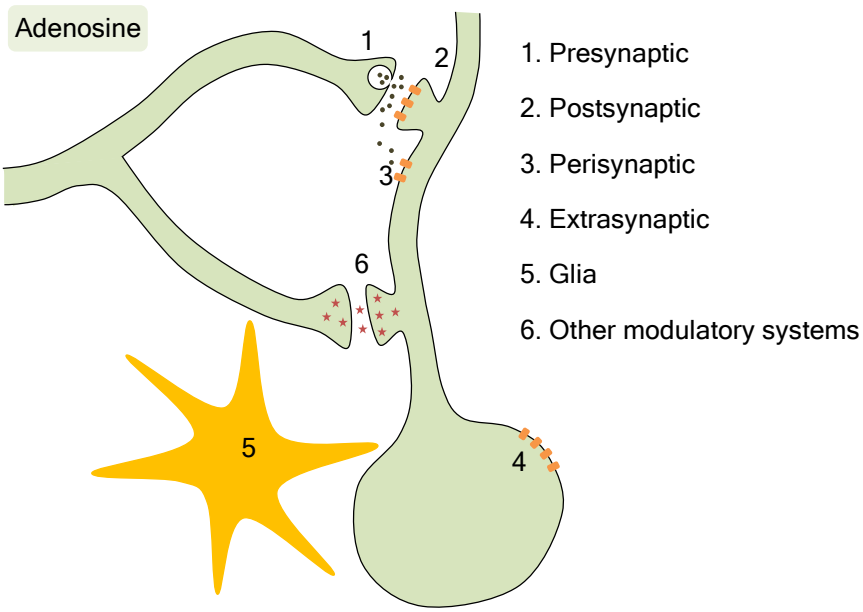

Figure 1.6. Adenosine modulation sites
Different sites of adenosine modulatory influence on neuronal communication are outline. These include presynaptic (1), postsynaptic (2) and peri- and extrasynaptic (3, 4) effects as well as interaction with glia cells (5) and other modulatory systems (6) (namely, cannabinoid, VIP, ATP, BDNF or dopamine receptor actions). Excitatory synaptic connections of hippocampal CA1 pyramidal cells are taken as a representative neuronal model to indicate the sites of relevant adenosine actions. Original drawing, based on (Schubert et al. 1995). ATP: adenosine 5'-triphosphate; BDNF: brain derived neurotrophic factor; VIP: vasointestinal peptide.

To exert its actions, adenosine must be released to the extracellular space. The classical view is that there are two major sources of extracellular adenosine: extracellular production from hydrolysis of adenine nucleotides and transport to the extracellular space from intracellular adenosine sources (Figure 1.7).

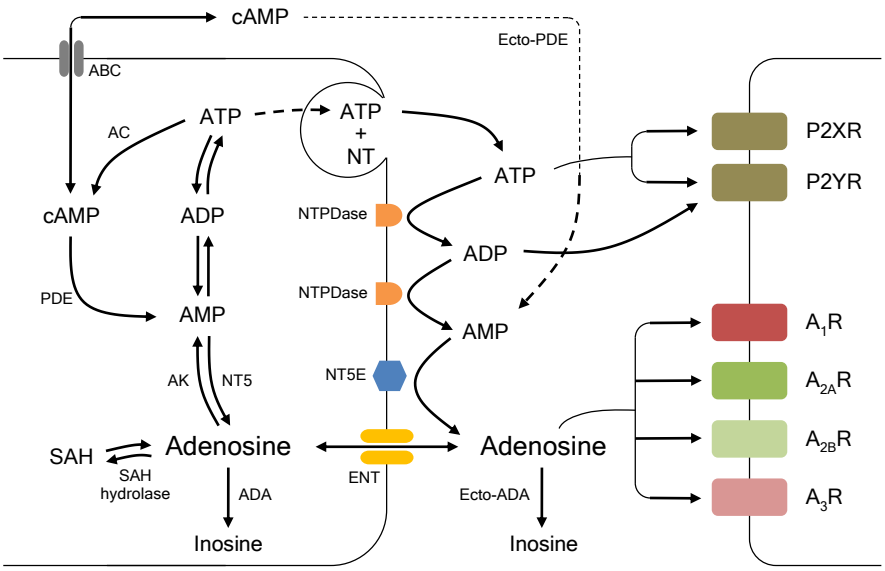

Figure 1.7. Schematic representation of adenosine metabolism and receptors
Adenosine can be synthesized intracellularly by the dephosphorylation of adenosine 5'-phosphates (ATP, ADP or AMP) by 5'-nucleotidases or by hydrolysis of SAH. Adenosine can also be generated extracellularly from rapid hydrolysis of nucleotides catalyzed by ecto-nucleotidases or from extracellular transport of cAMP. Extracellular adenosine concentrations are regulated by bi-directional transport through ENT. Once in the extracellular space, adenosine acts through four types of P1Rs - the high-affinity A_1R and $A_{2A}R$ and low-affinity $A_{2B}R$ and A_3R. ATP and ADP exert their actions through P2Rs - ionotropic P2XR and metabotropic P2YR. Elimination of adenosine occurs intracellularly through phosphorylation to AMP by AK and intra- or extracellularly by degradation to inosine by local ADA.
ABC: ATP-binding cassete transporter; AC: adenylate cyclase; ADA: adenosine deaminase; ADP: adenosine 5′-diphosphate; AK: adenosine kinase; AMP: adenosine 5′-monophosphate; ATP: adenosine 5′-triphosphate; cAMP: cyclic AMP; ENT: equilibrative nucleoside transporter; NT5: cytosolic 5'-nucleotidase; NT5E: ecto-5′-nucleotidase; NTPDase: ecto-nucleoside triphosphate diphosphohydrolase; PDE: phosphodiesterase; SAH: S-adenosyl-L-homocysteine.

The former mechanism is possibly the major contributor of external adenosine concentration in physiological conditions (Cunha et al. 1996c, Koizumi et al. 2003, Newman 2003, Pascual

et al. 2005). Released ATP is converted into adenosine through a cascade of ecto-enzymes that include a two-step reaction: (1) conversion of ATP and adenosine 5′-diphosphate (ADP) to adenosine 5′-monophosphate (AMP) by ecto-nucleoside triphosphate diphosphohydrolase (NTPDase); (2) hydrolysis of AMP to adenosine by ecto-5′-nucleotidase (NT5E) (Zimmermann et al. 1986, Richardson & Brown 1987, Richardson et al. 1987, Terrian et al. 1989). Extracellular transport of cyclic AMP (cAMP) (Rosenberg & Dichter 1989) can also contribute (although in a minor extent) to extracellular formation of adenosine through phosphodiesterase activity (Brundege et al. 1997). The second mechanism to generate extracellular adenosine involves passive adenosine transporters through equilibrative nucleoside transporter (ENT) that equilibrate its concentration across the cell membrane (Kong et al. 2004, King et al. 2006). In basal conditions, intracellular concentration of adenosine is relatively low compared to the extracellular space, so net flux through these transporters is inwardly directed. Indeed, in basal conditions, the intracellular concentration of adenosine is estimated to be less than 50 nM, whereas the extracellular synaptic concentration of adenosine range from 25 to 250 nM (Ballarín et al. 1991, Dunwiddie & Diao 1994) with small variations in-between brain regions (Delaney & Geiger 1996). However, in many circumstances such as hypoxia, ischemia or intense neuronal activity, intracellular adenosine concentration may increase to levels that outweigh the extracellular levels leading to reverse transport of adenosine and conferring an additional source of the nucleoside (Jonzon & Fredholm 1985, Lloyd et al. 1993, Frenguelli et al. 2007, Martín et al. 2007, Lovatt et al. 2012). This occurs because in metabolic

demanding situations, energy requirements increase and intracellular ATP concentrations suffer minor oscillations. Small changes in steady-state ATP levels lead to several fold increase in intracellular adenosine levels in a reaction that is controlled by the equilibrium between the activity of cytosolic 5'-nucleotidase (NT5) (Montero & Fes 1982, Kroll et al. 1993) and adenosine kinase (AK) (Caputto 1951, Newby 1985, Park & Gupta 2008). There are one other source of intracellular adenosine: hydrolysis of S-adenosy-L-homocysteine (SAH) by SAH hydrolase (SAHH) (De La Haba & Cantoni 1959, Palmer & Abeles 1979, Schrader et al. 1981). Adenosine degradation occurs through adenosine deaminase (ADA) activity that converts adenosine into its inactive metabolite, inosine (Dunwiddie & Hoffer 1980). ADA activity, although with an important function in stressful conditions like hypoxia or ischemia (Lloyd & Fredholm 1995, Barankiewicz et al. 1997), has little or no influence in basal conditions (Pak et al. 1994, Zhu & Krnjević 1994) where adenosine reuptake assumes the prominent role (Dunwiddie & Diao 1994).

1.3.1.1 Adenosine receptors

Once released, adenosine can act through four different types of G protein-coupled receptors (GPCRs) from the P1 receptor family, namely the high affinity A_1 and A_{2A} receptors (A_1R, $A_{2A}R$, respectively) and low affinity A_{2B} and A_3 receptors ($A_{2B}R$, A_3R, respectively) (Fredholm et al. 2001, 2011) (see Table 1.1 and Figure 1.8). Early pharmacological evidence for the existence of adenosine receptors was provided by the ability of methylxanthines to block the effect of adenosine on accumulation

of cAMP in brain slices (Sattin & Rall 1970). However, only some years later Burnstock first proposed the existence of a separate family of adenosine-selective receptors called P1-receptors, clearly differencing them from P2-receptors that recognized ATP and ADP (Burnstock 1978). Later work by van Calker and co-workers identified two subforms of adenosine receptors (the terms "adenosine receptor" and "P1 receptor" are synonymous) – the A_1R and the A_2R (van Calker et al. 1979). Careful pharmacological experiments revealed that adenosine was able to either inhibit, via A_1R, or stimulate, via A_2R, adenylate cyclase (AC) activity and accumulation of cAMP in cultured mouse brain cells (van Calker et al. 1979, Londos et al. 1980). The A_2R was further subdivided into two distinct forms based on the recognition that increased levels of cAMP were achieved through activation of a high-affinity receptor in striatal membranes (later named $A_{2A}R$) and a low affinity receptor ubiquitously present throughout the brain (the $A_{2B}R$) (Daly et al. 1983, Bruns et al. 1986). The existence of a fourth type of adenosine receptor, the A_3R, was proposed in the 80s by several independent groups (Phillis & Wu 1981, Stone 1985, Ribeiro & Sebastião 1986) but only identified and cloned in early 90s from rat testis (Meyerhof et al. 1991) and striatum (Zhou et al. 1992). By now these four receptors have been already cloned in a variety of species, including Human (Olah & Stiles 1995).

Table 1.1. Adenosine Receptors in CNS

Receptor Type	A_1R	$A_{2A}R$	$A_{2B}R$	A_3R
Adenosine Affinity	70 nM	150 nM	5100 nM	6500 nM
G-protein coupling	G_i and G_0	G_s and G_{olf}	G_s	G_{i3} and G_q
Transduction Mechanisms	Inhibits AC; Inhibits Ca^{2+} channels; Activates GIRKs; Activates PLC;	Activates AC; Activates Ca^{2+} channels; Inhibits Ca^{2+} channels;	Activates AC; Activates PLC;	Inhibits AC; Activates PLC; Increases intracellular Ca^{2+};
Physiological Actions	Inhibits synaptic transmission; Hyperpolarizes neurons;	Facilitates transmitter release; Inhibits transmitter release;	Increases cAMP in brain slices; Modulation of Ca^{2+} channel function;	Inhibits A_1R-mediated responses(1); Inhibits mGluR-mediated responses(2);
High Abundance	Hippocampus; Neocortex; Cerebellum; Spinal cord;	Striatum; Olfatpry bulb;	-	-
Medium/Low Abundance	Amygdala; Olfatory bulb; Striatum; Thalamus; Substancia nigra;	Hippocampus; Neocortex; Thalamus;	Uniform low level of expression;	Hippocampus; Cerebellum;

AC: adenylate cyclase; GIRKs: G-protein-dependent inwardly rectifying K^+ channels; mGluR: metabotropic glutamate receptor; PLC: phospholipase C. (1) Dunwiddie et al. 1997; (2) Macek et al. 1998; Adapted from Dunwiddie & Masino 2001, Boison 2005.

Adenosine receptors are seven transmembrane domain receptors linked to a variety of transduction mechanisms (see Figure 1.8 for details on signaling pathways).

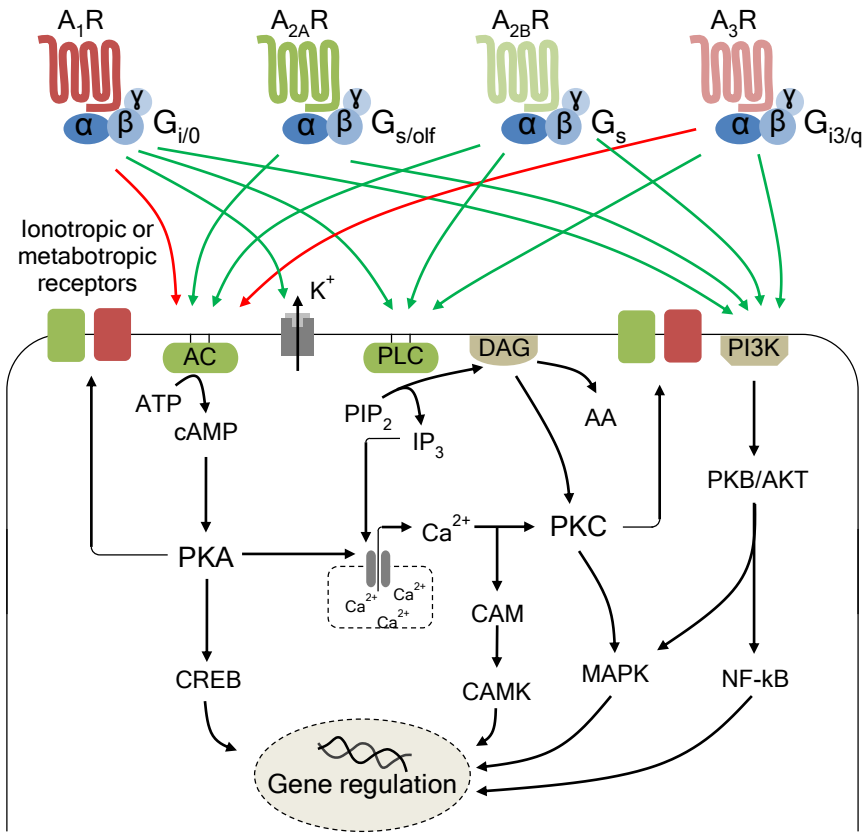

Figure 1.8. Adenosine receptors and classical signaling pathways
Adenosine A_1R and A_3R are coupled to pertussis-sensitive $G_{i/0}$ proteins inhibiting the activity of AC (via G_α subunit) and increasing the activity of PLC (via $G_{\beta\gamma}$ subunits). The A_1R also activates inwardly rectifying K^+ channels. Activation of the $A_{2A}R$ and $A_{2B}R$ increases AC activity through activation of G_s proteins. $A_{2B}R$ is also positively coupled to PLC via $G_{\beta\gamma}$ subunits. All four subtypes of adenosine receptors induce the activation of PI3K that may result in activation of NF-kB and MAPK, giving them a role in cell growth, survival, death and differentiation.
AA: arachidonic acid; AC: adenylate cyclase; ATP: adenosine 5´-triphosphate; Ca^{2+}: calcium ion; CAM: Ca^{2+}/calmodulin-dependent protein; CAMK: CAM kinase; cAMP: cyclic adenosine 5′-monophosphate; CREB: cAMP response element binding protein; DAG: diacylglycerol; IP_3: inositol 1,4,5-trisphosphate; K+: potassium ion; MAPK: mitogen-activated protein kinase; NF-kB: nuclear factor-κB; PI3K: phosphatidylinositol 3-kinase; PIP_2: phosphatidylinositol-4,5-bisphosphate; PKA: protein kinase A; PKB/AKT: protein kinase B; PKC: protein kinase C; PLC: phospholipase C; green arrow: activate; red arrow: inhibit.

Classically, A_1R and A_3R are preferably coupled to G_i or G_0 proteins inhibiting AC, while $A_{2A}R$ and $A_{2B}R$ are most frequently coupled to G_s proteins, promoting AC activity (Table 1.1). As mentioned before, A_1R and $A_{2A}R$ display high affinity for adenosine, suggesting that basal purinergic concentrations occurring in brain tissue are capable of activating these receptors. On the other hand, $A_{2B}R$ and A_3R are low affinity receptors with increased relevance in pathophysiological conditions, when adenosine levels also tend to increase. Noteworthy, A_3Rs display high affinity for adenosine in humans, unlike what occurs in the rat (Fredholm et al. 2001).

The A_1R is widely distributed in CNS with prominent abundance in the hippocampus, cerebral cortex, cerebellum and dorsal horn of spinal cord (Goodman & Synder 1982, Mahan et al. 1991, Reppert et al. 1991) (Table 1.1). It can be found heterogeneously expressed within neurons in the pre- and postsynaptic density (Rebola et al. 2003) as well as in non-neuronal cells such as astrocytes (Biber et al. 1997), microglia (Gebicke-Haerter et al. 1996) and oligodendrocytes (Othman et al. 2003). Neuronal actions involve the inhibition of synaptic transmission and excitability at pre-, post- and extrasynaptic sites. Presynaptically, A_1R decrease neurotransmitter release (Fredholm & Dunwiddie 1988) through G-protein–coupled inhibition of voltage-dependent Ca^{2+} channels (VDCCs) (MacDonald et al. 1986, Schubert et al. 1986, Wu & Saggau 1994, Ribeiro 1995) or through inhibition of Ca^{2+}-independent spontaneous release of neurotransmitter (Scanziani et al. 1992). Postsynaptically at proximal dendrites and in the cell body, activation of A_1R induces G-protein–dependent activation of inwardly rectifying K^+ channels (GIRKs) (Segal 1982,

Greene & Haas 1985, Trussell & Jackson 1985, Gerber et al. 1989) that regulate local depolarization of neurons through hyperpolarization (Ponce et al. 1996, Ehrengruber et al. 1997) and control burst-like activity in CNS (Dragunow 1988). Moreover, adenosine A_1R restrain activity-evoked neuronal Ca^{2+} influx mediated by postsynaptic VDCCs (Schubert 1988, Mogul et al. 1993, Klishin et al. 1995a) and N-methyl-D-aspartate receptors (NMDARs) (Schubert & Mager 1991, Canhão et al. 1994, de Mendonça et al. 1995, Klishin et al. 1995b). These neuromodulatory A_1R actions result in a reduction of neuronal excitability and constitute an important neuroprotective role of adenosine during excitotoxic events such as hypoxia/ischemia or increased neuronal firing (de Mendonça et al. 2000). Anatomical studies have shown that A_1Rs are also present in interneurons from hippocampal *stratum oriens* and *stratum radiatum*, suggesting that adenosine may also have an important role in controlling interneurons (Rivkees et al. 1995, Ochiishi et al. 1999). A_1Rs have been implicated in sedative, anticonvulsant, anxiolytic and locomotor depressant effects with potential therapeutic application (Jacobson & Gao 2006).

Regarding the $A_{2A}R$, it is highly enriched in the enkephalin-containing striatopallidal GABAergic neurons and olfactory bulb (Schiffmann et al. 1991, Fink et al. 1992, Svenningsson et al. 1997), and found at much lower levels in the hippocampus, neocortex and thalamus (Cunha et al. 1996b, Dixon et al. 1996, Svenningsson et al. 1997) (see Table 1.1). Like A_1R, $A_{2A}R$ can also be found in astrocytes (Li et al. 2001, Nishizaki et al. 2002) and microglia (Küst et al. 1999). Neuromodulatory actions of $A_{2A}R$ include modulation of neuronal excitability by facilitating synaptic

transmission (Sebastião & Ribeiro 1992, Cunha et al. 1994a, Dias et al. 2012), regulation of resting membrane properties (Ameri & Jurna 1991, Barajas-Lopez et al. 1991, Li & Henry 1998), synaptic plasticity (Sekino et al. 1991, de Mendonça & Ribeiro 1994, Dias et al. 2012) and neurotransmitter release, including acetylcholine (Cunha et al. 1994b, Jin & Fredholm 1997), glutamate (Okada et al. 1992, Cunha et al. 1994a, Ambrósio et al. 1997) and GABA (O'Regan et al. 1992, Mayfield et al. 1993, Gubitz et al. 1996, Cunha & Ribeiro 2000a, Brooke et al. 2004).

An important aspect to comprehend the neuromodulatory actions of adenosine in the brain is the understanding of how adenosine "chooses" between the two high-affinity receptors since A_1R and $A_{2A}R$ can coexist in the same nerve terminal with opposite effects (Correia-de-Sá et al. 1991). The explanation is believed to rely on the different localization of A_1R and $A_{2A}R$ in relation to adenosine release sites, to the location of NT5E that converts adenine nucleotides into adenosine and/or the intensity of neuronal activity at a particular moment (Sebastião & Ribeiro 2000). Indeed, during low frequency neuronal firing, the amount of ATP released into synapses is low (Wieraszko et al. 1989, Pedata et al. 1990) and the adenosinergic tonus result predominantly from basal concentrations of adenosine occurring extrasynaptically, that are insufficient to trigger $A_{2A}R$ actions but preferentially activate A_1Rs (Correia-de-Sá et al. 1996). In these conditions, tonic adenosine A_1R-mediated refraining of neuronal excitability and neuroprotection predominate (Cunha et al. 1996a). On the other hand, burst-like formation of adenosine from released ATP (Wieraszko et al. 1989, Cunha et al. 1996c) will preferentially activate $A_{2A}Rs$ (Correia-de-Sá et al. 1996, Cunha et al. 1996a).

Indeed, there is a non-linear relation between neuronal activity and adenine nucleotide release (namely, ATP). Adenosine formed during intense neuronal firing from ATP degradation by ecto-enzymes will favor $A_{2A}R$ actions. In these conditions besides direct $A_{2A}R$ influence on synaptic transmission, A_1R responses will also be attenuated by two $A_{2A}R$-dependent mechanisms: $A_{2A}Rs$ will enhance inward-directed adenosine transport through ENT, decreasing the availability of adenosine for A_1Rs (Pinto-Duarte et al. 2005); there will be a cross-talk between $A_{2A}R$ and A_1R leading to decreased affinity of A_1R to its ligand (Cunha et al. 1994a, Lopes et al. 1999).

Many examples of interactions between adenosine and other receptor systems can be found in the CNS. In fact, adenosine can be also considered an important metamodulator, or in other words, a modulator of the modulators (Sebastião & Ribeiro 2000). This is exemplified by A_1R and $A_{2A}R$ interactions with calcitonin gene-related peptide (CGRP) that results in facilitation synaptic efficiency in the hippocampus (Sebastião et al. 2000); $A_{2A}R$-dependent brain-derived neurotrophic factor (BDNF)-actions in hippocampal preparations (Diógenes et al. 2004); formation of several oligomeric forms with other receptors such as $A_1R/P2Y_1R$ (Yoshioka et al. 2002), A_1R/mGluR1 (Ciruela et al. 2001), $A_{2A}R$/mGluR5 (Ferré et al. 2002), $A_{2A}R$-Cannabinoid receptor type 1 (CB_1R) (Carriba et al. 2007), apart from the more explored interactions with dopamine receptors (DRs), the A_1R/D_1R and $A_{2A}R/D_2R$ interactions (Ferré et al. 1997), and the $A_1R/A_{2A}R$ heterodimers (Ciruela et al. 2006, Cristóvão-Ferreira et al. 2013). All these interactions, and many others not detailed here

(Sebastião & Ribeiro 2009), increase exponentially the potential of adenosine as a regulator of brain function.

1.3.1.2 Modulation of hippocampal GABA transmission

Opposite to what is known for hippocampal glutamatergic transmission, modulation of GABAergic transmission by adenosine is much less explored. This is even more evident if considering only $A_{2A}R$ actions on GABA-mediated communication. In fact, the first indirect evidence for $A_{2A}R$ control of inhibition came from a study in cortical neurons showing a depressant effect of $A_{2A}R$ on neuronal firing that was mediated by increased GABAergic inhibition (Phillis 1998). Later was shown that $A_{2A}R$ but not A_1R could enhance the evoked release of GABA from hippocampal nerve terminals (Cunha & Ribeiro 2000a). Besides presynaptic modulation, there is evidence for a postsynaptic control by $A_{2A}Rs$ of human epileptic inhibitory currents, that seem to prevent $GABA_AR$ run-down and desensitization (Roseti et al. 2008, 2009). These studies, although indicative of the contribution of $A_{2A}Rs$ in the control of GABA responses, lack the specificity and selectivity necessary for a complete understanding of inhibitory network operations. In fact, as detailed in Chapter 1.1.2, p12, GABA-releasing neurons are an extremely heterogeneous population with different anatomical, biochemical and physiological characteristics and distinct modes of operation. A careful examination of $A_{2A}R$ effects on different neuronal populations and subcellular locations is necessary for a full comprehension of its actions. This should reveal even more

relevance in pathological conditions and during altered neuronal communication.

Regarding A_1Rs, there is convincing and widely accepted evidence for a lack of effect on hippocampal phasic GABAergic transmission (Dolphin & Archer 1983, Burke & Nadler 1988, Kamiya 1991, Lambert & Teyler 1991, Yoon & Rothman 1991, Cunha & Ribeiro 2000a). This is not the case, however, for early hippocampal developmental stages, a period when A_1R activation is associated with a reduction of depolarizing GABA release (Jeong et al. 2003, Kirmse et al. 2008) (see Chapter 1.2, p16 for details on depolarizing GABA responses). This regulatory mechanism of A_1R is consistent with the neuroprotective actions of adenosine in the adult brain and may confer an important developmental control of excitation during neuronal maturation. Despite the absence of direct A_1R modulation on phasic GABA communication in adult hippocampus, adenosine can influence other receptor systems commonly associated with the control of GABA responses. Two examples are: the influence of adenosine A_1Rs on cannabinoid CB_1R-mediated control of GABA release, a phenomena with important functional implications for spatial memory (Sousa et al. 2011); the enhancement of GABA release caused by vasoactive intestinal peptide (VIP) in hippocampal nerve terminals that is dependent on tonic A_1R actions (Cunha-Reis et al. 2008). These two mechanisms further reinforce the idea that high affinity adenosine receptors are important fine tuners of neuronal activity able to modulate the action of other neuromodulators.

2 Aim

Considering the relevance of GABAergic transmission for the control of hippocampal function and the lack of detailed knowledge on the neuromodulatory actions of adenosine in the GABAergic system, the overall aim of this thesis was to evaluate the influence of high affinity adenosine receptors upon inhibitory neuronal communication at the hippocampus and its impact on the control of epileptiform discharges (Figure 2.1).

To accomplish this, the following objectives were pursued:

- Evaluate the actions of A_1Rs on phasic and tonic GABAergic transmission expressed directly onto pyramidal cells and onto anatomical/biochemical identified interneurons.
- Comprehend whether A_{2A}R-mediated effect upon hippocampal excitability is influenced by modulatory actions on inhibitory interneurons and assess its mechanisms.
- Understand the consequences of a putative modulatory role of A_{2A}Rs for the control of spontaneous epileptiform pyramidal cell discharge in hyperexcitable conditions.

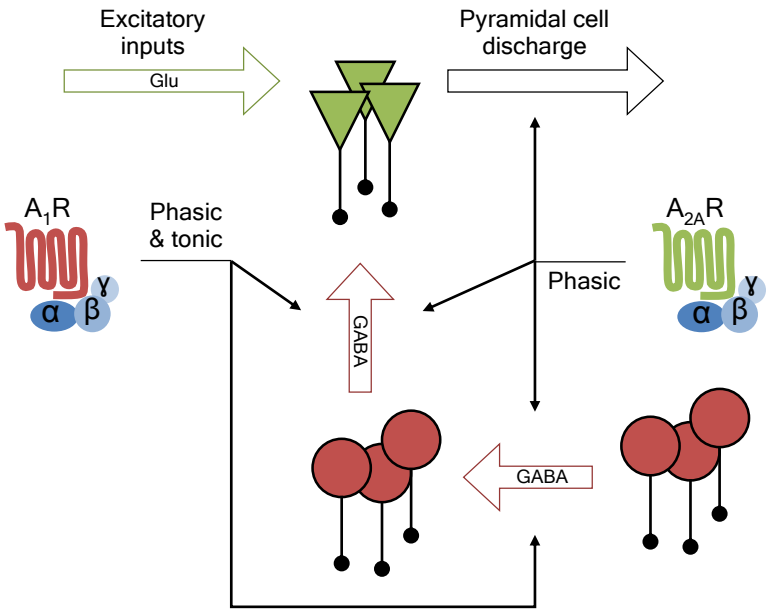

Figure 2.1. Schematic representation of the context and main targets of this study. Pyramidal cells from CA1 region of the hippocampus receive their major input signal from excitatory CA3 pyramidal cell fibers. The output corresponds to CA1 pyramidal cell discharge that mainly propagates to the subiculum (see Chapter 1.1.1, p9 for details). A diverse population of interneurons project inhibitory GABAergic inputs to pyramidal cells, restraining their excitability. A restrict balance between excitatory and inhibitory projections to pyramidal cells will regulate cellular excitability and control neuronal discharge. The main purpose of this thesis was to evaluate how adenosine, an ubiquitous neuromodulator of the CNS, regulate phasic and tonic forms of GABAergic inhibition into both pyramidal cells and interneurons and evaluate its implications for pyramidal cell excitability. Green triangles represent CA1 pyramidal cells; red circles represent interneurons; glu: glutamate;

3 Techniques

The main goal of this section is to provide the reader with fundamental information associated with some of the techniques used in this thesis, which are important for a complete comprehension of the results. It mostly has an educational purpose for students not familiarized with the methodologies performed. It will mostly focus on basic electrophysiological concepts and the principles behind optogenetic technology.

3.1 Patch-clamp recordings

Until the late 70s, the measurement of current flow through ion channels of excitable membranes was carried out with intracellular electrode under voltage-clamp recording conditions, a technique developed by Kenneth Cole and George Marmont (Cole 1949, Marmont 1949) but adopted by Alan Hodgkin and Andrew Huxley for their famous work concerning the ionic mechanisms involved in action potential initiation and propagation (Hodgkin & Huxley 1952a,b–d; Hodgkin et al. 1952). During the 70s, Erwin Neher and Bert Sakmann revolutionized the study in neurobiology with the development of the patch-clamp technique, permitting the characterization of the elemental currents that flow when a single ion channel undergoes a transition from a closed to an open conformation (Neher & Sakmann 1976). This technical advance had two major consequences: (1) the patch-clamping could be applied to cells as small as 2-5 µm in diameter (compared to the 50 µm cells needed for intracellular recordings); (2) allowed

the study of biophysical properties of neuronal and nonneuronal cells.

In its early form, the resolution of patch-clamp technique was limited by the relatively low (≈50MΩ) resistances that isolated the interior of the pipette from the bath, leading to a high background electrical noise due to current leaks. This was only resolved in 1981 when Neher, Sakmann, Sigworth, Marty and Hamill (Hamill et al. 1981) developed a high resistance (giga-ohm; GΩ) seal (named “gigaseal”) between the highly cleaned micropipette tips and the smooth surface of the cell membranes, by applying a gentle suction to the pipette interior. This high resistance seal ensured that almost all of the current from the membrane patch flows into the pipette. When in gigaseal cell-attached mode, it was found that the patch of membrane under the pipette tip could be removed, and once this had happened a direct electrical contact with the cell interior could be achieved. As a result, the voltage across the entire cell membrane could be clamped. This is how the technique came to be known as the whole-cell voltage-clamp mode. Many variations to this technique were elaborated afterword. For example, by gently pulling the membrane patch attached to the pipette off the cell in cell-attached or whole-cell configurations, it was possible to study its trapped ion channels and obtain inside-out and outside-out configurations, respectively. In inside-out patch, the intracellular side of the membrane patch is facing the external solution while in outside-out configuration, the same intracellular portion is facing the solution inside the electrode. A resume of the procedure to establish cell-attached mode and whole-cell configuration is shown and explained in Figure 3.1.

Once in whole-cell configuration, the neuron can be voltage or current-clamped. Within minutes after establishing whole-cell and gaining access to the interior of the cell there will be perfusion of the pipette content into the cytosolic compartment (Fenwick et al. 1982). This implicates that the reading of the real membrane potential of the cell (in current-clamp mode, I = 0 pA) should be obtained immediately after rupturing the cell membrane. The perfusion of intracellular solution into the interior of the neuron has the advantage of being able to manipulate the internal milieu of the cell. By changing the concentration of specific ions in the internal solution and by controlling the membrane potential at which the cells are clamped during the recording we are able to isolate currents mediated by a particular receptors of interest (see Figure 3.3). Also, drugs can be added directly into the cell through recording electrode to study intracellular signaling cascades. However, there are biological phenomena that involve protein synthesis that may be affected by internal dilution that occurs in this configuration.

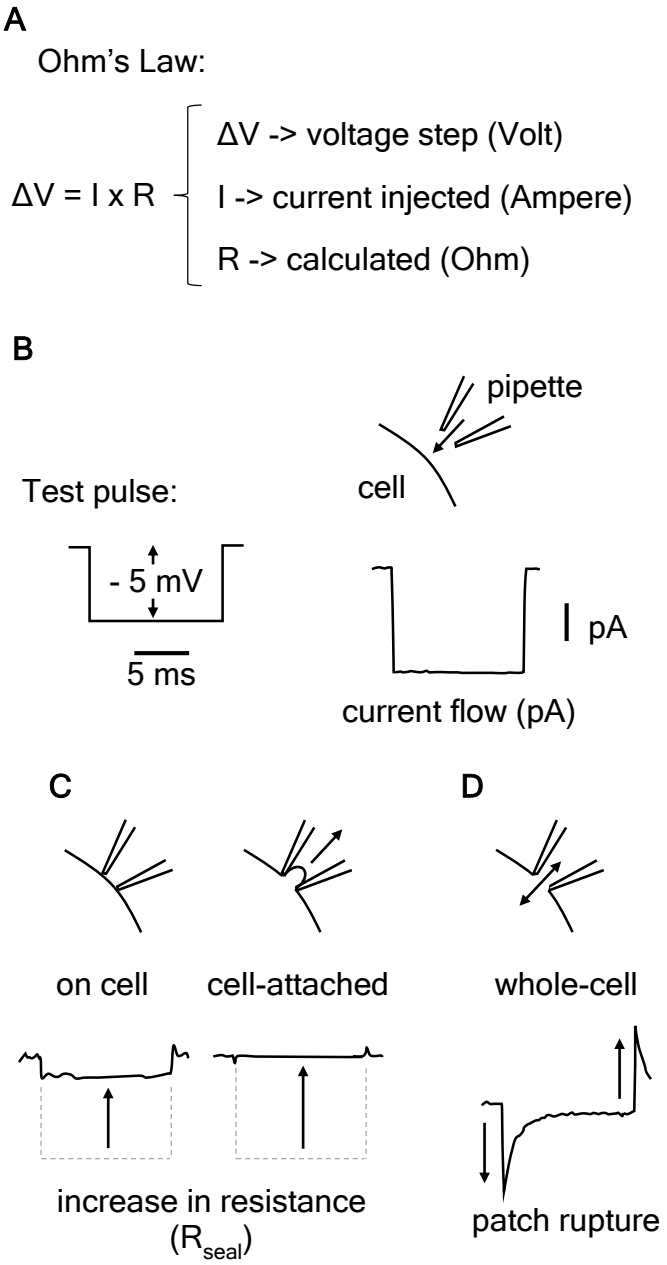

Figure 3.1. Oscilloscope traces obtained in response to constant test pulses for establishment of whole-cell recording

(A) According to Ohm's law, the electric potential difference between two points on a circuit (ΔV) is equivalent to the product of the current between those two points (I) and the total resistance of all electrical devices present between those two points (R). ΔV corresponds to the square voltage step delivered through the recording electrode, in units of volts (V); I is the measured current injected into the cell to induce ΔV, in units of amperes (A); R is the total resistance across the patch electrode tip, in units of ohms (Ω).

(B) During electrode placement, current injected through the electrode is monitored and the pipette resistance is calculated continuously by applying a small voltage pulse (-5 mV, 10 ms). While the electrode is in the bath and not in direct contact with the cell, the resistance is very low, (corresponding to the electrode resistance, usually around 4-9 MΩ) and the test pulse current is large (around -500 pA).
(C) The size of the current change produced by the test pulse goes down as the resistance across the patch electrode tip goes up. Thus, a reduction in test-pulse current indicates closer contact between the electrode tip and the cell (increase in seal resistance (R_{seal})). Once contact is made with the cell, electrode resistance spontaneously increases and application of gentle suction to the electrode, by mouth or a small syringe, quickly results in the formation of a gigaseal (cell attached mode). At this point, seal quality can be improved by changing the amplifier to voltage-clamp mode and applying a negative holding potential to the pipette until reaching the holding current that will be used during the recording (Vh = – 70 mV).
(D) Whole-cell configuration is achieved with brief pulses of suction that will rupture the membrane patch under the electrode, leaving the seal and the cell intact. This will result in a low-resistance access to the cell and in the appearance of large capacity transient arising from the added membrane capacitance.

All patch-clamp recordings reported in this thesis were performed in voltage-clamp mode, thus, details on the principles involved in voltage-clamping are displayed and briefly described in Figure 3.2.

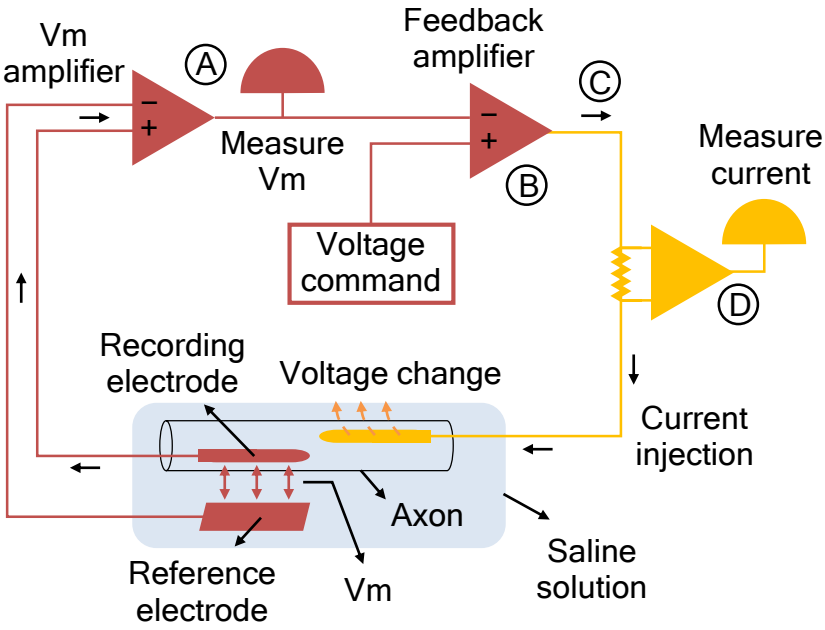

Figure 3.2. The voltage-clamp technique
Membrane potential (Vm) is measured by an amplifier (Vm amplifier) connected to an intracellular electrode (recording electrode) and an extracellular electrode in the bath (reference electrode). After amplification, the Vm signal is displayed on an oscilloscope (measure Vm) and is also fed into the negative terminal of the voltage-clamp feedback amplifier. The command potential (voltage command), which is selected by the experimenter and can be of any desired amplitude and waveform, is fed into the positive terminal of the feedback amplifier. The feedback amplifier then subtracts the membrane potential from the command potential and amplifies any difference between these two signals. This clamp amplifier will then inject a known amount of current into the axon through a second electrode that is egual and of opposite direction to that flowing through the ion channels. This negative feedback prevents a change in the membrane voltage and holds the membrane potential in the same value as the command potential. **(A)** Measure of Vm; **(B)** Feedback amplifier compares Vm to the desired command potential; **(C)** When Vm is different from the command potential, the clamp amplifier injects or withdraws current from the axon to minimize differences between the two. **(D)** The current injected into the axon is measured and shown to the experimenter.
The scheme refers to the initially developed voltage-clamp technique with two electrodes placed intracellularly (Cole 1949, Marmont 1949). It then evolved to a single intracellular electrode that was able to alternate from recording Vm and injecting current to keep the command potential. The patch-clamp technique was later developed allowing the recording of intact cells and following the same principles already described. Based on Kandel et al. 2013.

Figure 3.3 schematically representsis how neuronal synaptic activity is recorded in whole-cell voltage-clamp mode and how the

control of internal ion concentrations and the membrane potential of the neuron influences the recordings.

An important aspect that should always be accounted when performing patch-clamp in voltage-clamp mode is that the quality of recording will depend on the capacity of the amplifier to accurately inject current that compensate any membrane potential alteration due to changes in membrane conductivity (as explained before in Figure 3.3). Thus, voltage-clamp recordings are strongly influenced by fluctuations in the resistance that is in series with the pipette (R_s) and that will affect the passage of current into the interior of the cell. Therefore, a constant monitoring of the quality of the seal in voltage-clamp mode is of great importance to discard that any alteration in the recording is indeed a biological phenomenon and not caused by technical pitfalls associated with R_s. This is achieved by calculating R_s throughout all experiment as shown in Figure 3.4.

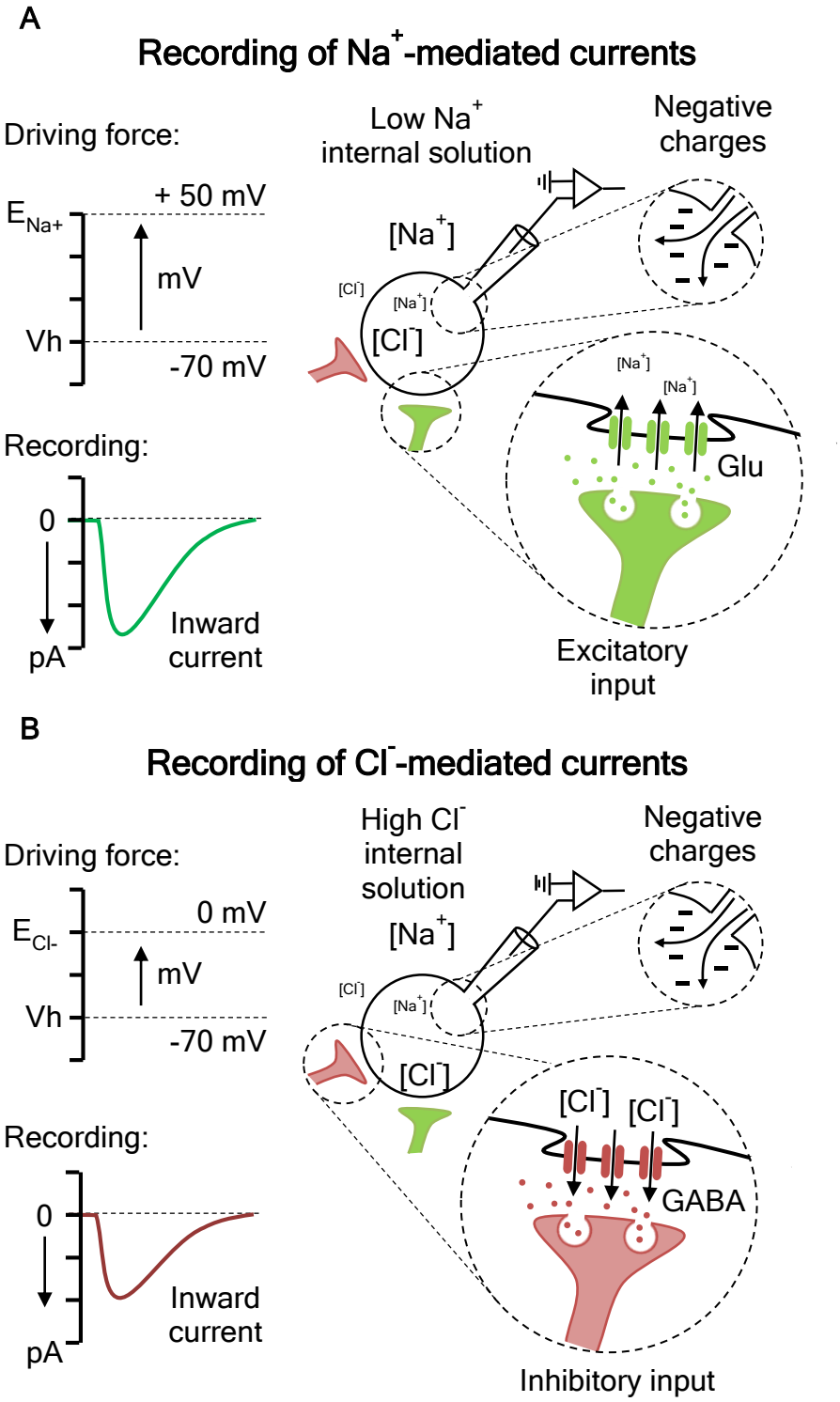
A
Recording of Na+-mediated currents
Driving force:
+ 50 mV
ENa+
mV
Vh
-70 mV
Recording:
0
pA
Inward current
Low Na+ internal solution
Negative charges
[Na+]
[Cl-]
[Na+]
[Cl-]
[Na+]
[Na+]
Glu
Excitatory input
B
Recording of Cl--mediated currents
Driving force:
0 mV
ECl-
mV
Vh
-70 mV
Recording:
0
pA
Inward current
High Cl- internal solution
Negative charges
[Na+]
[Cl-]
[Na+]
[Cl-]
[Cl-]
[Cl-]
GABA
Inhibitory input

Figure 3.3. Whole-cell voltage-clamp recordings
(A) For recording Na^+-mediated currents (e.g. α-amino-3-hydroxy-5-methyl-4-isoxazolepropionic acid receptor (AMPAR)-mediated currents) it is frequently used an internal solution that has low concentration of Na^+ when compared to the extracellular saline solution, mimicking what occurs in physiological situation. In this conditions, the equilibrium potential for Na^+ (E_{Na}) will be positive in relation to the holding membrane potential (Vh) (in this schematic, E_{Na} is shown as +50 mV for representative purposes only), creating a strong driving force for Na^+. Electrically stimulating glutamatergic fibers will induce a synchronous release of glutamate into the synaptic cleft. Glutamate will activate AMPARs at the postsynaptic site increasing AMPAR conductance and entry of Na^+ into the cell, according to the electrochemical gradient. In voltage-clamp, the AMPAR-mediated inward current will be detected by the feedback amplifier that injects an opposing current (injection of negative ions) to prevent membrane potential change and keep the cell at the voltage command (Vh = -70 mV). The injected current will be equal and of opposite polarity to that flowing through the cell membrane and used as a measure of synaptic activity. **(B)** The principle behind the recording of Cl^--mediated currents (e.g. $GABA_AR$-mediated currents) is the same as described before for Na^+. An important aspect to consider is the use a Cl^--based intracellular solution with a concentration of Cl^- similar to what is found in external solution. This will result in an equilibrium potential for Cl^- (E_{Cl}) close to 0 mV that will increase the driving force for this ion and facilitate the recording and measurement of these currents. In this condition, when GABA is released from presynaptic terminal and activate $GABA_ARs$, a Cl^--mediated inward current (chloride negative ions exiting the cell) occurs, according to the electrochemical gradient. The feedback amplifier will then inject negative ions into the cell through the pipette, compensating the exiting of Cl^- from the cell and preventing changes in the membrane potential.

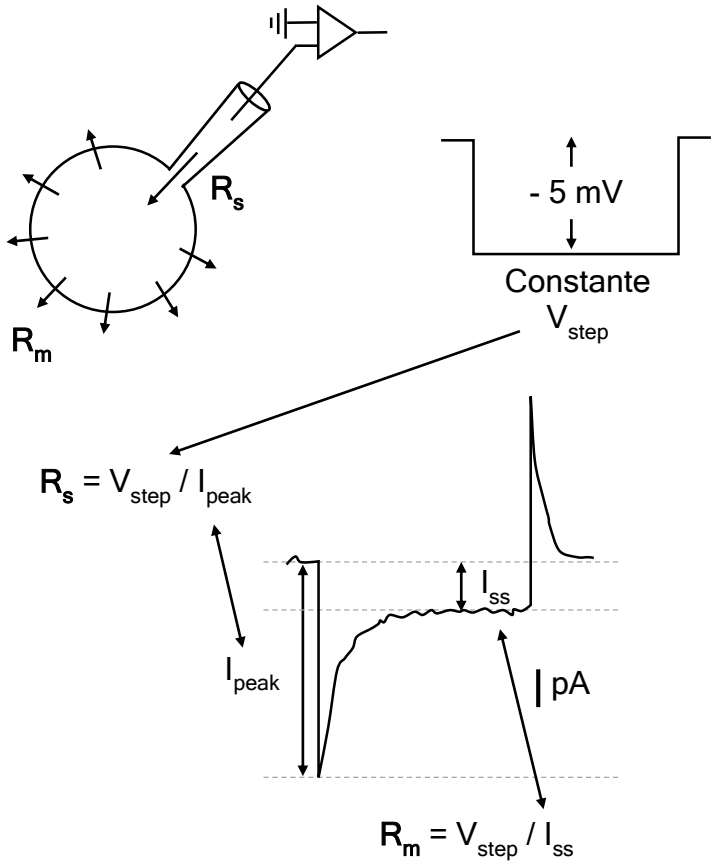

Figure 3.4. Method for approximate series resistance and membrane resistance calculation

During an experiment, accurate measurement of series resistance (R_s) and membrane resistance (R_m) is essential since small changes in these parameters can affect dramatically the amplitude of postsynaptic currents. R_s corresponds to the resistance that is in series with the pipette. This is the resistance that is opposing the passage of the current into the cell that maintain the voltage command stable. Rm, on the other hand, corresponds to the resistance that the cell membrane exerts to the passage of the current. It is mostly dependent on the size of the neuron and its overall membrane permeability. In this figure, V_{step} is the amplitude of the voltage step, which is constant and around -5 mV. For R_m calculation it is used the steady-state current (I_{ss}) which corresponds to the difference between the holding current before the voltage step and the later part of the voltage step ($R_m = V_{step} / I_{ss}$). Patch electrode R_s can be calculated by measuring the peak amplitude of the transient current immediately after the step is applied ($R_s = V_{step} / I_{peak}$). The correct compensation of fast transients after reaching the cell-attached mode and before goint into whole-cell is necessary for good estimate of R_s. Nevertheless, this method of measuring R_s is still an approximation of R_s and tends to overestimate its real value. However, it allows the experimenter to easily calculate and detect fluctuations and changes in the series resistance that may influence the recording. For a detailed description of methods to calculate these and other parameters of the neuron see Gentet et al. (2000).

For a deep understanding of whole-cell patch-clamp recordings consider reading Ogden (1994).

3.2 Field recordings

Extracellular electrophysiological recordings are performed to record the activity of an entire population of neurons that are in the vicinity of the recording electrode. A detailed explanation on the different components of the tracing obtained when recording from CA1 *stratum radiatum* region of the hippocampus are described in Figure 3.5.

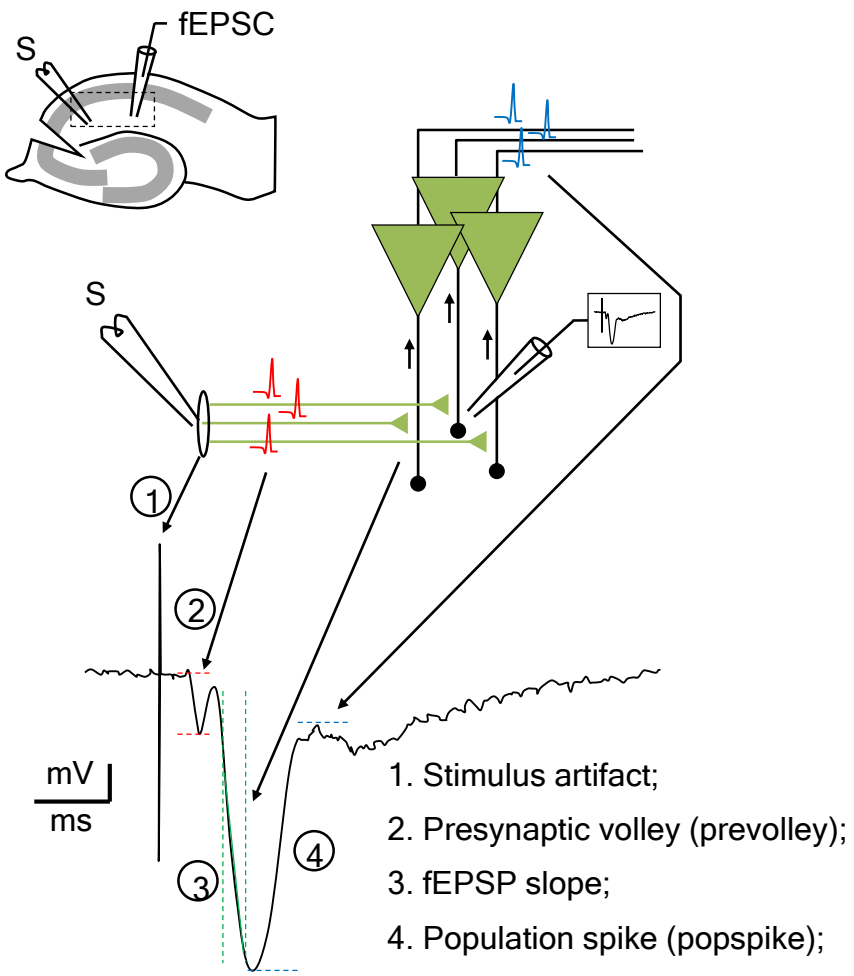

Figure 3.5. Schematic representation of a field excitatory postsynaptic potential (fEPSP) recorded in *stratum radiatum* of hippocampal CA1 region
A field excitatory postsynaptic potential (fEPSP) can be recorded from hippocampal CA1 *stratum radiatum* region while stimulating Schaffer Collateral fibers that project from hippocampal CA3 region. The arrow in **(1)** is pointing to the stimulus artifact that results from electrical stimulation of Schaffer Collaterals. This stimulation will induce the firing of action potential in all fibers surrounding the electrode that will propagate and reach the presynaptic terminal. This synchronous firing and propagation of action potentials will originate the presynaptic volley (prevolley) that follows the stimulus artifact in **(2)** and is measured between horizontal red dotted lines. Synchronous release of neurotransmitters, glutamate and GABA, in the presynaptic terminals, will result in activation of the respective postsynaptic receptors and the consequent synaptic potential (sum of inhibitory and excitatory postsynaptic potentials). The combination of synaptic potentials of the group of recorded postsynaptic neurons result in a fEPSP pointed in **(3)**. Changes in the initial slope of fEPSPs (measured between vertical dotted lines in green) are taken as a measure of synaptic strength, as they are less prone to contamination compared to fEPSP amplitude, which is more frequently influenced by disynaptic potentials or population spiking. The postsynaptic potential from each pyramidal cell will propagate through the dendrites and reach the soma. Here, synaptic potentials will be summated and, in case of reaching the

threshold for activation of voltage-dependent sodium channels, it will fire an action potential. The sum of all action potentials from the group of pyramidal cells recorded will originate a population spike, as shown in **(4)** that is measured between blue horizontal dotted lines.

3.3 Optogenetics

Optogenetics is a technique that involves the integration of optic and genetic tools to achieve a gain- or loss-of-function within a specific cell of living tissue (Deisseroth et al. 2006) (Figure 3.6).
Almost forty years ago, in 1979, the Nobel laureate Francis Crick wrote an article in Scientific American suggesting that one important challenge for the upcoming years in neuroscience field would be to develop “a method by which all neurons of just one type” could be controlled, “leaving the others more or less unaltered” (Crick 1979). With the tools available at the time this was very hard or even impossible to achieve since with electrical stimulation all fibers at the insertion site of the electrode were activated without distinguishing between different cell types. By the time Crick wrote the article, two scientists from the University of San Francisco, Walther Stoeckenius and Dieter Oesterhelt, were working on the study of light-activated ion-pump proteins (called microbial opsins) that were isolated from bacteria (Oesterhelt & Stoeckenius 1971). This initial finding by Stoeckenius and Oesterhelt led to a huge interest all over the world on the research and discover of other members of the opsin family and on the engineering of related proteins.

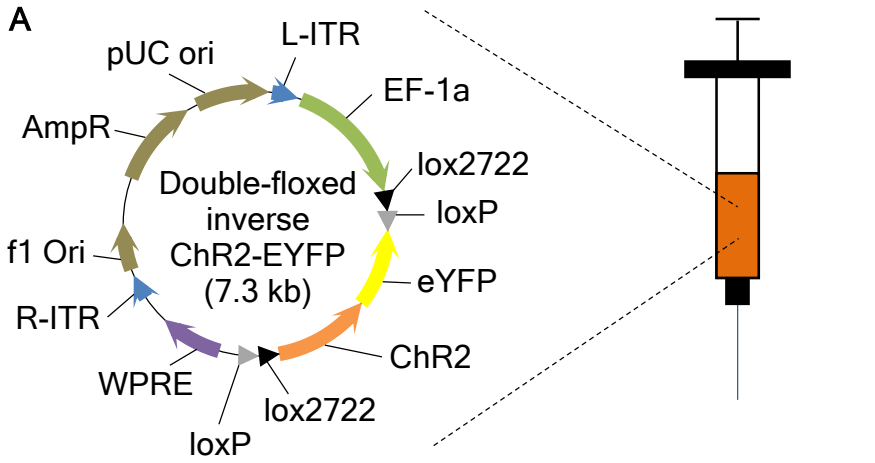

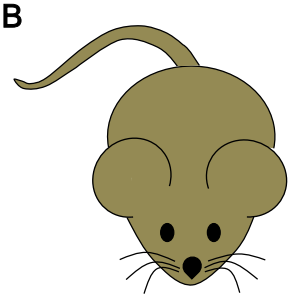

Trangenic mouse expressing Cre in specific population of neurons

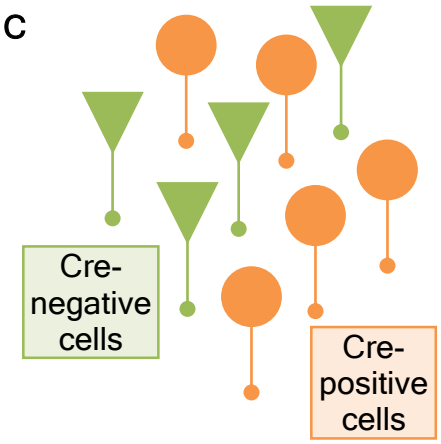

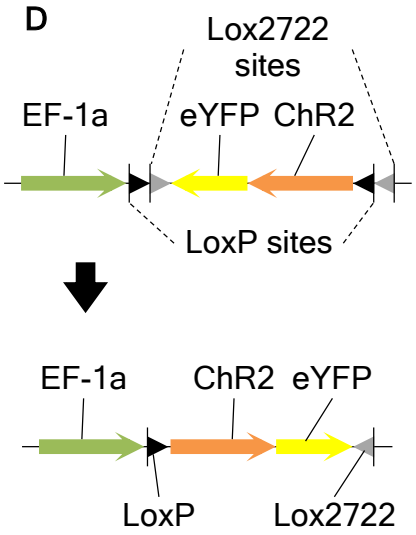

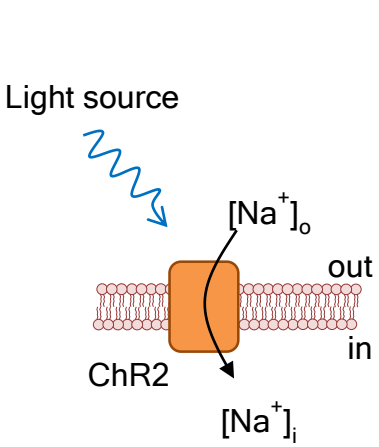

Depolarization!

Figure 3.6. Cell specific targeting of adeno-associated virus (AAV2/5:ChR2-eYFP) into transgenic Cre-recombinase mice
(A) Plasmid map showing the features of the double-floxed inverse ChR2-eYFP vector. The vector is inserted into an adeno-associated virus serotype 2 or 5 (AAV2/5) and stereotactically injected bilaterally into CA1 hippocampus. AAV2/5 was chosen because of its safety when compared to other viral systems (e.g. lentivirus) and because it is known to transfect neurons but not astroglia (Bartlett et al. 1998) **(B)** The animals used are transgenic mice expressing Cre protein in a specific population of neurons. One example of transgenic animals used in this thesis are the heterozygous PV-Cre mice (see Chapter 4.1, p63 for details on the animals). In this example, the animals will selectively express the Cre protein in all PV-positive interneurons. **(C)** When the virus is injected into a specific region of the brain, it will infect all neurons in that region, but only cells that are expressing the Cre protein (which in this example are the PV-positive neurons) will be able to recognize the LoxP sites that are flanking the ChR2-eYFP gene in the vector transported by the virus (see also A). **(D)** Only cells infected by the virus and expressing the Cre protein (PV-positive cells) will be able to express ChR2-eYFP fusion protein. The mechanism of Cre recombinase-mediated activation of the double-floxed-inverse ChR2-eYFP transgene is here shown. **(E)** Once Cre-LoxP system is activated, PV-positive cells will start expressing ChR2-eYFP fusion protein. The eYFP tag will allow the identification of cells that are successfully expressing ChR2 and that can be activated by light. A light source with a specific wavelength will be able to activate the ChR2 and allow the entry of Na^+ into the cell with consequent depolarization of neuron. If strong enough, the depolarization will induce the firing of action potentials specifically in these activated cells, allowing the measure of IPSCs in the neurons that are targeted by these cells. For details on optogenetic recordings see Chapter 4.4.2, p79 and on injection procedure see Chapter 4.5, p88. ChR2: Channelrhodopsin-2; eYFP: enhanced yellow fluorescent protein; loxP: locus of X-over P1; WPRE: woodchuck hepatitis post-transcriptional regulatory element; R-ITR: right-inverted terminal repeat; f1 Ori: f1 origin of replication for single-stranded DNA production; AmpR: ampicillin resistance; pUC ori: pUC origin of replication for propagation in *E. coli*; L-ITR: left-inverted terminal repeat; EF-1a: EF-1 alpha promoter.

All the effort resulted on the finding of several types of rhodopsins that included bacteriorhodopsins, halorhodopsins, and channelrhodopsins (Matsuno-Yagi & Mukohata 1977, Harz & Hegemann 1991, Nagel et al. 2002, Fenno et al. 2011, Yizhar et al. 2011). Later on, in 2005, the microbial opsin gene was applied to neuroscience and first introduced into mammalian dissociated neurons (Boyden et al. 2005), and in 2007 into behaving mice (Adamantidis et al. 2007, Aravanis et al. 2007), resulting in the control and induction of precisely-timed neuronal firing in response to light.

The principle behind the use of opsins to activate or suppress neurons consists on expressing the proteins in specific populations of cells. These light-gated pumps can be permeable to different ions: opsins permeable to Na^+ induce photoexcitation while opsins permeable to Cl^- induce photoinhibition. Several different recombinase-dependent systems can be used to achieve the cellular selectivity needed. One largely applied strategy is the Cre-recombinase system. It implies viral delivery of the opsin gene into a Cre-recombinase transgenic mouse line. A brief description on the principles associated to viral-targeting of opsins into Cre-recombinase mice is shown in Figure 3.6.

For a complete understanding of the technology, consider reading the following articles (Fenno et al. 2011, Yizhar et al. 2011).

4 Material and Methods

All procedures were conducted in accordance with the United Kingdom Home Office Animals (Scientific Procedures) Act (1986), the Portuguese law on animal care and the European Community guidelines (86/609/EEC).

4.1 Animals

Animals were housed in groups of 2-6 animals or individually (young/adult males), kept under standardized temperature, humidity and lighting conditions (12h/12h dark-light cycles) and had *ad libitum* access to water and food.

Two species of rodents were subjects in this thesis: *Rattus norvegicus* (rats) and *Mus Musculus* (mice). The experiments on Chapter 5.1 (p99) were conducted on 3-5 week-old male Wistar rats (Harlan, Italy). Experiments in Chapter 5.2 (p143) were conducted on 4-8 week-old mice from different strains:

- Wild-type mice (strain name: C57BL/6J; stock number: 000664) (The Jackson Laboratory, Bar Harbor, ME, USA);
- Heterozygous PV-Cre mice (strain name: B6;129P2-Pvalb$^{tm1(cre)Arbr}$/J; stock number: 008069) (The Jackson Laboratory, Bar Harbor, ME, USA);
- Heterozygous CCK-Cre mice (BAC-CCK-Cre$^{tg/+}$) (Geibel et al. 2014);
- Heterozygous CaMKII-Cre mice (strain name: B6.Cg-Tg(Camk2a-cre)T29-1Stl/J; stock number: 005359) and

their wild type littermates (The Jackson Laboratory, Bar Harbor, ME, USA);

- Heterozygous PV-Cre/Ai9 mice obtained from crossbred between homozygous PV-Cre mice and homozygous Ai9 mice (strain name: B6.Cg-Gt(ROSA)26Sor$^{tm9(CAG-tdTomato)Hze}$/J; stock number: 007909) (The Jackson Laboratory, Bar Harbor, ME, USA) to produce tdTomato fluorophore expression (emission wavelength, 581 nm) specifically in PV^+ cells.

4.2 Hippocampal slice preparation

Rats were anaesthetized with halothane (Sigma-Aldrich, St. Louis, MO, USA) or isoflurane (IsoFlo, Esteve Veterinaria, Spain) and mice were anaesthetized with intraperitoneal injection of pentobarbitone sodium (20% w/v, dosage ±0.2 mg/g; Pharmasol, Andover, UK). All animals were sacrificed by decapitation when the breathing had slowed down to ±1 breath per second and the response to stimulation of the limb withdrawal reflex had ceased. The dissection procedure and solutions slightly differed between rat and mice and are specified in the text and in Table 4.1. After decapitation, the brain was rapidly remove and placed in oxygenated (95% O_2, 5% CO_2), ice-cold (0-4°C) cutting solution (Table 4.1). The hemispheres were separated and the two hemispheres (for mice) or the two isolated hippocampi (for rat) were cut simultaneously. Transverse slices were obtained using a vibratome (Leica VT 1000S; Leica Microsystems, Germany or Microm HM650V, Carl Zeiss, UK) and the thickness was adjusted according to requirements: 300 µm thick slices for experiments

performed in rats (Chapter 5.1, p99); 250 µm or 400 µm thick hippocampal slices for experiments performed in mice (250 µm being used for patch-clamp recordings and 400 µm for spontaneous epileptiform discharges) (Chapters 5.2, p143). Once cut, all slices were immersed in oxygenated cutting solution at 35°C for 20–25 min to allow metabolic recovery. Following recovery, slices were transferred to a submerged (rat) or interface (mice) storage chamber that contained oxygenated artificial cerebrospinal fluid (aCSF) (Table 4.1) at room temperature (20-25°C). Slices were stored for at least 60min before starting experiments.

Table 4.1 Solutions for preparation, storage and recording of hippocampal slices

Solution type	Rats		Mice	
Cutting and recovering solutions	Sucrose	110 mM	Sucrose	75 mM
	KCl	2.5 mM	NaCl	87 mM
	$CaCl_2$	0.5 mM	KCl	2.5 mM
	$MgCl_2$	7.0 mM	$CaCl_2$	0.5mM
	$NaHCO_3$	25 mM	$MgCl_2$	7 mM
	NaH_2PO_4	1.25 mM	$NaHCO_3$	25 mM
	Glucose	7.0 mM	NaH_2PO_4	1.0 mM
	pH	7.4	Glucose	25 mM
			pH	7.4
Storage and recording solutions (aCSF)	NaCl	124 mM	NaCl	119 mM
	KCl	3 mM	KCl	2.5 mM
	NaH_2PO_4	1.25 mM	$NaH2PO_4$	1.25 mM
	$NaHCO_3$	26 mM	$NaHCO_3$	2 mM
	$MgSO_4$	1.0 mM	$MgSO_4$	1.3 mM
	$CaCl_2$	2.0 mM	$CaCl_2$	2.5 mM
	Glucose	10 mM	Glucose	10 mM
	pH	7.4	pH	7.4

Differences in solution between rats and mice were solely related with the protocols routinely implemented in the different labs where the experiments were performed.

4.3 Chemicals

Unless otherwise stated, drugs were added via the superfusion solution and their final concentration diluted from concentrated stocks. The complete list of drugs used in this study can be viewed in Table 4.2.

Table 4.2. Pharmacological tolls

Drug	Chemical name	Supp.	Biolog. activity	Stock sol.	Final [ ]
AM-251	N-(Piperidin-1-yl)-5-(4-iodophenyl)-1-(2,4-dichlorophenyl)-4-methyl-1H-pyrazole-3-carboxamide	Tocris Bioscience, Bristol, UK	CB_1R antagonist	2 mM in DMSO	2 µM
CGP55845	(2S)-3-[[(1S)-1-(3,4-Dichlorophenyl)ethyl] amino-2-hydroxypropyl] (phenylmethyl) phosphinic acid hydrochloride	Tocris Bioscience, Bristol, UK	$GABA_BR$ antagonist	1 mM in DMSO	1 µM
CGS21680	4-[2-[[6-Amino-9-(N-ethyl-β-D-ribofuranuronamidosyl)-9H-purin-2-yl] amino]ethyl] benzenepropanoic acid hydrochloride	Tocris Bioscience, Bristol, UK	$A_{2A}R$ agonist	5 mM in DMSO	30 nM
CNQX	6-cyano-7-nitroquinoxaline-2,3-dione disodium salt	Abcam Biochemicals, Cambridge, UK	AMPAR/ KAR antagonist	10 mM in ddH_2O	10 µM
CPA	N6-cyclopentyladenosine	Tocris Bioscience, Bristol, UK	A_1R agonist	5 mM in DMSO	10-30 nM
DL-AP5	DL-2-Amino-5-phosphonopentanoic acid sodium salt	Abcam Biochemicals, Cambridge, UK	NMDAR antagonist	50 mM in ddH_2O	50-100 µM
DPCPX	1,3-dipropyl-8-cyclopentylxanthine	Tocris Bioscience, Bristol, UK	A_1R antagonist	5 mM in DMSO	50-100 nM
Forskolin	[3R-(3α,4aβ,5β,6β, 6aα,10α,10aβ,10bα)]-5-(Acetyloxy)-3-ethenyldodecahydro-6,10,10b-trihydroxy-3,4a,7,7,10a-pentamethyl-1H-naphtho[2,1-b]pyran-1-one	Tocris Bioscience, Bristol, UK	Cell-permeable activator of adenylyl cyclase	5 mM in DMSO	5 µM

continue next page

Table 4.2. Pharmacological tolls (continue)

Drug	Chemical name	Supp.	Biolog. activity	Stock sol.	Final [ ]
Gabazine (SR-95531)	2-(3-Carboxypropyl)-3-amino-6-(4 methoxyphenyl) pyridazinium bromide	Abcam Biochemicals, Cambridge, UK	Selective, competitive $GABA_AR$ antagonist	10 mM in ddH_2O	100 µM
GF109203x	2-[1-(3-Dimethyl aminopropyl)indol-3-yl]-3-(indol-3-yl) maleimide	Tocris Bioscience, Bristol, UK	Protein kinase C inhibitor	1 mM in DMSO	1 µM
H-89	N-[2-[[3-(4-Bromophenyl)-2-propenyl] amino]ethyl]-5-isoquinoline sulfonamide dihydrochloride	Tocris Bioscience, Bristol, UK	Protein kinase A inhibitor	1 mM in ddH_2O	1 µM
KN-62	4-[(2S)-2-[(5-isoquinolinylsulfonyl) methylamino]-3-oxo-3-(4-phenyl-1-piperazinyl) propyl] phenyl isoquinoline sulfonic acid ester	Tocris Bioscience, Bristol, UK	Cell-permeable inhibitor of CaM kinase II	3 mM in DMSO	3 µM
MCPG	(RS)-α-Methyl-4-carboxyphenylglycine disodium salt	Tocris Bioscience, Bristol, UK	Non-selective mGluR I/II antagonist	100 mM in NaOH (100mM in ddH_2O)	200 µM
Muscimol	5-Aminomethyl-3-hydroxyisoxazole	Sigma-Aldrich, St Louis, MO, USA	$GABA_AR$ agonist	10 mM in NaOH (10mM, in ddH_2O)	30 µM
NBQX	2,3-Dioxo-6-nitro-1,2,3,4-tetrahydrobenzo[f] quinoxaline-7-sulfonamide disodium salt	Abcam Biochemicals, Cambridge, UK	AMPAR / KAR antagonist	25 mM in ddH_2O	25 µM

continue next page

Table 4.2. Pharmacological tolls (continue)

Drug	Chemical name	Supp.	Biolog. activity	Stock sol.	Final [ ]
PDD	Phorbol 12,13-didecanoate	Sigma-Aldrich, St Louis, MO, USA	Protein kinase C activator	5 mM in DMSO	250 nM
Picrotoxin (PiTX)	1:1 mixture of picrotoxinin and picrotin	Tocris Bioscience, Bristol, UK	$GABA_AR$ antagonist	50 mM in ethanol	100 µM
QX-314	N-(2,6-Dimethylphenyl carbamoylmethyl) triethylammonium bromide	Tocris Bioscience, Bristol, UK	Membrane imper-meable blocker of voltage-dependent Na^+ channel	-	5 mM
Rp-cAMPs	R)-Adenosine, cyclic 3',5'-(hydrogen phosphorothioate) triethylammonium	Tocris Bioscience, Bristol, UK	Cell-permeable cAMP analog	100 mM in ddH_2O	100 µM
SCH58261	2-(2-Furanyl)-7-(2-phenylethyl)-7H-pyrazolo[4,3-e][1,2,4]triazolo[1,5-c]pyrimidin-5-amine	Tocris Bioscience, Bristol, UK	$A_{2A}R$ antagonist	5 mM in DMSO	100 nM
SFK-89976A	1-(4,4-Diphenyl-3-butenyl)-3-piperidinecarboxylic acid hydrochloride	Abcam Biochemicals, Cambridge, UK	GAT-1 inhibitor	100 mM in ddH_2O	20 µM
SNAP5114	1-[2-[tris(4-methoxyphenyl) methoxy]ethyl]-(S)-3-piperidinecarboxylic acid	Tocris Bioscience, Bristol, UK	GAT-3 and GAT-2 inhibitor	100 mM in DMSO	20 µM

continue next page

Table 4.2. Pharmacological tolls (continue)

Drug	Chemical name	Supp.	Biolog. activity	Stock sol.	Final [ ]
Tetrodotoxin (TTX)	Octahydro-12-(hydroxymethyl)-2-imino-5,9:7,10a-dimethano-10aH-[1,3]dioxocino[6,5-d]pyrimidine-4,7,10,11,12-pentol + citrate buffer	Abcam Biochemicals, Cambridge, UK	Selective inhibitor of voltage-dependent Na^+ channel	1 mM in ddH_2O	0.5 µM
WIN 55,212-2	(R)-(+)-[2,3-Dihydro-5-methyl-3-(4-morpholinylmethyl) pyrrolo[1,2,3-de]-1,4-benzoxazin-6-yl]-1-naphthalenyl methanone mesylate	Tocris Bioscience, Bristol, UK	CB_1R and CB_2R agonist	5 mM in DMSO	5 µM

Drugs are listed in alphabetic order. DMSO: Dimethyl sulfoxide; ddH_2O: double distillated water; GAT: GABA transporter; KA: kainate.

4.4 Electrophysiological recordings

Whole-cell patch-clamp and field potential recordings were performed using electrodes pulled from borosilicate glass capillaries (1.5mm outer diameter, 0.86mm inner diameter, GC150F-10, Harvard Apparatus, Holliston, MA, USA) in a PC-10 vertical (Narishige Group, London, UK) or a P-97 horizontal (Sutter Instrument Co., Novato, CA, USA) microelectrode puller. All intracellular solutions used in this study are described in Table 4.3.

Table 4.3 Intracellular solutions

Intracellular	Composition		Experiment
K-based (1)	K-gluconate	125 mM	- Muscimol-evoked postsynaptic currents
	KCl	11 mM	
	CaCl2	0.1 mM	
	MgCl2	2 mM	
	EGTA	1 mM	
	HEPES	10 mM	
	MgATP	2 mM	
	NaGTP	0.3 mM	
	Phospocreatine	10 mM	
	pH	7.3	
	Osmolarity	280-290 mOsm	
	Biocytin	0.2 - 0.5%	
K-based (2)	K-gluconate	145 mM	- Electrical-evoked excitatory postsynaptic currents
	HEPES	20 mM	
	KOH	10 mM	
	NaCl	8 mM	
	EGTA	0.2 mM	
	MgATP	2 mM	
	NaGTP	0.3 mM	
	pH	7.2	
	Osmolarity	290-300 mOsm	
	Neurobiotin	0.2 - 0.5%	

continue next page

Table 4.3. Intracellular solutions (continue)

Intracellular	Composition		Experiment
Cs-based (1)	CsCl	125 mM	- Electrical-evoked inhibitory postsynaptic currents - Miniature inhibitory postsynaptic currents - Tonic inhibitory currents
	NaCl	8 mM	
	CaCl2	1 mM	
	EGTA	10 mM	
	HEPES	10 mM	
	Glucose	10 mM	
	MgATP	5 mM	
	NaGTP	0.4 mM	
	pH	7.2	
	Osmolarity	280-290 mOsm	
	QX-314	5 mM	
	Biocytin	0.2 - 0.5%	
Cs-based (2)	CsCl	145 mM	- Light-evoked IPSCs
	HEPES	20 mM	
	CsOH	10 mM	
	NaCl	8 mM	
	EGTA	0.2 mM	
	MgATP	2 mM	
	NaGTP	0.3 mM	
	pH	7.2 mM	
	Osmolarity	290-300 mOsm	
	QX-314	5 mM	
	Neurobiotin	0.2 - 0.5%	

continue next page

Table 4.3. Intracellular solutions (continue)

Intracellular	Composition		Experiment
Cs-Methanesulfonate	Cs-Methanesulfonate	145 mM	- Light-evoked EPSCs/disynaptic IPSCs
	HEPES	20 mM	
	CsOH	10 mM	
	NaCl	8 mM	
	EGTA	0.2 mM	
	MgATP	2 mM	
	NaATP	0.3 mM	
	pH	7.2	
	Osmolarity	290-300 mOsm	
	QX-314	5 mM	
	Neurobiotin	0.2 – 0.5%	

Schematics for all experimental designs used in this study is shown in Table 4.4, p88.

4.4.1 Patch-clamp recordings

All patch-clamp recordings were performed in a submerged recording chamber (Luigs & Neumann, Ratingen, Germany) and individual hippocampal slices were clamped with a harp slice grid with nylon strings (HSG-5BD, ALA Scientific Instruments, Farmingdale, NY, USA) to minimize agitation.

In experiments described in Chapters 5.1 (p99) and 5.2.5 (p157) slices were mounted at the stage of a Carl Zeiss Axioskop 2FS upright microscope (Jena, Germany) equipped with a 40x immersion objective with 2 and 4 zoom (i.e. up to 160x magnification) and a differential interference contrast-infrared (DIC-IR) CCD video camera (VX44, Till Photonics, Gräfelfing,

Germany) (Stuart et al. 1993). Data were recorded with an EPC-7 electrical amplifier (List Biologic, Campbell, CA, USA). The recording chamber was continuously superfused by an open gravitational superfusion system at 2-3 mL/min with aCSF at room temperature. Cells were voltage-clamped at Vh = -70 mV and recordings were low-pass filtered using a 3 and 10kHz three-pole Bessel filter of the EPC-7 amplifier, digitized at 5 or 10kHz using a Digidata 1322A board and registered by Clampex software version 10.2 (Molecular devices, Sunnyvale, CA, USA).

Experiments in Chapters 5.2 (p143) except experiments in Chapter 5.2.5 (p157) and Chapter 5.2.8 (p173) were performed under the stage of a BX51WI upright microscope (Olympus, Southend, UK) and slices continuously superfused with oxygenated aCSF in a closed pump-driven circuit (Watson-Marlow, Falmouth, UK) at 5 mL/min flow rates and at 32°C. Hippocampal cells were visualised digitally using a 20x immersion objective with 2 and 4 zoom (i.e. up to 80x magnification) and DIC-IR in combination with a CCD camera (SensiCam, PCO imaging, Kelheim, Germany). Data were recorded with a Multiclamp 700B amplifier (Molecular Devices, Sunnyvale, CA, USA), recordings were low-pass filtered at 2 kHz using the built-in Bessel filter, digitized at 10 kHz with a Digidata 1400 and acquired with Clampex software version 10.2 (Molecular devices, Sunnyvale, CA, USA).

For all patch-clamp recordings whole-cell access was established following formation of a gigaseal (>1 GΩ) between pipette tip and cell membrane. Recordings were started not before the first 5–10 min after break-in to enable diffusion of intracellular solution in the soma and proximal dendrites. Series resistance was not

compensated for during voltage-clamp recordings but was regularly monitored throughout each experiment with a -5mV, 50ms pulse, and cells with more than 20% change in series resistance were excluded from the data. Access and input resistance were derived from currents in response to the test pulses according to Ohm's law (Ogden 1994). Biocytin (Tocris Bioscience, Bristol, UK) or neurobiotin (Vector Laboratories, Burlingame, CA, USA) was regularly added to intracellular solution for *post hoc* anatomical analyses of neurons.

4.4.1.1 Muscimol-evoked postsynaptic currents

Whole-cell recordings of muscimol-evoked postsynaptic currents (muscimol-PSC) were performed with an intracellular filling solution containing (in mM): 125 K-gluconate, 11 KCl, 0.1 CaCl2, 2 MgCl2, 1 EGTA, 10 HEPES, 2 MgATP, 0.3 NaGTP, 10 phosphocreatine, pH 7.3, adjusted with KOH (1M), 280-290 mOsm; biocytin (0.2 - 0.5%) was added in to some cells for *post hoc* analyses (see Table 4.3, p71). Data were sampled at 5 kHz and muscimol-PSC evoked through a micropipette (2-4MΩ) containing muscimol ($GABA_AR$ agonist; 30µM in aCSF) coupled to a pressure application system (Picopump PV820, World Precision Instruments, Stevenage, UK) and positioned close to the soma of the recorded cell (Table 4.4, p88). Single pulses of 10-20ms and 6-8psi were applied every 2min and the amplitude of the resulting current analysed. For statistical purposes it was considered the 10 min period immediately before the application of the tested drug and the 10 min period starting 40 min after the

start of its perfusion. Muscimol-evoked currents are shown along Chapter 5.1 (p99).

4.4.1.2 Electrical-evoked inhibitory postsynaptic currents

Inhibitory postsynaptic currents (IPSCs) were recorded with a pipette solution containing (in mM): 125 CsCl, 8 NaCl, 1 CaCl2, 10 EGTA, 10 HEPES, 10 glucose, 5 MgATP, 0.4 NaGTP, pH 7.2, adjusted with CsOH (50wt% in H2O), 280-290 mOsm; biocytin (0.2 - 0.5%) was added to some recordings for *post hoc* structural analyses and QX-314 (5mM) to block the firing of action potentials (see Table 4.3, p71). IPSCs were evoked as previously described elsewhere (Chevaleyre et al. 2007) with alterations. Rectangular pulses stimuli at 0.067Hz (15 sec interval), 1-15µA and 0.1 ms were delivered via monopolar stimulation with a patch-type pipette filled with aCSF and positioned in *stratum radiatum*, *stratum oriens* or *stratum pyramidale*, 80-120µm from the recorded cell (Table 4.4, p88). Recordings were sampled at 5 kHz and performed in the continuous presence of NMDA and AMPA/KA receptor antagonists (50µM DL-AP5 and 10µM CNQX, respectively) to exclude the influence of glutamatergic transmission. The amplitude of eight consecutive currents (2 min period, to match the time course of experiments with muscimol-PSCs) were averaged and the 10 min period immediately before the application of the tested drug and the 10 min period starting 40 min after its perfusion were considered for statistical purposes.
Electrical-evoked IPSCs are shown in Chapter 5.1.4 (p108) and Chapter 5.1.7 (p121).

4.4.1.3 Miniature inhibitory postsynaptic currents

The miniature inhibitory postsynaptic currents (mIPSCs) were recorded with the same intracellular solutions described for IPSCs (see Chapter 4.4.1.2, p76 and Table 4.3, p71). The aCSF was supplemented with NMDA (50µM DL-AP5) and AMPA/KA (10µM CNQX) receptor antagonists, to block glutamatergic transmission, as well as TTX (0.5 µM) to block voltage-dependent Na^+ channels and firing of action potential, allowing the exclusive recording of spontaneous GABA release-mediated events (Table 4.4, p88). The events were recorded with a sampling rate of 10 kHz and analyzed off-line using spontaneous events detection parameters of the Mini Analysis software (Synaptosoft, GA, USA). Averaged amplitude and frequency of events obtained from 100 sec interval window were plotted in graphs and statistical analysis was performed by comparing the period 10 min immediately before adding the test drug and the 10 min period starting 40 min after its perfusion.
Experiments on mIPSCs are described in Chapter 5.1.4 (p108).

4.4.1.4 Tonic inhibitory currents

Tonic inhibitory currents (tonic-ICs) were recorded with the same intracellular solutions described for IPSCs and mIPSCs recordings (see Chapter 4.4.1.2, p76 and Table 4.3, p71). For tonic-ICs, SFK89976A (GABA transporter (GAT)-1 inhibitor; 20µM) and SNAP5114 (GAT-3 inhibitor; 20µM) were added to the aCSF. GABA (5µM) was also added where mentioned. SR95531 (gabazine, a $GABA_AR$ inhibitor; 100µM) was fast applied using a

DAD-12 Superfusion System (ALA Scientific Instruments, Farmingdale, NY, USA) (Table 4.4, p88). The tonic current measurements were performed as previously described elsewhere (Glykys & Mody 2007b). The digitized recording acquired at 10 kHz (0.1ms) was binned to 5ms. Binned data was loaded with Prism Version 5.00 for Windows (GraphPad Software, La Jolla, CA, USA) and an all-point histogram was plotted for every 200 points (every 1 s) and smoothed by Savitzky-Golay algorithm to obtain the peak value. A Gaussian was fitted to the part of the distribution from a point 3pA to the left of the peak value to the rightmost (most positive) value of the histogram distribution. The mean of the fitted Gaussian was considered to be the mean holding current. This process was repeated for the entire recording. For statistical purposes the 20-30 s period before applying gabazine (in control or CPA conditions) was compared with the 10-15 s period in the presence of gabazine (100μM) under the same drug conditions. For a given neuron it was obtained the magnitude of the tonic current by subtracting the tonic current before perfusing gabazine from that recorded in the presence of gabazine. Slices were incubated for 50 min at room temperature with CPA (30nM) for test conditions and with DMSO (0.0006%, v/v; same concentration of solvent as in test conditions) for control conditions.

Tonic-ICs are represented in Chapter 5.1.5 (p112) and Chapter 5.1.7 (p121).

4.4.1.5 Electrical-evoked excitatory postsynaptic currents

Afferent-evoked excitatory postsynaptic currents (EPSCs) were elicited by 0.1 ms rectangular pulses, delivered once every 15 s through a bipolar concentric wire electrode manually fabricated from platinum/iridium wire (25 µm diameter, <800 kΩ impedance (Advent Research Materials)) positioned in the Schaffer collaterals afferents. EPSCs were recorded from pyramidal cells or interneurons from CA1 area (Table 4.4, p88), voltage-clamped at Vh = -70 mV and perfused with aCSF containing picrotoxin (PiTX, $GABA_AR$ antagonist, 100 mM), and CGP55845 ($GABA_BR$ antagonist, 1 mM) to block GABAergic transmission. The intracellular solution contained (in mM): 145 K-gluconate, 20 HEPES, 10 KOH, 8 NaCl, 0.2 KOH-EGTA, 2 ATP-Mg, 0.3 GTP-Na, pH 7.2 adjusted with KOH (1M), 290-300 mOsm, neurobiotin (0.2 - 0.5%). Averages of four consecutive individual recordings were used to plot and analyse data and the 5 min period before bath application of the drug was compared to the 15-20 min following its application.
EPSCs experiments are presented in Chapter 5.2.5 (p157).

4.4.2 Optogenetic recordings

Experiments for optogenetic recordings were performed in 250 µm thick hippocampal slices from transgenic-Cre animals (see Chapter 4.1, p63) that had been previously injected with viral ChR2-eYFP constructs (for *in vivo* injections see Chapter 4.5, p91). During slice preparation, storage and recording light was minimised to avoid photoactivation of ChR2. Prior to storage,

slices were screened for ChR2-eYFP-transfected neurons in a standalone microscope (Leica DM5000B, Wetzlar, Germany) equipped with a CCD camera (ORCA-ER, Hamamatsu Photonics K.K., Iwata, Japan) and appropriate eYFP filter sets (excitation: 450-490nm; emission: 515-565 nm; beam splitter: 510 nm; Leica, Wetzlar, Germany). Slices that contained a dense tangle of eYFP expression in area CA1 were stored in the interface chamber for subsequent recording. Individual slices were mounted in the stage of a BX51WI upright microscope (see Chapter 4.4.1, p73) and eYFP-positive cells and axons were identified in the computer screen using TILLvisION software (Till Photonics, Gräfelfing, Germany) using the 'EYFP/Venus/Citrine/Topaz band-pass filter set' (#41028, excitation: HQ500/20x; beam splitter: Q515lp; emission: HQ535/30m; Chroma, Bellows Falls, VT, USA). Activation of ChR2 (excitation range 450 ± 25 nm) was achieved by blue laser light (473 nm) using a standard 'Endow GFP/EGFP band-pass filter set' (#41017, excitation: HQ470/40x; beam splitter: Q495LP; emission: HQ525/50m; Chroma, Bellows Falls, VT, USA). A blue light spot of 20-80 µm diameter (achieved by a 113 µm fibre light guide for laser-microscope coupling; Rapp OptoElectronic, Hamburg, Germany) was systematically moved along the *stratum pyramidale*, *stratum radiatum* or *stratum oriens* to a location that reliably elicited PSCs in the postsynaptic recorded cell. The intensity of the laser varied between 50 - 90% of maximum laser power (maximum laser unit output prior entry to the optic fibre is 100 mW) and was adjusted to the minimum intensity required to obtain consistent afferent firing that resulted in regular PSC and minimal number of failures.

4.4.2.1 Light-evoked EPSCs/disynaptic IPSCs

Slices used for recordings of light-evoked EPSCs and disynaptic-IPSCs (dIPSCs) were prepared from hippocampi of heterozygous CaMKII-Cre mice transduced with adeno-associated virus serotype 2 or 5 (AAV2/5)-ChR2-eYFP to express ChR2 in a Cre-dependent manner on glutamatergic cells (see Chapter 4.5, p91 for details on injection procedure). The intracellular solution contained (in mM): 145 Cs-Methanesulfonate, 20 HEPES, 10 CsOH, 8 NaCl, 0.2 CsOH-EGTA, 2 ATP-Mg, 0.3 GTP-Na, pH 7.2 adjusted with CsOH (1M), 290-300 mOsm, neurobiotin (0.2 - 0.5%) and QX-314 (5mM). All slices were continuously stored and recorded in the presence of KN-62 (3 µM) and MCPG (200 µM) (see Table 4.2, p67) to prevent long-term plasticity resulting from repetitive glutamatergic fiber burst stimulation (Perez et al. 2001, Lamsa et al. 2007, Campanac et al. 2013). To elicit light-evoked EPSCs and dIPSCs, a fixed-spot laser was positioned in CA1 Schaffer collateral fibers showing strong eYFP labelling (Table 4.4, p88). Five consecutive 473 nm laser light-pulses of 3 ms each and separated by a 50 ms interval (20 Hz) were delivered every 30 s to activate ChR2 in glutamatergic neurons. Recorded postsynaptic cells were voltage-clamped sequentially at two different holding potentials to record glutamatergic EPSCs and disynaptic GABAergic IPSCs. Neurons were clamped at Vh = -70 mV (potential close to the calculated E_{Cl} of -71 mV) to record isolated EPSCs that result from glutamate release after light-activated glutamatergic axons. The reversal potential of EPSCs was determined at Vh = 11 ± 1 mV (n = 7) by depolarizing the cell until the inward-directed EPSCs were abolished with consequent

isolation of outward-directed GABAergic IPSCs ($GABA_AR$ and $GABA_BR$ blockers were not added to perfusion). Since only glutamatergic fibers are being optically recruited, any GABA-mediated response obtained in this conditions is necessarily from disynaptic or polysynaptic recruitment of interneurons that feedback or feedforward to the recorded postsynaptic pyramidal neuron. This was regularly confirmed at the end of each experiment since blockage of glutamatergic transmission with NBQX (25 µM) and DL-APV (100 µM) also blocked dIPSCs. Data were analysed by measuring the charge (area under the curve) for EPSCs and dIPSCs in the 500 ms window from current onset. For statistical purposes was considered the 5 min period before drug application and the 15-20 min period after the start of drug perfusion.

The experiments of light-evoked EPSCs/dIPSCs are represented in Chapter 5.2.4 (p153).

4.4.2.2 Light-evoked IPSCs

Recordings of light-evoked IPSCs were performed in heterozygous PV-Cre and CCK-Cre mice that had been previously injected with viral AAV2/5-ChR2-eYFP constructs (for *in vivo* injections see Chapter 4.5, p91). The intracellular solution contained (in mM): 145 CsCl, 20 HEPES, 10 CsOH, 8 NaCl, 0.2 CsOH-EGTA, 2 ATP-Mg, 0.3 GTP-Na, pH 7.2 adjusted with CsOH (1M), 290-300 mOsm, neurobiotin (0.2 - 0.5%) and QX-314 (5mM). Excitatory transmission was pharmacologically blocked with NBQX (25 µM) and DL-AP5 (100 µM) and cells were clamped at Vh = -70 mV. The fixed-spot laser was moved along *stratum*

oriens, *stratum pyramidale* or *stratum radiadum* to a position with intense ChR2-eYFP labelling and that regularly elicited IPSCs in the recorded cell (Table 4.4, p88). Two consecutive 473 nm laser light-pulses of 3 ms each and separated by a 50 ms interval were delivered every 15 s to activate ChR2 in GABAergic interneurons. Paired-pulse ratios are presented as 2nd versus 1st IPSC amplitude. The amplitude of four consecutive currents (1 min period) were averaged and the 5 min period immediately before the application of the tested drug and the 5 min period starting 15 min after its perfusion were considered for statistical purposes. The experiments of light-evoked IPSCs are represented in Chapter 5.2.6 (p161).

4.4.3 Firing patterns

Firing patterns of interneurons were determined in current-clamp mode immediately after achieving whole-cell configuration by a series of hyperpolarizing and depolarizing steps (1200ms) of current injection. After recording the firing pattern, cells were tested for adenosine actions with muscimol-PSCs. The firing pattern was characterized according to the Petilla convention (Ascoli et al. 2008) and Lamsa and co-workers (Lamsa et al. 2007). Four neuronal populations were distinguished: regular-spiking non-pyramidal neurons (RSNP) that were further divided in non-reboundind (NR-RSNP) or rebounding (R-RSNP), burst-spiking non-pyramidal cells (BSNP) and fast-spiking interneurons (FSI). Rebounding interneurons generated action potentials on release from hyperpolarizing current injection (hyperpolarization to more than 25 mV from resting membrane potential). FSI had a

high maximal spiking frequency and small reduction in the spiking frequency when comparing initial (0-100 ms) and later (400-500 ms) periods. BSNP cells are characterized by generating high frequency bursts of action potentials (≥3) during depolarizing current injection and on release from hyperpolarizing current injection. The firing patterns of different interneurons are further described in Figure 5.16 (p124).

4.4.4 Field recordings

All field recordings were performed under the stage of a BX51WI upright microscope (Olympus, Southend, UK) as described in Chapter 4.4.1, p73 for patch-clamp recordings. Extracellular field excitatory post-synaptic potentials (fEPSPs) were recorded through an extracellular microelectrode filled with aCSF and placed in the *stratum radiatum* of the CA1 area. Stimulation was delivered through a bipolar concentric wire electrode manually fabricated from platinum/iridium wire (25 µm diameter, <800 kΩ impedance, Advent Research Materials) positioned in the Schaffer collaterals afferents, in the *stratum radiatum* near the CA3-CA1 border. The CA3 area was regularly removed by surgical cut to avoid recurrent excitation.

For experiments showed in Chapter 5.2.3 (p146), paired-pulse (50 ms interval) electrical stimulation (S1) was delivered in the CA1 area (Table 4.4, p88) and fEPSPs were elicited in every experiment with five stimulation intensities gradually increasing stimulus pulse duration from 50 to 150 µs. The fEPSP slope and population spike (popspike) amplitude were measured as showed in Figure 5.22 (p148). Ratio of baseline fEPSP slope values and

popspike amplitudes evoked with different intensities were fitted with regression line in each experiment baseline. The fEPSP slope / popspike relation was considered linear when regression fitting index was > 0.8 (0.89 ± 0.03, n = 11, mean ± SEM, SigmaPlot). All fEPSP slope values recorded following wash-in of drug were fitted in the baseline condition regression line. Then, measured popspike amplitude after drug perfusion and popspike estimate given to same fEPSP value in baseline linear slope / popspike relation were compared. This gave a Δ popspike / fEPSP used for analysis. Because lowest intensity often failed to elicit stable popspike in baseline, intensities from 75 µs till 150 µs stimulus duration were used to determine linear relation of fEPSP slope and popspike amplitude in baseline conditions with regression line. The fEPSP values in the presence of agonist, which were potentiated out of the baseline fEPSP slope range, were excluded in analyses because no linear relation between fEPSP slope and popspike could be confirmed.

For experiments showed in Chapter 5.2.7 (p170), two stimulating electrodes were used. The S1 was positioned as described before and was used to elicit paired pulses (50 ms interval) while recording fEPSP in the CA1 area. A second electrode (S2) was positioned in the vicinity of recording electrode and used to apply high-frequency stimulation (HFS, 50 Hz 100 pulse) and elicit local release of adenosine (Table 4.4, p88). Schaffer collaterals were stimulated with S1 every 5 s and HFS delivered with S2 every 2 min. The experiments were performed in continuous presence of blockers for CB_1R (AM-251, 2 µM), $GABA_BR$ (CGP55485, 1 µM), adenosine A_1R (DPCPX, 100 nM) as well as DL-APV (100 µM). The fEPSPs slope and popspike were analysed as described

above. A time-period of 35 s before HFS and 5 s after HFS was used for statistical purposes.

4.4.5 Spontaneous epileptiform discharges

For spontaneous epileptiform discharge recordings, slices with 400 µm thick were constantly perfused with aCSF at a flow rate of 3 mL/min and the temperature was maintained at 32°C. Slices were visualised with a stereo-microscope (Leica MZ8, Micro Instruments, Long Hanborough, Oxon, UK) mounted above an interface chamber. Extracellular microelectrodes were filled with aCSF. Data were recorded with an alternating current preamplifier and AC/DC amplifier Neurolog NL104 and NL106 (0.3 Hz high-pass filtering) (Digitimer Ltd., Welwyn Garden City, UK). The signal was digitized by a Power 1401 plus (Cambridge Electronic Design, Cambridge, UK). Additionally, a Humbug 50/60 Hz (Digitimer Ltd., Welwyn Garden City, UK) was used to remove noise locked to the electrical mains supply. Data were stored for off-line analysis using Signal5 software (Cambridge Electronic Design, Cambridge, UK) at 10 kHz acquisition rate. A single-pulse electrical stimuli was delivered (every 20 s), and elicited fEPSPs (100 ms from stimulation) that were excluded from spontaneous activity analysis. Spontaneous seizure-like events were induced by perfusion of slices with elevated (8-9 mM) extracellular potassium ($[K_o]$) (Table 4.4, p88) (Korn et al. 1987, Sagratella et al. 1987). Recordings were band-pass (1 -100 Hz) filtered off-line to uncover low-frequency deflections and analyze event occurrence. Amplitude threshold was set to 0.25 mV, and event detection was visually verified. Parallel high-pass filtering (> 60

Hz) of recordings was used to uncovered extracellular spikes associated with the events. Occurrence of events was plotted in 2 min bin period. For statistical purposes the 10 min period before and the 20–30 min after test drug application was used. The experiments of spontaneous epileptiform discharge are showed in Chapter 5.2.8 (p173).

Table 4.4 Schematic of all experimental designs performed in electrophysiological recordings

Schematic	Name
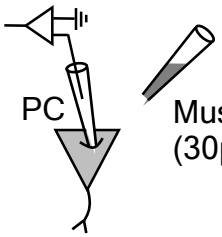	Muscimol-evoked postsynaptic currents in pyramical cells
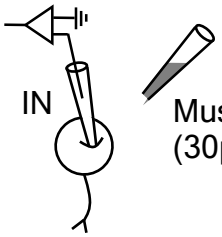	Muscimol-evoked postsynaptic currents in interneurons
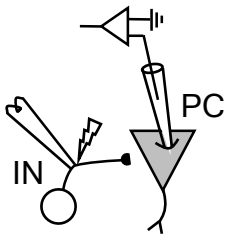	Electrical-evoked inhibitory postsynaptic currents in pyramidal cells
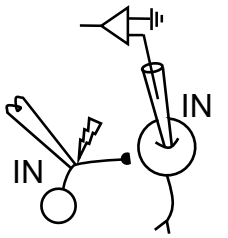	Electrical-evoked inhibitory postsynaptic currents in interneurons
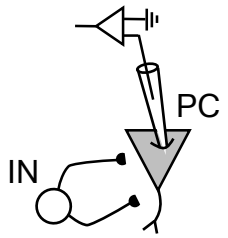	Miniature inhibitory postsynaptic currents in pyramidal cells

continue next page

Table 4.4. Schematic of all experimental designs performed in electrophysiological recordings (continue)

Schematic	Name
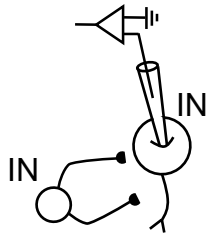	Miniature inhibitory postsynaptic currents in interneurons
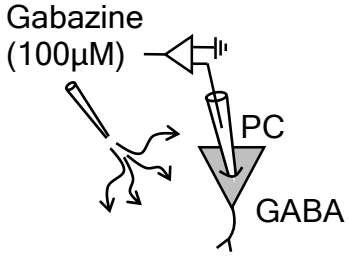	Tonic inhibitory currents in pyramidal cells
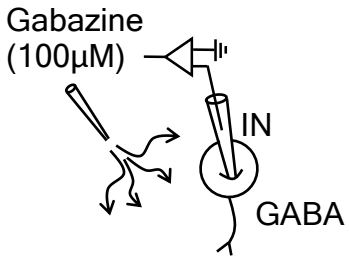	Tonic inhibitory currents in interneurons
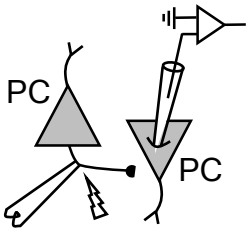	Electrical-evoked excitatory postsynaptic currents in pyramidal cells

continue next page

Table 4.4. Schematic of all experimental designs performed in electrophysiological recordings (continue)

Schematic	Name
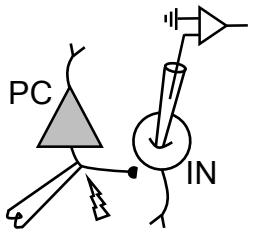	Electrical-evoked excitatory postsynaptic currents in interneurons
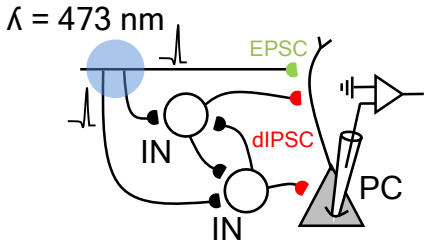	Light-evoked EPSCs/disynaptic IPSCs
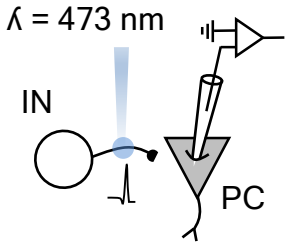	Light-evoked IPSCs in pyramidal cells
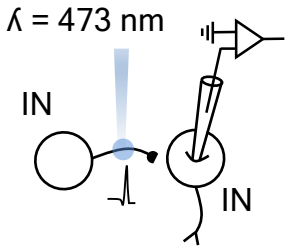	Light-evoked IPSCs in interneurons

continue next page

Table 4.4. Schematic of all experimental designs performed in electrophysiological recordings (continue)

Schematic	Name
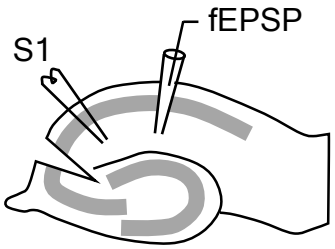	Field recordings with single stimulation
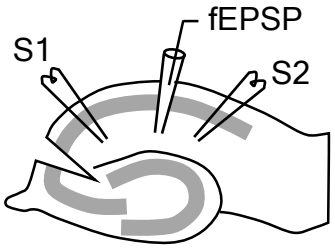	Field recordings with dual stimulation
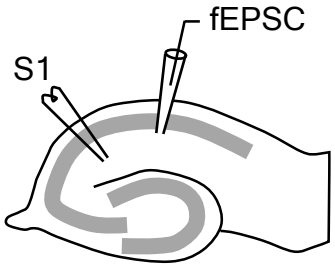 $[K_o]$ = 8 - 9 mM	Spontaneous epileptiform discharges

PC: Pyramidal cell; IN: Interneuron; dIPSC: disynaptic IPSC; fEPSP: field EPSP.

4.5 Stereotaxic injections

An adeno-associated virus serotype 2 or 5 construct (AAV2/5:ChR2-eYFP) was stereotaxically injected into dorsal hippocampus of heterozygous PV-Cre, CCK-Cre, and CaMKII-Cre mice (CA1-CA3 area). The AAV2/5 particle suspension (titre:

±4 x 10^{12} per mL) carrying fusion genes for ChR2 and eYFP (Figure 3.6A, p61) (Boyden et al. 2005) were produced by Vector Core Services, Gene Therapy Centre Virus, University of North Carolina, USA. For *in vivo* delivery of virus to Cre-expressing interneurons, mice were anesthetized in a chamber with 2 – 4% isoflurane in 99.5% oxygen. The depth of anaesthesia was monitored throughout the procedure, and peri-operative analgesia was administered (buprenorphine 0.1 mg/kg body weight, subcutaneous injection; Vetergesic, Alstoe Animal Health, York, UK). The mouse was laid on the heated platform of a stereotaxic frame (Model 1900; Kopf Instruments, California, USA) and its head secured. Ocular lubricant (Allergan, Marlow, UK) was applied, and the scalp was shaved with an electric razor and swabbed with iodine then lidocaine 5% m/m ointment. Under a surgical microscope (Wild Heerbrugg M655, Gais, Switzerland), a small area of cranium was exposed and a hole drilled on bilaterally, 1.70 mm caudal from Bregma and 1.40 mm lateral from Lambda using a Microtorque II drill (Ram Products) bathed periodically with saline (NaCl 0.9% w/v). A 33-gauge needle attached to a Hamilton Microlitre Syringe (UK) was placed 1.20 to 1.60 mm below the brain surface. In each hemisphere, 800 nL of virus suspension was delivered at a rate of 80 nL/min through a pump-driven syringe (Ultra Microsyringe pump / Micro4 controller; World Precision Instruments, Sarasota, FL, USA). Injections were distributed such that ±200–300 nL of virus suspension was injected at each of three positions, ±0.20 mm apart. After injection at the lowest site, the needle was retracted by 0.20 mm for another injection, and then again by 0.20 mm for a third injection. After each injection and before retracting the needle, there was a 2 min

wait to ensure that virus settled and diffused at the selected injection sites. After the third injection and following the 2 min wait, the needle was slowly retracted fully. Staggered injections served to increase transfection along the horizontal brain axis and thus maximise the yield of horizontal brain slices. Finally, the scalp incision was sutured with biodegradable thread and with tissue adhesive (Vetbond, 3M, Bracknell, UK), and bupivicaine hydrochloride 0.25% ointment applied to the wound. A subcutaneous injection of 200 µl glucose saline (NaCl 0.9% w/v + glucose 5% w/v) was administered to compensate for dehydration during surgery. Isofluorane was then withdrawn and the mouse released from the stereotaxic frame and allowed to breathe 99.5% oxygen for a few minutes until conscious, then removed to a heated cage for recovery and monitoring. Injected mice recovered for 10–21 days prior preparation of slices to allow good transfection and viral ChR2-eYFP expression.

4.6 Morphologic and immunohistochemical analysis

4.6.1 Tissue fixation and re-sectioning

After whole cell recordings the pipette was carefully detached from the cell under IR-DIC observation then rapidly withdrawn from the slice. Neurons filled with biocytin (0.4%) during whole-cell recordings (at least 30 min) were fixed overnight at 4°C in fixative solution containing 4% paraformaldehyde and 15% picric acid in 0.1 M phosphate buffer (PB; pH 7.4). During fixation, some slices were kept between 2 mixed cellulose ester membrane filter papers (Millipore, Durham, UK) to minimize deformation. Next day, slices

were thoroughly washed in 0.1 M PB, and stored in PB supplemented with 0.05% sodium azide at 4°C. For resectioning, slices were embedded in 20% gelatine and fixed for 1 h. The base of the gelatine block was glued to a microtome plate using cyanoacrylate adhesive, and embedded slices were re-sectioned at 60-70 µm thickness with a Leica VT1000S vibrating microtome in 0.1 M PB.

4.6.2 Cell reconstructions

All sections obtained from a re-sectioned slice were washed in 50 mM Tris-buffered saline (TBS; pH 7.4) with 0.3% Triton X-100 (TBS-Tx) and incubated overnight with streptavidin conjugated to either Alexa Fluor 488 (diluted 1:1000, Invitrogen, Eugene, OR, USA) or Cy3 (diluted 1:2000, Jackson ImmunoResearch Laboratories, Inc., USA) in TBS-Tx. The next day, sections were washed in TBS-Tx, mounted in Vectashield (H-1000, Vector Laboratories, Peterborough, UK) and examined with a DM5000 B epifluorescent microscope (Leica Microsystems Ltd., Milton Keynes, UK) using an appropriate filter set (L5, Y3) and an ORCA-ER CCD camera (Hamamatsu, Welwyn Garden City, UK). Digital micrographs were constructed from z-stack images recorded with epifluorescence microscope, collapsed and analyzed with Image-J software (v1.43u, NIH, MD, USA; NeuronJ plugin) or Microsoft Office Powerpoint software (Microsoft Corporation, Redmond, USA).

4.6.3 Immunohistochemistry

Free-floating 60- to 70-µm-thick sections were washed in TBS-Tx, blocked in 20% normal horse serum (NHS, Vector Laboratories) in TBS-Tx for at least 1 h at room temperature, and incubated with the relevant primary antibodies (Table 4.5) at 4 °C for 48 h. Appropriate fluorochrome-conjugated secondary antibodies (Table 4.5) were applied overnight at 4 °C after thorough washing (3 x 20 min in TBS-Tx) to remove unbound primary antibody. After another wash in TBS-Tx (3 x 20 min), sections were mounted in Vectashield (H-1000, Vector Laboratories, Peterborough, UK) under coverslips. Immunoreactivity was evaluated in laser scanning confocal microscope at x40 or higher magnification using either a Zeiss LSM 510 META (Carl Zeiss, Jena, Germany) with LSM software or a Zeiss LSM710 (Carl Zeiss, Jena, Germany) with Zen2008 software. Micrographs were adjusted for brightness and contrast only. Immunoreactivity was declared negative when fluorescence was not detected in relevant parts of the cell in an area where similar parts of unfilled cells were immunopositive. Immunonegativity to CB_1R was confirmed on at least two separate regions with successful antibody staining. Immunoreactivity was considered inconclusive (‘not tested’) if antibody staining was insufficient at the tissue depth of Streptavidin-visualised axon.

Table 4.5 Primary and seconday antibodies

Antigen / Conjugate	Species	Type[a]	Supplier	Product Code	Dilution[b]
CB_1R	Guinea pig	P	Frontier Science Co., Ltd, Japan	Cb1-GP-Af530-1	1:1000
Pro-CCK	Rabbit	P	Dr. A. Varro, University of Liverpool, UK	-	1:1000
CCK	Mouse	M	Antibody/RIA Core, UCLA, USA	9303	1:5000
PV	Rabbit	P	Swant, Bellinzona, Swizterland	PV 28	1:5000
$GABA_AR$ δ subunit	Rabbit	P	Phospho Solutions, CO, USA	868-GDN	1:500
Ab-Cy3	Donkey anti-Mouse	-	Jackson Immuno Research, PA, USA	715-165-151	1:400
Ab-Cy5	Donkey anti-Rabbit	-	Jackson Immuno Research, PA, USA	711-175-152	1:250
Streptavidin-Alexa 488	-	-	Invitrogen, Eugene, OR, USA	S-32354	1:1000
Streptavidin-Cy3	-	-	Jackson Immuno Research, PA, USA	016-160-084	1:2000
Anti-Rabbit Horseradish Peroxidase	Mouse	P	Bio-Rad Laboratories, CA, USA	1706515	1:7500

[a]M: Monoclonal; P: Polyclonal.

[b]Dilutions in TBS-Tx containing 1% normal horse serum (NHS).

4.7 Immunoblot assay

Hippocampal slices were prepared as described for electrophysiological recordings (Chapter 4.4, p70) and incubated with tested drug as described for tonic inhibitory currents (Chapter 4.4.1.4, p77). After the incubation period, the tissue (12-14 slices per condition) was stored at -80ºC. Samples were sonicated in 1% NP-40 lysis buffer containing (in mM): 50 Tris-HCl (pH 7.5), 150 NaCl, 5 ethylenediamine tetra-acetic acid (EDTA), 2 dithiothreitol (DTT), sodium dodecyl sulfate (SDS) 0.1% and protease inhibitors (Roche). The lysate was incubated on ice and then the supernatant was collected following centrifugation at 14,000 rpm (16000 x g) for 10min at 4°C. Protein concentrations were determined using a commercial Bradford assay (Sigma-Aldrich, St. Louis, MO, USA). Total protein (100µg) was loaded onto a 10% SDS polyacrylamide gel, subjected to gel electrophoresis, transferred to a polyvinylidene fluoride (PVDF) membrane (GE Healthcare, Little Chalfont, UK), blocked in 10% nonfat milk, and probed with an antibody specific for the $GABA_AR$ δ subunit (1:500, 868-GDN, PhosphoSolutions, CO, USA) (Table 4.5, p96). After washing (3 x 5 min in TBS-T (10 mM Tris, 150 mM NaCl, 0,05% Tween 20 in H_2O)), blots were incubated with secondary antibodies conjugated with horseradish peroxidase (Table 4.5, p96) and bands were visualized with a commercial enhanced chemiluminescence detection method (ECL) kit (PerkinElmer Life Sciences, MA, USA). Values were normalized to glyceraldehyde-3- phosphate dehydrogenase (GAPDH) loading control and the relative intensities were normalized to the control sample.

Densitometry of the bands was performed using the ImageJ software (v1.43u, NIH, MD, USA).

4.8 Statistical analysis

Data are expressed as the mean ± SEM of *n* cells from different slices (electrophysiological recordings) or *n* measurements from independent experiments (immunoblot assay). Normal distribution was tested by Shapiro-Wilk test. When passed, statistical significance was assessed either by two-tailed Student's t-test, when comparing 2 groups, or by performing one-way ANOVA followed by Bonferroni´s post-hoc test for comparison between multiple experimental groups. Otherwise, Mann-Whitney was used instead and data shown as median and quartiles. A P-value of less than 0.05 was considered to account for significant differences. Analyses were conducted with the GraphPad Software (La Jolla, CA, USA) or SigmaPlot software (Systat Software Inc., London, UK).

5 Results

5.1 Adenosine A_1R suppresses tonic $GABA_A$R currents in hippocampal pyramidal cells and in a defined subpopulation of interneurons

The work presented in this Chapter was published in:

- *Rombo DM, Dias RB, Duarte ST, Ribeiro JA, Lamsa KP, Sebastião AM (2014). Adenosine A1 receptors suppress tonic GABAA receptor currents in hippocampal pyramidal cells and in a defined subpopulation of interneurons. Cerebral Cortex. (Epub ahead of print).*

***DMR** performed all experiments described in this chapter except experiments shown in Figure 5.13 (p120) performed by **STD**.*

5.1.1 Summary

Adenosine is an endogenous neuromodulator that decreases excitability of hippocampal circuits activating membrane-bound metabotropic A_1R. The presynaptic inhibitory action of adenosine A_1R in glutamatergic synapses is well documented, but its influence on inhibitory GABAergic transmission is poorly known. Here is reported that $GABA_AR$-mediated tonic, but not phasic, transmission is suppressed by A_1R in hippocampal neurons. Adenosine A_1R activation strongly inhibits $GABA_AR$ agonist (muscimol)-evoked currents in CA1 pyramidal neurons and in a specific subpopulation of interneurons expressing axonal CB_1R. In addition A_1R suppresses tonic $GABA_AR$ currents measured in the presence of elevated ambient GABA as well as in naïve slices. The inhibition of GABAergic currents involves both PKA and PKC signaling pathways and decreases $GABA_AR$ δ-subunit expression. On the contrary, no A_1R-mediated modulation was detected in phasic IPSCs evoked either by afferent electrical stimulation or spontaneous quantal release. The results show that A_1R modulates extrasynaptic rather than synaptic $GABA_AR$-mediated signaling and that this modulation selectively occurs in hippocampal pyramidal neurons and in a specific subpopulation of inhibitory interneurons. It is concluded that modulation of tonic $GABA_AR$ signaling by adenosine A_1R in specific neuron types may regulate neuronal gain and excitability in the hippocampus.

5.1.2 Rational

GABA-releasing hippocampal interneurons regulate excitability of postsynaptic neurons via phasic and tonic $GABA_AR$-mediated signaling (McBain & Fisahn 2001, Klausberger & Somogyi 2008). GABAergic phasic transmission shows fast and precisely-timed current kinetics generated by synaptic $GABA_AR$. Tonic inhibition is generated by sustained or persistent activity of mainly extrasynaptic (Brickley et al. 1996, Salin & Prince 1996, Semyanov et al. 2003) high-affinity and slowly-desensitizing $GABA_AR$ (Nusser et al. 1998, Haas & Macdonald 1999, Bianchi & Macdonald 2003, Caraiscos et al. 2004b). In the hippocampus, tonic $GABA_AR$-mediated currents have been characterized in pyramidal cells (Bai et al. 2001) and in inhibitory interneurons (Semyanov et al. 2003). Tonic and phasic inhibition exhibit distinct pharmacological properties (Semyanov et al. 2004, Farrant & Nusser 2005, Mann & Paulsen 2007) and hence these can be selectively modulated (Farrant & Nusser 2005). Adenosine, acting through high-affinity A_1R, is a well characterized endogenous modulator of neuronal activity in the brain (Sebastião & Ribeiro 2009). Adenosine A_1R modulates excitatory glutamatergic synapses both at pre- and postsynaptic site (Boison 2012, Dias et al. 2013). On the contrary, phasic GABAergic transmission in pyramidal cells is not modulated by A_1R (Burke & Nadler 1988, Kamiya 1991, Lambert & Teyler 1991, Yoon & Rothman 1991, Cunha & Ribeiro 2000a). However, in pyramidal cells immunohistochemical studies show intense labeling of A_1R not only in dendritic glutamatergic synapses, but also in the perisomatic region where synapses are mainly GABAergic and

inhibitory (Kasugai et al. 2010). Adenosine A_1R are also expressed postsynaptically in GABAergic interneurons (Rivkees et al. 1995, Ochiishi et al. 1999). Although phasic $GABA_AR$ currents are unaffected by A_1R activity, it is unknown whether tonic inhibitory currents in pyramidal cells are modulated by the receptor. In addition, how adenosine A_1R acts on disinhibitory signaling, i.e. GABAergic transmission in inhibitory interneurons has not been studied. The work described in this chapter was designed to evaluate the influence of A_1R actions on hippocampal inhibitory responses, namely on tonic $GABA_AR$ responses in pyramidal cells and different subpopulations of interneurons.

5.1.3 Adenosine A_1R inhibits agonist-evoked $GABA_AR$-mediated currents in CA1 pyramidal cells

To investigate whether activation of adenosine A_1R influences $GABA_AR$-mediated responses in the postsynaptic neuron, it was performed whole-cell patch-clamp recordings (Vh = -70 mV). In a first set of experiments, a selective $GABA_AR$ agonist, muscimol (30 µM), was pressure applied close to the soma of the recorded CA1 pyramidal cell (Figure 5.1A) eliciting postsynaptic currents (muscimol-PSCs) that were blocked by $GABA_AR$ antagonist gabazine (10 µM; n = 4; Figure 5.1D). Pyramidal cells were identified by their localization inside pyramidal cell layer (*stratum pyramidale*) (Figure 5.1B) and in some recordings biocytin was added to the internal solution for anatomical reconstruction (Figure 5.1C).

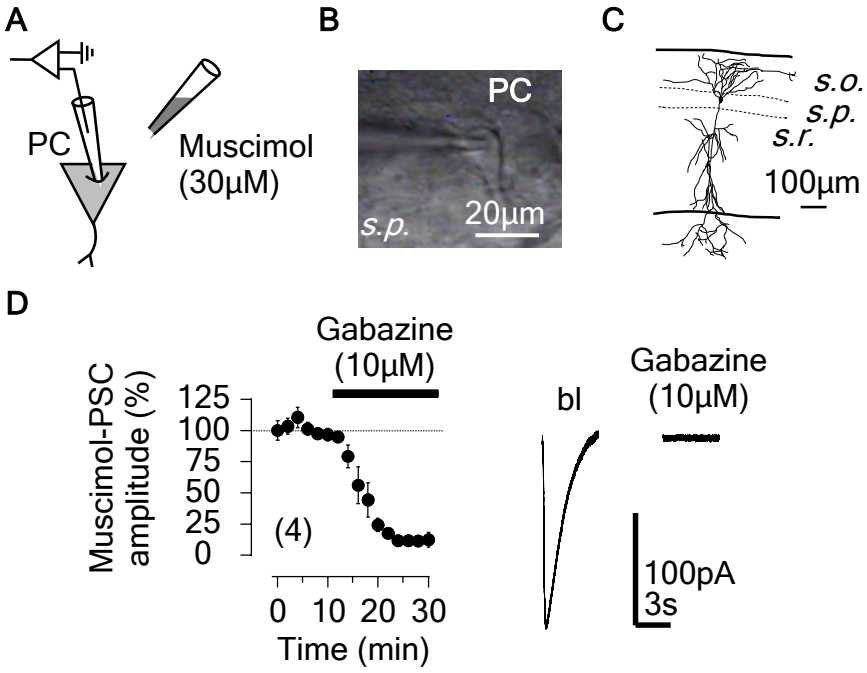

Figure 5.1. Local agonist (muscimol)-evoked $GABA_A$ currents in pyramidal cells
(A) Schematic representation of the experimental design to evoke postsynaptic $GABA_A$ currents by local application of a $GABA_AR$ agonist, muscimol (30 µM, muscimol-PSC) on the soma of a voltage-clamped pyramidal cell. **(B)** Differential interference contrast-infrared (DIC-IR) image. **(C)** Illustration of a recorded pyramidal cell. **(D)** Left: Gabazine (10 µM) completely abolishes the agonist-evoked $GABA_AR$ currents (baseline-normalized mean ± SEM, n = 4); right: Representative PSCs from one cell in baseline (bl) and after application of gabazine (10 µM); each trace is the average of 5 consecutive responses. In all panels, the number of experiments is shown in brackets; PC: pyramidal cell; *s.r.*: *stratum radiatum*; *s.p.*: *stratum pyramidale*; *s.o.*: *stratum oriens*.

It was found that the adenosine A_1R agonist CPA (30 nM) (Moos et al. 1985) decreased the amplitude of muscimol-PSCs and the suppression reached a steady-state within 40 min from wash-in of CPA (Figure 5.2A). The amplitude of muscimol-PSCs was significantly reduced in 14 of 16 cells tested (effect showing a Gaussian distribution, Shapiro-Wilk test, n = 16; Figure 5.2B) indicating consistency of effect in pyramidal cells. CPA induced an average decrease to 62.1 ± 4.5% of the baseline (n = 16, $P < 0.001$, t-test; Figure 5.2A,B). During CPA wash out, the

suppression persisted for at least 40min (Figure 5.2A,C). Data from all individual neurons are shown in a separate panel (Figure 5.2C).

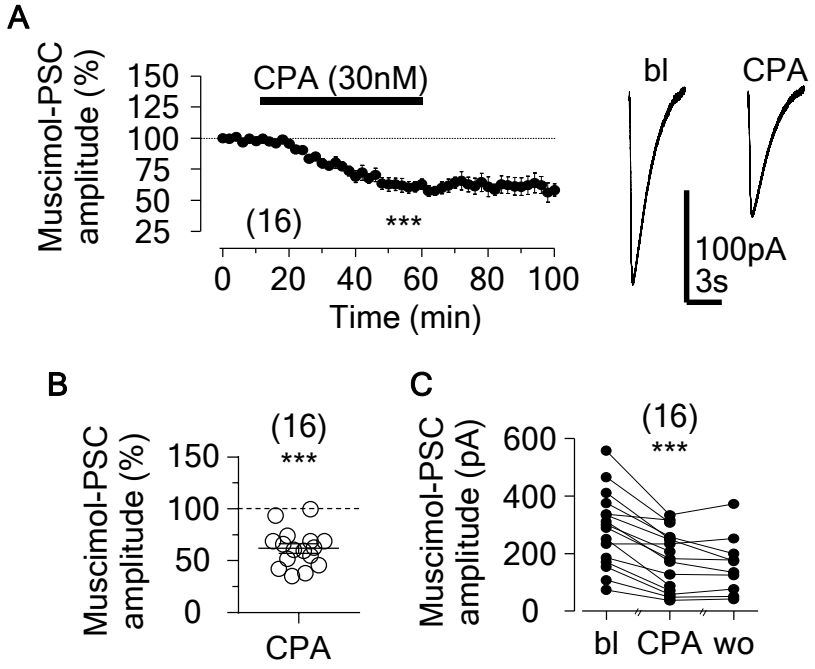

Figure 5.2. Adenosine A_1R suppresses muscimol-PSC in pyramidal cells.
(A) Left: A_1R agonist, CPA (30 nM) reduces the agonist-evoked $GABA_AR$ current amplitude (baseline-normalized mean ± SEM, n = 16); right: Representative PSCs from one cell in baseline (bl) and in the presence of CPA; each trace is the average of 5 consecutive responses. **(B)** Plot showing baseline-normalized PSC amplitude in all studied cells showing effect of CPA (30 nM) after baseline. **(C)** Muscimol-PSC amplitude (pA) of all cells in A and B, in baseline (bl), following wash-in of CPA and after 30 min washout of CPA (wo). Values from each cell are connected with line. In all panels, the number of experiments is shown in brackets; ***P < 0.001 (Student's t-test).

In a next set of experiments it was applied a high-affinity A_1R antagonist, DPCPX (100 nM) (Sebastião et al. 1990), to revert the suppressive effect of CPA on GABAergic currents. This restored muscimol-PSCs in all tested cells (average to 96.2 ± 3.7% of original baseline, n = 7, P < 0.001, t-test; Figure 5.3A,B), demonstrating that the CPA effect on $GABA_AR$ currents is reversible.

A lower concentration of CPA (10nM) was also capable of decreasing amplitude of muscimol-PSCs significantly in 12 out of 17 cells (Figure 5.3C). The magnitude of effect with 10nM CPA was not statistically different from 30 nM CPA (73.0 ± 5.4% of the baseline, n = 17 *vs* 60.3 ± 3.9% of the baseline, n = 23, P = 0.06; see Figure 5.3).

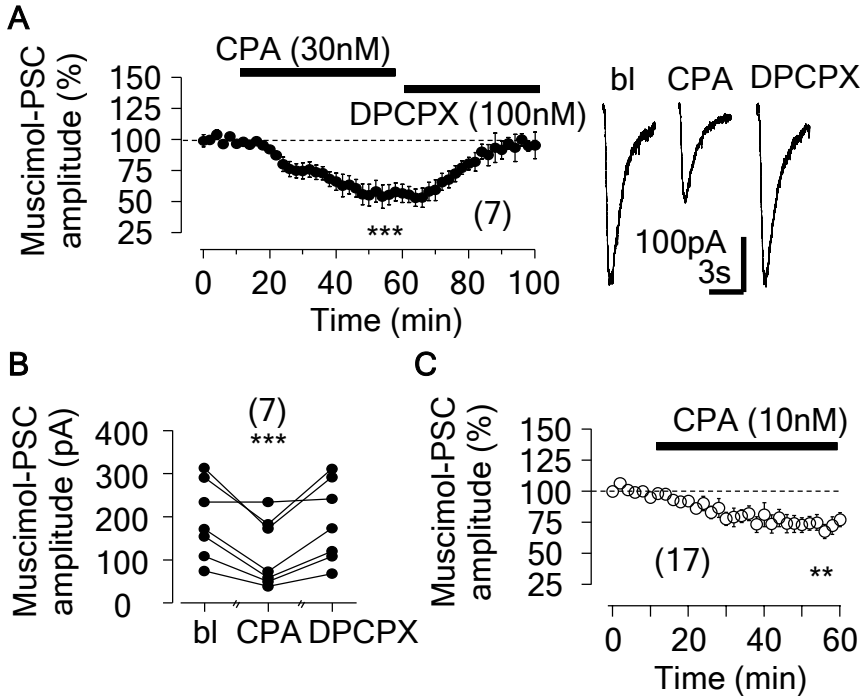

Figure 5.3. Adenosine A_1R antagonist facilitates recovery of muscimol.PSC after agonist action.
(A) Left: Wash-in of A_1R antagonist DPCPX (100 nM), fully restored CPA-inhibited muscimol-PSCs to the baseline level (baseline-normalized mean ± SEM, n = 7); right: Representative PSCs from one cell in the baseline (bl), in the presence on CPA and following further application of DPCPX; each trace is the average of 5 consecutive responses. **(B)** Muscimol-PSC amplitudes (in pA) of all cells in A, in baseline (bl), in the presence of CPA and following DPCPX application. Values from each cell are connected with line. **(C)** Lower concentration of the A_1R agonist, CPA (10 nM) also reduces muscimol-PSC amplitude (baseline-normalized mean ± SEM, n = 17). In all panels, the number of experiments is shown in brackets; **P < 0.01; ***P < 0.001 (Student's t-test).

In addition, CPA (30 nM) failed to change muscimol-PSC when washed in the presence of A_1R antagonist DPCPX (100 nM) (103.7 ± 1.4% of the baseline, n = 6, P = 0.17, t-test; Figure 5.4A). Interestingly it was found a significant increase in muscimol-PSCs following wash-in of DPCPX in naïve slices to 115.3 ± 4.9% of the baseline (n = 6, P < 0.05, t-test; Figure 5.4B), which suggests tonically activated-A_1R and suppression of $GABA_AR$-mediated currents in standard physiological conditions.

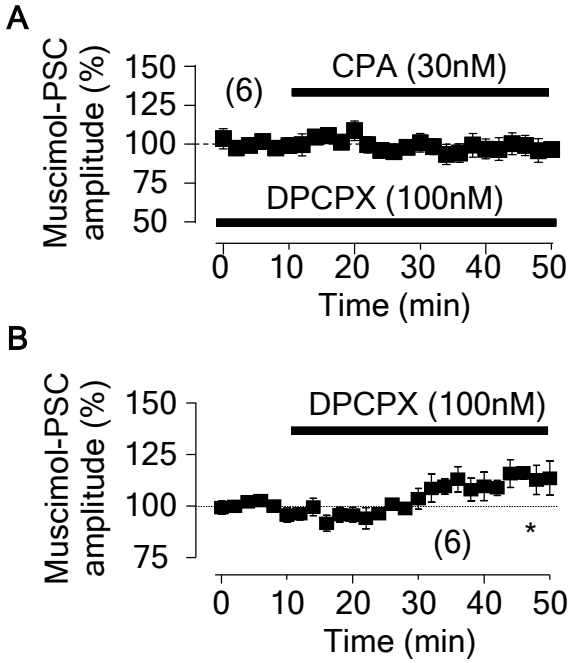

Figure 5.4. Endogenous activation of A_1R suppresses muscimol-PSCs
(A) Timecourse plot showing full prevention of CPA effect on muscimol-PSCs amplitude in the presence of DPCPX (100 nM) (baseline-normalized mean ± SEM, n = 6); **(B)** DPCPX (100 nM) alone had a facilitatory effect on muscimol-PSCs (baseline-normalized mean ± SEM, n = 6). In all panels, the number of experiments is shown in brackets; *P < 0.05 (Student's t-test).

To confirm that the observed inhibitory action of adenosine A_1R on $GABA_AR$ currents was not caused via an indirect effect on glutamatergic transmission or axonal GABAergic excitation (Alle & Geiger 2007, Ruiz et al. 2010), previous experiments were

reproduced in the continuous presence of NMDA and AMPA/Kainate (KA) receptor antagonists (50 µM DL-AP5 and 10 µM CNQX, respectively), and tetrodotoxin (TTX, 0.5 µM) to block action potential firing. Indeed in these conditions there was a similar suppression of muscimol-PSC by CPA (30 nM) as observed above (decrease in amplitude to 69.5 ± 8.0% of the baseline, n = 8, P < 0.001, t-test; Figure 5.5A).

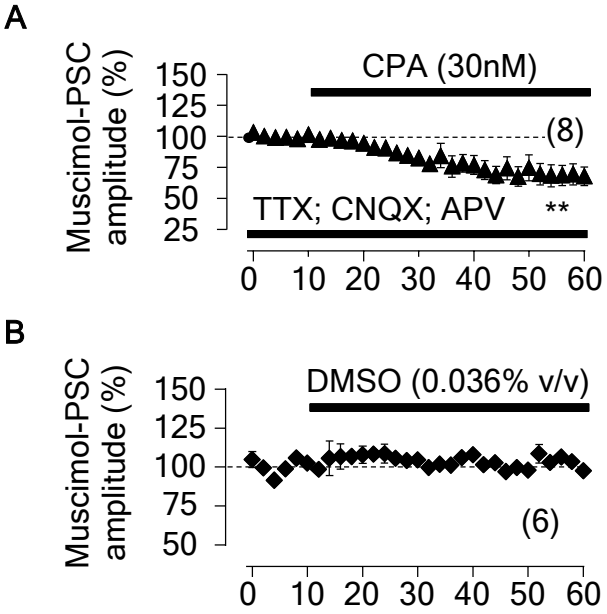

Figure 5.5. A_1R-mediated suppression of muscimol-PSC is independent of glutamatergic transmission and neuronal firing
(A) CPA-induced suppression of $GABA_AR$ currents in the presence of glutamate blockers (CNQX, 10 µM; APV, 50 µM), and TTX (0.5 µM; mean ± SEM, baseline-normalized, n = 8). **(B)** DMSO (maximal final concentration in aCSF was 0.036% v/v of DMSO) did not affected muscimol-PSCs (baseline-normalized mean ± SEM, n = 6). In all panels, the number of experiments is shown in brackets; **P < 0.01; (Student's t-test).

Also, the CPA solvent, DMSO (0.036% v/v) had no effect on $GABA_AR$ amplitude (104.0 ± 2.3% of the baseline, n = 6, P = 0.140, Figure 5.5B). Although previous studies have reported that GABAergic synapses may not be directly modulated by A_1R (Lambert & Teyler 1991) the results show suppression of agonist-

evoked postsynaptic $GABA_AR$-mediated currents in pyramidal cells.

A resume with most of the pharmacology performed to describe the A_1R-mediated effect on muscimol-PSC can be visualized in Figure 5.6.

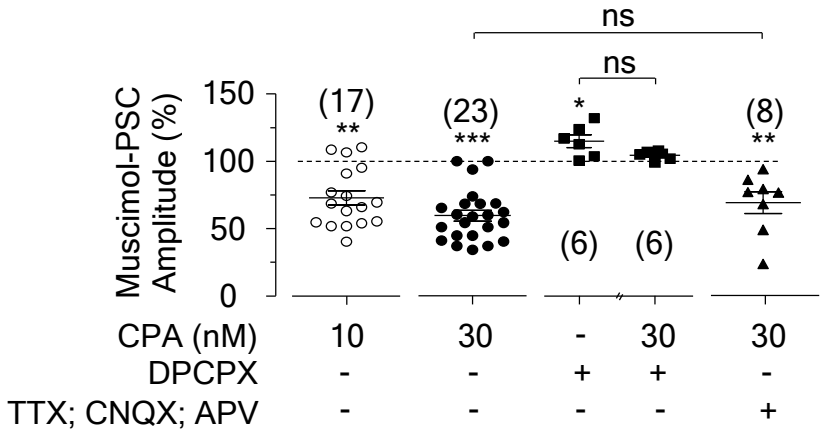

Figure 5.6. Pharmacology on A_1R-mediated suppression of muscimol-PSCs
Plot showing baseline-normalized PSC amplitude in different conditions in all studied cells; from left: Effect of CPA (10 nM) after baseline; effect of CPA (30 nM) after baseline; effect of DPCPX (100 nM) after baseline; full prevention of CPA effect on PSC amplitude in the presence of DPCPX; CPA-induced suppression of $GABA_AR$ currents in the presence of glutamate blockers (CNQX, 10 µM; APV, 50 µM), and TTX (0.5 µM) (mean ± SEM, baseline-normalized). In all panels, the number of experiments is shown in brackets; ns: not statistically significant; *P < 0.05; **P < 0.01 (Student's t-test).

5.1.4 Phasic $GABA_AR$-mediated currents are not affected by adenosine A_1R in CA1 pyramidal cells

I next explored whether adenosine A_1R modulates $GABA_AR$-mediated IPSCs evoked by electrical afferent fiber stimulation. Stimulation was in *stratum radiatum* or *stratum oriens* and monosynaptic IPSCs in pyramidal cells were recorded in the presence of CNQX (10 µM) and DL-AP5 (50 µM). The IPSCs were fully blocked with gabazine (10 µM) at the end of experiment (Figure 5.7A,B) indicating isolation of GABA-mediated currents. It

was found that in contrast to muscimol-PSCs, synaptic $GABA_AR$ IPSCs were not significantly modulated by CPA (30 nM) (89.3 ± 6.4% of the baseline, n = 9, P = 0.14, t-test; Figure 5.7C-E).

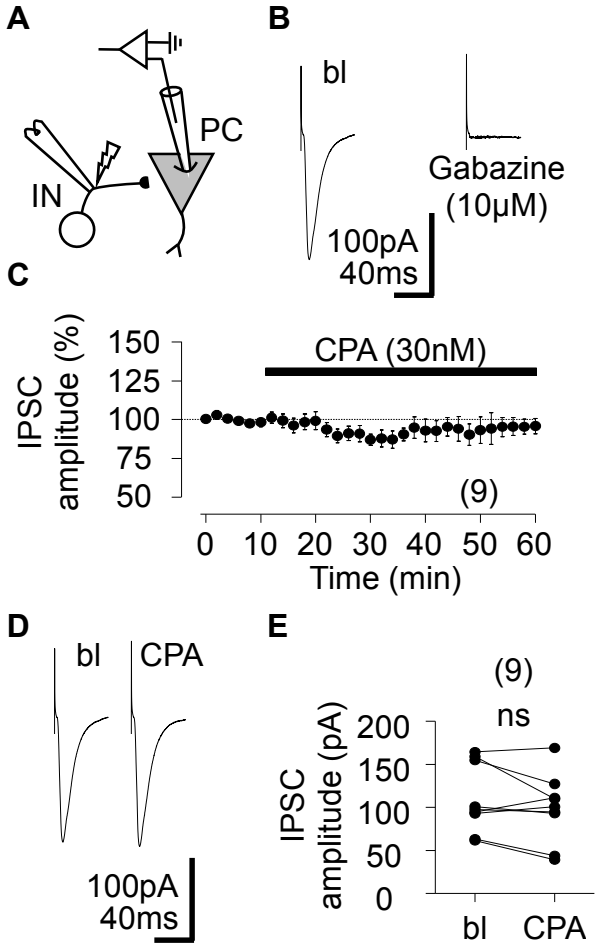

Figure 5.7. Adenosine A_1R agonist fails to suppress electrical-evoked IPSCs
(A) Schematic representation of the experimental design for IPSC recordings in pyramidal cells. **(B)** Representative IPSCs in baseline (bl) and after wash-in of gabazine (10 μM); each trace is the average of 10 consecutive responses. **(C)** IPSCs evoked in CA1 pyramidal cells by electrical stimulation of inhibitory afferents are not modulated by CPA (30 nM; baseline-normalized mean ± SEM, n = 9). **(D)** Representative IPSCs in baseline (bl) and after wash-in of CPA (30 nM). **(E)** IPSC amplitude (pA) in all cells during baseline (bl) and following wash-in of CPA; values from each cell are connected with line. In all panels, the number of experiments is shown in brackets; ns: not statistically significant (Student's t-test); PC: pyramidal cell; IN: interneuron.

It was also studied in separate experiments GABAergic miniature IPSCs (mIPSCs) in the presence of CNQX (10 μM), DL-AP5 (50 μM) and TTX (0.5 μM) (Figure 5.8A). Wash-in of CPA (30 nM for at least 50 min) failed to change either mIPSCs frequency (99.4 ± 2.2% of baseline, n = 13, P = 0.80, t-test; Figure 5.8B,D) or amplitude (100.1 ± 1.2% of baseline, n = 13, p = 0.96, t-test; Figure 5.8B,E), confirming a lack of modulation of synaptic IPSCs by A_1R.

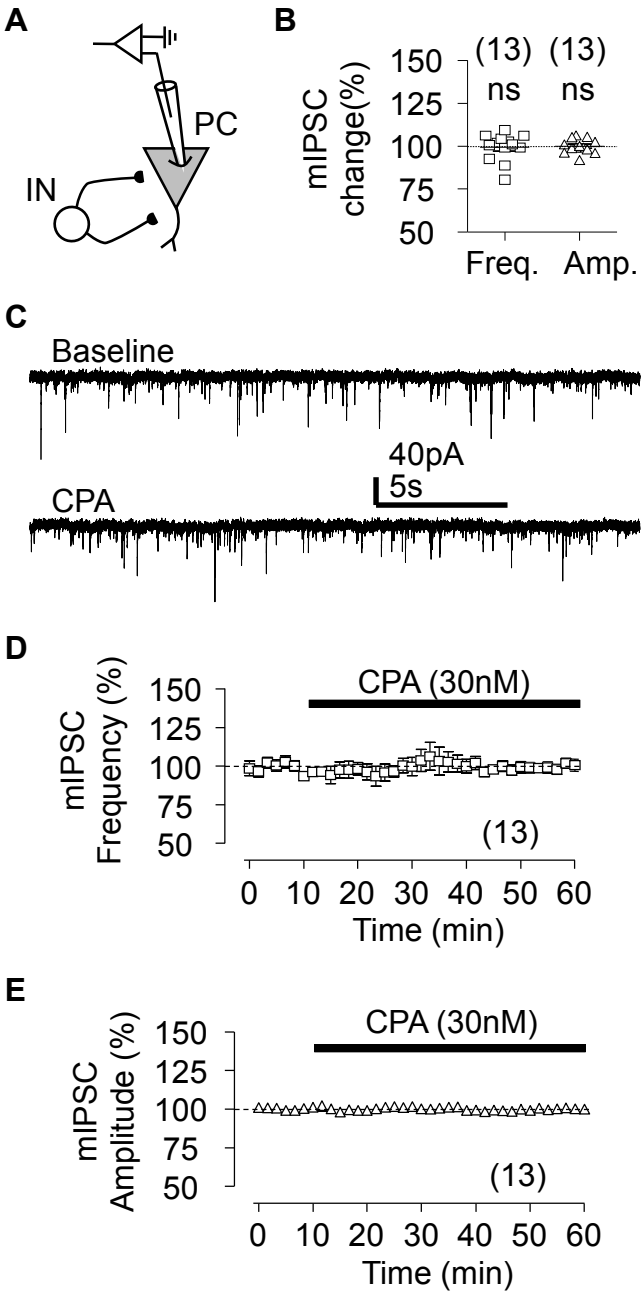

Figure 5.8. Spontaneous inhibitory activity is not affected by A1R activation
(A) Experimental design for mIPSC recordings in pyramidal cells. **(B)** mIPSC frequency and amplitude in individual cells (baseline-normalized; 100% corresponds to 9.6 ± 1.7 Hz and 11.8 ± 1.6 pA); **(C)** Sample traces from one cell in baseline and following wash-in of CPA. **(D and E)** CPA has no significant effect on either miniature frequency (D) or amplitude (E) of mIPSCs (baseline-normalized mean ± SEM, n = 13). In all panels, the number of experiments is shown in brackets; ns: not statistically significant (Student's t-test); PC: pyramidal cell; IN: interneuron.

5.1.5 Adenosine A_1R suppresses tonic GABAergic currents in CA1 pyramidal cells

Next, it was hypothesized that A_1R modulation could be selective to extrasynaptic $GABA_AR$. To test this it was studied adenosine A_1R agonist effects on tonic inhibitory currents (tonic-IC) in pyramidal cells. Whole-cell voltage clamp recordings (Vh = -70 mV) were performed in CA1 pyramidal cells in the continuous presence of glutamate receptor blockers (CNQX, 10 µM; DL-AP5, 50 µM) and TTX (0.5 µM). In addition, and to avoid any interference of adenosine receptors upon GAT activity (Cristóvão-Ferreira et al. 2009, 2013), which could indirectly affect tonic-ICs, the GABA transporters blockers, SFK89976A (20 µM; GAT-1 inhibitor) and SNAP5114 (20 µM; GAT-3 inhibitor), were added to the superfusion solution. Also, unless indicated otherwise, tonic currents were recorded in aCSF with 5 µM GABA added to standardize the ambient GABA levels around the recorded neurons, which might otherwise vary with the depth of the neuron in the slice, the level of local spontaneous GABA release or type of neuron. Indeed, consistent with previous reports (Semyanov et al. 2003, Glykys & Mody 2007b), pyramidal cells did not express measurable tonic $GABA_AR$-mediated conductance (-3.1 ± 1.1pA, n = 4), unless the extracellular concentration of GABA was enhanced (Glykys & Mody 2007b), which also increased the signal-to-noise ratio. Therefore, in the remaining experiments aiming to evaluate tonic-ICs in pyramidal cells, GABA (5 µM) was added to the superfusion solution (Figure 5.9A). Tonic currents were determined as described in Chapter 4.4.1.4 (p77). Briefly, an all-point histogram was plotted every 1 s, obtaining a distribution

skewed to the left side, where synaptic events occur (see inboxes in Figure 5.9C). The mean of a Gaussian fit to the non-skewed side of the distribution was considered as the mean holding current that formed the basis for the determination of the tonic current (Figure 5.9C). Tonic-IC magnitude was measured comparing the mean holding current before and in the presence of gabazine (100 µM, Figure 5.9B).

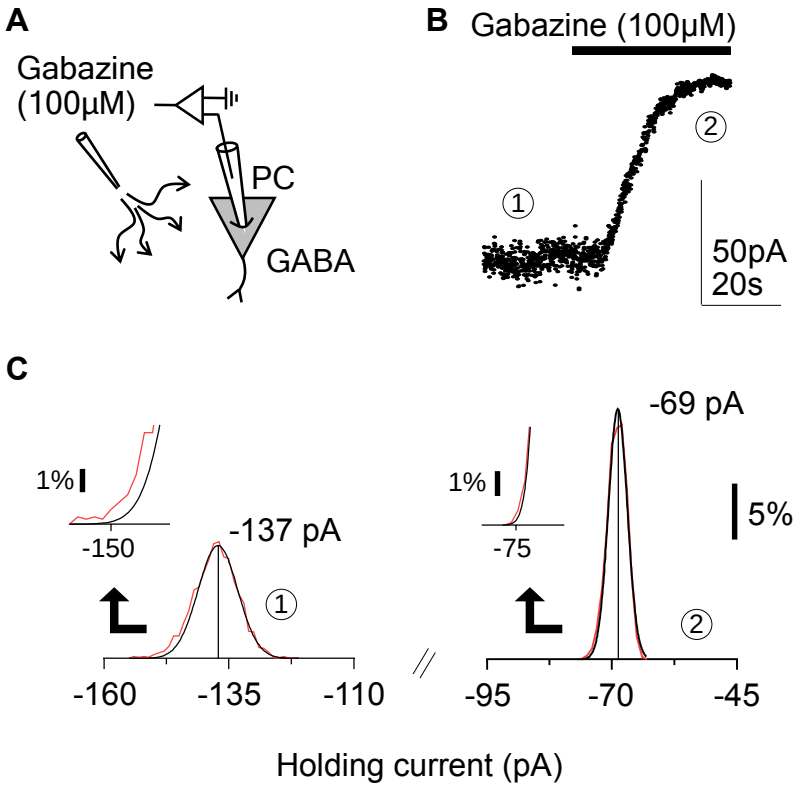

Figure 5.9. Recording and measurement of tonic inhibitory currents
(A) Schematic representation of the experimental design used to access tonic currents; whole-cell voltage-clamp recording from a CA1 pyramidal cell (Vh = -70 mV) revealed tonic $GABA_AR$ inhibition (amplified by adding 5 µM ambient GABA) after application of gabazine (100 µM); the difference between the holding current in the absence and presence of gabazine was used as tonic current measurement (see Chapter 4.4.1.4, p77). **(B)** Tonic current (plotted at 5 ms intervals) recorded from an individual pyramidal cell in a control slice. **(C)** Gaussian fits (black line) to the all-points histograms (red line) of the indicated periods in B. The peak of the Gaussian denotes the mean tonic current while all the points outside of the Gaussian distribution (skewed to the left) constitute the phasic current; insets: higher magnifications of the corresponding graphs to show the contribution of phasic transmission for the histogram in 1 (left panel) that disappears in 2 (right panel). Numbers indicate the corresponding time periods in B. PC: pyramidal cell.

Interestingly, in the presence of CPA (30 nM, incubated for at least 50 min) tonic-ICs were significantly lower than in control slices (Figure 5.10A). The average of tonic-IC in control conditions was -119.7 ± 12.5 pA (n = 8), and decreased to -57.7 ± 14.8 pA (n = 7) when incubated with CPA ($P < 0.01$, t-test; Figure 5.10B,C).

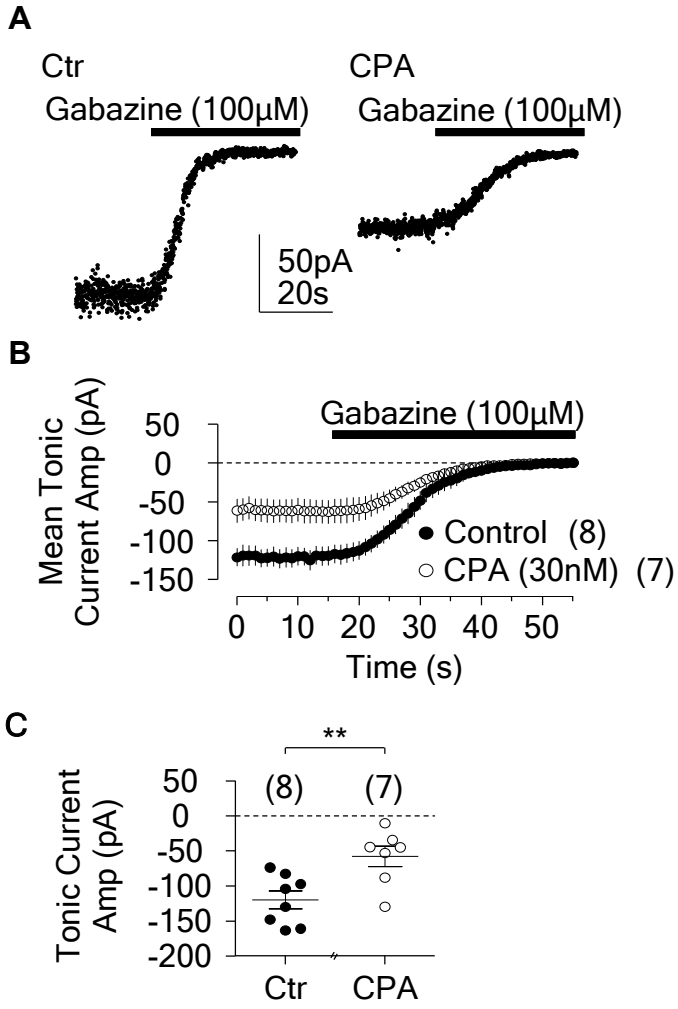

Figure 5.10. Tonic-ICs are suppressed by A_1R activation
(A) Tonic current (plotted at 5 ms intervals) recorded from an individual pyramidal cell in a control slice (left) and in a CPA (30 nM)-incubated slice (right). **(B)** Averaged tonic current (mean ± SEM, pA) recorded from pyramidal cells in control slices (filled circles, n = 8) and in slices where CPA (30 nM) was added at least 50 min prior gabazine (open circles; n = 7); note that tonic $GABA_A$ currents were quantitatively smaller in the presence of CPA. **(C)** Plot showing tonic $GABA_AR$ current in all studied cells in control slices and in slices incubated with CPA. In all panels, the number of experiments is shown in brackets; **P < 0.01 (Student's t-test).

These results, taken together with the absence of effect of CPA upon afferent evoked IPSCs and mIPSCs, allow to conclude that adenosine A_1R in pyramidal neurons selectively suppress tonic

inhibitory currents, known to be mediated by extra- and perisynaptically-localized $GABA_AR$.

5.1.6 Adenosine A_1R-mediated effect on $GABA_A$ currents is PKA/PKC-dependent

Adenosine A_1R is $G_{i/o}$ coupled (Freissmuth et al. 1991, Jockers et al. 1994, Nanoff et al. 1995) and involve signaling cascades that require PKA and in some cases, PKC (Akbar et al. 1994, Cascalheira & Sebastião 1998). $GABA_AR$-mediated currents are affected by activity of both PKA (Kano & Konnerth 1992, Kano et al. 1992, Moss et al. 1992, Robello et al. 1993, Nusser et al. 1999, Poisbeau et al. 1999) and PKC signalling pathways (Poisbeau et al. 1999, Brandon et al. 2002b, Bright & Smart 2013). Therefore, it was tested whether activity of those kinases could be involved in A_1R suppression of tonic $GABA_AR$ currents. The PKC or the PKA blockers (GF109203x, 1 µM, or Rp-cAMPs, 100 µM, respectively) were added intracellularly through the whole-cell patch pipette filling solution (Figure 5.11A). In either situation (intracellular inhibition of PKA or PKC) the effect of CPA (30 nM) on muscimol-PSC was blocked. Muscimol-PSCs amplitude in the presence of CPA and GF109203x was 97.1 ± 4.3% (n = 6, P = 0.53, t-test; Figure 5.11B-D) and in the presence of CPA and Rp-cAMPs 101.0 ± 4.0% (n = 6, P = 0.80, t-test; Figure 5.11C-E) of the pre-CPA values. These results show the involvement of both kinases in A_1R modulation of GABAergic currents.

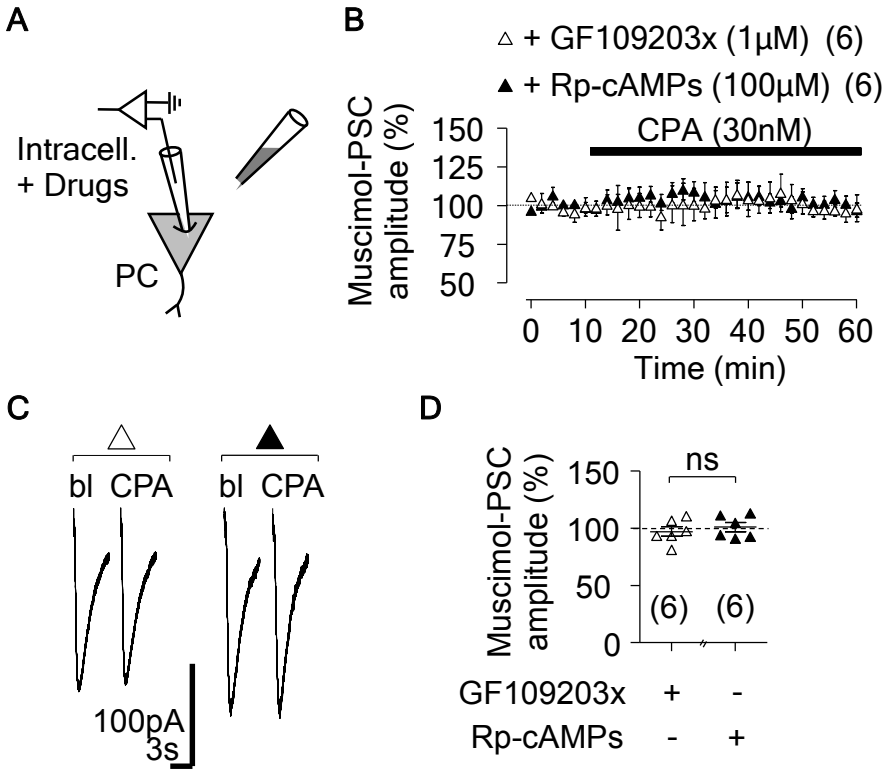

Figure 5.11. PKA and PKC are involved in A_1R-mediated suppression of muscimol-PSCs

(A) Schematic experimental design; drugs were added to the intracellular solution when mentioned. **(B)** Either a PKC inhibitor (GF109203x, 1 µM) or a PKA blocker (Rp-cAMPs, 100 µM) in pipette filling solution prevents suppression of GABAergic currents by CPA (30 nM; baseline-normalised mean ± SEM; n = 6 for both conditions). **(C)** Representative muscimol-PSCs in the presence of GF109203x (open triangle) or Rp-cAMPs (filled triangle) in baseline (bl) and following application of CPA. **(D)** Baseline-normalized muscimol-PSCs in all studied cells in the presence of either GF109203x or Rp-cAMP. In all panels, the number of experiments is shown in brackets; the representative PSCs correspond to the average of 5 consecutive responses; ns: not statistically significant (Student's t-test).

Then it was questioned whether the sequence of kinase activation cascade involved in this processes could be uncovered. The muscimol-PSCs modulation was evaluated while activating one of the signaling pathways and blocking the other one.

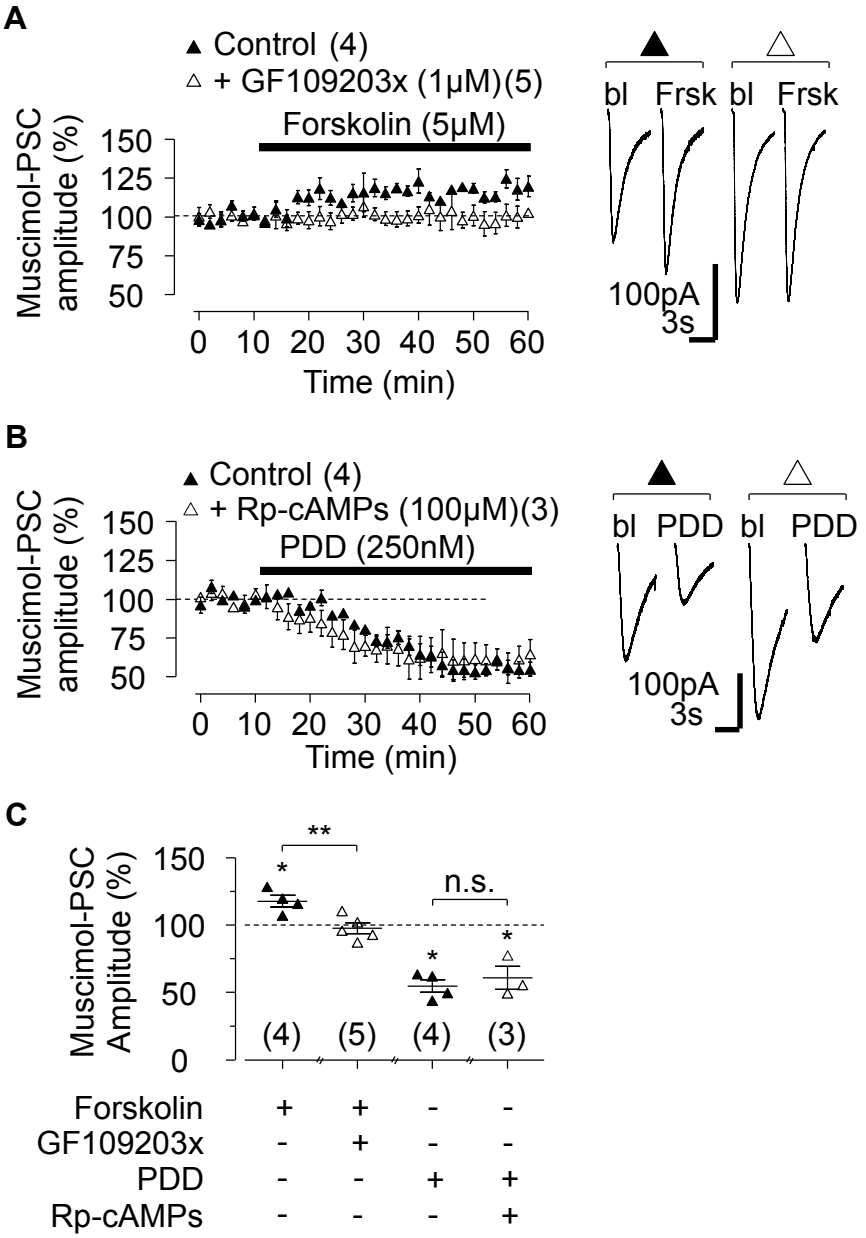

Figure 5.12. PKC activity is downstream PKA activity to suppress muscimol-PSCs
(A) Left: Plot showing that intracellular application of GF109203x completely prevented the facilitatory effect of Forskolin (5 μM) on muscimol-PSCs (baseline-normalized mean ± SEM; n = 4-5 as indicated). Right: Representative muscimol-PSCs in one pyramidal cell in baseline (bl) and after Forskolin application (Frsk), in the absence (filled triangle) or presence (open triangle) of GF109203x. **(B)** Left: Plot showing that intracellular Rp-cAMPs failed to prevent a PKC activator PDD (250 nM)-elicited suppression of muscimol-PSCs (baseline-normalized mean ± SEM; n = 3-4 as indicated). Right: Representative muscimol-PSCs in baseline (bl) and after PPD perfusion, in the absence (filled triangle) or presence (open triangle) of intracellular

Rp-cAMPs. **(C)** Baseline-normalized muscimol-PSC in all studied pyramidal cells shown in A and B; from left: application of Forskolin after baseline; intracellular GF109203x with forskolin; application of PDD after baseline; and intracellular Rp-cAMPs with forskolin. In all panels, the number of experiments is shown in brackets; the representative PSCs correspond to the average of 5 consecutive responses; ns: not statistically significant; *P < 0.05; **P < 0.01 (Student's t-test).

First, the adenylate cyclase (AC) activator, forskolin (5 μM) (Seamon et al. 1981) was bath applied to activate cAMP/PKA signaling. Forskolin increased the amplitude of muscimol-PSC to 117.5 ± 4.4% of baseline (n = 4, P = 0.029, t-test; Figure 5.12A,C). The effect was similar to blockade of A_1R in naïve slices with DCPCX (see Figure 5.4). Loading the patch pipette with PKC inhibitor, GF109203x (1 μM), completely prevented forskolin effect on muscimol-PCSs (96.0 ± 4.1% of baseline, n = 5, P = 0.38, t-test; Figure 5.12A,C). These results suggest that PKA signaling is upstream of PKC in the $GABA_AR$ current suppression cascade. To further test this idea, an activator of PKC, Phorbol 12,13 Didecanoate (PDD, 250 nM) was washed-in. This suppressed muscimol-PSCs to 54.4 ± 4.8% of baseline (n = 4, P = 0.002, t-test; Figure 5.12B,C), akin to the generated by A_1R activation with CPA (see Figure 5.2). Adding a PKA inhibitor, Rp-cAMPs to the pipette filling solution failed to prevent the suppression of muscimol-PSCs by PDD (60.5 ± 8.6% of baseline; n = 3, P = 0.04, t-test; Figure 5.12B,C). Altogether these results show that PKC is downstream to PKA activation in the $GABA_AR$ current suppression cascade.

Knowing that $GABA_ARs$ are substrate for kinases and that PKC activity decreases extrasynaptic $GABA_AR$ expression (Bright & Smart 2013), it was evaluated if A_1R actions on tonic inhibition could be associated with decreased expression of $GABA_AR$. It was performed immunoblot assays against the δ-subunit of $GABA_AR$,

a subunit present exclusively in extrasynaptic and perisynaptic $GABA_AR$s in the hippocampus (Nusser et al. 1998, Wei et al. 2003, Sun et al. 2004, Glykys & Mody 2007a), therefore most relevant for tonic-ICs. It was found that in slices that had been incubated with CPA (30 nM, for at least 50 min) $GABA_AR$ δ-subunit immunoreactivity was significantly decreased to 68.5 ± 9.5% when compared to the control slices (n = 4, P = 0.04, paired t-test; Figure 5.13).

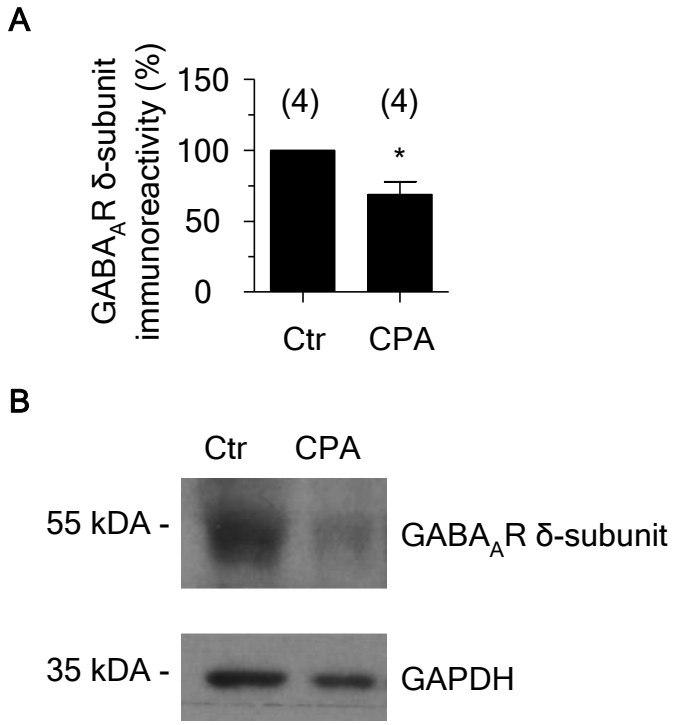

Figure 5.13. Adenosine A_1R decreases $GABA_AR$ δ-subunit immunoreactivity
(A) Plot showing control-normalized $GABA_AR$ δ-subunit immunoreactivity after incubation of hippocampal slices in the absence (control: Ctr) or presence of CPA (30 nM) for at least 50 min (see Chapter 4.7, p97 for details). **(B)** Representative western blot obtained from control slices (left lane) and from slices treated with CPA (30 nM) for at least 50 min (right lane). GAPDH was used as a loading control (bottom lanes).

Together, these results demonstrate that A_1R actions upon GABAergic currents involve postsynaptic signaling requiring both PKA and PKC pathways and suggest that A_1R activation leads to

inhibition of PKA signaling, releasing PKC activity which then suppresses $GABA_AR$ currents (Figure 5.14).

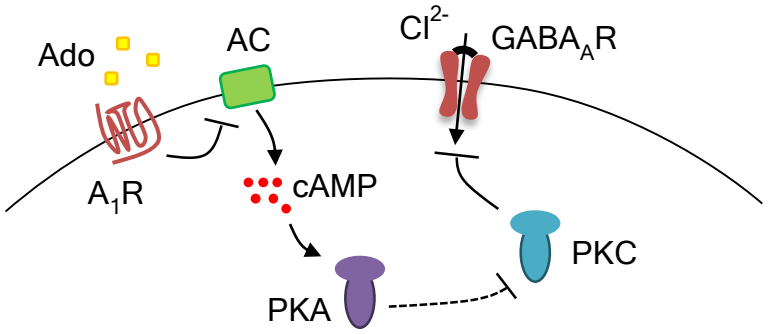

Figure 5.14. Schematic representation of the signaling cascade involved in A_1R-mediated suppression of $GABA_AR$
Schematic diagram of suggested postsynaptic cascade of PKC and PKA action underlying A_1R-mediated inhibition of $GABA_AR$ currents. AC: adenylate cyclase; Ado: adenosine; cAMP: cyclic adenosine 5′-monophosphate; Cl^-: chloride; PKA: protein kinase A; PKC: protein kinase C.

Results from immunoblot assays fit this idea, suggesting that A_1R mediated-decrease in tonic inhibition is associated with decreased expression of extrasynaptic $GABA_AR$ δ-subunit.

5.1.7 Adenosine A_1R suppresses tonic $GABA_AR$ currents in a specific subpopulation of hippocampal interneurons

Despite the relatively homogeneity of hippocampal CA1 pyramidal neurons, inhibitory interneurons are a diverse population of cells innervating different domains of principal cells and other interneurons (Klausberger and Somogyi 2008) and are markedly involved in neuronal network operations (Whittington et al. 1995; Whittington and Traub 2003; Mann and Paulsen 2007). Because of the profound influence of interneurons in controlling neuronal excitability and hippocampal output signaling and the lack of knowledge about the influence of adenosine modulation on these

cells, it was investigated A_1R actions on $GABA_AR$ responses from interneurons (Figure 5.15A). It was recorded muscimol-PSCs in CA1 area interneurons whose soma was located in *stratum radiatum* or *stratum oriens*. The interneuron population showed non-parametric distribution in response to CPA (30nM) (Shapiro-Wilk test, n=17; Figure 5.15B), and in fact it was found two different populations of cells. A subset of interneurons showed a significant and robust suppression of muscimol-PSCs following CPA application (average reduction to 66.3 ± 2.2% of baseline, n = 7, $P < 0.001$, t-test; Figure 5.15C) similar to that observed in pyramidal cells (see Figure 5.2). In the remaining tested interneurons, muscimol-PSC was unchanged by CPA (amplitude 101.2 ± 2.0% of the baseline, n = 10, $P = 0.58$, t-test; Figure 5.15D).

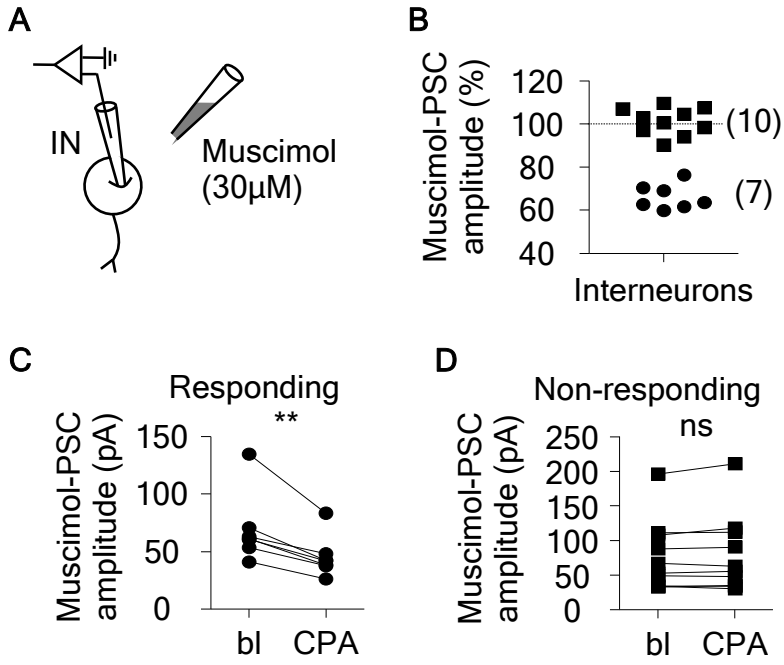

Figure 5.15. Hippocampal interneurons are affected differently by A_1R activation
(A) Schematic representation of the experimental design to record muscimol-PSCs from interneurons. **(B)** Circles: A_1R activation with CPA (30 nM) significantly depressed baseline-normalized muscimol-PSCs in 7 interneurons. Squares: 10 interneurons where CPA (30 nM) failed to show an effect (baseline-normalized, t-test). **(C and D)** Muscimol-PSC amplitudes (in pA) of studied interneurons before (bl) and after CPA superfusion, where data from cells with significant suppression are shown in C and data from cells with no effect of CPA are shown in D; values from each cell are connected with line. In all panels, the number of experiments is shown in brackets; ns, not statistically significant; **P < 0.01 (Student's t-test); IN: interneuron.

The interneurons were tested for their physiological properties by injecting steps of hyperpolarizing and depolarizing current pulses (1200 ms each) to reveal the neuronal firing pattern. The observed adenosine A_1R modulation on interneurons did not correlate with their neuronal firing properties. In fact, both groups of cells (responding and non-responding cells) showed diverse physiological properties characteristic of different populations of interneurons (Figure 5.16). These included regular-spiking non-pyramidal cells (RSNP), further classified as non-rebounding (NR-

RSNP) (Figure 5.16A) or rebounding (R-RSNP) (Figure 5.16B), burst-spiking nonpyramidal cells (BSNP) (Figure 5.16C) and fast-spiking interneurons (FSI) (Figure 5.16D) (characterization followed the Petilla convention (Ascoli et al. 2008) and (Lamsa et al. 2007)) (see Chapter 4.4.3, p83 for detail on methods).

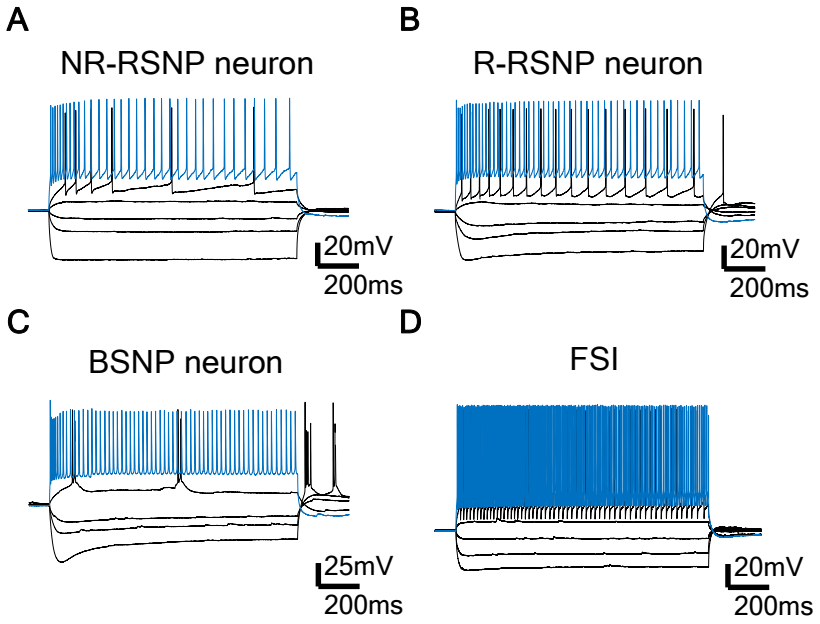

Figure 5.16. Characterization of interneurons by their firing pattern
Interneurons were characterized eletrophysiologically by their firing pattern and divided in four different categories: non-rebounding regular-spiking non-pyramidal cells (NR-RSNP) **(A)**; rebounding regular-spiking non-pyramidal cell (R-RSNP) **(B)**; Burst-spiking non-pyramidal neuron (BSNP) **(C)**; and fast-spiking interneurons (FSI) **(D)**. See Chapter 4.4.3, p83 for further information.

It was then hypothesized whether A_1R actions correlated with expression of a specific marker, the CB_1R, which corresponds to one of the most represented populations of interneurons in the hippocampus and correlated with the CCK-positive population (Katona et al. 1999, Klausberger et al. 2005). It was discovered that the A_1R effect on $GABA_AR$ currents correlated with the expression of axonal CB_1R, in the studied cells. This was tested

by recording muscimol-PSC in interneurons (Figure 5.17A) that were filled with biocytin and visualized with streptavidin-fluorophore. All successfully visualized cells were tested in immunohistochemical reaction for axonal CB_1R expression (Katona et al. 1999, Klausberger et al. 2005, Nissen et al. 2010). Importantly, it was found that 9 of 10 cells responding to CPA in muscimol-PSCs were immunopositive for CB_1R (CB_1R-positive). In CB_1R-positive interneurons, average muscimol-PSC inhibition by CPA was to 58.8 ± 5.0% of baseline responses ($n = 10$, $P < 0.001$, t-test; Figure 5.17B,C,E). Analyses on the laminar distribution of CB_1R-positive interneuron axon revealed basket cells ($n = 4$; Figure 5.17D) and dendritic targeting Schaffer collateral-associated cells (Figure 5.17F) indicating that $GABA_AR$ current modulation by A_1R occurs in various types of CB_1R-positive interneurons (Somogyi & Klausberger 2005, Lee et al. 2010b). Interestingly, the A_1R agonist (CPA, 30 nM) failed to significantly suppress muscimol-PSCs in any CB_1R immunonegative (CB_1R-negative) interneuron. Indeed, muscimol-PSCs in CB_1R-negative interneurons were 99.0 ± 1.4% of baseline ($n = 10$, $P = 0.60$, t-test; Figure 5.17B,C,G) in the presence of CPA. This population of CB_1R-negative neurons included three basket-cells. Also, CB_1R-positive neurons were characterized as R-RSNP or NR-RSNP and CB_1R-negative neurons characterized as R-RSNP, NR-RSNP or FSI.

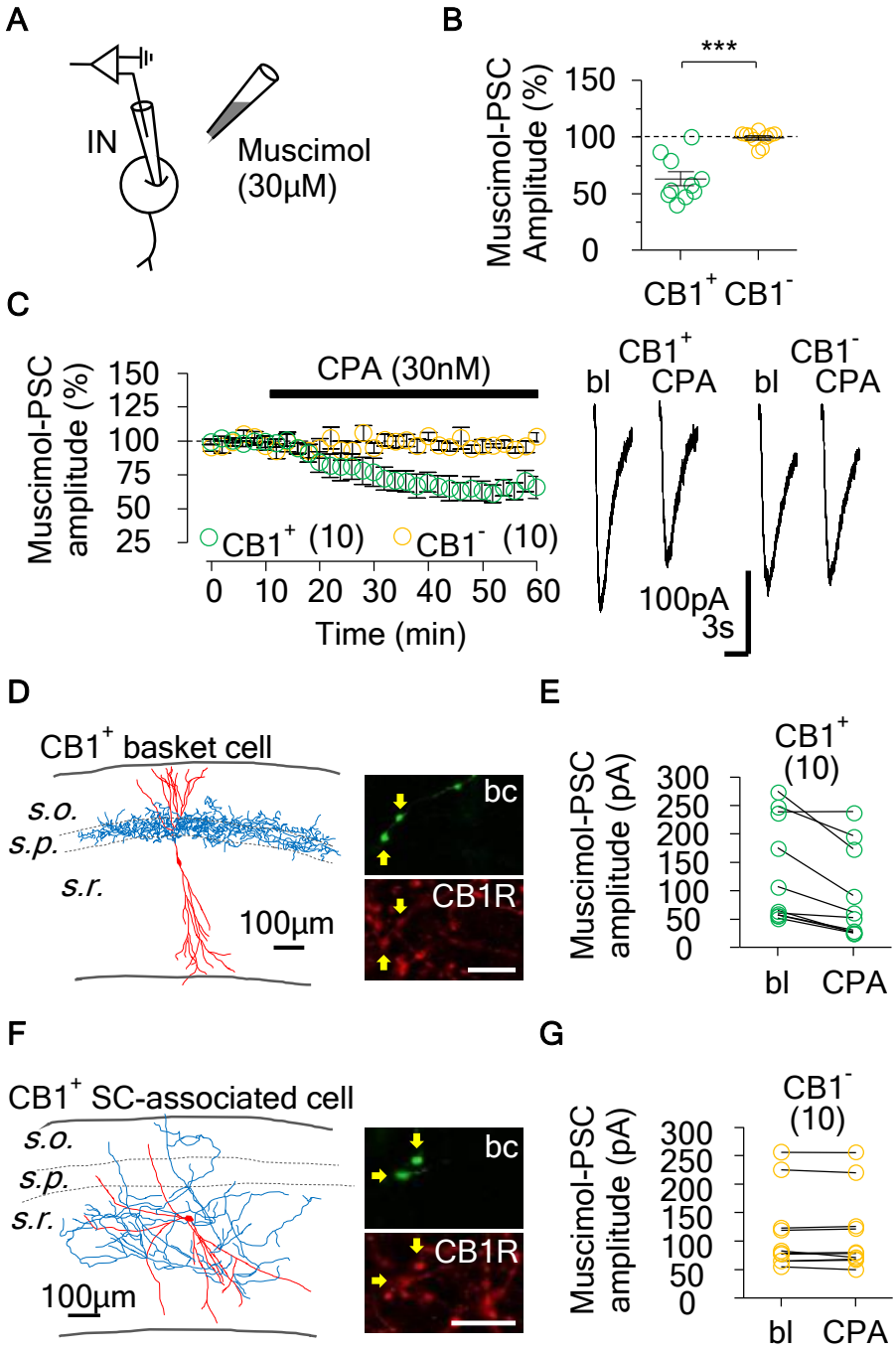

Figure 5.17. A_1R activation suppresses muscimol-PSCs in GABAergic interneurons expressing axonal CB1R, but not in CB1-immunonegative interneurons.
(A) Schematic representation of the experimental design to record muscimol-PSCs from interneurons. **(B)** Baseline-normalized muscimol-PSCs recorded in the presence of CPA from individual interneurons expressing axonal CB1R (CB1+, green) and

CB1-immunonegative interneurons (CB1−, yellow) **(C)** Left: baseline-normalized muscimol-PSCs (mean ± SEM) recorded from CB1+ (n = 10) and from CB1− (n = 10) neurons; right: representative traces of muscimol-PSCs from one CB1+ and one CB1− interneuron in baseline (bl) and in CPA. **(D and F)** Left: Reconstructed studied CB1+ basket cell (D) and Schaffer collateral (SC)-associated cell (F) (soma and dendrites in red; axon in blue); right: confocal images showing positive axonal immunoreaction for CB1R (red, Cy3; scale bar corresponds to 5 µm) in Biocytin/Alexa-Streptavidin reaction-visualized axon (green, bc). Arrows show co-localization. **(E and G)** Muscimol-PSCs (in pA) of all CB1+ (E, green) and CB1− interneurons (G, yellow) in baseline (bl) and in the presence of CPA; values from each cell are connected with line. In all panels, the number of experiments is shown in brackets; the representative current traces correspond to 5 consecutive responses; ***P < 0.001 (Student's t-test); IN: interneuron; *s.r.: stratum radiatum; s.p.: stratum pyramidale; s.o.: stratum oriens*.

To directly assess A_1R-mediated actions on tonic inhibitory responses, it was recorded tonic-IC in immuhistochemical-identified CB_1R-positive and CB_1R-negative interneurons. In the first set of experiments and to allow better comparison with results from pyramidal cells, GABA (5 µM) was added to the aCSF together with GABA transport blockers (SFK89976A, 20 µM and SNAP5114, 20 µM), glutamate receptor antagonists (CNQX, 10 µM and DL-AP5, 50 µM) and TTX (0.5 µM) (Figure 5.18A). In these experiments averaged tonic-ICs recorded from interneurons in control slices was -153.3 ± 10.8 pA (n = 5; Figure 5.18C). In slices incubated with CPA (30 nM for at least 50 min), tonic-ICs were significantly lower than control in 4 out of 5 CB_1R-positive interneurons (-47.9 ± 7.0 pA, n = 4, P < 0.001, t-test; Figure 5.18B,C) but not in CB_1R-negative interneurons (-144.1 ± 8.7 pA, n = 5, CB_1R-negative in CPA, P = 0.53, t-test; Figure 5.18C).

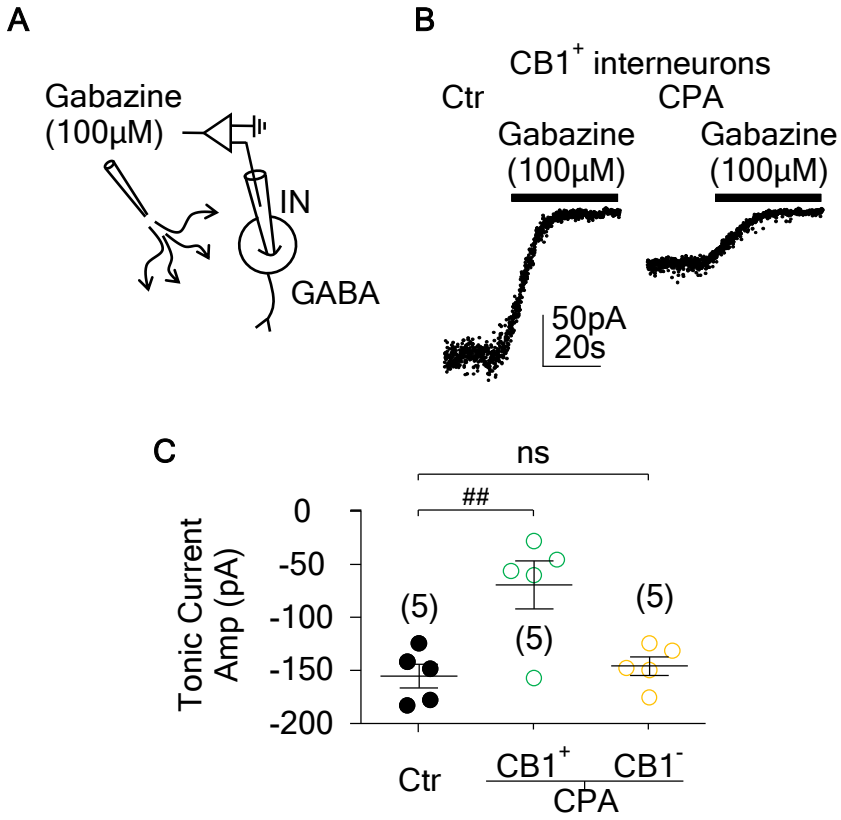

Figure 5.18. Tonic $GABA_AR$ currents in CB_1R-immunoposivite interneurons are inhibited by adenosine A_1R activation
(A) Schematic representation of experimental design used to access tonic currents; ambient GABA (5 µM) was added to aCSF and tonic-IC was revealed by application of gabazine (100 µM). **(B)** Representative tonic current (plotted at 5 ms intervals) recorded from a CB1+ interneuron in a control slice (left) and in a CPA (30 nM)-incubated slice (right). **(C)** Averaged tonic current (mean ± SEM, pA) recorded from interneurons (green correspond to CB1+ interneurons; yellow correspond to CB1R− interneurons) in control slices (Ctr, filled circles) and in slices where CPA (30 nM) was added at least 50 min prior gabazine (CPA, open symbols). In all panels, the number of experiments is shown in brackets; ns, not statistically significant; $^{\#\#}P < 0.01$ (one-way ANOVA followed by Bonferroni's multiple comparison test); IN: interneuron.

It was then evaluated if adenosine A_1R could also affect tonic transmission in the presence of endogenous concentrations of GABA and recorded tonic-ICs in interneurons without supplying the aCSF with GABA (Figure 5.19). Contrary to what was observed for pyramidal cells, naïve interneurons showed a significant tonic-IC (-15.4 ± 1.4 pA, n = 4, Figure 5.19B,C). Upon

incubation with CPA, tonic-IC was clearly smaller in 5 of 7 anatomically identified interneurons (-8.8 ± 1.0 pA, n = 5, in CPA, P < 0.05, t-test; Figure 5.19B,C).

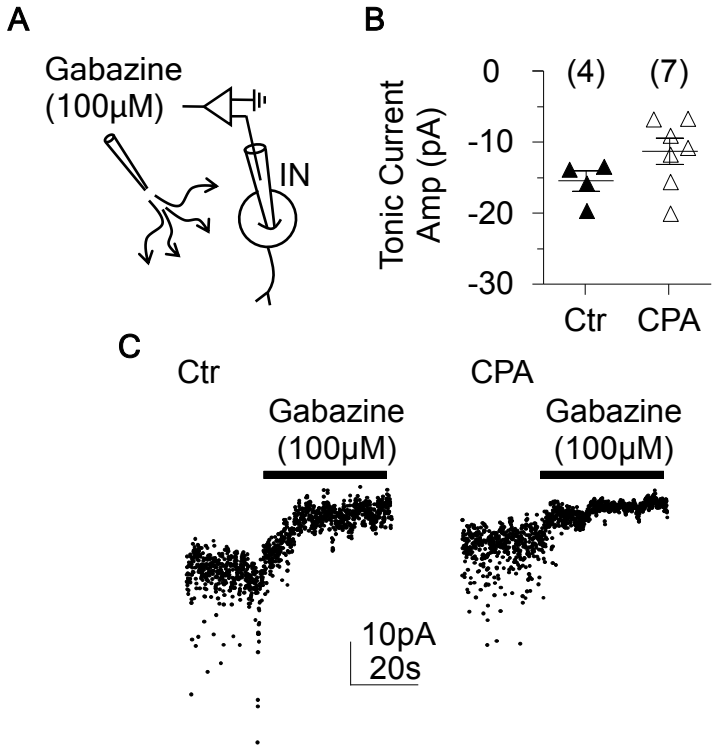

Figure 5.19. Adenosine A_1R suppresses tonic-ICs recorded in the presence of endogenous concentrations of GABA
(A) Schematic representation of the experimental design used to access endogenous tonic currents; no GABA was added to aCSF, tonic-IC was revealed by application of gabazine (100 µM). **(B)** Averaged tonic current (mean ± SEM, pA) recorded from interneurons in control slices (filled triangles, n = 4) and in slices where CPA (30 nM) was added at least 50 min prior gabazine (open triangles, n = 7). **(C)** Representative tonic current (plotted at 5 ms intervals) recorded from interneurons in control (left) and in a CPA (30 nM)-incubated slices (right). In all panels, the number of experiments is shown in brackets; IN: interneuron.

Finally, it was tested whether, similar to that observed in pyramidal cells, A_1R modulation of inhibitory currents in interneurons was restricted to extrasynaptic $GABA_AR$-mediated currents. It was recorded electrical stimulation-evoked IPSCs in the CA1 area interneurons (Figure 5.20).

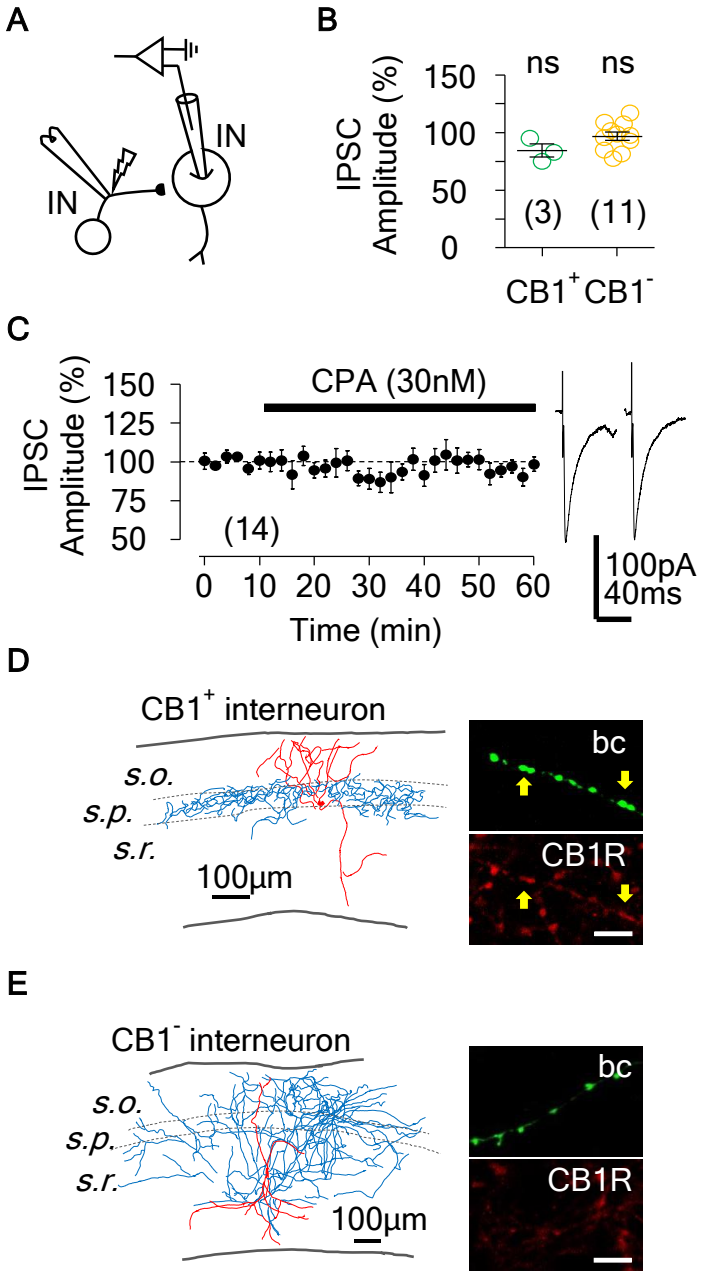

Figure 5.20. Phasic synaptic IPSCs in interneurons are not suppressed by adenosine A_1R

(A) Schematic experimental design to record IPSCs from interneurons; **(B)** Baseline-normalized IPSCs recorded in the presence of CPA from all individual cells studied and tested for CB1R immunoreactivity; note that IPSCs were not affected by CPA, either in CB1+ (green) or CB1R− (yellow) interneurons. **(C)** left: time course plot showing that synaptic IPSCs evoked by electrical stimulation were not altered by CPA; right: representative IPSC recorded from one CB1+ interneuron in baseline (bl) and in the presence of CPA; each trace corresponds to the average of 10 consecutive

responses. **(D and E)** Left: reconstructed studied CB1+ (D) and CB1− (E) interneurons (soma and dendrites in red; axons in blue); right: Confocal images of positive (D) and negative (E) CB1R immunoreaction (red, Cy3, scale bar corresponds to 5 µm) in Biocytin/Alexa-Sterptavidin reaction (green, bc). Arrows point at co-staining. In all panels, the number of experiments is shown in brackets; ns, not statistically significant (Student's t-test); IN: interneuron; *s.r.: stratum radiatum; s.p.: stratum pyramidale; s.o.: stratum oriens*.

Cells were visualized post-hoc and tested for axonal CB_1R immunoreaction. Similar to the results obtained with pyramidal cells, A_1R activation failed to significantly modulate IPSCs in either CB_1R-positive (84.0 ± 5.7% of baseline, n = 3, P = 0.10, t-test; Figure 5.20B,C,D) or CB_1R-negative (96.1 ± 3.6% of baseline, n = 11, P = 0.3, t-test; Figure 5.20B,C,E) interneurons, indicating a lack of modulation of phasic interneuron inhibition by A_1R. Cells showed heterogenous anatomical characteristics (Figure 5.20D,E).

Together, the above results show A_1R modulation of tonic $GABA_AR$ currents in a specific subpopulation of GABAergic interneurons expressing axonal CB_1Rs.

5.1.8 Discussion

The results show that adenosine A_1R selectively modulates tonic $GABA_AR$ currents generated by extrasynaptic receptors, but has no effect on phasic synaptic $GABA_AR$ currents. The modulation is consistent in CA1 pyramidal cells, but present only in a specific population of postsynaptic CA1 GABAergic inhibitory interneurons with axonal CB_1R. A_1R-mediated modulation requires intracellular PKA/PKC signaling. Sustained A_1R activity results in a decreased expression of $GABA_AR$ δ-subunit, a key component of

extrasynaptic receptors mediating tonic $GABA_AR$ currents (Farrant & Nusser 2005).

Adenosine has a broad spectrum of modulatory actions in the brain. Through A_1R, it acts as an anticonvulsant agent with neuroprotective effects (Sebastião & Ribeiro 2009, Boison 2012). These actions are partly based on suppression of glutamatergic transmission either by presynaptically reducing calcium influx (Scanziani et al. 1992, Yawo & Chuhma 1993) and neurotransmitter release (Schubert et al. 1986, Proctor & Dunwiddie 1987, Barrie & Nicholls 1993) or postsynaptically facilitating potassium currents (Gerber et al. 1989, Thompson et al. 1992) and inhibiting ionotropic glutamatergic receptors (de Mendonça et al. 1995, Li & Henry 2000). Thus, the effect of adenosine via A_1R on glutamatergic transmission is well known. A role of adenosine in regulation of inhibitory GABAergic transmission has received much less attention and is much less investigated. This is surprising because already in early 90's, it was demonstrated that adenosine strongly modulates disynaptic inhibition in the hippocampus, although it has no direct effect on GABAergic synapses to pyramidal cells (Kamiya 1991, Lambert & Teyler 1991, Yoon & Rothman 1991, Thompson et al. 1992).

During the past two decades, tonic $GABA_AR$-mediated inhibition has been described in neurons in the hippocampus and in many other brain areas (Semyanov et al. 2004, Farrant & Nusser 2005, Glykys & Mody 2007a). Tonic $GABA_AR$-mediated membrane conductance plays a role in regulation of synaptic integration, input to output signal transformation and firing rate of individual neurons and ultimately overall excitability of the hippocampus (Hamann et al. 2002, Mitchell & Silver 2003, Semyanov et al.

2003, Bright et al. 2007, Rothman et al. 2009). Deregulation of tonic inhibition has also been implicated in pathophysiological conditions including schizophrenia (Damgaard et al. 2011, Gill et al. 2011, Hines et al. 2012), stroke (Clarkson et al. 2010) and epilepsy (Dibbens et al. 2004, Peng et al. 2004, Naylor et al. 2005, Scimemi et al. 2005, Feng et al. 2006, Zhang et al. 2007). This makes tonic GABAergic responses an important target to modulation via endogenous or exogenous drugs. Indeed, neuroactive steroids, ethanol and some anticonvulsant drugs act on extrasynaptic $GABA_AR$ and modulate tonic GABAergic conductance (Stell et al. 2003, Cope et al. 2005, Ferando & Mody 2012). Interestingly, $GABA_AR$ responsible for tonic currents and postsynaptic adenosine A_1R mainly locate in extra- and perisynaptic areas (Rivkees et al. 1995, Swanson et al. 1995, Ochiishi et al. 1999, Glykys & Mody 2007b), which makes them potential candidates to interact. This idea is further supported by A_1R coupling to $G_{i/o}$ signaling pathways since $GABA_AR$ is strongly modulated by PKA and PKC-mediated phosphorylation (Kano & Konnerth 1992, Kano et al. 1992, Moss et al. 1992, Robello et al. 1993, Nusser et al. 1999, Poisbeau et al. 1999, Brandon et al. 2002b, Bright & Smart 2013). This possibility was evaluated by recording afferent-evoked synaptic IPSCs and agonist-evoked $GABA_AR$ currents in hippocampal neurons. These two ways to generate postsynaptic GABAergic currents allowed us to discriminate responses mediated by synaptic and extrasynaptic $GABA_AR$. Local application of muscimol (a selective $GABA_AR$ agonist) through a micropipette positioned close to the recorded cell soma predominantly activates extrasynaptic $GABA_AR$, which are prominent in the perisomatic postsynaptic area (Kasugai et al.

2010). Accordingly, the resulting muscimol-PSC exhibited slow current kinetics characteristic of extrasynaptic $GABA_AR$-mediated responses (Pearce 1993, Banks et al. 1998, Banks & Pearce 2000). As herein reported, in all studied pyramidal cells and in a subpopulation of interneurons, the muscimol-evoked $GABA_AR$ currents were inhibited by the A_1R agonist. In contrast, the A_1R agonist failed to change phasic synaptic $GABA_AR$ currents generated by quantal release or by afferent stimulation (Kamiya 1991, Lambert & Teyler 1991, Yoon & Rothman 1991, Thompson et al. 1992). Such selective modulation of tonic $GABA_AR$ signaling might be important in controlling neuronal synchronization (Maex & De Schutter 1998, Glykys & Mody 2007a). However, it is worth noting the tendency of evoked IPSCs, but not mIPSCs, to decrease after A_1R activation, although not statistically significant (the suppression reached statistical significance if the period between 16 to 24 min after CPA perfusion is considered, see Figure 5.7C, p109). This observation on phasic transmission may very possibly be related to the fact that afferent electrical stimulation to evoke IPSCs leads to synchronized multiple vesicle release and consequent activation of adjacent perisynaptic or even extrasynaptic receptors that are functionally affected by adenosine A_1R actions. This modulatory strategy might be particularly important to allow discrete control of synapse specific inhibitory inputs arriving to pyramidal cells in response to local release of adenosine, in contrast with changes in tonic responses that would influence the overall excitability of the cell in response to widespread changes of adenosine concentrations (Maex & De Schutter 1998). Also, our data on the facilitation of muscimol-PSCs by the A_1R antagonist in naïve slices demonstrate that

endogenous adenosine can tonicaly suppress extrasynaptic $GABA_AR$ conductance. Because adenosine is paracrinally released from neurons and astrocytes (Boison 2006, Haydon & Carmignoto 2006), changes in ambient levels of endogenous adenosine are likely to occur and, therefore, tune peri- and extrasynaptic $GABA_AR$ activity. Interestingly, as compared to glutamatergic neurons, interneurons are easily disconnected by hypoxia due to A_1R activation (Khazipov et al. 1995), an indication that adenosine levels around GABAergic neurons is higher.

Many signaling mechanisms are involved in the modulation of $GABA_AR$ that are relevant to both phasic and tonic inhibition. Various protein kinases phosphorylate serine/threonine residues of $GABA_AR$ subunits (Brandon et al. 2002a), including PKA and PKC phosphorylation mechanism (Moss et al. 1995, Brandon et al. 2001, 2002b). Adenosine A_1R are coupled to $G_{i/o}$ proteins (Freissmuth et al. 1991, Jockers et al. 1994, Nanoff et al. 1995) but also affect phospholipase C and phosphoinositol-3-kinase activity (Akbar et al. 1994, Cascalheira & Sebastião 1998, Dickenson & Hill 1998, Schulte & Fredholm 2000, Cascalheira et al. 2002). It was found that PKA and PKC signaling cascades were responsible for A_1R-mediated inhibition of tonic $GABA_A$ currents. The results also indicated that A_1R-mediated inhibition of adenylate cyclase activity relieves a negative regulation of PKA over PKC. Disinhibition of PKC then promotes suppression of tonic $GABA_A$ currents in hippocampal neurons (see Figure 5.14, p121). In support of such mechanism our data shows that (1) both GF109203x and Rp-cAMPs (blockers of PKC and PKA, respectively), when loaded into the neurons, were able to prevent A_1R actions, clearly indicating the involvement of these kinases on

$GABA_AR$ modulation; (2) PKA activation with forskolin, per se, had the opposite effect of A_1R activation, suggesting that A_1R are negatively coupled to AC/PKA signaling; (3) by loading the cells with a PKC inhibitor, GF109203x, the effect of forskolin was completely prevented, indicating the involvement of PKC signaling downstream of PKA activation; (4) perfusion of an activator of PKC, PDD, mimicked A_1R activation and its actions were not prevented by Rp-cAMPs, confirming that PKC is downstream PKA and is negatively controlling $GABA_AR$ function. Our results also imply that the influence of PKC upon $GABA_ARs$ is constitutively under check by PKA activation, preventing $GABA_AR$ inhibition. When A_1Rs are activated, PKA-mediated inhibition of PKC is reduced and therefore the inhibition of $GABA_ARs$ by PKC is exacerbated. PKC is known to directly phosphorylate $GABA_ARs$ at serine residues of β3 subunit, decreasing receptor function (Brandon et al. 2000). This activity can also be modulated by PKA phosphorylation resulting in a decrease of PKC binding to $GABA_ARs$ (Brandon et al. 2000, 2002b). Since most described PKC and PKA phosphorylation sites occur in $GABA_AR$ subunits that are common to synaptic and extrasynaptic receptors, it remains to be evaluated how selectivity to phasic and/or tonic responses is achieved. Regarding adenosine effects, one possibility would be the selective localization of A_1Rs close to peri- and extrasynaptic $GABA_ARs$ exert cell-type and cell-compartment specific modulatory actions as observed for prefrontal and somatosensory neurons (van Aerde et al. 2013). Also, PKC-mediated phosphorylation of extrasynaptic $GABA_AR$ in the hippocampus causes a decrease in their expression level (Bright & Smart 2013). Accordingly, it was detected that upon incubation

with an A_1R agonist there is a decrease in the expression of $GABA_AR$ δ-subunit, a marker of extrasynaptic $GABA_AR$.

Pyramidal cells were sensitive to A_1R-mediated modulation of tonic GABAergic currents, somehow contrasting what occurs in pyramidal neurons from the somatosensory cortex, which are heterogeneous for the sensitivity to post-synaptic A_1R-mediated modulation (van Aerde et al. 2013). Among the interneurons, is shown that those that exhibit modulation of tonic $GABA_A$ currents by A_1R are also immunopositive for CB_1R, whereas CB_1R negative interneurons are insensitive to A_1R activation. Similarly to the pyramidal neurons, A_1R-mediated suppression of GABAergic responses in interneurons was significant only for tonic $GABA_A$ currents. In the hippocampus, axonal expression of CB_1R strongly correlates with expression of CCK in interneurons (Katona et al. 1999). These neurons are characterized by discharging at moderate frequencies (Lee et al. 2011), recruited with low reliability, being able to integrate incoming inputs over longer time windows (Glickfeld & Scanziani 2006), receive high proportion of inhibitory inputs (Mátyás et al. 2004) and generate asynchronous, fluctuating and unstable inhibitory output signals (Hefft & Jonas 2005, Daw et al. 2009, Ali & Todorova 2010). Endogenous modulators such as CCK and endocannabinoids (eCB) are known to influence differently CCK-positive and CCK-negative cells (Armstrong & Soltesz 2012). In fact, released CCK can act on pyramidal cells leading to eCB release and retrograde actions on CCK-positive cells suppressing GABA release (Földy et al. 2007) or depolarize CCK-negative interneurons (namely PV-positive cells) with consequent increase in firing rate and GABA release (Lee et al. 2011). The intrinsic and extrinsic signaling

properties of CCK-positive interneurons confer to these cells a unique gain control mechanism to regulate the balance between excitation and inhibition (Mitchell & Silver 2003). By acting selectively on tonic responses from CB1-positive/CCK-positive cells, adenosine can act as a homeostatic modulator of synaptic inhibition to pyramidal cells. Also, suppression of extrasynaptic $GABA_AR$ function without changes in phasic transmission may increase inhibition of pyramidal cells through CCK-positive interneurons, resulting in decreased hippocampal excitability (Mitchell & Silver 2003). In fact, low concentration of picrotoxin (1 μM), aimed to predominantly inhibit tonic currents in interneurons increases spontaneous output from GABAergic cells to pyramidal cells, seen as the increased frequency of spontaneous IPSCs (Semyanov et al. 2003). Discharge of interneurons expressing CCK is coupled to co-ordinated oscillatory activities in hippocampus *in vivo* (Klausberger & Somogyi 2008). Firing of hippocampal CCK-positive inhibitory neurons is coupled to synchronous network oscillations in theta (4-8 Hz) and gamma (30-80 Hz) rhythms, which occur during cognitive processes in the hippocampus (Klausberger et al. 2005, Tukker et al. 2007, Lasztoczi et al. 2011). Controlling excitability and discharge by robust tonic $GABA_AR$ conductance in these neurons (Pietersen et al. 2009, Oke et al. 2010, Schulz et al. 2012) could allow adenosine A_1R modulation of hippocampal rhythm generation and information processing associated with coordinated rhythmic activities.

Adenosine A_1R actions decrease hippocampal excitability and hence adenosine is a suitable endogenous anticonvulsant compound (Boison 2012, Dias et al. 2013). Most documented

actions of A_1R as an anticonvulsant substance rely on its ability to refrain glutamatergic transmission (Khan et al. 2001, Boison 2012). Here is demonstrated a direct suppression of tonic GABAergic inhibition by A_1R in inhibitory interneurons, therefore highlighting another target for A_1R-mediated neuromodulation and excitability control. The resulting reduction of the disinhibition of interneurons caused by A_1R-mediated suppression of tonic GABAergic inhibition can increase inhibitory GABAergic output to hippocampal principal cell population. In parallel, adenosine A_1R also reduce tonic GABAergic inhibition in pyramidal cells. However in low ambient GABA levels, tonic $GABA_AR$ inhibition is likely to be more pronounced in interneurons than in pyramidal cells (Bai et al. 2001, Semyanov et al. 2003). Therefore, the net effect of A_1R-mediated modulation of tonic $GABA_AR$ on hippocampal pyramidal cell excitability may depend on ambient GABA concentrations as well as other conditions that control extrasynaptic $GABA_AR$ activation levels in the two cell populations (Scimemi et al. 2005, Wlodarczyk et al. 2013) (Figure 5.21).

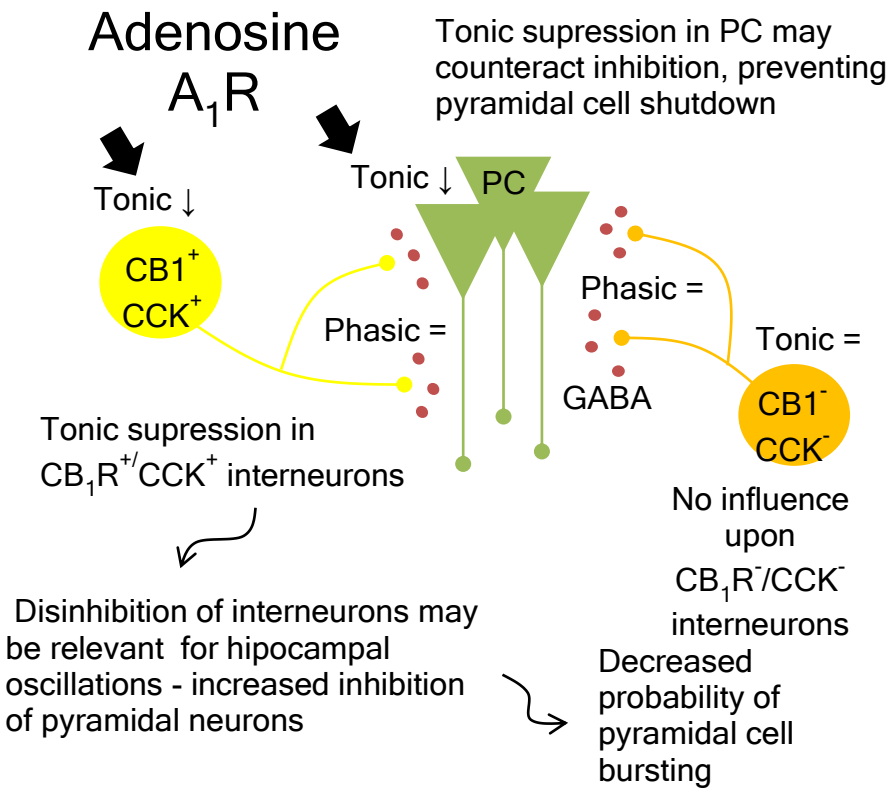

Figure 5.21. Schematic representation of the A_1R-mediated actions upon GABAergic transmission into CA1 hippocampal pyramidal cells and interneurons.
Green neuron: pyramidal cells: blue neuron: CB1R-positive, CCK-positive interneuron; orange neuron: CB_1R-negative, CCK-negative interneuron; "=": not altered; "↓": decreases.

Ambient GABA and adenosine levels are dynamic in the brain and both are increased during episodes of epileptiform activity (Chin et al. 1995, Berman et al. 2000, Pavlov & Walker 2013). Decreasing tonic $GABA_AR$ conductance in pyramidal cells during high ambient GABA levels should increase pyramidal cell excitability. However, during epileptiform discharges when ambient GABA concentrations reach peak, $GABA_AR$ currents can turn to depolarizing and excitatory (Köhling et al. 2000, Cohen et al. 2002, Ellender et al. 2014). This means that A_1R-mediated suppression of tonic $GABA_AR$ conductance in pyramidal cells can

also have an antiepileptic effect by shunting the Cl^- conductance during epileptiform activity (Ilie et al. 2012). In contrast, adenosine $A_{2A}R$ and A_3R may promote excitability in epileptic tissues by exacerbating use-dependent run-down of phasic $GABA_A$ currents (Roseti et al. 2009). These opposite actions of adenosine receptors are particularly relevant when planning adenosine-mediated therapies in pathological conditions such as epilepsy.

In conclusion, it is proposed that adenosine A_1Rs, by changing the inhibitory tonus of neurons without affecting phasic inhibitory synaptic transmission, can homeostatically regulate inhibition and control neuronal gain without disrupting fidelity of synaptic GABAergic inhibition (Pouille & Scanziani 2001, Lamsa et al. 2005). Its selectivity to specific interneuron populations may confer to adenosine an important modulatory action on hippocampal network oscillations that are the critical bases for hippocampal dependent behavior and cognitive processes.

5.2 Synaptic mechanisms of adenosine A_{2A}R-mediated hyperexcitability in the hippocampus

The work presented in this Chapter was published in:

- *Rombo DM, Newton K, Nissen W, Badurek S, Horn J, Minichiello L, Jefferys J, Sebastiao AM, Lamsa K (2015). Synaptic mechanims of adenosine A2A receptor mediated hyperexcitability in the hippocampus. Hippocampus 25, 566-80.*

***DMR** performed all experiments described in this Chapter.*
*Cell reconstructions and immunohistochemistry shown in Figure 5.27 (p158), Figure 5.28 (p160), Figure 5.29 (p163), Figure 5.32(p167) and Figure 5.33(p168) were performed together with **KN**.*
*Electrophysiological recordings shown in Figure 5.35 (p172) were performed together with **KL** and in Figure 5.36 (p175) and Figure 5.37 (p177) together with **AMS**.*

5.2.1 Summary

Adenosine inhibits excitatory neurons widely in the brain through adenosine A_1R, but activation of adenosine $A_{2A}R$ has an opposite effect promoting discharge in neuronal networks. In the hippocampus $A_{2A}R$ expression level is low, and its effect on identified neuronal circuits is unknown. Using optogenetic afferent stimulation and whole-cell recording from identified postsynaptic neurons it is shown that $A_{2A}R$ facilitates excitatory glutamatergic Schaffer collateral synapses to CA1 pyramidal cells, but not to GABAergic inhibitory interneurons. In addition, $A_{2A}R$ enhances GABAergic inhibitory transmission between CA1 area interneurons leading to disinhibition of pyramidal cells. Adenosine $A_{2A}R$ has no direct modulatory effect on GABAergic synapses to pyramidal cells. As a result adenosine $A_{2A}R$ activation alters the synaptic excitation - inhibition balance in the CA1 area resulting in increased pyramidal cell discharge to glutamatergic Schaffer collateral stimulation. In line with this, it is shown that $A_{2A}R$ promotes synchronous pyramidal cell firing in hyperexcitable conditions with elevated extracellular potassium or following high-frequency electrical stimulation. Our results revealed selective synapse and cell type specific adenosine $A_{2A}R$ effects in hippocampal CA1 area. The uncovered mechanisms help to understand the facilitatory effect of $A_{2A}R$ on cortical network activity.

5.2.2 Rational

Adenosine is well known for its inhibitory effect on neocortical and hippocampal glutamatergic principal cells via the A_1R (Dias et al. 2013). In addition, the high affinity adenosine $A_{2A}R$ is expressed in the brain, and although present at low levels in the neocortex and hippocampus (Schiffmann et al. 1991, Dixon et al. 1996) its activation in pathological conditions promotes epileptiform activity and facilitates excitotoxic neuronal death (Jones et al. 1998, Etherington & Frenguelli 2004, Zeraati et al. 2006, El Yacoubi et al. 2009). However, evidence for $A_{2A}R$-mediated facilitation of cortical excitatory neuron discharge is largely based on results in epilepsy and neuronal trauma models, and function of $A_{2A}R$ in physiological conditions in the cortex is less well known. Facilitatory effect of $A_{2A}R$ on excitatory neurons in healthy brain is well characterized in basal ganglia where it is involved in controlling arousal and motor responses (Rebola et al. 2005a, Ciruela et al. 2006, Shook & Jackson 2011, Wei et al. 2011, Lazarus et al. 2012). Adenosine $A_{2A}R$-mediated modulation of neuronal activity has also been reported in the hippocampus where the receptor activation facilitates excitatory input from the CA3 area to CA1 enhancing glutamatergic synapses directly and via altering glutamate transport (Cunha et al. 1994a, Rebola et al. 2005c, Dias et al. 2012, Matos et al. 2013). In physiological conditions adenosine $A_{2A}Rs$ are involved in synaptic long-term plasticity in hippocampal glutamatergic mossy fibers (Rebola et al. 2008, Chamberlain et al. 2013), and a recent study demonstrated that deletion of $A_{2A}R$ selectively in hippocampus compromises contextual memory formation (Wei et al. 2014).

The paucity of apparent adenosine $A_{2A}R$ expression in the hippocampus hints that the receptor may be localized to specific neuron subpopulations or subtypes of synapses (Schiffmann et al. 1991, Dixon et al. 1996). Although reported facilitatory effects on glutamatergic transmission between pyramidal cells could explain, at least partly, why $A_{2A}R$ activation promotes cortical pyramidal cell discharge (Jones et al. 1998, Zeraati et al. 2006, El Yacoubi et al. 2008, 2009; Moschovos et al. 2012), it is unknown if modulation of GABAergic inhibitory interneurons contributes to $A_{2A}R$-mediated effects on hippocampal function. Adenosine $A_{2A}R$ expression level increases in posttraumatic and epileptic neocortex and hippocampus (Dixon et al. 1996, Rebola et al. 2005b), and this may emphasize a role of the receptor in the activity modulation in pathological conditions. Knowledge of the action of $A_{2A}R$ on identified hippocampal synaptic circuits is crucial for understanding adenosine function in physiological conditions in the cortex and the therapeutic potential of high affinity adenosine receptors in pathological conditions such as epilepsy.

5.2.3 Adenosine $A_{2A}R$ facilitates glutamatergic synapses and amplifies CA1 pyramidal cell input-output transformation

To evaluate the effect of $A_{2A}R$ activation on hippocampal Schaffer collateral synapses in the CA1 area it was used paired-pulse microelectrode stimulation (50 ms interval, delivered every 15 s) in field potential recording from mouse hippocampal slices. The CA3 area was removed by surgical cut to avoid recurrent excitation (see schematic in Figure 5.22A). The fEPSPs were elicited in every experiment with five stimulation intensities

gradually increasing stimulus pulse duration from 50 to 150 µs. The fEPSP slope and popspike amplitude were measured as showed in Figure 5.22B. The lowest intensity (50 µs) often failed to elicit stable popspike in baseline so only intensities from 75 µs till 150 µs stimulus duration were used for analysis of popskike. Further details on fEPSP measurement and analysis are described in Chapter 4.4.4, p84.

Wash-in of the selective $A_{2A}R$ agonist CGS21680 (30 nM) after a baseline period of at least 10 min enhanced stimulus-evoked fEPSP slope (Figure 5.22C) and increased popspike amplitude (Figure 5.22D).

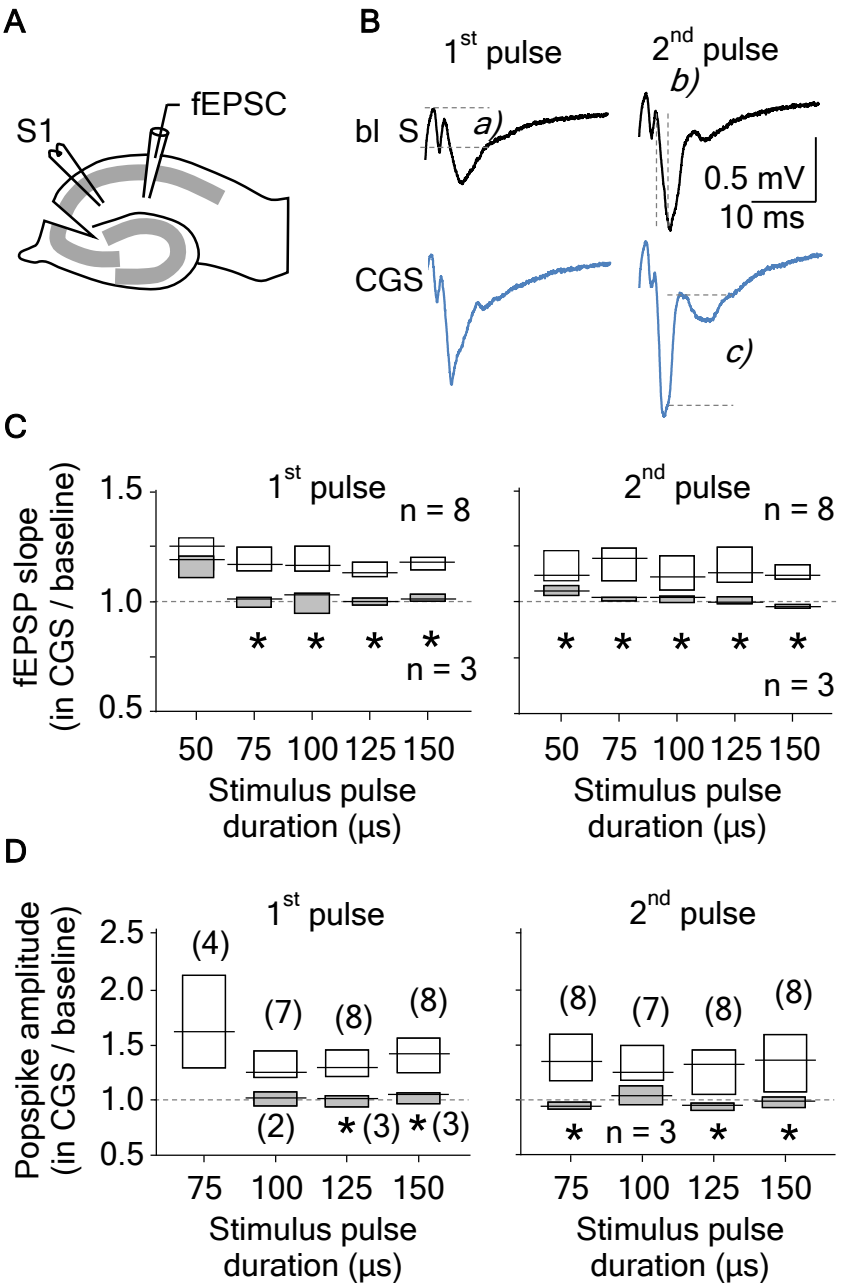

Figure 5.22. Activation of adenosine $A_{2A}R$ facilitates glutamatergic transmission in hippocampal Schaffer collaterals

A selective agonist CGS21680 (30 nM) increases fEPSP slope and population spike amplitude evoked by stimulation of Schaffer collaterals. **(A)** Schematic shows experimental design. Paired-pulse (50 ms interval) electrical stimulation (S1) was delivered in the CA1 area. The CA3 area was removed by surgical cut to avoid recurrent excitation. **(B)** Averaged field potential traces (10) evoked with mid-strength stimulation (100 µs pulse duration) in baseline (bl, black) and following application of

CGS21680 (30 nM) (CGS, blue); (a) shows prespike volley amplitude (between horizontal dotted lines); (b) fEPSP slope was measured between dotted vertical lines; and (c) popspike amplitude between horizontal lines; stimulation artifact (S1) is truncated. **(C)** Increase of fEPSP slope by CGS21680 (30 nM); fEPSPs were elicited in every experiment with five stimulation intensities gradually increasing stimulus pulse duration from 50 to 150 µs. Open boxes show median (with 25% and 75% quartiles) of baseline-normalized fEPSP slope in 8 experiments following wash-in of CGS21680; solid boxes show CGS21680 wash-in effect in presence of the $A_{2A}R$ antagonist SCH58261 (100 nM) (n = 3); significant difference between open and solid boxes is indicated by asterisk; *P < 0.05, Mann-Whitney test. **(D)** Increase of popspike amplitude by CGS21680 (30 nM) in the same experiments shown in C. When popspike data are not available in all experiments *n* is indicated in parenthesis. Asterisks show difference between the open and solid boxes; *P < 0.05, Mann-Whitney test. For C and D, left panels show results for first stimulus pulse and right panel for the second pulse generated from stimulation of paired-pulse.

Values and statistics for baseline-normalised CGS21680 effect for each stimulus intensities can be visualized in Table 5.1. The facilitatory effects of CGS21680 on fEPSP slope and popspike amplitude were fully blocked in experiments with continuous presence of the $A_{2A}R$ antagonist SCH58261 (100 nM) (Figure 5.22C,D).

The baseline-normalized presynaptic spike (prespike) volley in all CGS21680 experiments (agonist alone plus agonist in the presence of antagonist, SCH58261), measured for 100 µs stimulus duration was not changed (1.02 ± 0.02 for 1st stimulation pulse and 1.01 ± 0.03 for 2nd, n = 11, P > 0.05, Mann-Whitney test) (Sebastião & Ribeiro 1992). The averaged baseline popspike amplitude measured for 100 µs stimulus duration was 0.25 ± 0.06 mV for 1st pulse, and 0.59 ± 0.17 mV for 2nd pulse (n = 11, mean ± SEM) which corresponded to a fEPSP slope of 0.32 ± 0.06 mV / ms and 0.57 ± 0.11 mV / ms, respectively.

Table 5.1. Baseline-normalised slope values of CGS21680 (agonist) effect alone or in the presence of SCH58261 (antagonist)

		Intensity (ms)	Mean ± SEM (N) (in agonist)	Mean ± SEM (N) (in antagonist)	Statistics [1]
fEPSP slope	1st pulse	50	1.21 ± 0.04 (8)	1.16 ± 0.04 (3)	P > 0.05
		75	1.18 ± 0.02 (8)	1.00 ± 0.02 (3)	*P = 0.01
		100	1.19 ± 0.03 (8)	1.00 ± 0.04 (3)	*P = 0.01
		125	1.14 ± 0.02 (8)	1.00 ± 0.01 (3)	*P = 0.01
		150	1.17 ± 0.02 (8)	1.02 ± 0.01 (3)	*P = 0.01
	2nd pulse	50	1.15 ± 0.03 (8)	1.05 ± 0.02 (3)	*P = 0.02
		75	1.20 ± 0.05 (8)	1.01 ± 0.01 (3)	*P = 0.01
		100	1.14 ± 0.04 (8)	1.01 ± 0.01 (3)	*P = 0.02
		125	1.16 ± 0.03 (8)	1.00 ± 0.01 (3)	*P = 0.01
		150	1.13 ± 0.02 (8)	0.98 ± 0.01 (3)	*P = 0.01
Popspike	1st pulse	50	-	-	-
		75	1.72 ± 0.28 (4)	-	-
		100	1.67 ± 0.39 (7)	1.02 ± 0.07 (2)	P > 0.05
		125	1.75 ± 0.47 (8)	0.99 ±0.04 (3)	*P = 0.02
		150	1.74 ± 0.37 (8)	1.02 ± 0.04 (3)	*P = 0.01
	2nd pulse	50	-	-	-
		75	1.61 ± 0.29 (8)	0.95 ± 0.02 (3)	*P = 0.01
		100	1.43 ± 0.16 (7)	1.04 ± 0.07 (3)	*P = 0.04
		125	1.35 ± 0.13 (8)	0.94 ± 0.03 (3)	*P = 0.01
		150	1.39 ± 0.12 (8)	0.98 ± 0.04 (3)	*P = 0.02

[1] Mann-Whitney test.

In the presence of CGS21680, fEPSPs were associated with a higher increase in popspikes amplitude than fEPSP slope (Figure 5.23A). It was used a linear regression to fit fEPSP slope and popspike amplitude values (evoked with various stimulus intensities) in baseline conditions for each experiment (see Chapter 4.4.4, p84 for detailed description of the procedure). Following wash-in of CGS21680 (30 nM), fEPSPs did not significantly change 1st pulse stimulation Δ popspike / fEPSP relation, but upon 2nd pulse stimulation it generated a significantly higher amplitude popspikes than similar magnitude fEPSPs during baseline ($P < 0.05$, Mann-Whitney test) (Figure 5.23B). Popspike amplitude / fEPSP slope relation details are shown in Figure 5.23.

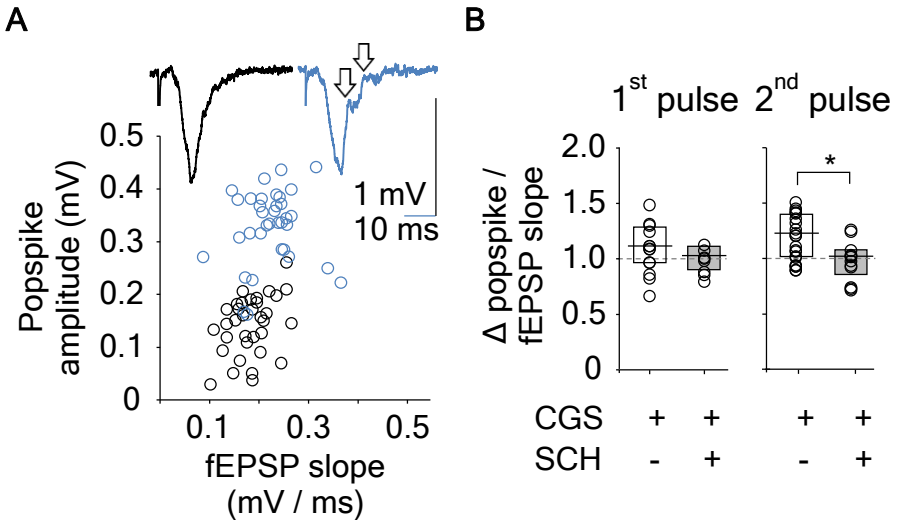

Figure 5.23. Activation of adenosine $A_{2A}R$ amplifies CA1 pyramidal cell input-output function

CGS21680 increases popspike amplitude - fEPSP slope ratio. **(A)** Relation of popspike amplitude and fEPSP slope in one experiment in baseline (black trace and symbols) and following wash-in of CGS21680 (blue); fEPSPs were evoked with various intensities using stimulation pulse duration from 75 to 125 μs; inset: average of 10 field potential responses in baseline (black) and following wash-in of CGS21680 (blue). Popspikes appearing in the fEPSP following wash-in of CGS21680 are indicated by arrows (data in the plot show first popspike amplitude when more than one popspike is elicited in CGS21680). **(B)** Effect of CGS21680 on popspike amplitude - fEPSP slope relation in all experiments. In baseline conditions popspike - fEPSP slope relation was determined in each experiment (see Chapter 4.4.4, p84). Plot shows a relation of popspike amplitude associated with similar size fEPSP slope in CGS21680 and baseline. This is indicated as Δ popspike/fEPSP slope. Open boxes represent median of means of individual experiments (circles); fEPSPs upon 2nd stimulation of paired-pulse generated significantly higher popspikes than similar magnitude fEPSPs in baseline; *P < 0.05, Mann-Whitney test. For 1st stimulation pulse response, there was no significant difference between baseline and CGS21680; solid boxes correspond to control experiments where CGS21680 was applied in the presence of $A_{2A}R$ blocker SCH58261 (30 nM). Antagonist blocks the agonist-induced increase in A popspike/fEPSP slope; *P < 0.05, Mann-Whitney test.

The results show that $A_{2A}R$ facilitates glutamatergic synapses in the hippocampus, and in addition increases CA1 pyramidal cells output in response to Schaffer collateral excitation.

5.2.4 Adenosine $A_{2A}R$ increases excitation and suppresses feedforward inhibition to pyramidal cells

Next, it was investigated how $A_{2A}R$ activation modulates monosynaptic excitatory and disynaptic inhibitory currents in the CA1 hippocampal pyramidal cells. It was selectively stimulated Schaffer collaterals delivering 473 nm laser light-pulses (3 ms, 5 pulses at 50 ms interval, delivered every 30 s) to CA1 *stratum radiatum* in slices expressing ChR2 in glutamatergic neurons (Figure 5.24A).

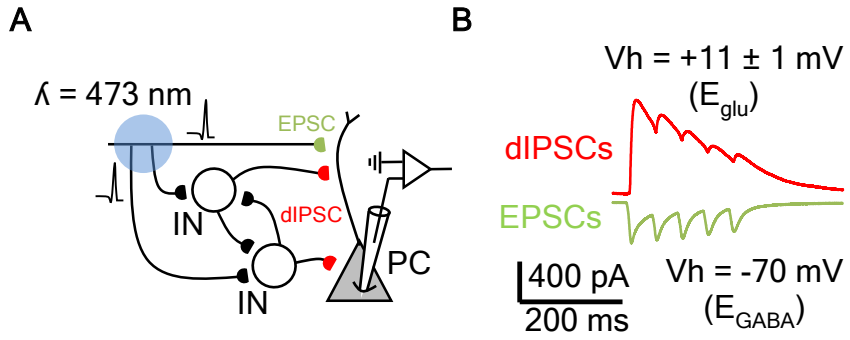

Figure 5.24. Schematic of light-evoked EPSCs/disynaptic IPSCs
(A) Experimental design; optogenetic fixed-spot laser stimulation (blue dot, λ = 473 nm) of Schaffer collateral fibers in the CA1 area, and recording in a postsynaptic pyramidal cell (gray). ChR2 is expressed in glutamatergic cells in Cre-dependent manner. GABAergic interneuron somata in the schematic are shown white. Action potentials indicate activation of axons between neurons. **(B)** Shaffer collateral stimulation with the fixed-spot laser will result in the recording of EPSCs (green trace) originated from monosynaptic recruitment of glutamatergic fibers (when the cell is voltage-clamped at E_{GABA}, Vh = -70 mV) and the recording of disynaptic IPSCs (dIPSCs, red trace) that result from recruitment of interneurons activated by Schaffer collaterals that will then project to the recorded pyramidal cell (when the neuron is voltage-clamped at E_{glu} (Vh = +11 ± 1 mV)). IN: interneuron; PC: pyramidal cell.

Slices were prepared from hippocampi of heterozygous CaMKII-Cre (CaMKII-Cre$^{tg/+}$) mice transduced with AAV2/5-ChR2-eYFP to express ChR2 in a Cre-dependent manner in CA1-CA3 pyramidal cells (see Chapter 4.5, p91).

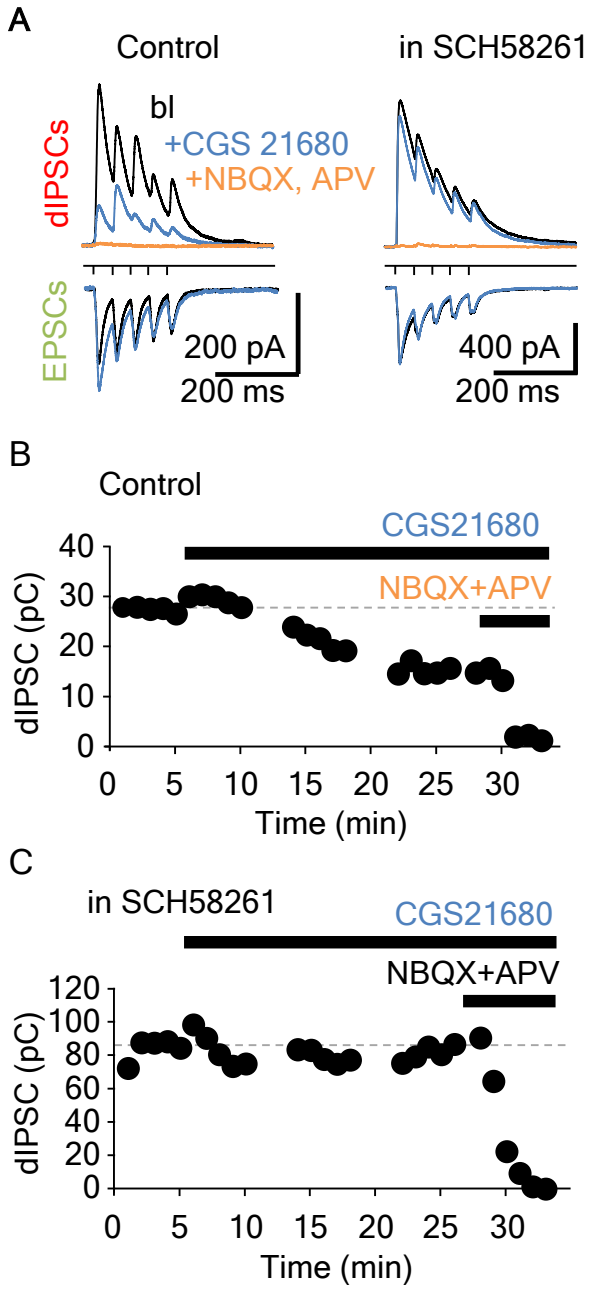

Figure 5.25. Adenosine A2A receptor facilitates excitatory Schaffer collateral synapses and suppresses feed-forward GABAergic inhibitory input to CA1 pyramidal cells

(A) $A_{2A}R$ agonist CGS21680 (30 nM) suppresses disynaptic feed-forward GABAergic IPSCs (dIPSCs) and enhances glutamatergic EPSCs evoked by a train (5 pulses 20 Hz) of stimuli; left: averaged traces (5) from two sample experiments illustrate the effect of CGS21680 (blue) on EPSCs and dIPSC following a baseline (black); right: the effects of CGS21680 are blocked in the presence of $A_{2A}R$ antagonist SCH58261

(100 nM). The dIPSCs are fully abolished with glutamate receptor blockers NBQX (25 mM) and DL-APV (100 mM) (orange). Stimulus train is shown in the middle between traces. **(B,C)** Time course of the effect of CGS21680 (horizontal bar) on dISPCs charge in control (B) and in the presence of antagonist (C). The dIPSCs were recorded at EPSC reversal potential and blocked by NBQX and DL-APV at the end. Gaps in IPSC data during agonist wash-in show time points when determining IPSC reversal potential.

Postsynaptic cells were voltage-clamped sequentially at -70 mV and at a reversal potential of EPSCs (11 ± 1 mV, n = 7 cells) to record glutamatergic EPSCs and disynaptic GABAergic IPSCs (dIPSCs), respectively (Figure 5.24B). Wash-in of $A_{2A}R$ agonist CGS21680 (30 nM) potentiated glutamatergic EPSCs and simultaneously suppressed disynaptic GABAergic IPSCs in CA1 pyramidal cells (Figure 5.25A,B).

Charge of baseline-normalized EPSCs increased to 1.25 ± 0.08 ($P < 0.05$, n = 7 cells, t-test), and disynaptic IPSCs decreased to 0.77 ± 0.07 ($P < 0.05$, n = 7 cells, t-test) (Figure 5.26A). Baseline EPSC and dIPSC were 25.3 ± 4.7 pC and 55.2 ± 12.6 pC, respectively. When experiments in the presence of the $A_{2A}R$ antagonist SCH58261 (100 nM, applied at least 30 min prior to agonist wash-in) were repeated, $A_{2A}R$ agonist effect was fully blocked and neither EPSCs nor dIPSCs were altered (Figure 5.25A,C). Baseline-normalized EPSCs and dIPSCs were 0.98 ± 0.02 and 0.94 ± 0.03, respectively (n = 6, t-test) (Figure 5.26B). During baseline, mean ± SEM of EPSCs was 48.0 ± 8.5 pC and dIPSCs was 70.1 ± 7.6 pC).

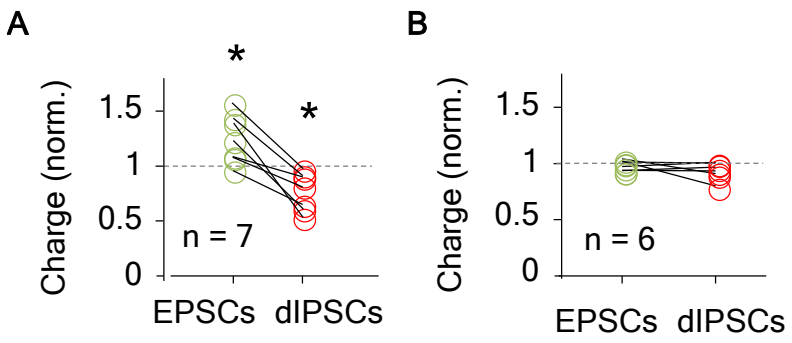

Figure 5.26. Effect of CGS21680 on EPSC and disynaptic IPSC charge in all experiments.
Baseline-normalized effect of CGS21680 on EPSCs and disynaptic IPSCs (dIPSCs) charge in all experiments. Values from each cell are connected with line. **(A)** EPSCs are significantly enhanced and dIPSCs suppressed by CGS21680. **(B)** The effect is blocked in the presence of $A_{2A}R$ antagonist SCH58261 (100 nM). In all panels, the number of experiments is shown in brackets; *P < 0.05 (Student's t-test).

Because pyramidal cells in the CA1 area can express low levels of CamKII and Cre, light-evoked ChR2 currents could mask synaptic EPSCs in these experiments (Geibel et al. 2014). Therefore, it was washed-in the glutamate receptor blockers NBQX (25 µM) and DL-APV (100 µM) at the end of experiments to measure ChR2-contribution to light stimulation-evoked excitatory currents (Figure 5.25). In all tested cells glutamatergic current was predominant (78 ± 8% of total charge, n = 7 cells) showing that the facilitatory of effect of $A_{2A}R$ agonist on excitatory currents is caused by increased glutamatergic EPSCs.

The results show that $A_{2A}R$ activation modulates Schaffer collateral-driven synaptic input from CA3 area to CA1 pyramidal cells in two ways; facilitating monosynaptic glutamatergic excitation and suppressing network-driven disynaptic GABAergic inhibition simultaneously. These changes can at least partially explain the above findings on $A_{2A}R$-mediated facilitation of Schaffer collateral fEPSP slope and popspike upon Schaffer

collateral paired pulse stimulation (see Figure 5.22), and the observed facilitation in CA1 pyramidal cells input / output transformation (see Figure 5.23).

5.2.5 Adenosine A_{2A}R facilitates glutamatergic Schaffer collateral synapses selectively to pyramidal cells

The experiments with Schaffer collateral electrical stimulation were repeated (see Figure 5.22) while recording intracellularly from postsynaptic CA1 pyramidal cells (Figure 5.27A). Bath-applied adenosine A_{2A}R agonist CGS21680 (30 nM) facilitated glutamatergic EPSC amplitude to 1.30 ± 0.04 from baseline (10-15 min following application, $P < 0.001$, $n = 9$, t-test) in synapses onto identified CA1 pyramidal cells (Figure 5.27B,C). Wash-in of A_{2A}R antagonist SCH58261 (100 nM) after baseline failed to change EPSCs, and baseline-normalized EPSC amplitude in SCH58261 was 0.94 ± 0.04 ($n = 6$, t-test) indicating that A_{2A}Rs are not activated by endogenous adenosine under the experimental conditions (Figure 5.27D).

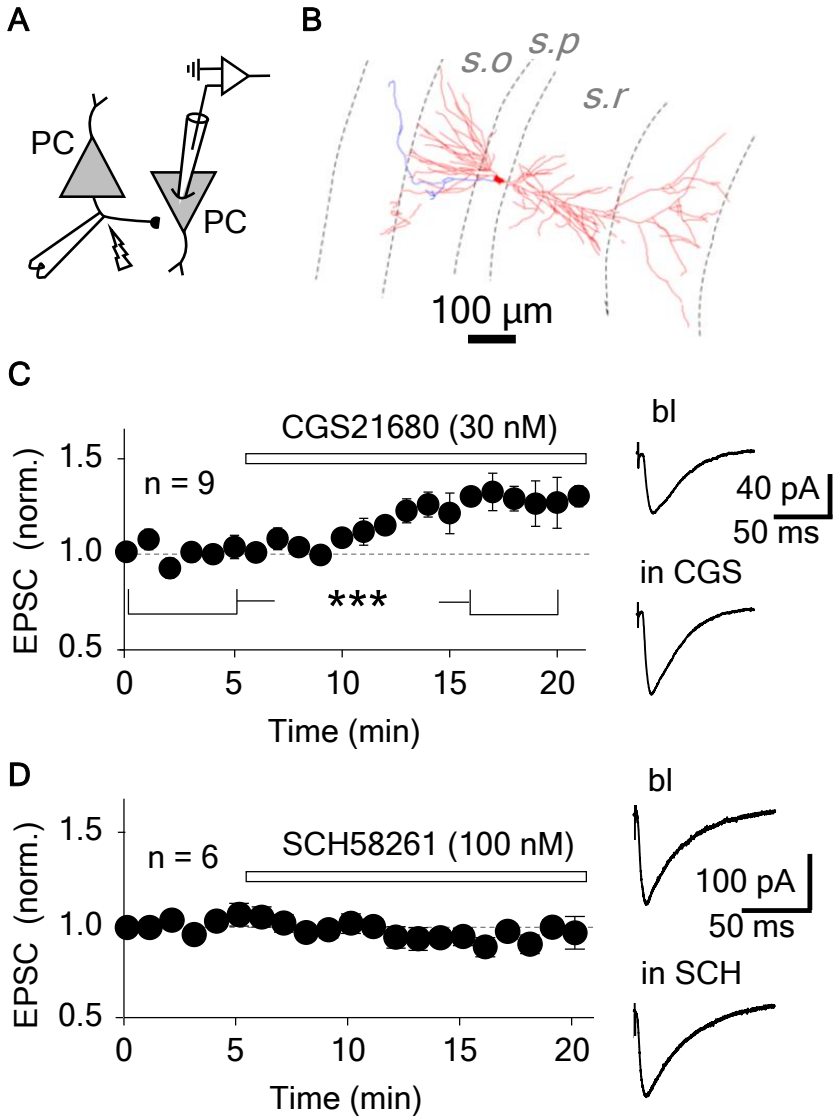

Figure 5.27. Adenosine A2AR facilitates glutamatergic synapses to pyramidal cells
(A) Schematic showing electrical stimulation of Schaffer collaterals and recording from pyramidal cells. Recordings were performed in the presence of GABA receptors blockers (PiTX, 100 mM) and CGP55845, 1 mM). **(B)** Illustration of one recorded, neurobiotin-filled and visualized pyramidal cell (soma and dendrites red; axon blue). **(C)** Left: bath-applied $A_{2A}R$ agonist CGS21680 (30 nM) facilitates glutamatergic EPSC amplitude (mean ± SEM, baseline-normalized); right: averaged EPSCs (10) from one cell in baseline (bl) and following CGS21680 application (at 15-20 min time point). **(D)** Left: adenosine $A_{2A}R$ antagonist SCH58261 (100 nM) has no effect on EPSC amplitude in the experimental conditions. Plot (mean ± SEM) and averaged EPSCs as in C. In all panels, the number of experiments is shown; the representative PSCs correspond to the average of 10 consecutive responses; ***P < 0.001 (Student's t-test); *s.r.: stratum radiatum, s.p.: stratum pyramidale, s.o.: stratum oriens*.

Next, it was studied EPSCs in two major interneuron populations involved in feedforward inhibition in area CA1; GABAergic cells expressing either PV-positive (Figure 5.28A,B) or CCK-positive with axonal CB_1R (Figure 5.28D,E) (Katona et al. 1999, Glickfeld & Scanziani 2006, Nissen et al. 2010, Armstrong & Soltesz 2012).

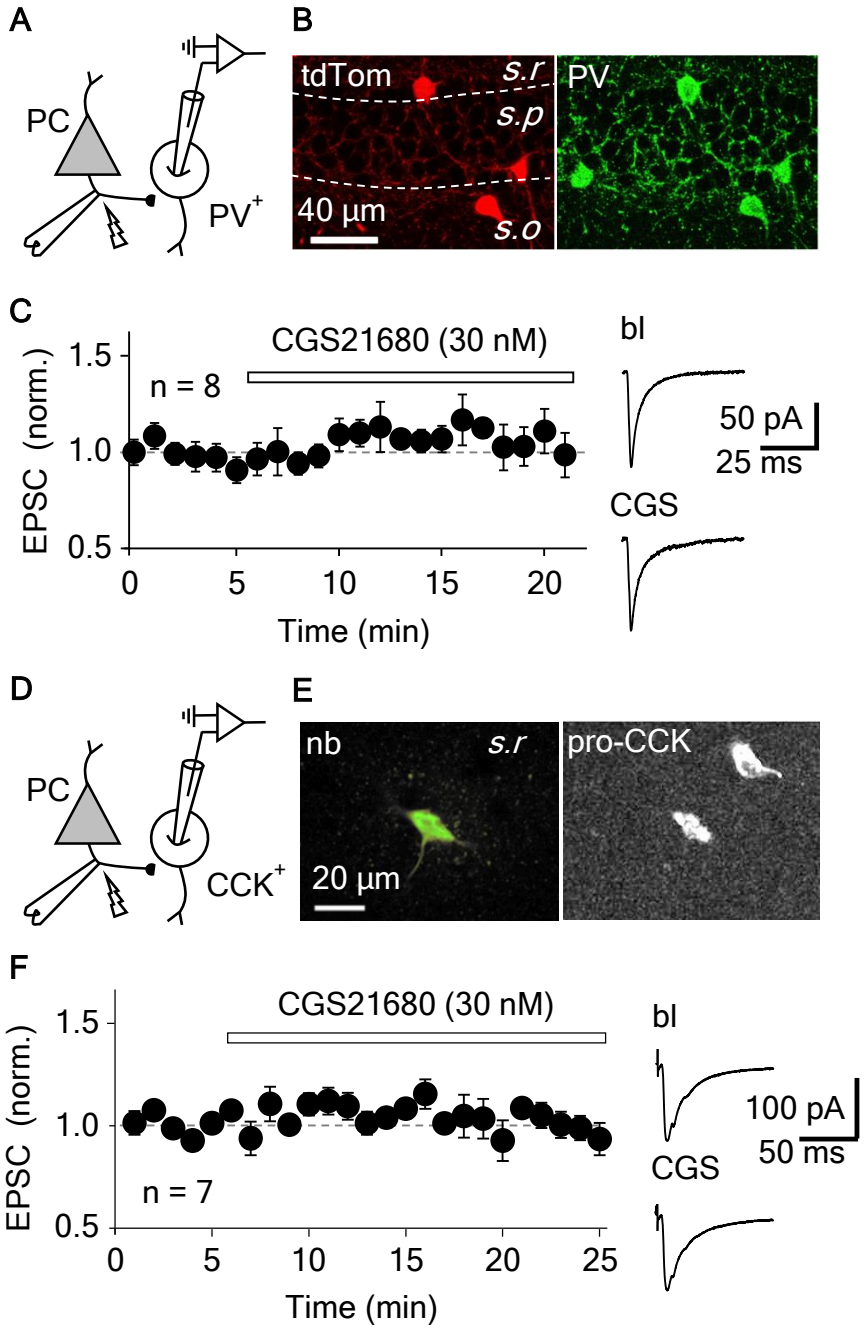

Figure 5.28. Adenosine $A_{2A}R$ does not affect synapses to two major feed-forward GABAergic inhibitory interneuron populations expressing either PV or CCK
(A) Schematic representation of the experimental design to record electrical-evoked EPSCs in PV-positive interneurons. **(B)** PV-positive cells were identified by Cre-dependent fluorophore (tdTomato, tdTom) expression. Confocal images showing tdTom (above) and immunoreaction for PV (below, visualized with Alexa-488) in the CA1 area in a fixed slice. **(C)** Left: EPSCs in PV-positive interneurons were not altered

by CGS21680 (baseline-normalized, mean ± SEM); right: averaged EPSCs (10) from one postsynaptic PV-positive cell. **(D)** Schematic representation of the experimental design to record electrical-evoked EPSCs in CCK-positive interneurons. **(E)** Postsynaptic CCK-positive interneurons were identified by positive immunoreaction for pro-CCK in *post hoc* analysis. Confocal images from one postsynaptic neurobiotin filled (nb, Alexa-488) and pro-CCK (Cy5) interneuron. **(F)** Left: adenosine $A_{2A}R$ agonist CGS21680 does not change EPSCs in CCK-positive GABAergic interneurons (baseline-normalized, mean ± SEM); right: averaged EPSCs (10) in one pro-CCK interneuron. In all panels, the number of experiments is shown; the representative PSCs correspond to the average of 10 consecutive responses; Student's t-test; *s.r.: stratum radiatum, s.p.: stratum pyramidale, s.o.: stratum oriens*.

Electrical-evoked EPSCs in PV-positive and CCK-positive interneurons were not altered by $A_{2A}R$ agonist (t-test), and baseline-normalized EPSC amplitudes in CGS21680 (30 nM) were 1.05 ± 0.05 (n = 8, Figure 5.28C) and 1.04 ± 0.02 (n = 7, Figure 5.28F) accordingly.

Thus, activation of $A_{2A}R$ facilitates excitatory Schaffer collateral synapses in target-specific manner. Mean ± SEM of EPSCs during baseline was 79.6 ± 8.1 pA in pyramidal cells (n = 9) and 77.8 ± 15.8 pA in the interneurons (n = 15). GABA receptors were blocked with PiTX (100 µM) and CGP55845 (1 µM), and cells were filled with neurobiotin for post-hoc anatomical and immunohistochemical studies (Figure 5.28B,E).

5.2.6 Adenosine $A_{2A}R$ enhances GABAergic inhibition in the CA1 area selectively between interneurons

The results described above do not explain why feedforward IPSCs were strongly suppressed by $A_{2A}R$ activation in experiments above (see Figure 5.22 and Figure 5.26). To explore this, it was investigated whether GABAergic synapses from interneurons to pyramidal cells are modulated by $A_{2A}R$ agonist, or if GABAergic synapses between interneurons are altered. Cre-

dependent ChR2 expression were used to optogenetically activate GABAergic synapses from either PV or CCK-expressing CA1 interneurons. Slices were prepared from heterozygous PV-Cre (Figure 5.29A) and BAC-CCK-Cre$^{tg/+}$ mice (Figure 5.33A) transduced with AAV:ChR2-eYFP (see Chapter 4.5, p88). It was first stimulated ChR2-expressing PV-positive GABAergic interneuron axons with paired-pulse laser light pulses (3 ms, 50 ms interval) in the CA1 area (Figure 5.29A,B), and found that wash-in of the agonist CGS21680 (30 nM) increased IPSC amplitude in postsynaptic interneurons to 1.35 ± 0.04 of baseline ($P < 0.001$, $n = 12$, t-test) (Figure 5.29C,D). The facilitation was significant in 11 of 12 anatomically verified interneurons, and was fully blocked when studied in the presence of the $A_{2A}R$ antagonist SCH58261 (100 nM) ($n = 5$, t-test) (Figure 5.29D).

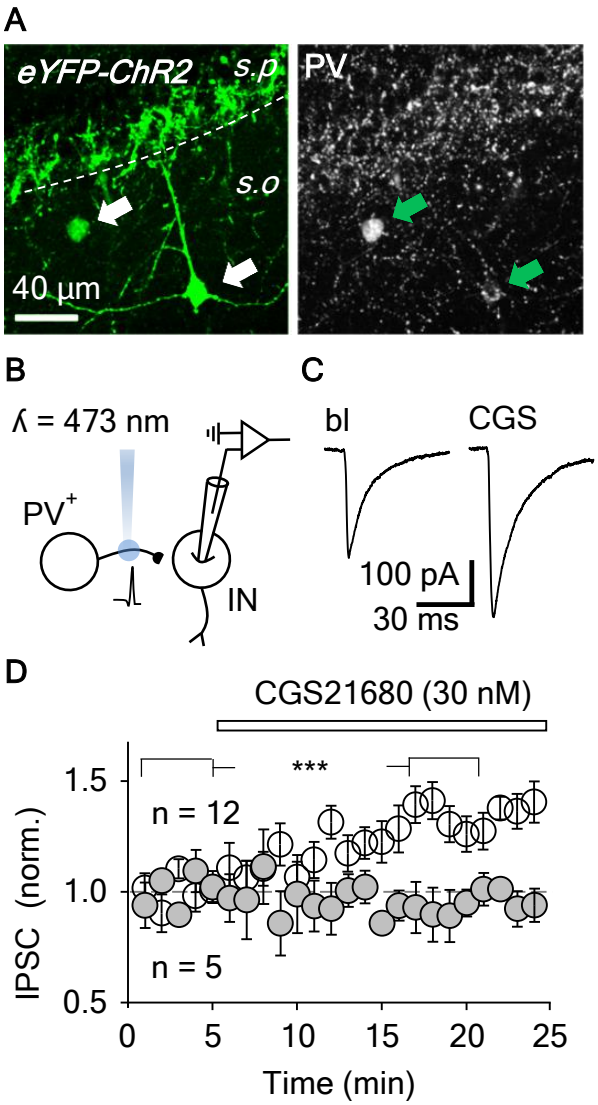

Figure 5.29. Adenosine $A_{2A}R$ agonist facilitates IPSCs elicited from GABAergic PV-positive cells to various inhibitory interneurons
(A) Optogenetic stimulation of GABAergic synapses from PV-positive interneurons. ChR2 is expressed in Cre-dependent manner. Confocal images show eYFP-ChR2 (above) in PV-positive cells (below, Cy5). Arrows point to positive somata (fixed slice). **(B)** Schematic of experimental design; **(C)** Averaged IPSCs (10) in baseline and after 15 min in CGS21680. **(D)** Plot shows that CGS21680 (30 nM) facilitates IPSC amplitude in postsynaptic interneurons (open symbols; mean ± SEM of baseline-normalized IPSCs; facilitation by CGS21680 is blocked in the presence of $A_{2A}R$ antagonist (SCH58261, 100 nM; gray symbols). The number of experiments is shown in the panel; the representative PSCs correspond to the average of 10 consecutive responses; ***P < 0.001 (Student's t-test*); s.p.: stratum pyramidale, s.o.: stratum oriens*.

However, CGS21680 (30 nM) failed to directly modulate GABAergic synapses from PV-positive cells to postsynaptic pyramidal cells (t-test) (Figure 5.30). Baseline-normalized IPSC amplitude in postsynaptic pyramidal cells was 0.93 ± 0.04 in the presence of CGS21680 (30 nM) (n = 12).

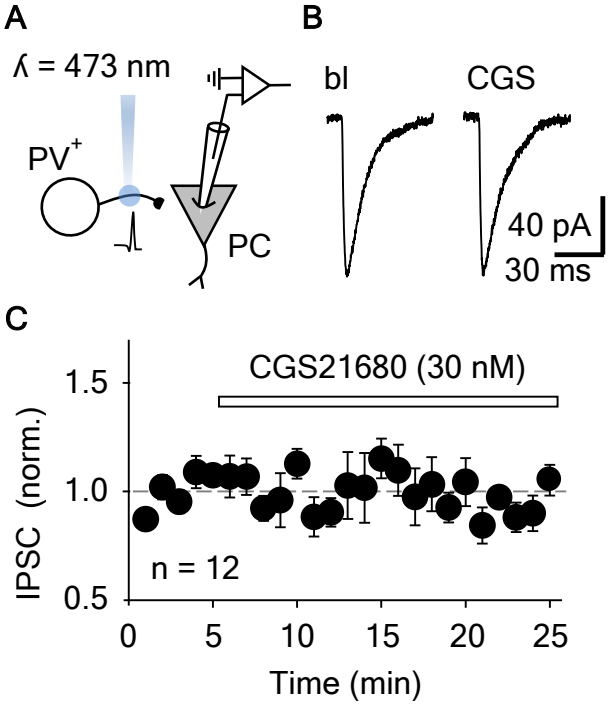

Figure 5.30. Adenosine $A_{2A}R$ fails to modulate IPSCs from PV-positive GABAergic synapses to identified pyramidal cells
(A) Schematic showing experimental design to record PV-positive mediated IPSCs. **(B)** Averaged IPSCs (10) in baseline and after 15 min in CGS21680 **(C)** CGS21680 fails to modulate IPSCs from PV-positive GABAergic synapses to identified pyramidal cells (mean ± SEM of baseline-normalized IPSCs). The number of experiments is shown in the panel; the representative PSCs correspond to the average of 10 consecutive responses; Student's t-test; PC: pyramidal cell; PV^+: Parvalbumin-positive interneuron.

The IPSC facilitation by CGS21680 (30 nM) in interneurons was associated with a decrease in the paired-pulse ratio to 0.67 ± 0.08 from baseline ($P < 0.001$, n = 10, t-test), suggesting presynaptic modulation of transmission by $A_{2A}R$ in GABAergic fibers (Figure

5.31A). In addition, facilitation of IPSC by CGS21680 was blocked in the presence of a PKA inhibitor H-89 dihydrochloride hydrate (1 μM) (baseline-normalized IPSC amplitude was to 1.02 ± 0.01, n = 5) (Figure 5.31B). In PKA-inhibitor studies, IPSCs were elicited with afferent electrical stimulation in the presence of glutamate receptor blockers (NBQX, 25 μM and DL-APV, 100 μM) and in control experiments IPSC increased to 1.14 ± 0.03 from baseline by CGS21680 (30 nM) ($P < 0.01$, 15 min wash-in, n = 6, t-test). Wash-in of $A_{2A}R$ antagonist SCH58261 after baseline (100 nM) failed to change IPSCs (amplitude 0.99 ± 0.11 of baseline, n = 6, t-test) (Figure 5.31B).

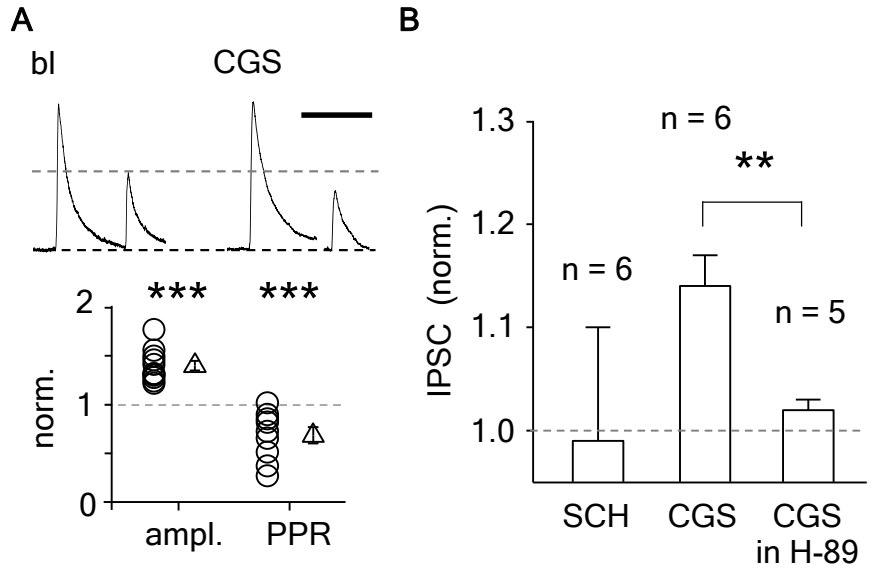

Figure 5.31. The CGS21680-induced IPSC facilitation in interneurons is associated with reduced paired-pulse ratio (PPR)
(A) Above: averaged IPSCs (10) in baseline and after perfusion with CGS21680 (30 nM), scale 50 ms; traces are scaled by 1st IPSC amplitude and dotted line indicates 2nd IPSC peak in baseline; below: plot shows baseline-normalized IPSC amplitude (for 1st IPSC) and PPR (2nd vs. 1st IPSC amplitude) following wash-in of CGS21680; Circles represent individual experiments; triangles correspond to mean ± SEM. **(B)** Facilitation of IPSCs by CGS21680 in interneurons involves protein kinase A (PKA). Histogram shows baseline normalized IPSC amplitude following CGS21680 application in control (mean ± SEM, n = 6), and in the presence of a PKA inhibitor H-89 (1 mM, n = 5). IPSCs were elicited by electrical stimulation of GABAergic fibers (glutamate receptors blocked with NBQX, 25 mM and DL-APV, 100 mM). The number of experiments is shown in the panels; the representative PSCs correspond to the average of 10 consecutive responses; **P < 0.01; ***P < 0.001 (Student's t-test); PPR: paired-pulse ratio.

The results on IPSCs in postsynaptic pyramidal cells and interneurons show that A_{2A}R-mediated modulation of inhibitory synapses from PV-positive GABAergic fibers depends on the postsynaptic cell type. Postsynaptic neurons were filled with neurobiotin during recording for post-hoc analysis of the cells (see Chapter 4.6, p93). This confirmed that A_{2A}R-mediated facilitation of IPSCs occurs in various postsynaptic interneuron types including O-LM cells (n = 2), and basket cells with negative (n = 2) or positive (n = 6) axonal immunoreaction for CB_1R (Figure 5.32)

(Glickfeld & Scanziani 2006, Lawrence et al. 2006, Klausberger & Somogyi 2008). Two interneurons, of which one showed IPSC facilitation by $A_{2A}R$, remained unidentified (Figure 5.32D).

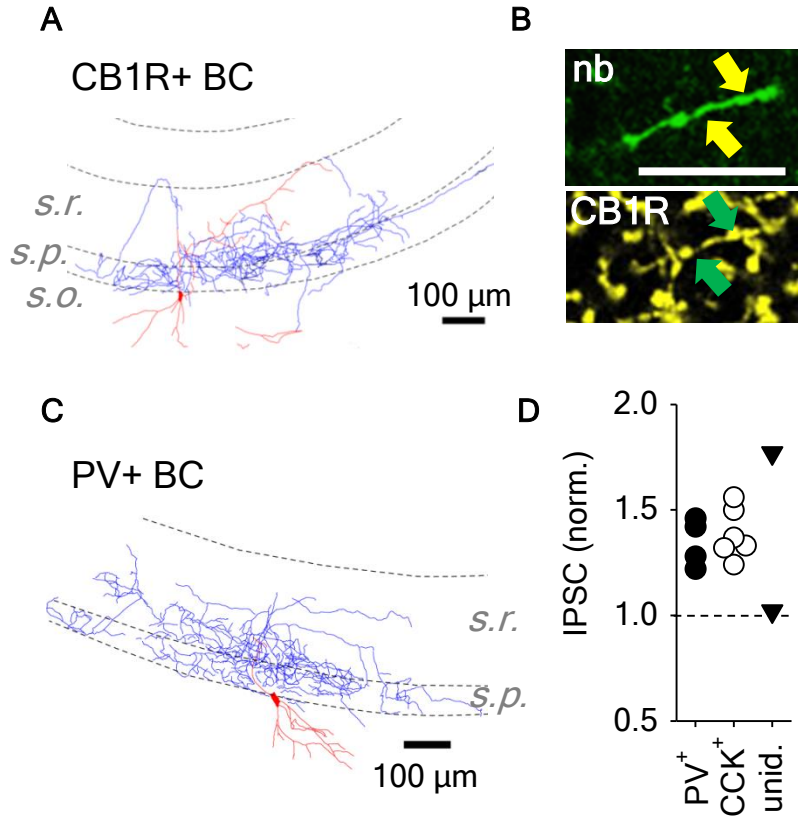

Figure 5.32. Optogenetic-evoked IPSC facilitation by CGS21680 occurs in various different postsynaptic interneuron types
(A and C) Illustration of a basket cell; collapsed z-stack epifluorescence image from one 60 mm-thick section (soma and dendrites in red, axon in blue) with positive (A) or negative (C) axonal immunoreaction for CB1R. **(B)** Confocal images of CB1R at Cy3 and a neurobiotin-filled axon in Alexa488, pointed by arrows; scale 20 mm. **(D)** Histogram shows baseline-normalized IPSC in CGS21680 in all recorded interneurons (n = 12). Analyses revealed four putatively PV-positive cells (two O-LM cells and two CB1R-negative basket cells) and six putative CCK-positive cells immunopositive for axonal CB1R. Two interneurons remained unidentified. *s.r.: stratum radiatum; s.p.: stratum pyramidale*,

Conversely, IPSCs elicited from CCK-positive GABAergic fibers (Figure 5.33A) were not modulated by $A_{2A}R$.

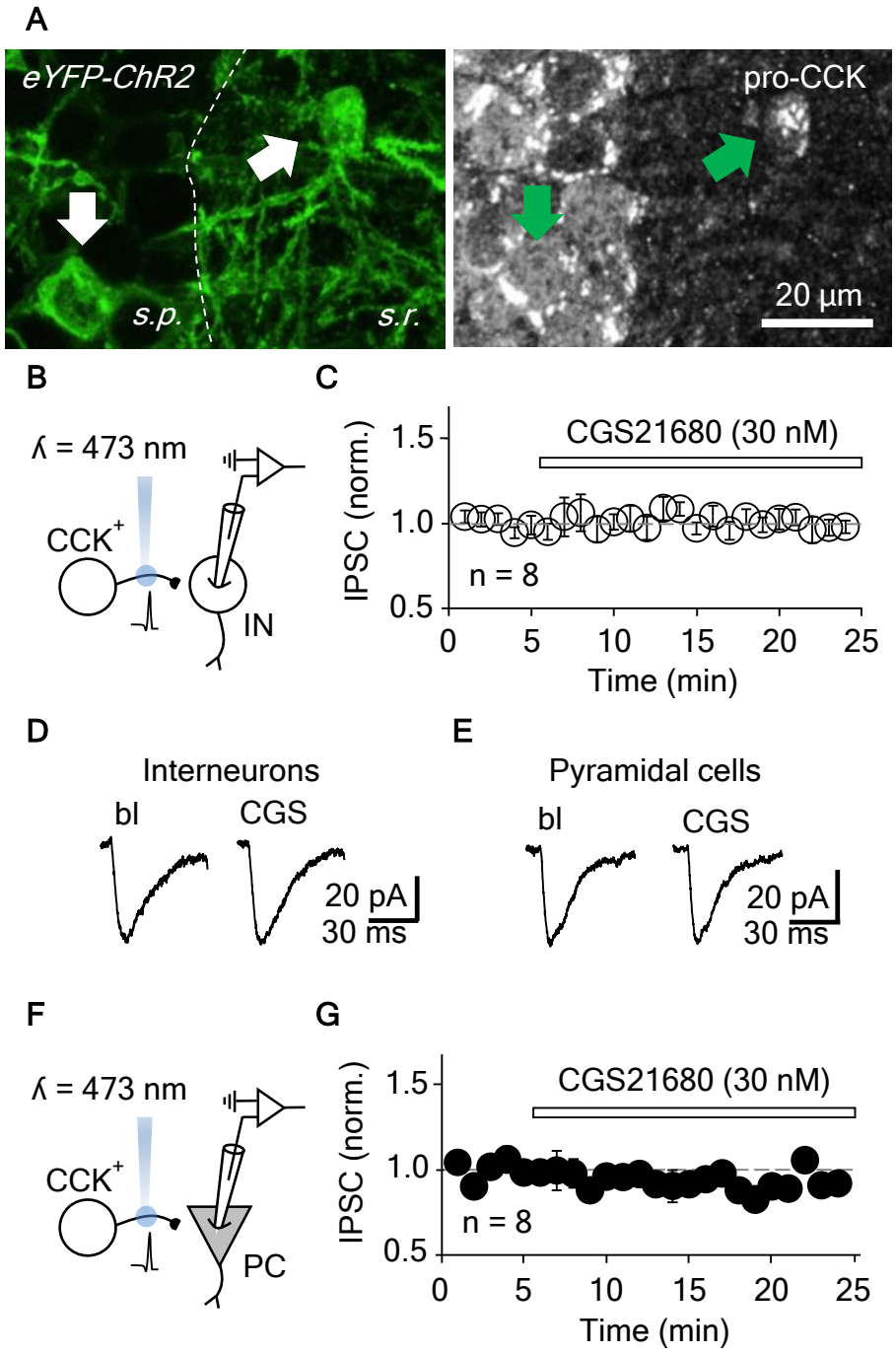

Figure 5.33. The IPSCs elicited from CCK-positive interneurons are not modulated by the $A_{2A}R$ agonist

(A) Optogenetic stimulation of axons from CCK-expressing GABAergic cells. Confocal images of AAV-transduced Cre-dependent eYFP-ChR2 (left) in pro-CCK neurons (right; at Cy5). Fluorophore-positive somata are pointed with arrows (fixed

slice). **(B and F)** Schematic representation of experimental CCK-positive mediated IPSCs evoked with laser stimulation and recorded from different populations of interneurons (B) or pyramidal cells (F). IPSCs evoked from CCK+ cells are not modulated by CGS21680 (30 nM) either in postsynaptic interneurons **(C)** nor in pyramidal cells **(G)**. **(D and E)** Averaged IPSCs (10) from sample recordings. All recordings were in the presence of NBQX (25 mM) and DL-APV (100 mM); the number of experiments is shown in the panels; the representative PSCs correspond to the average of 10 consecutive responses; Student's t-test. *s.r.: stratum radiatum; s.p.: stratum pyramidale*,

Exposure to CGS21680 (30 nM) failed to alter IPSCs either in postsynaptic interneurons (n = 8) (Figure 5.33B-D) or pyramidal cells (n = 5) (Figure 5.33E-G) (t-test, baseline IPSCs = 94.0 ± 25.2 pA and 52.7 ± 9.9 pA, respectively). Inhibitory PSCs were elicited by paired-pulse optical stimulation in slices from BAC-CCK-Cre$^{tg/+}$ mice transfected with AAV:ChR2-eYFP (Figure 5.33A). Ionotropic glutamate receptors were blocked with NBQX (25 μM) and DL-APV (100 μM), because in addition to GABAergic neurons also CCK-containing glutamatergic fibers in the CA1 area may express Cre (Geibel et al. 2014).

It was also confirmed that optogenetically-evoked IPSCs in the slices were elicited from CCK-positive interneuron axons demonstrating suppression of the IPSCs by CB_1R agonist WIN55,212-2 (5 μM) to 0.62 ± 0.03 of baseline ($P < 0.001$, n = 6, t-test) with a characteristic increase in paired-pulse ratio (to 1.49 ± 0.18 from baseline, $P < 0.05$, n = 5, t-test) (Figure 5.34) (Katona et al. 1999, Glickfeld & Scanziani 2006, Nissen et al. 2010).

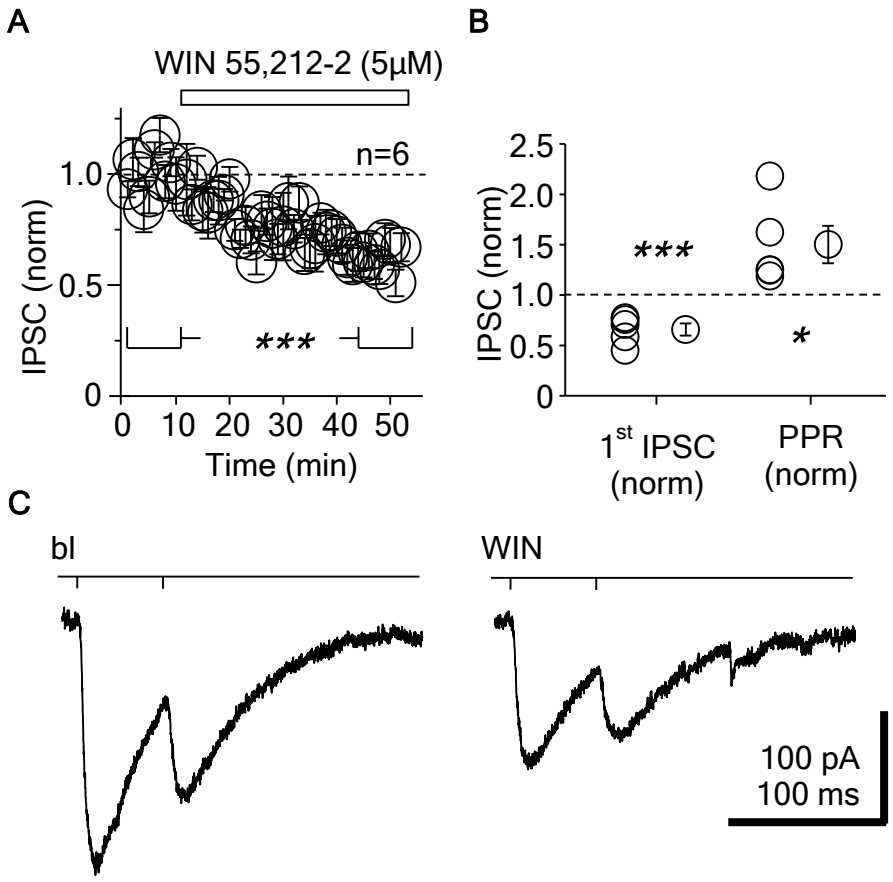

Figure 5.34. Optogenetically-evoked IPSCs from CCK-positive interneurons are inhibited by CB_1R activation

(A) Application of CB1R agonist WIN 55,212-2 (5 μM) shown with horizontal bar (mean ± SEM of baseline-normalized IPSCs in CA1 pyramidal cells). Glutamatergic ionotropic receptors were blocked with NBQX (25 μM) and D-APV (100 μM). **(B)** IPSC suppression is associated with increased paired-pulse ratio characteristic of GABAergic fibers from CCK+ interneurons. **(C)** Averaged IPSCs from one cell (stimuli indicated in horizontal time line) in baseline and after perfusion with WIN 55,212-2. The number of experiments is shown in the panel; the representative PSCs correspond to the average of 10 consecutive responses; *P < 0.05; ***P < 0.001 (paired t-test, normality test passed, Shapiro-Wilk test); PPR: paired-pulse ratio.

5.2.7 Endogenous adenosine promotes synchronous pyramidal cell discharge via $A_{2A}Rs$ in hippocampal slices

I next studied whether endogenous adenosine released by high-frequency electrical stimulation is sufficient to modulate

hippocampal pyramidal cell discharge through adenosine $A_{2A}R$ (Chamberlain et al. 2013). The experimental design is the same described above in Figure 5.22 (p148) to electrically stimulate Schaffer collaterals with paired pulses (50 ms interval), while recording field potential in the CA1 area. In addition, high-frequency stimulation (HFS, 50 Hz, 100 pulse) was applied with second stimulation electrode (S2) positioned in the vicinity of recording electrode aiming to elicit local release of adenosine (Figure 5.35A) (Chamberlain et al. 2013). Schaffer collaterals were stimulated every 5 s and HFS delivered with second electrode every 2 min. To uncover adenosine $A_{2A}R$-mediated modulation the experiments were performed in continuous presence of blockers for CB_1R (AM-251 2 µM), $GABA_BR$ (CGP55485, 1 µM), adenosine A_1R (DPCPX, 200 nM) as well as with DL-APV (100 µM). The fEPSP parameters were analyzed as in Figure 5.22 (p148) and found that HFS was followed by significant increase of popspike amplitude in Schaffer collateral –mediated field potential response. Popspike were elicited by 2^{nd} stimulation pulse of the paired-pulse and they were significantly increased from baseline up to 40 s following the HFS (Figure 5.35B,C). Importantly, the facilitation was blocked after wash-in of SCH58261 (100 nM) ($P < 0.001$, ANOVA, Tukey's HSD test) (Figure 5.35B,C). Although HFS also transiently modulated fEPSP slope in the experiments, application of the $A_{2A}R$ blocker failed to cause any change in the effect on slope. Neither did HFS or SCH58261 affect prespike volley (ANOVA, Tukey's HSD test). The HFS and $A_{2A}R$ antagonists effects on popspike are shown in detail in Figure 5.35.

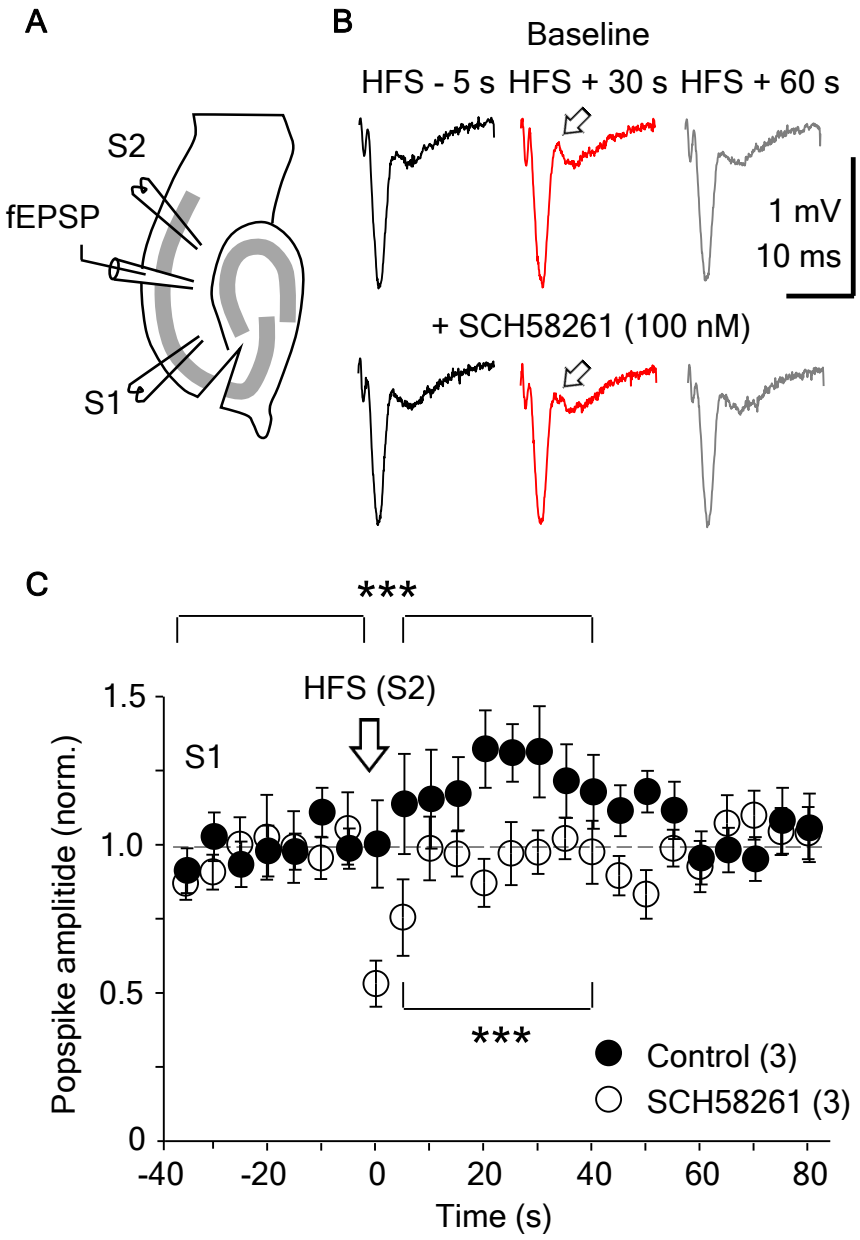

Figure 5.35. Facilitation of hippocampal pyramidal cell discharge through A_{2A}Rs activated by high-frequency electrical stimulation.
Transient facilitation of Schaffer collateral stimulation (S1)-evoked popspike following high-frequency stimulation with another electrode (S2) in the vicinity of recording site. **(A)** A schematic shows experimental design in the CA1 area. Paired-pulse (50 ms interval) electrical stimulation of Schaffer collaterals (S1) was delivered every 5 s, and high frequency local stimulation (HFS, 50 Hz with 100 pulses) applied with electrode S2 every 2 min. The S2 electrode was positioned approximately 100 mm from field potential (fEPSP) recording. **(B)** Averaged (5) traces from one experiment show facilitation of fEPSP associated popspike (pointed with arrow) following S2 HFS.

Wash-in of $A_{2A}R$ antagonist SCH58261 (100 nM, 10 min) abolished facilitation in the same experiment. Traces at different time points in relation to HFS are shown in distinct colors. Arrow points to increased popspike 30 s after HFS in baseline conditions, and below shows same response following wash-in of SCH58261 (10 min). Popspikes was elicited in 2nd pulse of paired-pulse stimulation. **(C)** Mean ± SEM of baseline-normalized popspike amplitude in three experiments. Solid symbols indicate baseline conditions (before SCH58261 wash-in) and open circles following 10 min wash-in of SCH58261 (100 nM). The number of experiments is shown in the panel; the representative PSCs correspond to the average of 5 consecutive responses; ***P < 0.001 (Single-way ANOVA and Tukey's *post hoc* test); in each experiment 5 cycles were recorded at each time point; timing of HFS is indicated by arrow (delivered immediately before abscissa 0-time point); HFS: high frequency stimulation.

5.2.8 Modulation of spontaneous epileptiform pyramidal cell discharge by adenosine $A_{2A}R$

Finally, it was investigated whether $A_{2A}R$ activation by endogenous adenosine modulates spontaneous epileptiform discharge of hippocampal pyramidal cells in hyperexcitable conditions. Spontaneous inter-ictal like pyramidal cell population bursts were generated exposing slices to elevated (8-9 mM) [K_o] in perfusion solution (Korn et al. 1987, Sagratella et al. 1987). Field potential was recorded in the CA3 area in an interface chamber. Following stable baseline (at least 10 minutes), either $A_{2A}R$ blocker SCH58261 (100 nM) or agonist CGS21680 (30 nM) was washed in. Epileptiform activity was quantified analyzing the occurrence of spontaneous inter-ictal like events characterized by a low frequency content field potential deflection associated with a barrage of extracellular spikes. Recordings were band-pass (1 - 100 Hz) filtered off-line to uncover low-frequency deflections and analyze event occurrence (Figure 5.36A,B). Amplitude threshold was set to 0.25 mV, and event detection was visually verified. Parallel high-pass filtering (> 60 Hz) of recordings uncovered

extracellular spikes associated with the events (Figure 5.36B). Occurrence of inter-ictal like events in baseline conditions was 32.7 ± 11.7 events / min, ranging from 6.3 to 97.4 events / min (n = 7) (Figure 5.36C). The adenosine $A_{2A}R$ blocker SCH58261 strongly inhibited the occurrence spontaneous population bursts to 36 ± 9% ($P < 0.01$, n = 3, t-test) of baseline in 20 - 30 min following drug application (Figure 5.36A,C). The activity-suppressing effect of antagonist persisted and in 40 - 50 min from drug application the burst occurrence dropped to 16 ± 5% of baseline level ($P < 0.001$, n = 3, t-test) (Figure 5.36C).

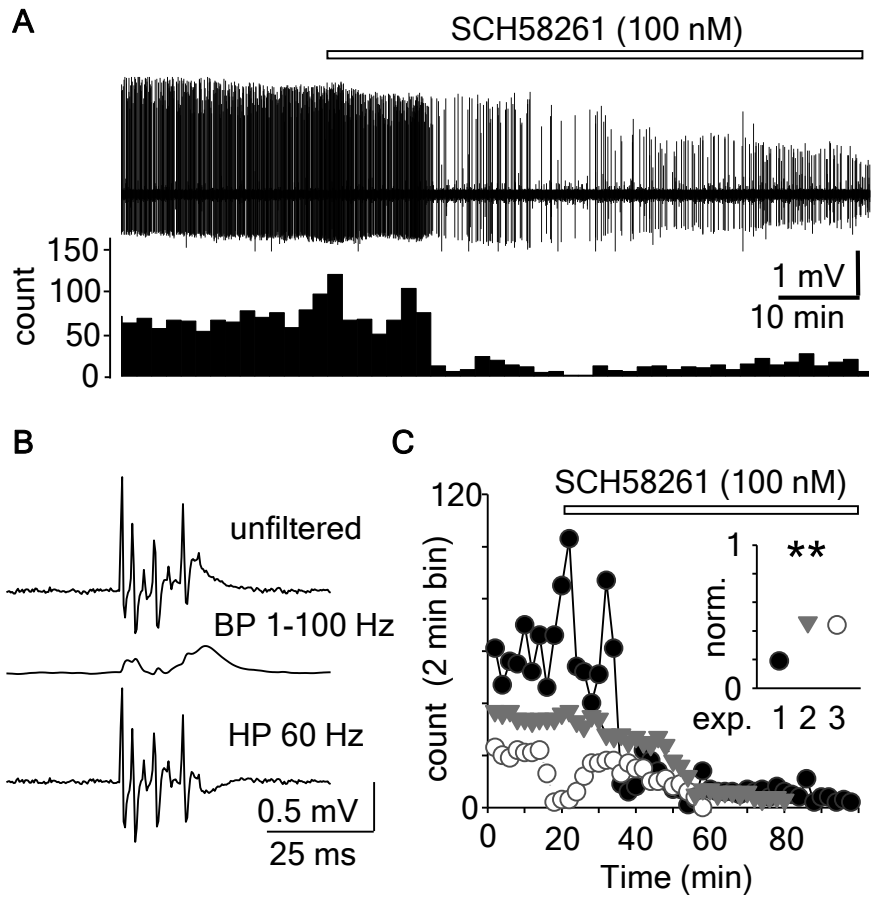

Figure 5.36. Modulation of spontaneous epileptiform pyramidal cell discharge by A_{2A}R antagonist.

Adenosine A_{2A}R blocker SCH58261 (100 nM) suppresses spontaneous epileptiform discharges in hippocampal slices exposed to elevated (8-9 mM) extracellular potassium. Spontaneous interictal-like synchronous bursting activity was recorded with field potential electrode in CA3 area. **(A)** A sample trace from one experiment showing inhibition of spontaneous epileptiform burst activity by SCH58261 (unfiltered trace). Timing for wash-in of A_{2A}R antagonist SCH58261 (100 nM) is indicated by horizontal bar. Histogram below shows occurrence of spontaneous epileptiform bursts in 2 min bins. For burst occurrence analysis data were band-pass filtered (1-100 Hz) to avoid detection of occasional single unitary extracellular spikes. **(B)** Epileptiform population bursts are characterized by 1-100 Hz band-pass filtered (BP 1-100 Hz) field potential deflection associated with extracellular spikes (high-pass filtered at 60 Hz, HP 60 Hz). An unfiltered epoch shown on top with filtering below as indicated. **(C)** Plot shows suppression in occurrence of spontaneous epileptiform events by SCH58261 in the three of three experiments. Occurrence of events is shown in 2 min bins. Horizontal bar indicates wash-in of the antagonist. Inset plot shows baseline-normalized effect of the antagonist on burst occurrence (indicated with same symbols as in main plot). Inhibitory effect of SCH58261 was highly significant; **P < 0.01, Student's t-test, at 20-30 min after drug application.

Adenosine $A_{2A}R$ agonist CGS21680 (100 nM) increased spontaneous epileptiform burst occurrence from baseline to 140 ± 16% ($P < 0.05$, $n = 4$, t-test) in 20 - 30 min following drug application (Figure 5.37A,B). Increase of burst occurrence was significant in three of four experiments, but varied in magnitude (Figure 5.37B,D). Samples of band-pass and high-pass -filtered events are illustrated in Figure 5.37A,C.

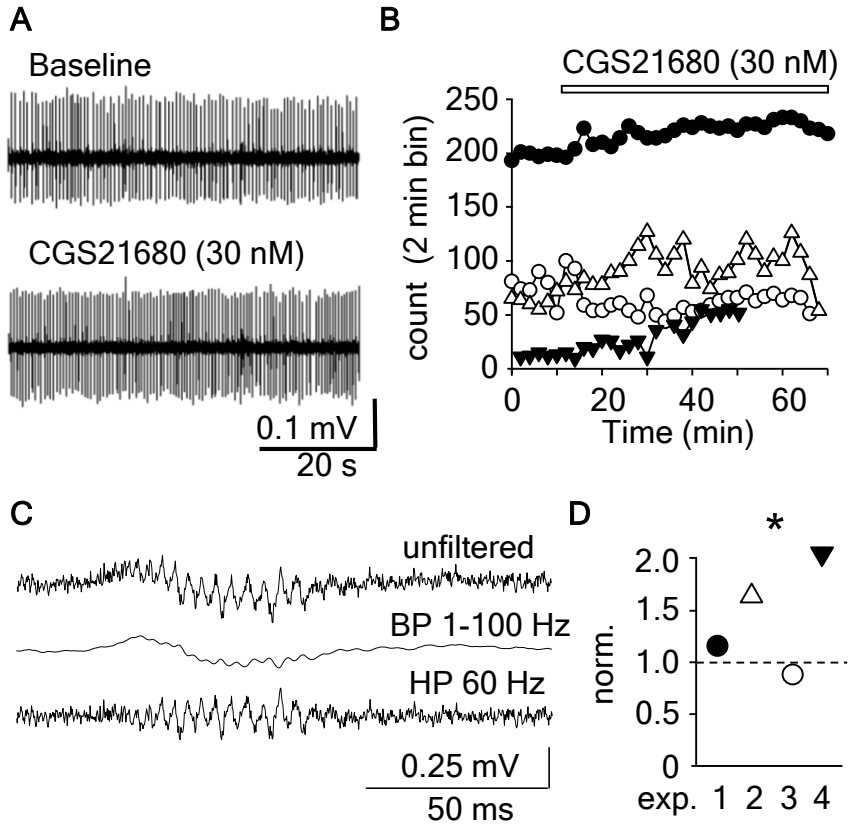

Figure 5.37. Modulation of spontaneous epileptiform pyramidal cell discharge by $A_{2A}R$ agonist.
Wash-in of $A_{2A}R$ agonist CGS21680 (30 nM) is associated with increased spontaneous occurrence of epileptiform bursts. **(A)** Traces from one experiment illustrate spontaneous burst activity in baseline and following agonist application (20-30 min wash-in). **(B)** Plot shows effect of $A_{2A}R$ agonist (CGS21680, 30 nM) on occurrence of spontaneous epileptiform bursts in four experiments (2 min bin). Wash-in of the antagonist is indicated by horizontal bar. **(C)** Illustration of one burst event from same experiment. Unfiltered (top) and filtered (band-pass 1-100 Hz and high-pass 60 Hz) traces of the same event are illustrated as indicated. **(D)** Baseline-normalized burst occurrence in the presence of agonist in the four experiments above (indicated with same symbols). Burst occurrence is variably modulated, but significantly increased in pool of four experiments; *P < 0.05, Student's t-test, at 20-30 min time point following agonist application. BP: band-pass; HP: high-pass; norm: normalized.

Modulation of spontaneous activity with $A_{2A}R$ drugs suggests the receptors are tonically activated in slices with elevated [K_o], possibly because of increased ambient adenosine levels

(Marichich & Nasello 1973, Etherington & Frenguelli 2004, Dias et al. 2013).

5.2.9 Discussion

Adenosine has a well-established role as an endogenous neuronal inhibitor in the brain. The suppressive effect of adenosine on excitatory glutamatergic transmission via A_1R is well characterized, but its effect via other adenosine receptor types is not as well known (Dunwiddie & Masino 2001, Sebastião & Ribeiro 2009). In the hippocampus and neocortex the high-affinity $A_{2A}R$ is expressed in low quantities (Dixon et al. 1996), but elevated levels of extracellular adenosine activate these receptors to facilitate neuronal discharge (Etherington & Frenguelli 2004, Zeraati et al. 2006, El Yacoubi et al. 2008, 2009). It has been proposed that excitatory effects of adenosine in the cortex may mainly occur in pathological conditions, because $A_{2A}R$ expression levels increase in those circumstances in parallel with desensitization and down-regulation of A_1R (Rebola et al. 2005b, D'Alimonte et al. 2009, Hamil et al. 2012, Moschovos et al. 2012). In addition evidence for $A_{2A}R$-mediated modulation of activity in the hippocampus in physiological conditions is emerging (Cunha & Ribeiro 2000b, Rebola et al. 2005a, 2008; Dias et al. 2012, 2013; Chamberlain et al. 2013, Wei et al. 2014), but $A_{2A}R$ effect on identified neuronal circuits in this area is still poorly known.

Here are identified two sites of synaptic modulation by which $A_{2A}R$ acts to shift the balance between synaptic excitation and inhibition in mouse hippocampus to facilitate principal cell discharge. Adenosine $A_{2A}R$ activation directly enhances excitatory

glutamatergic Schaffer collateral synapses to CA1 pyramidal cells, and simultaneously suppresses feedforward GABAergic inhibition to same neurons. This at least partially explains the facilitatory effects of $A_{2A}R$ agonist on Schaffer collateral field potential responses in the CA1 area with increased fEPSP slope and popspike amplitude (shown in Figure 5.22, p148 and Figure 5.35, 172) (Sebastião & Ribeiro 1992). Our results also demonstrate that adenosine $A_{2A}R$ is unlikely to modulate glutamatergic Schaffer collateral axon excitability, for example through axonal receptors (Kullmann et al. 2005), because the agonist did not have effect on extracellular prespike volley. Together our findings provide a simple mechanistic explanation how $A_{2A}R$ activity increases excitability in the hippocampal CA3-CA1 circuitry modulating identified excitatory and inhibitory synapses. Although modulatory effects of $A_{2A}R$ are not restricted to synapses, but in addition can include alterations in intrinsic properties of neurons (Rebola et al. 2011) as well as glial glutamate transport (Matos et al. 2013), the synaptic modulatory action can at least partly explain pro-convulsive effect of $A_{2A}R$ reported previously and also demonstrated here (Jones et al. 1998, Zeraati et al. 2006, El Yacoubi et al. 2008, 2009).

Facilitation of epileptiform activity through low $A_{2A}R$ expression level in the hippocampus (Dixon et al. 1996) can be explained by synergistic action of the synaptic modulatory actions shown here. Increased Schaffer collateral excitation of pyramidal cells, but not feedforward interneurons, increases CA1 pyramidal firing to glutamatergic input from the CA3 area (Pouille & Scanziani 2001, Lamsa et al. 2005, Xiao et al. 2006, Pavlov et al. 2009, Lovett-Barron et al. 2012). It was studied two major subpopulations of

CA1 area GABAergic interneurons, either expressing PV or CCK, which both contribute to CA3-CA1 feedforward inhibition controlling CA1 area pyramidal cell firing and their input-output transformation (Cobb et al. 1995, Halasy et al. 1996, Glickfeld & Scanziani 2006, Klausberger & Somogyi 2008, Lovett-Barron et al. 2012). Inhibitory transmission through these interneurons to CA1 pyramidal cells was not enhanced by A_{2A}R. Instead A_{2A}R activation suppressed feedforward GABAergic inhibition in pyramidal cells through a mechanism which is likely to include disinhibition. Facilitation of inhibitory synapses between CA1 interneurons has been demonstrated to effectively suppress network activity-driven GABAergic inhibition in the CA1 area pyramidal cells (Chamberland & Topolnik 2012, Lovett-Barron et al. 2012). This promotes synaptically-driven pyramidal cell discharge and increases their input-output transformation (Tóth et al. 1997, Mastakov et al. 2001, Letzkus et al. 2011, Lovett-Barron et al. 2012). Here is reported that A_{2A}R-mediated facilitation of IPSCs was present in various postsynaptic CA1 area interneuron types, including O-LM cells specialized to inhibit distal dendrites of pyramidal cells, and basket cells that directly control pyramidal cell action potential firing via perisomatic inhibitory synapses (Zhang & McBain 1995, Glickfeld & Scanziani 2006, Klausberger & Somogyi 2008). Through modulation of the GABAergic circuits A_{2A}Rs can control co-ordinated rhythmic neuronal activities in the hippocampus (Cobb et al. 1995, Klausberger et al. 2005, Wulff et al. 2009). Interestingly, the A_{2A}R-mediated facilitation of GABAergic efferents was specific to PV-expressing interneurons, and was not detected in CCK-positive GABAergic interneuron fibers (Armstrong & Soltesz 2012).

Importantly, it is showed that $A_{2A}R$-mediated facilitation of CA1 pyramidal cell activity also occurs through endogenous adenosine. High-frequency electrical stimulation experiment demonstrated that CA1 area pyramidal cell input-output transformation to Schaffer collateral stimulation is similarly facilitated via endogenous and agonist-induced $A_{2A}R$ activity. Although high-frequency stimulation-evoked $A_{2A}R$ activation failed to significantly change synaptic Schaffer collateral responses in the experiments, this can be explained by higher sensitivity of the network-driven input-output function than a monosynaptic pathway to synaptic modulations (Lovett-Barron et al. 2012).

Our results on spontaneous activity modulation by $A_{2A}R$ antagonist and agonist in hyperexcitable conditions confirm the previously reported findings that $A_{2A}R$ controls spontaneous epileptiform pyramidal cell discharge in the hippocampus (Sebastião & Ribeiro 2009). In addition, the results indicate that in slices with elevated extracellular potassium adenosine $A_{2A}Rs$ are tonically active promoting synchronous discharge in the hippocampus. This was evidenced by robust effect with $A_{2A}R$ antagonist suppressing the spontaneous interictal like events in the CA3 area. Variability and occasionally a lack of $A_{2A}R$ agonist effect to promote synchronous discharge in these conditions could also be explained by vigorous tonic $A_{2A}R$ activity in baseline conditions (Dias et al. 2013). Given that ambient adenosine levels elevate in epileptic tissue and $A_{2A}R$ expression increases whereas A_1R levels go down, $A_{2A}R$ blockers might provide an effective supplementary treatment in specific forms of epilepsy (Sebastião & Ribeiro 2009, Gomes et al. 2011). Therapeutic effects of adenosine via A_1R might benefit from inhibition of $A_{2A}Rs$. A seizure

promoting role of $A_{2A}R$ in humans has recently been highlighted (Shinohara et al. 2013), and adenosine $A_{2A}R$ antagonists have already entered clinical trials and are safe to use with relatively mild side effects (Lopes et al. 2011, Shook & Jackson 2011, Müller 2013). Our findings here identify specific synaptic targets for $A_{2A}R$-modulation. This helps to understand how these receptors are involved in generation of aberrant hippocampal activity and can point out specific therapeutic targets in cortical microcircuits.

6 General Discussion and Conclusions

The present work was designed to investigate the actions of adenosine, through A_1R and $A_{2A}R$, on hippocampal inhibitory circuitry functioning. Before this work, little was known about how adenosine receptors influence GABA-mediated transmission to principal excitatory cells and in-between interneurons. In fact, most adenosine neuromodulatory actions on hippocampal excitability were considered to be mediated through the control of principal cells, either by influencing glutamatergic actions (pre- and postsynaptically) or by directly changing neuronal excitability through potassium channels. The reason for this lack of information about the influence of adenosine on inhibitory networks was most probably related to the technical difficulties to record and isolate monosynaptic inhibitory inputs to different populations of neurons as well as to investigate how selective modulation of these synapses would contribute to changes of excitability in intact circuits. Attempts were made by Lambert group and others to evaluate adenosine influence on mono- and disynaptic inhibitory responses in the hippocampus (Kamiya 1991, Lambert & Teyler 1991, Yoon & Rothman 1991, Thompson et al. 1992), however, many of the obtained results remained to be further explored and clarified. Taking advantage of the most recent technology that allows to selectively explore synapses in the brain and by methodically exploring individual connections and forms of transmission between different players in hippocampal inhibitory circuitry, I aimed with my PhD work to clarify this long-to-answer

question of whether and how adenosine influences GABA transmission in the hippocampus.

From the results obtained in this work three main conclusions could be drawn (also see Figure 6.1):

(1) Adenosine A_1R and $A_{2A}R$ indeed modulate GABAergic transmission in the hippocampus by selectively acting on specific populations of neurons;

(2) Activation of A_1R affects tonic, but not phasic, $GABA_AR$-mediated transmission in pyramidal cells and in CB_1R-expressing interneurons;

(3) Modulation of $A_{2A}R$ leads to increased inhibitory monosynaptic inputs through PV-positive neurons to other interneurons leading to disinhibition of principal cells and increased hippocampal excitability.

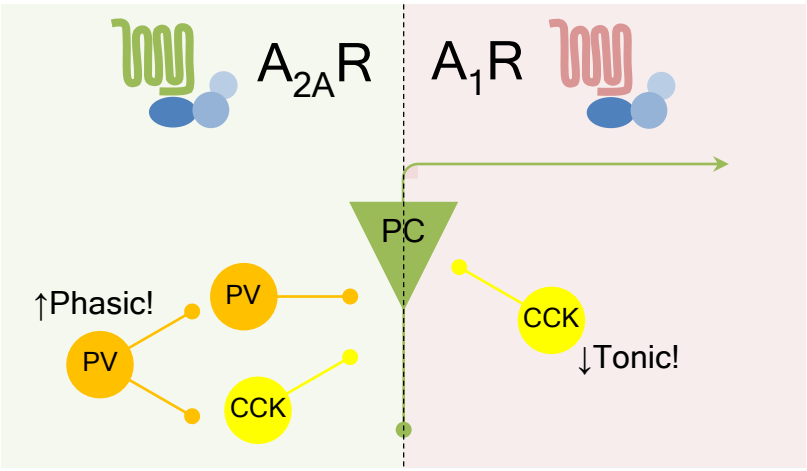

Figure 6.1 Schematic with the main achievements of the work presented in this thesis.

Together these results open new promising lines of investigation to further explore adenosine actions on GABA-mediated responses and emphasize the need to take into account its diversity, frequently opposite, and highly selective modes of action on diverse neuronal populations, while planning adenosine use for therapeutic purposes.

Above all, this work points out important aspects about adenosine control and modulation of hippocampal excitability that are summarized next:

(1) Modulation of tonic *versus* phasic inhibitory transmission;
(2) Modulation of pyramidal cells *versus* interneurons;
(3) Modulation of different populations of interneurons (CCK-positive *versus* PV-positive interneurons);
(4) Modulation of mono- *versus* disynaptic inhibitory transmission and its impact for principal cells excitability;
(5) Modulation through A_1R *versus* $A_{2A}R$;
(6) Consequences for pathophysiological conditions (the example of epilepsy).

This summary clearly reveals that selectivity is a hallmark of adenosine actions on GABAergic transmission. Through A_1Rs, tonic, but not phasic, inhibition is controlled with greater physiological relevance on CCK-positive interneurons. Through $A_{2A}Rs$, on the other hand, presynaptic phasic inhibitory transmission is enhanced selectively on PV-positive interneurons, explaining the adenosine-mediated increase of hippocampal principal cells excitability.

Together, the results also reveal the strong versatility of actions mediated by adenosine. In fact, modulating tonic actions on CCK-positive neurons or phasic PV-positive interneuron outputs will

have completely different consequences for the operations of neuronal networks. As mentioned in the Introduction (Chapter 1.1.2, p12), there is a functional dichotomy between PV-positive and CCK-positive interneurons in the hippocampus (Armstrong & Soltesz 2012, Bartos & Elgueta 2012). This dichotomy is evidenced by their distinct intrinsic neuronal properties that will consequently generate different but complementary tasks in network functioning and animal behavior. In general, PV-cells are considered to have characteristics that are well-suited to control the precise timing and oscillatory activity of the network, by reliably translating rapid excitatory inputs into fast short-latency inhibitory outputs (Jonas 2004, Doischer et al. 2008). In contrast, CCK-neurons receive information from distinct sources and multiple modulatory systems (Freund & Katona 2007), integrate these inputs over longer time windows and respond less readily in a form of tonic inhibition (Hefft & Jonas 2005, Daw et al. 2009, Ali & Todorova 2010). Several modulators of the CNS have already been described to differently control these two populations of inhibitory neurons. Examples include CCK peptide, best known for its gastrointestinal actions, but also extremely abundant in the brain where it suppresses GABA release from CCK-positive neurons (Földy et al. 2007) but also causes a robust depolarization of PV-positive cells with consequent increase in its firing rate (Lee et al. 2011). Also endocannabinoids, a group of lipid messenger molecules (Piomelli 2003), are known to act selectively on CCK-positive neurons (Katona et al. 1999, Freund & Katona 2007) where they mediate suppression of GABA release in response to postsynaptic pyramidal cell production (Földy et al. 2006, Neu et al. 2007, Lawrence 2008, Kano et al. 2009). Many

other substances, such as acetylcholine, serotonin or opioids, can be added to the list, all with the common characteristic of altering differently and selectively the actions of CCK- or PV-interneurons (Armstrong & Soltesz 2012).

Adenosine emerges now as a new modulator with long-known effects on hippocampal neuronal communication that also shows selective actions mediated by A_1Rs or A_{2A}Rs on CCK- or PV-positive neurons, respectively. In fact, adenosine seems to contribute, in this case, to further exaggerate the dichotomy between these two populations of cells. In one hand, it is responsible for decreasing peri- and extrasynaptic $GABA_A$R activity in CCK-positive interneurons that will contribute to dislocate the inhibitory tone from interneurons to pyramidal cells and explain the decreased principal cells excitability after A_1R activation. This reduced GABA tonus in CCK interneurons will determine its increased excitability and firing output to principal cells, exacerbating the role of CCK cells in balancing excitation and inhibition and implementing gain control mechanisms in hippocampal networks (Mitchell & Silver 2003). On the other hand, increased phasic GABA release from PV neurons will disinhibit pyramidal cells and mediate A_{2A}R increased excitability. Through A_{2A}Rs, adenosine is then involved in controlling connectivity between PV-cells to other interneurons, which may play a major role in the increase of spike fidelity in these cells, ensure their temporally precise firing (Bacci & Huguenard 2006) and coherence of network oscillations (Whittington et al. 1995, Traub et al. 1996, Bartos et al. 2001, 2002; Bartos & Elgueta 2012). Given the importance of these two populations of interneurons in hippocampal network functioning and consequently, in many

cognitive operations such as learning and memory, this work comes to confirm and further stablish the influence of adenosine, through novel and diverse mechanism, in the control and regulation of these processes.

Besides the knowledge of adenosine effects during physiological situations, a major interest in the adenosine field is concerned with understanding its actions during pathophysiological conditions such as epilepsy. In fact, the results shown in this thesis highlight the necessity for careful planning of adenosine therapies. Conjugation of A_1R activation and $A_{2A}R$ inhibition might prove of great benefit in the treatment of several forms of pharmacoresistant epilepsy. Although this was not directly tested in this work, results herein described provide additional and strong evidence in this direction.

Further research on the understanding of adenosine role in physiology and pathophysiology of GABA-related diseases, would be, indeed, extremely advantageous. Namely, there are some top priority questions that are still awaiting to be answered. These are mostly related with the specificity and selectivity of adenosine actions in hippocampal circuitry and its role in cognition and include: (1) in what conditions during neuronal oscillatory processes are A_1Rs and $A_{2A}Rs$ activated; (2) in what cells are these actions physiologically relevant; and (3) what are the overall consequences of this modulatory actions for hippocampal network processes and ultimately for animal behavior. The answer to these questions will be also important to provide a great base of knowledge to develop new approaches for the use of adenosine in different neuropathological conditions.

7 Future Perspectives

The previous chapter finishes with some of the questions I believe would be of great importance to be pursued in the next decade of investigation about adenosine to fully understand its role in hippocampal functioning and animal behavior. Here, I will narrow my considerations into what I consider to be the next steps for a research work on adenosine control of inhibitory network operations and try to describe, whenever possible, the experiments I would carry on for its accomplishment.

The data presented in this thesis reveals, for the first time, novel mechanisms and modes of actions of adenosine that involve the regulation of inhibitory neuronal transmission in the hippocampus. Although not directly tested in this work, it is likely that the actions described here may indeed support and explain, at least partially, the marked effects of this neuromodulator on neuronal excitability. This statement lacks, however, direct evidence and investigation, namely whether neuronal operations such as hippocampal oscillations or inhibitory plasticity phenomena are affected by A_1R and $A_{2A}R$. In fact, different forms of plasticity at GABAergic synapses onto different target cells (either pyramidal cells or interneurons) were already observed (Chevaleyre & Castillo 2003, Ali & Todorova 2010, Evstratova et al. 2011). Similar to the great heterogeneity among interneurons, plastic events are also variable and diversified in these cells. Indeed, both short-term and long-lasting forms of plasticity were described, which are expressed either pre- or postsynaptically and may involve or not glutamatergic receptor activation (Chevaleyre & Castillo 2003,

Patenaude et al. 2005, Ali & Todorova 2010, Ali 2011, Evstratova et al. 2011). Interestingly, most mechanisms are highly dependent on the release of modulators such as eCB, nitric oxide, opioids or growth factors (Jinno & Kosaka 2002, Chevaleyre & Castillo 2003, Nugent et al. 2007), which emphasize the importance of continuous activity control of interneurons by neuromodulatory molecules. Taking advantage of recent optogenetic tools (as described in Chapter 4.4.2, p79) and by carefully recording and identifying postsynaptic interneurons (as described in Chapter 4.6, p93 of this thesis) it would be important to further explore these forms of plasticity phenomena and evaluate the influence of endogenous adenosine on its expression. This is particularly relevant in a context of synchronized activity of the hippocampus, since interconnectivity between interneurons and plasticity phenomena among them are the substrate for coordinated network activity responsible for maintaining different frequency oscillations (Bragin et al. 1995, Cobb et al. 1995, Whittington et al. 1995, Traub et al. 1996, 2001; Wang & Buzsáki 1996, Bartos et al. 2001, 2002). In line with this, it becomes also relevant to study the role of adenosine during gamma- and theta-oscillations both *in vitro* and *in vivo*. In the hippocampus, theta-oscillations (3-12 Hz) co-emerge with gamma-rhythms (30-120 Hz) during exploratory behavior (Bragin et al. 1995, Buzsáki & Draguhn 2004) which underlie cognitive functions such as learning, memory formation and information retrieval (Buzsáki & Draguhn 2004). Both PV-positive cells and CCK-expressing interneurons play key roles in the emergence and maintenance of this frequency oscillations, respectively. Moreover, it was recently reported that adenosine formation from extracellular released ATP is implicated in changes

of gamma rhythms *in vitro* (Schulz et al. 2012). However, no mechanism or the receptors involved were explored. It is, thus, reasonable to hypothesize that both A_1Rs and A_{2A}Rs may participate in these processes. In this way, further exploration of adenosine effects on *in vitro* gamma-oscillations induced by cholinergic agonist carbachol (mimicking cholinergic input from the septum) (Fisahn et al. 1998, Gulyás et al. 2010) or by KA receptor agonist (Hájos et al. 2000, Fisahn et al. 2004) and by combining field recordings (as described in Chapter 4.4.4, p84), to monitor hippocampal oscillations, and patch-clamp recordings (as described in Chapter 4.4.1, p73), to selectively evaluate the activity of interneurons, would elucidate some of this mechanisms. Moreover, the involvement of non-neuronal cells, such as astrocytes, the most abundant glial cell in the brain, on neuronal information processing should not be disregarded. In fact, cutting edge experiments have recently revealed the involvement of astrocytes as an active component of synaptic function and neuronal activity (Perea et al. 2014). The ability of adenosine to direct control astrocyte function and its release by astrocytes to regulate the tripartite synapse have also been target of great attention (Boison et al. 2010). Further exploration of these astrocyte-neuron interations may reveal novel forms of network processes that might explain higher congnitive function.

The ultimate goal for the understanding of adenosine actions on hippocampal operations *in vitro* is to create a ground of knowledge for exploring and comprehending how it affects *in vivo* neuronal functioning and changes animal behavior. However, attempts to identify and characterize neuromodulators affecting cognitive processes *in vivo* may profit from a deep investigation into how

specific neuron types shape higher brain functions, up to the level of animal behavior. The recording of neuronal activity with field recordings or single cell recordings (from PV-positive or CCK-positive cells) in awake and behaving animals is one possible way to approach this. These studies would benefit from the use of transgenic Cre animals (as used in this work, see Chapter 4.1, p63) alongside with optogenetic or pharmacogenetic manipulations for ablation or activation of defined neurons (Deisseroth et al. 2006, Magnus et al. 2011). Regarding a putative role of adenosine, it is already accepted its involvement in learning and memory (Daly & Fredholm 1998, Fredholm et al. 1999, Takahashi et al. 2008, Nehlig 2010). Whether adenosine exerts its actions by changing hippocampal network oscillations *in vivo* is still unknown. One way to explore this would be to record hippocampal network activity in behaving animals that were previously treated with agonists or antagonists of adenosine receptors. For these tests a particular care should be taken to clearly distinguish acute from chronic effects, which may largely differ or even appear contradictory (Sousa et al. 2011). Given the meta-modulatory functions of adenosine (Sebastião & Ribeiro 2009) special attentions should be made to interactions with other modulatory systems such as the cannabinoid system. This gained particularly relevance on the light of the results herein described showing a direct effect of adenosine, through A_1Rs, in CB_1R-expressing interneurons.

Finally, another major challenge in adenosine field is to understand how it is involved in neurological and psychiatric diseases and how it can be used to ameliorate these disorders. In fact, a great interest has been given to the use of adenosine as an

anticonvulsant agent to control pharmacoresistant epilepsy. The work described in this thesis further substantiate this line of thinking. However, it also calls the attention for, and points to a direction where the use of the therapeutic potential of adenosine should take into consideration the highly specificity and selectivity of its actions. Indeed, one of the main causes for the etiology of epilepsy is a dysregulation of the GABAergic system, which has as its main player the inhibitory interneurons (the principal source of GABA). Thus, molecules like adenosine that are able to directly act to control the activity of these neurons should be considered important targets. The challenge will be to take advantage of these selective effects (A_1Rs onto tonic CCK-positive responses and A_{2A}Rs onto phasic disinhibitory PV-positive actions) and develop drugs that are directed to affect relevant neuronal targets, leaving untouched the ones not involved in the pathology.

Overall, it is fundamental that neuroscience and pharmacology research continue progressing together in pursuing relevant questions and innovative approaches for the understanding of brain functioning in physiological and pathological conditions.

8 Acknowledgements

As últimas palavras desta dissertação de Doutoramento são dedicadas a todas as pessoas que directa ou indirectamente contribuiram para a minha caminhada nos últimos cinco anos. Foi uma aventura extraordinária, com experiências únicas! Muitas destas aparecem registadas neste trabalho que agora termina; muitas outras podem apenas ficar marcadas na minha memória e de quem comigo as partilhou. Aos que contribuiram para as primeiras e aos que comigo viveram as segundas, segue agora meu eterno agradecimento.

Começo pela minha orientadora, Professora Ana Sebastião, a quem realmente devo a concretização deste Doutoramento. O agradecimento estende-se para lá destes últimos cinco anos, estende-se ao dia em que comecei as minhas visitas regulares ao laboratório, ainda enquanto estudante de Biologia, para ver experiências a decorrer, fazer perguntas aos colegas e conhecer um laboratório a funcionar. Desde aí tem sido um enorme orgulho e privilégio crescer para a ciência a seu lado. Para além da sua extraordinária qualidade na produção de ciência e competência na formação de doutorandos, a Professora Ana mostra uma sensibilidade ímpar a lidar com os seus alunos. Agradeço pela dedicação e entrega que colocou na minha orientação, pelo entusiasmo na planificação e discussão de experiências, pela paixão contagiante à eletrofisiologia, pela aptidão inata em ensinar, que me fez aprender tanto e motivou a querer saber mais,

mas sobretudo pela forma como olha para a pessoa acima do cientista. Espero ter estado à altura das suas expectativas.
Ao Professor Alexandre Ribeiro dedico também umas palavras de grande consideração e respeito, pelo seu exemplo de carreira como cientista e professor. A sua forma de ensinar ciência e transmitir o gosto pela investigação e pelo conhecimento são tremendamente inspiradores não só para mim, mas decerto para todos os seus alunos. Agradeço também a fantástica oportunidade que me concedeu em trabalhar no seu laboratório e pela ideia inicial de revisitar a modulação da transmissão GABAérgica pela sua tão amada adenosina, também ela rainha do trabalho que agora apresento.
À Raquel Dias! Foi sem dúvida um enorme privilégio ter-te conhecido e ter partilhado contigo todos estes anos. És a minha "irmã" de laboratório, que partilha comigo este gostinho tão especial que é o patch-clamp. Fizeste muito mais do que me introduzir uma técnica de eletrofisiologia… ensinaste-me a trabalhar num laboratório, a pensar ciência, a fazer perguntas e procurar respostas. Apesar de todos os teus afazeres (percebo e dou ainda mais valor agora) estás sempre disponível para ajudar, não só a mim, mas a qualquer um. Isso faz de ti não só uma cientista execional, como também uma pessoa extraordinária, com um coração enorme. Obrigado pela amizade e pelo exemplo que transmites aos que te rodeiam. Este trabalho também é teu.
Tenho também de agradecer a todos aqueles que partilharam comigo o dia-a-dia do laboratório. À Vânia Batalha, André Santos e Rita Aroeira, que aterraram no mesmo dia que eu no laboratório e partilharam comigo a vivência das primeiras reuniões, apresentações, viagens e conferências nacionais e

internacionais; todas estas vivências são inesquecíveis, assim como a vossa presença.

Aos que encontrei quando cheguei ao laboratório, Sofia Cristóvão-Ferreira, Sandra Vaz, Natália Assaífe, Vasco Sousa, Ana Rita Costenla; por receberem os "novatos" sempre de braços abertos, pela partilha da vossa visão mais experiente, pelos concelhos, pelas conversas, pela companhia, pelas discussões e divagações, científicas ou não, nas horas de almoço apertadinhos em cima de um banco alto no átrio central do laboratório.

Aos que chegaram a seguir, a Ana Filipa Ribeiro (pelas conversas fora da caixa que me punham a pensar, e pela companhia na viagem a Tarragona), Mariana Colino (pela visão aventureira que transmite, mas principalmente pela constante partilha das alegrias e frustrações sobre o nosso grande Sporting Clube de Portugal!!!), Francisco Mouro (a primeira pessoa a quem transmiti o pouquinho conhecimento que tenho de patch-clamp; tenho ainda a esperança de não ter sido eu a razão de fugires a sete pés da eletrofisiologia), Rita Ramalho (por todas as dicas sobre professores, trabalhos, aulas práticas, exames, estudo, etc, etc, que nos tem acompanhado nos últimos anos), Armando Cruz (pela boa disposição que trazes ao laboratório e pelas tuas visitas ocasionais a Oxford, trazendo uma cara familiar e a língua portuguesa). Também ao Jorge Valadas, Alexandra Marçal, Paula Pousinha, Daniela Calçada, Catarina Luís, que apesar de já terem deixado o laboratório à data da escrita deste trabalho, não poderão ser esquecidos.

Agradeço ainda à Mizé (ou direi respeitosamente, Professora Maria José Diógenes), pelos desafios experimentais que me proporcionou (com a memantina, a sinucleína, o Rett), pelos

ensinamentos farmacológicos (fui a todas as tuas aulas!), pelas discussões científicas e pelo sentido de justiça que defende para si e para os outros; também à Cláudia Valente, que me recebeu fresquinho no laboratório e pacientemente me ensinou a fazer imunos, por se prontificar sempre a ajudar quando um eletrofisiologista precisa de conselhos de "molecularices", e pelas nossas discussões sobre as fatias epiléticas que tanto me ajudaram a crescer no patch-clamp.

Também aos vários estudantes que tive a oportunidade de conhecer e ajudar, por me terem desafiado com as suas perguntas e com elas me terem ensinado tanto. À Cátia Domingos, uma aluna extraordinária que fervilha de ideias e planos, a quem tive o enorme prazer de transmitir um pouquinho daquilo que gosto de fazer.

Ao Sr. João, não só por toda a ajuda que me tem dado para o sucesso do trabalho experimental, mas também pelas conversas amigas, discussões futebolísticas e companhia nos intervalos entre experiências. À Elvira que também ajudou na organização do trabalho experimental que não se vê nos artigos. À Alexandra Botelho e Cristina Varandas, pelo incansável apoio a lidar com as burocracias que ninguém gosta, mas que sem elas seria impossível fazer ciência.

Também ao Prof. Alexandre Mendonça, Prof. Tiago Maia e Prof. Pedro Lima, pelo tempo dispendido a ouvir e discutir o meu trabalho, pelo *feedback*, sugestões e balanço que ofereceram.

In Oxford, I would like to thank first and foremost to Karri Lämsä, my co-supervisior. The time I spent in Oxford was an amazing experience spent in an enriching environment where I had the

oportunity to meet and discuss with extraordinary scientists and fascinating people. All of this was only possible with the huge support and availability of Karri, who prompt to help and advise a young PhD student from Portugal since the first e-mail we exchanged more than 4 years ago. With him I learned science, electrophysiology, many techniques and working methods, I learned new ways of thinking. But I also learned from his career, his enthusiasm, his motivation, his willingness that were trully inspirational and that will definitely guide my future work. For all of these and also for the discussions, support, advices and chats I would like to express my deepest thanks.

I would also like to thank Wiebke Nissen and Petrina Lau for welcoming me in Oxford, for all the help and patience with the adaptation to a new lab and a new environment. Wiebke, also for taking me out of the lab to live Oxford's culture; Petrina, for offering me a room to stay and for all the chats inbetween experiments.

A special thanks to Dimitrios Kotzadimitriou, my partner in patching, dissections and surgeries, for all the companionship inside and outside the lab, for the support, the stimulating discussions, the political and cultural debates, for receiving me in his house and introducing me to his friends with whom I spent such worderfull times. A word to all of them as well (and specially to Panos), for making the time outside the lab much more pleasurable.

I cannot forget Lorenz Müller for the really nice time we spent lunching at the 5th floor of the Pharmacology Department, for all the great dinners with his housemates, for all the discussions, ideas and perspectives we exchanged, inspiring and motivating me to pursuit a medical career.

To Kathryn Newton, Tommas Ellender, Matthew Prior, Liz Norman (from MRC ANU) and Liliana Minichiello for the help and advice with experimental procedures.
To the people in Birmingham, John Jefferys for receiving me in his lab, Andrew Powell for the support with field recordings and Gareth Morris and Alex Ferecskó for the experimental help and for showing me the city around.

I am grateful to the Fundação para a Ciência e a Tecnologia (FCT, SFRH/BD/ 60386/2009), Network of European Neuroscience Schools (NENS) and Medical Research Council (MRC) for the finantial support.

Termino agradecendo de forma muito especial a todas as pessoas que me acompanham desde muito antes do início desta caminhada. É com elas que partilho a maior aventura de todas e com quem sou realmente feliz.
À minha família e em especial aos pais, Pedro e Cristina, irmão, André, cunhada Raquel e o meu espetacular sobrinho, Zé Diogo!!! Aos meus avós, Rosário e Joaquim. A todos eles agradeço e dedico este trabalho. Por fazerem de mim a pessoa que sou hoje, por me ajudarem a conquistar tudo o que alcancei. Parcas serão sempre as palavras para vos agradecer e homenagear.
Aos meus amigos, que são verdadeiramente uma segunda família: Marco Lopes, Gonçalo Atalaia, Filipa Pinto, Ana Maria Alcafache, Ricardo Lopes, Diogo Lopes, Rodrigo Atalaia, João Pedro Pinto, António Mesquita, Pedro Silva, Catarina Machado, Eduardo Teixeira, João Lory, Pedro Charola. É com eles que passo os melhores e mais divertidos momentos da minha vida.

À minha família adquirida, Guida e Paulo, que me acompanham desde a adolescência e tornaram a sua casa também a minha.
Margarida Alcafache, infinitas são as razões que me fazem agradecer-te pela concretização deste trabalho, mas sobretudo por tudo o que trouxeste à minha vida. A ti agradeço a cumplicidade; agradeço a confiança; agradeço a presença, até mesmo na ausência; agradeço por me ouvires e por não deixares nada por dizer; agradeço-te pelo que és e pelo que me fazes ser; pelo que vivemos juntos e pelo que havemos de viver; agradeço-te pelo amor… Obrigado!

Diogo Rombo

9 References

Acsády L, Görcs TJ, Freund TF. 1996. Different populations of vasoactive intestinal polypeptide-immunoreactive interneurons are specialized to control pyramidal cells or interneurons in the hippocampus. *Neuroscience*. 73:317–34

Adamantidis AR, Zhang F, Aravanis AM, Deisseroth K, de Lecea L. 2007. Neural substrates of awakening probed with optogenetic control of hypocretin neurons. *Nature*. 450:420–24

Akbar M, Okajima F, Tomura H, Shimegi S, Kondo Y. 1994. A single species of A1 adenosine receptor expressed in Chinese hamster ovary cells not only inhibits cAMP accumulation but also stimulates phospholipase C and arachidonate release. *Mol. Pharmacol.* 45:1036–42

Albright TD, Jessell TM, Kandel ER, Posner MI. 2000. Neural science: a century of progress and the mysteries that remain. *Neuron*. 25:S1–55

Alger BE, Nicoll RA. 1982. Feed-forward dendritic inhibition in rat hippocampal pyramidal cells studied in vitro. *J. Physiol.* 328:105–23

Ali AB. 2011. CB1 modulation of temporally distinct synaptic facilitation among local circuit interneurons mediated by N-type calcium channels in CA1. *J. Neurophysiol.* 105:1051–62

Ali AB, Todorova M. 2010. Asynchronous release of GABA via tonic cannabinoid receptor activation at identified interneuron synapses in rat CA1. *Eur. J. Neurosci.* 31:1196–1207

Alle H, Geiger JRP. 2007. GABAergic spill-over transmission onto hippocampal mossy fiber boutons. *J. Neurosci.* 27:942–50

Amaral DG. 1993. Emerging principles of intrinsic hippocampal organization. *Curr. Opin. Neurobiol.* 3:225–29

Amaral DG, Witter MP. 1989. The three-dimensional organization of the hippocampal formation: a review of anatomical data. *Neuroscience*. 31:571–91

Ambrósio AF, Malva JO, Carvalho AP, Carvalho CM. 1997. Inhibition of N-,P/Q- and other types of Ca2+ channels in rat hippocampal nerve terminals by the adenosine A1 receptor. *Eur. J. Pharmacol.* 340:301–10

Ameri A, Jurna I. 1991. Adenosine A1 and non-A1 receptors: intracellular analysis of the actions of adenosine agonists and antagonists in rat hippocampal neurons. *Brain Res.* 546:69–78

Andersen P, Bliss T V, Skrede KK. 1971. Lamellar organization of hippocampal pathways. *Exp. brain Res.* 13:222–38

Aravanis AM, Wang L-P, Zhang F, Meltzer LA, Mogri MZ, et al. 2007. An optical neural interface: in vivo control of rodent motor cortex with integrated fiberoptic and optogenetic technology. *J. Neural Eng.* 4:S143–56

Armstrong C, Soltesz I. 2012. Basket cell dichotomy in microcircuit function. *J. Physiol.* 590:683–94

Ascoli GA, Alonso-Nanclares L, Anderson SA, Barrionuevo G, Benavides-Piccione R, et al. 2008. Petilla terminology: nomenclature of features of GABAergic interneurons of the cerebral cortex. *Nat. Rev. Neurosci.* 9:557–68

Attwell D, Barbour B, Szatkowski M. 1993. Nonvesicular release of neurotransmitter. *Neuron*. 11:401–7

Awapara J, Landua AJ, Fuerst R, Seale B. 1950. Free gamma-aminobutyric acid in brain. *J. Biol. Chem.* 187:35–39

Bacci A, Huguenard JR. 2006. Enhancement of spike-timing precision by autaptic transmission in neocortical inhibitory

interneurons. *Neuron*. 49:119–30

Bai D, Zhu G, Pennefather P, Jackson MF, MacDonald JF, Orser BA. 2001. Distinct functional and pharmacological properties of tonic and quantal inhibitory postsynaptic currents mediated by gamma-aminobutyric acid(A) receptors in hippocampal neurons. *Mol. Pharmacol.* 59:814–24

Bakker A, Kirwan CB, Miller M, Stark CEL. 2010. Pattern Separation in the Human Hippocampal CA3 and Dentate Gyrus. *Science*. 319:1640–42

Ballarín M, Fredholm BB, Ambrosio S, Mahy N. 1991. Extracellular levels of adenosine and its metabolites in the striatum of awake rats: inhibition of uptake and metabolism. *Acta Physiol. Scand.* 142:97–103

Banks MI, Li TB, Pearce RA. 1998. The synaptic basis of GABAA,slow. *J. Neurosci.* 18:1305–17

Banks MI, Pearce RA. 2000. Kinetic differences between synaptic and extrasynaptic GABA(A) receptors in CA1 pyramidal cells. *J. Neurosci.* 20:937–48

Barajas-Lopez C, Surprenant A, North RA. 1991. Adenosine A1 and A2 receptors mediate presynaptic inhibition and postsynaptic excitation in guinea pig submucosal neurons. *J. Pharmacol. Exp. Ther.* 258:490–95

Barankiewicz J, Danks AM, Abushanab E, Makings L, Wiemann T, et al. 1997. Regulation of adenosine concentration and cytoprotective effects of novel reversible adenosine deaminase inhibitors. *J. Pharmacol. Exp. Ther.* 283:1230–38

Barnard EA, Skolnick P, Olsen RW, Mohler H, Sieghart W, et al. 1998. International Union of Pharmacology. XV. Subtypes of gamma-aminobutyric acidA receptors: classification on the basis of subunit structure and receptor function. *Pharmacol. Rev.* 50:291–313

Barrie AP, Nicholls DG. 1993. Adenosine A1 receptor inhibition

of glutamate exocytosis and protein kinase C-mediated decoupling. *J. Neurochem.* 60:1081–86

Bartlett JS, Samulski RJ, McCown TJ. 1998. Selective and rapid uptake of adeno-associated virus type 2 in brain. *Hum. Gene Ther.* 9:1181–86

Bartos M, Elgueta C. 2012. Functional characteristics of parvalbumin- and cholecystokinin-expressing basket cells. *J. Physiol.* 590:669–81

Bartos M, Vida I, Frotscher M, Geiger JR, Jonas P. 2001. Rapid signaling at inhibitory synapses in a dentate gyrus interneuron network. *J. Neurosci.* 21:2687–98

Bartos M, Vida I, Frotscher M, Meyer A, Monyer H, et al. 2002. Fast synaptic inhibition promotes synchronized gamma oscillations in hippocampal interneuron networks. *Proc. Natl. Acad. Sci. U. S. A.* 99:13222–27

Beaulieu C, Kisvarday Z, Somogyi P, Cynader M, Cowey A. 1992. Quantitative distribution of GABA-immunopositive and -immunonegative neurons and synapses in the monkey striate cortex (area 17). *Cereb. Cortex*. 2:295–309

Ben-Ari Y, Cherubini E, Corradetti R, Gaiarsa JL. 1989. Giant synaptic potentials in immature rat CA3 hippocampal neurones. *J. Physiol.* 416:303–25

Berman RF, Fredholm BB, Aden U, O'Connor WT. 2000. Evidence for increased dorsal hippocampal adenosine release and metabolism during pharmacologically induced seizures in rats. *Brain Res.* 872:44–53

Bernstein J. 1902. Untersuchungen zur Thermodynamik der bioelektrischen Ströme. *Pflügers Arch. Gesamte Physiol. Menschen Tiere*. 92:521–62

Bianchi MT, Haas KF, Macdonald RL. 2001. Structural Determinants of Fast Desensitization and Desensitization – Deactivation Coupling in GABA A Receptors. *Currents*.

21:1127–36

Bianchi MT, Macdonald RL. 2001. Agonist Trapping by GABAA Receptor Channels. *J. Neurosci.* 21:9083–91

Bianchi MT, Macdonald RL. 2002. Slow phases of GABA(A) receptor desensitization: structural determinants and possible relevance for synaptic function. *J. Physiol.* 544:3–18

Bianchi MT, Macdonald RL. 2003. Neurosteroids shift partial agonist activation of GABA(A) receptor channels from low- to high-efficacy gating patterns. *J. Neurosci.* 23:10934–43

Biber K, Klotz KN, Berger M, Gebicke-Härter PJ, van Calker D. 1997. Adenosine A1 receptor-mediated activation of phospholipase C in cultured astrocytes depends on the level of receptor expression. *J. Neurosci.* 17:4956–64

Blackstad TW. 1956. Commissural connections of the hippocampal region in the rat, with special reference to their mode of termination. *J. Comp. Neurol.* 105:417–537

Blasco-Ibáñez JM, Freund TF. 1995. Synaptic input of horizontal interneurons in stratum oriens of the hippocampal CA1 subfield: structural basis of feed-back activation. *Eur. J. Neurosci.* 7:2170–80

Boison D. 2005. Adenosine and epilepsy: from therapeutic rationale to new therapeutic strategies. *Neuroscientist*. 11:25–36

Boison D. 2006. Adenosine kinase, epilepsy and stroke: mechanisms and therapies. *Trends Pharmacol. Sci.* 27:652–58

Boison D. 2012. Adenosine dysfunction in epilepsy. *Glia*. 60:1234–43

Boison D, Chen J-F, Fredholm BB. 2010. Adenosine signaling and function in glial cells. *Cell Death Differ.* 17:1071–82

Bormann J, Feigenspan A. 1995. GABAC receptors. *Trends*

Neurosci. 18:515–19

Bormann J, Hamill OP, Sakmann B. 1987. Mechanism of anion permeation through channels gated by glycine and gamma-aminobutyric acid in mouse cultured spinal neurones. *J. Physiol.* 385:243–86

Bowery NG, Doble A, Hill DR, Hudson AL, Shaw JS, et al. 1981. Bicuculline-insensitive GABA receptors on peripheral autonomic nerve terminals. *Eur. J. Pharmacol.* 71:53–70

Bowery NG, Hill DR, Hudson AL, Doble A, Middlemiss DN, et al. 1980. (-)Baclofen decreases neurotransmitter release in the mammalian CNS by an action at a novel GABA receptor. *Nature*. 283:92–94

Bowery NG, Smart TG. 2006. GABA and glycine as neurotransmitters: a brief history. *Br. J. Pharmacol.* 147 Suppl :S109–19

Boyden ES, Zhang F, Bamberg E, Nagel G, Deisseroth K. 2005. Millisecond-timescale, genetically targeted optical control of neural activity. *Nat. Neurosci.* 8:1263–68

Bragin A, Jandó G, Nádasdy Z, Hetke J, Wise K, Buzsáki G. 1995. Gamma (40-100 Hz) oscillation in the hippocampus of the behaving rat. *J. Neurosci.* 15:47–60

Brandon N, Jovanovic J, Moss S. 2002a. Multiple roles of protein kinases in the modulation of gamma-aminobutyric acid(A) receptor function and cell surface expression. *Pharmacol. Ther.* 94:113–22

Brandon NJ, Delmas P, Hill J, Smart TG, Moss SJ. 2001. Constitutive tyrosine phosphorylation of the GABA(A) receptor gamma 2 subunit in rat brain. *Neuropharmacology*. 41:745–52

Brandon NJ, Delmas P, Kittler JT, McDonald BJ, Sieghart W, et al. 2000. GABAA receptor phosphorylation and functional modulation in cortical neurons by a protein kinase C-

dependent pathway. *J. Biol. Chem.* 275:38856–62

Brandon NJ, Jovanovic JN, Smart TG, Moss SJ. 2002b. Receptor for activated C kinase-1 facilitates protein kinase C-dependent phosphorylation and functional modulation of GABA(A) receptors with the activation of G-protein-coupled receptors. *J. Neurosci.* 22:6353–61

Brickley SG, Cull-Candy SG, Farrant M. 1996. Development of a tonic form of synaptic inhibition in rat cerebellar granule cells resulting from persistent activation of GABAA receptors. *J. Physiol.* 497:753–59

Brickley SG, Cull-Candy SG, Farrant M. 2003. Vesicular release of GABA contributes to both phasic and tonic inhibition of granule cells in the mature cerebellum of mice. *J. Physiol.* 547P:C30

Bright DP, Aller MI, Brickley SG. 2007. Synaptic release generates a tonic GABA(A) receptor-mediated conductance that modulates burst precision in thalamic relay neurons. *J. Neurosci.* 27:2560–69

Bright DP, Smart TG. 2013. Protein kinase C regulates tonic GABAA receptor-mediated inhibition in the hippocampus and thalamus. *Eur. J. Neurosci.* 38:3408–23

Brooke RE, Deuchars J, Deuchars SA. 2004. Input-specific modulation of neurotransmitter release in the lateral horn of the spinal cord via adenosine receptors. *J. Neurosci.* 24:127–37

Brown N, Kerby J, Bonnert TP, Whiting PJ, Wafford K a. 2002. Pharmacological characterization of a novel cell line expressing human alpha(4)beta(3)delta GABA(A) receptors. *Br. J. Pharmacol.* 136:965–74

Brundege JM, Diao L, Proctor WR, Dunwiddie T V. 1997. The role of cyclic AMP as a precursor of extracellular adenosine in the rat hippocampus. *Neuropharmacology*. 36:1201–10

Brünig I, Scotti E, Sidler C, Fritschy JM. 2002. Intact sorting, targeting, and clustering of γ-aminobutyric acid A receptor subtypes in hippocampal neurons in vitro. *J. Comp. Neurol.* 443:43–55

Bruns RF, Lu GH, Pugsley TA. 1986. Characterization of the A2 adenosine receptor labeled by [3H]NECA in rat striatal membranes. *Mol. Pharmacol.* 29:331–46

Buhl EH, Halasy K, Somogyi P. 1994. Diverse sources of hippocampal unitary inhibitory postsynaptic potentials and the number of synaptic release sites. *Nature*. 368:823–28

Burke SP, Nadler J V. 1988. Regulation of glutamate and aspartate release from slices of the hippocampal CA1 area: effects of adenosine and baclofen. *J. Neurochem.* 51:1541–51

Burnstock G. 1972. Purinergic nerves. *Pharmacol. Rev.* 24:509–81

Burnstock G. 1978. A basis for distinguishing two types of purinergic receptor. In *Cell Membrane Receptors for Drugs and Hormones*, eds. L Bolis, RW Straub, pp. 107–18. New York: Raven Press

Burnstock G. 2006. Historical review: ATP as a neurotransmitter. *Trends Pharmacol. Sci.* 27:166–76

Buzsáki G, Draguhn A. 2004. Neuronal oscillations in cortical networks. *Science*. 304:1926–29

Campanac E, Gasselin C, Baude A, Rama S, Ankri N, Debanne D. 2013. Enhanced Intrinsic Excitability in Basket Cells Maintains Excitatory-Inhibitory Balance in Hippocampal Circuits. *Neuron*. 77:712–22

Canhão P, de Mendonça A, Ribeiro JA. 1994. 1,3-Dipropyl-8-cyclopentylxanthine attenuates the NMDA response to hypoxia in the rat hippocampus. *Brain Res.* 661:265–73

Caputto R. 1951. The enzymatic synthesis of adenylic acid; adenosinekinase. *J. Biol. Chem.* 189:801–14

Caraiscos VB, Elliott EM, You-Ten KE, Cheng VY, Belelli D, et al. 2004a. Tonic inhibition in mouse hippocampal CA1 pyramidal neurons is mediated by alpha5 subunit-containing gamma-aminobutyric acid type A receptors. *Proc. Natl. Acad. Sci. U. S. A.* 101:3662–67

Caraiscos VB, Newell JG, You-Ten KE, Elliott EM, Rosahl TW, et al. 2004b. Selective enhancement of tonic GABAergic inhibition in murine hippocampal neurons by low concentrations of the volatile anesthetic isoflurane. *J. Neurosci.* 24:8454–58

Carriba P, Ortiz O, Patkar K, Justinova Z, Stroik J, et al. 2007. Striatal adenosine A2A and cannabinoid CB1 receptors form functional heteromeric complexes that mediate the motor effects of cannabinoids. *Neuropsychopharmacology*. 32:2249–59

Cascalheira JF, Sebastião AM. 1998. Adenosine A1 receptor activation inhibits basal accumulation of inositol phosphates in rat hippocampus. *Pharmacol. Toxicol.* 82:189–92

Cascalheira JF, Sebastião AM, Ribeiro JA. 2002. Pertussis toxin-sensitive G proteins mediate the inhibition of basal phosphoinositide metabolism caused by adenosine A1 receptors in rat hippocampal slices. *Neurochem. Res.* 27:1707–11

Chamberlain SEL, Sadowski JHLP, Teles-Grilo Ruivo LM, Atherton LA, Mellor JR. 2013. Long-term depression of synaptic kainate receptors reduces excitability by relieving inhibition of the slow afterhyperpolarization. *J. Neurosci.* 33:9536–45

Chamberland S, Topolnik L. 2012. Inhibitory control of hippocampal inhibitory neurons. *Front. Neurosci.* 6:1–13

Chance FS, Abbott LF, Reyes AD. 2002. Gain modulation from background synaptic input. *Neuron*. 35:773–82

Chang Y, Weiss DS. 1999. Channel opening locks agonist onto the GABAC receptor. *Nat. Neurosci.* 2:219–25

Chen G, Trombley PQ, van den Pol AN. 1996. Excitatory actions of GABA in developing rat hypothalamic neurones. *J. Physiol.* 494:451–64

Chesler M. 1990. The regulation and modulation of pH in the nervous system. *Prog. Neurobiol.* 34:401–27

Chevaleyre V, Castillo PE. 2003. Heterosynaptic LTD of hippocampal GABAergic synapses: a novel role of endocannabinoids in regulating excitability. *Neuron*. 38:461–72

Chevaleyre V, Heifets BD, Kaeser PS, Südhof TC, Purpura DP, Castillo PE. 2007. Endocannabinoid-mediated long-term plasticity requires cAMP/PKA signaling and RIM1alpha. *Neuron*. 54:801–12

Chin JH, Wiesner JB, Fujitaki J. 1995. Increase in adenosine metabolites in human cerebrospinal fluid after status epilepticus. *J. Neurol. Neurosurg. Psychiatry*. 58:513–14

Ciruela F, Casadó V, Rodrigues RJ, Luján R, Burgueño J, et al. 2006. Presynaptic control of striatal glutamatergic neurotransmission by adenosine A1-A2A receptor heteromers. *J. Neurosci.* 26:2080–87

Ciruela F, Escriche M, Burgueno J, Angulo E, Casado V, et al. 2001. Metabotropic glutamate 1alpha and adenosine A1 receptors assemble into functionally interacting complexes. *J. Biol. Chem.* 276:18345–51

Claiborne BJ, Amaral DG, Cowan WM. 1986. A light and electron microscopic analysis of the mossy fibers of the rat dentate gyrus. *J. Comp. Neurol.* 246:435–58

Clarkson AN, Huang BS, Macisaac SE, Mody I, Carmichael ST. 2010. Reducing excessive GABA-mediated tonic inhibition promotes functional recovery after stroke. *Nature*. 468:305–9

Cobb SR, Buhl EH, Halasy K, Paulsen O, Somogyi P. 1995. Synchronization of neuronal activity in hippocampus by individual GABAergic interneurons. *Nature*. 378:75–78

Cohen I, Navarro V, Clemenceau S, Baulac M, Miles R. 2002. On the origin of interictal activity in human temporal lobe epilepsy in vitro. *Science*. 298:1418–21

Cole KS. 1949. Dynamic electrical characteristics of the squid axon membrane. *Arch Sci Physiol*. 3:253–58

Conti F, Minelli A, Melone M. 2004. GABA transporters in the mammalian cerebral cortex: Localization, development and pathological implications. *Brain Res. Rev.* 45:196–212

Cope DW, Hughes SW, Crunelli V. 2005. GABAA receptor-mediated tonic inhibition in thalamic neurons. *J. Neurosci.* 25:11553–63

Correia-de-Sá P, Sebastião AM, Ribeiro JA. 1991. Inhibitory and excitatory effects of adenosine receptor agonists on evoked transmitter release from phrenic nerve endings of the rat. *Br. J. Pharmacol.* 103:1614–20

Correia-de-Sá P, Timóteo MA, Ribeiro JA. 1996. Presynaptic A1 inhibitory/A2A facilitatory adenosine receptor activation balance depends on motor nerve stimulation paradigm at the rat hemidiaphragm. *J. Neurophysiol.* 76:3910–19

Crick FH. 1979. Thinking about the brain. *Sci. Am.* 241:219–32

Cristóvão-Ferreira S, Navarro G, Brugarolas M, Pérez-Capote K, Vaz SH, et al. 2013. A1R-A2AR heteromers coupled to Gs and G i/0 proteins modulate GABA transport into astrocytes. *Purinergic Signal.* 9:433–49

Cristóvão-Ferreira S, Vaz SH, Ribeiro JA, Sebastião AM. 2009.

Adenosine A2A receptors enhance GABA transport into nerve terminals by restraining PKC inhibition of GAT-1. *J. Neurochem.* 109:336–47

Cunha RA, Correia-de-Sá P, Sebastião AM, Ribeiro JA. 1996a. Preferential activation of excitatory adenosine receptors at rat hippocampal and neuromuscular synapses by adenosine formed from released adenine nucleotides. *Br. J. Pharmacol.* 119:253–60

Cunha RA, Johansson B, Constantino MD, Sebastião AM, Fredholm BB. 1996b. Evidence for high-affinity binding sites for the adenosine A2A receptor agonist [3H] CGS 21680 in the rat hippocampus and cerebral cortex that are different from striatal A2A receptors. *Naunyn. Schmiedebergs. Arch. Pharmacol.* 353:261–71

Cunha RA, Johansson B, van der Ploeg I, Sebastião AM, Ribeiro JA, Fredholm BB. 1994a. Evidence for functionally important adenosine A2a receptors in the rat hippocampus. *Brain Res.* 649:208–16

Cunha RA, Milusheva E, Vizi ES, Ribeiro JA, Sebastião AM. 1994b. Excitatory and inhibitory effects of A1 and A2A adenosine receptor activation on the electrically evoked [3H]acetylcholine release from different areas of the rat hippocampus. *J. Neurochem.* 63:207–14

Cunha RA, Ribeiro JA. 2000a. Purinergic modulation of [3H]GABA release from rat hippocampal nerve terminals. *Neuropharmacology*. 39:1156–67

Cunha RA, Ribeiro JA. 2000b. Adenosine A2A receptor facilitation of synaptic transmission in the CA1 area of the rat hippocampus requires protein kinase C but not protein kinase A activation. *Neurosci. Lett.* 289:127–30

Cunha RA, Vizi ES, Ribeiro JA, Sebastiao AM. 1996c. Preferential release of ATP and its extracellular catabolism as a source of adenosine upon high- but not low-frequency

stimulation of rat hippocampal slices. *J Neurochem*. 67:2180–87

Cunha-Reis D, Ribeiro JA, Sebastião AM. 2008. A1 and A2A receptor activation by endogenous adenosine is required for VIP enhancement of K+ -evoked [3H]-GABA release from rat hippocampal nerve terminals. *Neurosci Lett*. 430:207–12

Curtis DR. 1959. Pharmacological investigations upon inhibition of spinal motoneurones. *J. Physiol.* 145:175–92

Curtis DR, Duggan AW, Felix D, Johnston GA. 1970. GABA, bicuculline and central inhibition. *Nature*. 226:1222–24

Curtis DR, Phillis JW, Watkins JC. 1959. Chemical excitation of spinal neurones. *Nature*. 183:611–12

Cutting GR, Lu L, O'Hara BF, Kasch LM, Montrose-Rafizadeh C, et al. 1991. Cloning of the gamma-aminobutyric acid (GABA) rho 1 cDNA: a GABA receptor subunit highly expressed in the retina. *Proc. Natl. Acad. Sci. U. S. A.* 88:2673–77

D'Alimonte I, D'Auro M, Citraro R, Biagioni F, Jiang S, et al. 2009. Altered distribution and function of A2A adenosine receptors in the brain of WAG/Rij rats with genetic absence epilepsy, before and after appearance of the disease. *Eur. J. Neurosci.* 30:1023–35

Dale HH, Dudley HW. 1929. The presence of histamine and acetylcholine in the spleen of the ox and the horse. *J. Physiol.* 68:97–123

Daly JW, Butts-Lamb P, Padgett W. 1983. Subclasses of adenosine receptors in the central nervous system: interaction with caffeine and related methylxanthines. *Cell. Mol. Neurobiol.* 3:69–80

Daly JW, Fredholm BB. 1998. Caffeine--an atypical drug of dependence. *Drug Alcohol Depend.* 51:199–206

Damgaard T, Plath N, Neill JC, Hansen SL. 2011. Extrasynaptic

GABAA receptor activation reverses recognition memory deficits in an animal model of schizophrenia. *Psychopharmacology (Berl).* 214:403–13

Dammerman RS, Flint AC, Noctor S, Kriegstein AR. 2000. An excitatory GABAergic plexus in developing neocortical layer 1. *J. Neurophysiol.* 84:428–34

Daw MI, Tricoire L, Erdelyi F, Szabo G, McBain CJ. 2009. Asynchronous transmitter release from cholecystokinin-containing inhibitory interneurons is widespread and target-cell independent. *J. Neurosci.* 29:11112–22

De La Haba G, Cantoni GL. 1959. The enzymatic synthesis of S-adenosyl-L-homocysteine from adenosine and homocysteine. *J. Biol. Chem.* 234:603–8

de Mendonça A, Almeida T, Bashir ZI, Ribeiro JA. 1997. Endogenous adenosine attenuates long-term depression and depotentiation in the CA1 region of the rat hippocampus. *Neuropharmacology*. 36:161–67

de Mendonça A, Ribeiro JA. 1994. Endogenous adenosine modulates long-term potentiation in the hippocampus. *Neuroscience*. 62:385–90

de Mendonça A, Sebastião AM, Ribeiro JA. 1995. Inhibition of NMDA receptor-mediated currents in isolated rat hippocampal neurones by adenosine A1 receptor activation. *Neuroreport*. 6:1097–1100

de Mendonça A, Sebastião AM, Ribeiro JA. 2000. Adenosine: does it have a neuroprotective role after all? *Brain Res. Rev.* 33:258–74

DeFelipe J, López-Cruz PL, Benavides-Piccione R, Bielza C, Larrañaga P, et al. 2013. New insights into the classification and nomenclature of cortical GABAergic interneurons. *Nat. Rev. Neurosci.* 14:202–16

Deisseroth K, Feng G, Majewska AK, Miesenböck G, Ting A,

Schnitzer MJ. 2006. Next-generation optical technologies for illuminating genetically targeted brain circuits. *J. Neurosci.* 26:10380–86

Delaney SM, Geiger JD. 1996. Brain regional levels of adenosine and adenosine nucleotides in rats killed by high-energy focused microwave irradiation. *J. Neurosci. Methods*. 64:151–56

DeLorey TM, Olsen RW. 1992. Gamma-aminobutyric acidA receptor structure and function. *J. Biol. Chem.* 267:16747–50

Delpire E. 2000. Cation-Chloride Cotransporters in Neuronal Communication. *News Physiol. Sci.* 15:309–12

Deuchars J, Thomson AM. 1996. CA1 pyramid-pyramid connections in rat hippocampus in vitro: dual intracellular recordings with biocytin filling. *Neuroscience*. 74:1009–18

Dias RB, Ribeiro JA, Sebastião AM. 2012. Enhancement of AMPA currents and GluR1 membrane expression through PKA-coupled adenosine A(2A) receptors. *Hippocampus*. 22:276–91

Dias RB, Rombo DM, Ribeiro JA, Henley JM, Sebastião AM. 2013. Adenosine: setting the stage for plasticity. *Trends Neurosci.* 36:248–57

Dibbens LM, Feng H-J, Richards MC, Harkin LA, Hodgson BL, et al. 2004. GABRD encoding a protein for extra- or peri-synaptic GABAA receptors is a susceptibility locus for generalized epilepsies. *Hum. Mol. Genet.* 13:1315–19

Dickenson JM, Hill SJ. 1998. Involvement of G-protein betagamma subunits in coupling the adenosine A1 receptor to phospholipase C in transfected CHO cells. *Eur. J. Pharmacol.* 355:85–93

Diógenes MJ, Fernandes CC, Sebastião AM, Ribeiro JA. 2004. Activation of adenosine A2A receptor facilitates brain-derived neurotrophic factor modulation of synaptic

transmission in hippocampal slices. *J. Neurosci.* 24:2905–13

Dixon AK, Gubitz AK, Sirinathsinghji DJ, Richardson PJ, Freeman TC. 1996. Tissue distribution of adenosine receptor mRNAs in the rat. *Br. J. Pharmacol.* 118:1461–68

Doischer D, Hosp JA, Yanagawa Y, Obata K, Jonas P, et al. 2008. Postnatal differentiation of basket cells from slow to fast signaling devices. *J. Neurosci.* 28:12956–68

Dolleman-Van Der Weel MJ, Witter MP. 1996. Projections from the nucleus reuniens thalami to the entorhinal cortex, hippocampal field CA1, and the subiculum in the rat arise from different populations of neurons. *J. Comp. Neurol.* 364:637–50

Dolphin AC, Archer ER. 1983. An adenosine agonist inhibits and a cyclic AMP analogue enhances the release of glutamate but not GABA from slices of rat dentate gyrus. *Neurosci. Lett.* 43:49–54

Dragunow M. 1988. Purinergic mechanisms in epilepsy. *Prog. Neurobiol.* 31:85–108

Drew CA, Johnston GAR, Weatherby RP. 1984. Bicuculline-insensitive GABA receptors: Studies on the binding of (-)-baclofen to rat cerebellar membranes. *Neurosci. Lett.* 52:317–21

Drury AN, Szent-Györgyi A. 1929. The physiological activity of adenine compounds with especial reference to their action upon the mammalian heart. *J. Physiol.* 68:213–37

du Bois-Reymond E. 1848. *Untersuchungen über Thierische Elektricität*. Berlin: Reimer. 2 Bände ed.

Duncan K, Ketz N, Inati SJ, Davachi L. 2012. Evidence for area CA1 as a match/mismatch detector: a high-resolution fMRI study of the human hippocampus. *Hippocampus*. 22:389–98

Dunlap K, Fischbach GD. 1981. Neurotransmitters decrease the

calcium conductance activated by depolarization of embryonic chick sensory neurones. *J. Physiol.* 317:519–35

Dunwiddie T V, Diao L. 1994. Extracellular adenosine concentrations in hippocampal brain slices and the tonic inhibitory modulation of evoked excitatory responses. *J. Pharmacol. Exp. Ther.* 268:537–45

Dunwiddie T V, Diao L, Kim HO, Jiang JL, Jacobson KA. 1997. Activation of hippocampal adenosine A3 receptors produces a desensitization of A1 receptor-mediated responses in rat hippocampus. *J. Neurosci.* 17:607–14

Dunwiddie T V, Hoffer BJ. 1980. Adenine nucleotides and synaptic transmission in the in vitro rat hippocampus. *Br. J. Pharmacol.* 69:59–68

Dunwiddie T V, Masino SA. 2001. The role and regulation of adenosine in the central nervous system. *Annu. Rev. Neurosci.* 24:31–55

Edwards FA, Konnerth A, Sakmann B. 1990. Quantal analysis of inhibitory synaptic transmission in the dentate gyrus of rat hippocampal slices: a patch-clamp study. *J. Physiol.* 430:213–49

Ehrengruber MU, Doupnik CA, Xu Y, Garvey J, Jasek MC, et al. 1997. Activation of heteromeric G protein-gated inward rectifier K+ channels overexpressed by adenovirus gene transfer inhibits the excitability of hippocampal neurons. *Proc. Natl. Acad. Sci. U. S. A.* 94:7070–75

El Yacoubi M, Ledent C, Parmentier M, Costentin J, Vaugeois J-MM. 2008. Evidence for the involvement of the adenosine A2A receptor in the lowered susceptibility to pentylenetetrazol-induced seizures produced in mice by long-term treatment with caffeine. *Neuropharmacology*. 55:35–40

El Yacoubi M, Ledent C, Parmentier M, Costentin J, Vaugeois

JM. 2009. Adenosine A2A receptor deficient mice are partially resistant to limbic seizures. *Naunyn. Schmiedebergs. Arch. Pharmacol.* 380:223–32

Ellender TJ, Raimondo J V, Irkle A, Lamsa KP, Akerman CJ. 2014. Excitatory Effects of Parvalbumin-Expressing Interneurons Maintain Hippocampal Epileptiform Activity via Synchronous Afterdischarges. *J. Neurosci.* 34:15208–22

Elliott KA, Van Gelder NM. 1958. Occlusion and metabolism of gamma-aminobutyric acid by brain tissue. *J. Neurochem.* 3:28–40

Essrich C, Lorez M, Benson J a, Fritschy JM, Lüscher B. 1998. Postsynaptic clustering of major GABAA receptor subtypes requires the gamma 2 subunit and gephyrin. *Nat. Neurosci.* 1:563–71

Etherington L V, Frenguelli BG. 2004. Endogenous adenosine modulates epileptiform activity in rat hippocampus in a receptor subtype-dependent manner. *Eur. J. Neurosci.* 19:2539–50

Evstratova A, Chamberland S, Topolnik L. 2011. Cell type-specific and activity-dependent dynamics of action potential-evoked Ca2+ signals in dendrites of hippocampal inhibitory interneurons. *J. Physiol.* 589:1957–77

Farrant M, Nusser Z. 2005. Variations on an inhibitory theme: phasic and tonic activation of GABA(A) receptors. *Nat. Rev. Neurosci.* 6:215–29

Feigenspan A, Wässle H, Bormann J. 1993. Pharmacology of GABA receptor Cl- channels in rat retinal bipolar cells. *Nature*. 361:159–62

Feng H-J, Kang J-Q, Song L, Dibbens L, Mulley J, Macdonald RL. 2006. Delta subunit susceptibility variants E177A and R220H associated with complex epilepsy alter channel gating and surface expression of alpha4beta2delta GABAA

receptors. *J. Neurosci.* 26:1499–1506

Fenno L, Yizhar O, Deisseroth K. 2011. The development and application of optogenetics. *Annu. Rev. Neurosci.* 34:389–412

Fenwick EM, Marty A, Neher E. 1982. A patch-clamp study of bovine chromaffin cells and of their sensitivity to acetylcholine. *J. Physiol.* 331:577–97

Ferando I, Mody I. 2012. GABAA receptor modulation by neurosteroids in models of temporal lobe epilepsies. *Epilepsia*. 53 Suppl 9:89–101

Ferré S, Fredholm BB, Morelli M, Popoli P, Fuxe K. 1997. Adenosine-dopamine receptor-receptor interactions as an integrative mechanism in the basal ganglia. *Trends Neurosci.* 20:482–87

Ferré S, Karcz-Kubicha M, Hope BT, Popoli P, Burgueño J, et al. 2002. Synergistic interaction between adenosine A2A and glutamate mGlu5 receptors: implications for striatal neuronal function. *Proc. Natl. Acad. Sci. U. S. A.* 99:11940–45

Ferrier D. 1886. *The Functions of the Brain*. New York: G. P. Putnam's Sons

Fink JS, Weaver DR, Rivkees SA, Peterfreund RA, Pollack AE, et al. 1992. Molecular cloning of the rat A2 adenosine receptor: selective co-expression with D2 dopamine receptors in rat striatum. *Mol. brain Res.* 14:186–95

Fisahn A, Contractor A, Traub RD, Buhl EH, Heinemann SF, McBain CJ. 2004. Distinct roles for the kainate receptor subunits GluR5 and GluR6 in kainate-induced hippocampal gamma oscillations. *J. Neurosci.* 24:9658–68

Fisahn A, Pike FG, Buhl EH, Paulsen O. 1998. Cholinergic induction of network oscillations at 40 Hz in the hippocampus in vitro. *Nature*. 394:186–89

Fisher JL, Macdonald RL. 1997. Single channel properties of recombinant GABAA receptors containing gamma 2 or delta subtypes expressed with alpha 1 and beta 3 subtypes in mouse L929 cells. *J. Physiol.* 505:283–97

Földy C, Lee SY, Szabadics J, Neu A, Soltesz I. 2007. Cell type-specific gating of perisomatic inhibition by cholecystokinin. *Nat. Neurosci.* 10:1128–30

Földy C, Neu A, Jones M V, Soltesz I. 2006. Presynaptic, activity-dependent modulation of cannabinoid type 1 receptor-mediated inhibition of GABA release. *J. Neurosci.* 26:1465–69

Fontinha BM, Delgado-García JM, Madroñal N, Ribeiro JA, Sebastião AM, Gruart A. 2009. Adenosine A(2A) receptor modulation of hippocampal CA3-CA1 synapse plasticity during associative learning in behaving mice. *Neuropsychopharmacology*. 34:1865–74

Fredholm BB, Bättig K, Holmén J, Nehlig A, Zvartau EE. 1999. Actions of caffeine in the brain with special reference to factors that contribute to its widespread use. *Pharmacol. Rev.* 51:83–133

Fredholm BB, Dunwiddie T V. 1988. How does adenosine inhibit transmitter release? *Trends Pharmacol. Sci.* 9:130–34

Fredholm BB, IJzerman AP, Jacobson KA, Klotz KN, Linden J. 2001. International Union of Pharmacology. XXV. Nomenclature and classification of adenosine receptors. *Pharmacol. Rev.* 53:527–52

Fredholm BB, IJzerman AP, Jacobson KA, Linden J, Mu CE, Müller CE. 2011. International Union of Basic and Clinical Pharmacology . LXXXI . Nomenclature and Classification of Adenosine Receptors — An Update. *Pharmacol. Rev.* 63:1-34

Freissmuth M, Schütz W, Linder ME. 1991. Interactions of the

bovine brain A1-adenosine receptor with recombinant G protein alpha-subunits. Selectivity for rGi alpha-3. *J. Biol. Chem.* 266:17778–83

Frenguelli BG, Wigmore G, Llaudet E, Dale N. 2007. Temporal and mechanistic dissociation of ATP and adenosine release during ischaemia in the mammalian hippocampus. *J. Neurochem.* 101:1400–1413

Freund TF, Buzsáki G. 1996. Interneurons of the hippocampus. *Hippocampus*. 6:347–470

Freund TF, Katona I. 2007. Perisomatic inhibition. *Neuron*. 56:33–42

Fricke R, Cowan WM. 1978. An autoradiographic study of the commissural and ipsilateral hippocampo-dentate projections in the adult rat. *J. Comp. Neurol.* 181:253–69

Fyhn M, Molden S, Witter MP, Moser EI, Moser M-B. 2004. Spatial representation in the entorhinal cortex. *Science*. 305:1258–64

Gao XB, van den Pol AN. 2001. GABA, not glutamate, a primary transmitter driving action potentials in developing hypothalamic neurons. *J. Neurophysiol.* 85:425–34

Gebicke-Haerter PJ, Christoffel F, Timmer J, Northoff H, Berger M, Van Calker D. 1996. Both adenosine A1- and A2-receptors are required to stimulate microglial proliferation. *Neurochem. Int.* 29:37–42

Geibel M, Badurek S, Horn JM, Vatanashevanopakorn C, Koudelka J, et al. 2014. Ablation of TrkB signalling in CCK neurons results in hypercortisolism and obesity. *Nat. Commun.* 5:3427

Gentet LJ, Stuart GJ, Clements JD. 2000. Direct measurement of specific membrane capacitance in neurons. *Biophys. J.* 79:314–20

Gerber U, Greene RW, Haas HL, Stevens DR. 1989. Characterization of inhibition mediated by adenosine in the hippocampus of the rat in vitro. *J. Physiol.* 417:567–78

Gest H. 2004. The discovery of microorganisms by Robert Hooke and Antoni Van Leeuwenhoek, fellows of the Royal Society. *Notes Rec. R. Soc. Lond.* 58:187–201

Gill KM, Lodge DJ, Cook JM, Aras S, Grace AA. 2011. A novel α5GABA(A)R-positive allosteric modulator reverses hyperactivation of the dopamine system in the MAM model of schizophrenia. *Neuropsychopharmacology*. 36:1903–11

Glickfeld LL, Scanziani M. 2006. Distinct timing in the activity of cannabinoid-sensitive and cannabinoid-insensitive basket cells. *Nat. Neurosci.* 9:807–15

Glykys J, Mody I. 2007a. Activation of GABAA receptors: views from outside the synaptic cleft. *Neuron*. 56:763–70

Glykys J, Mody I. 2007b. The main source of ambient GABA responsible for tonic inhibition in the mouse hippocampus. *J. Physiol.* 582:1163–78

Gomes C V, Kaster MP, Tomé AR, Agostinho PM, Cunha RA. 2011. Adenosine receptors and brain diseases: neuroprotection and neurodegeneration. *Biochim. Biophys. Acta*. 1808:1380–99

Goodman RR, Synder SH. 1982. Autoradiographic localization of adenosine receptors in rat brain using [3H]cyclohexyladenosine. *J. Neurosci.* 2:1230–41

Gray EG. 1959a. Axo-somatic and axo-dendritic synapses of the cerebral cortex: an electron microscope study. *J. Anat.* 93:420–33

Gray EG. 1959b. Electron microscopy of synaptic contacts on dendrite spines of the cerebral cortex. *Nature*. 183:1592–93

Green JD, Arduini AA. 1954. Hippocampal electrical activity in

arousal. *J. Neurophysiol.* 17:533–57

Greene RW, Haas HL. 1985. Adenosine actions on CA1 pyramidal neurones in rat hippocampal slices. *J. Physiol.* 366:119–27

Gross CG. 1987. The Early History of Neuroscience. In *Encyclopedia of Neuroscience*, ed. G Adelman, pp. 843–47. Birkhauser

Grover LM, Lambert NA, Schwartzkroin PA, Teyler TJ. 1993. Role of HCO3- ions in depolarizing GABAA receptor-mediated responses in pyramidal cells of rat hippocampus. *J. Neurophysiol.* 69:1541–55

Gubitz AK, Widdowson L, Kurokawa M, Kirkpatrick KA, Richardson PJ. 1996. Dual signalling by the adenosine A2a receptor involves activation of both N- and P-type calcium channels by different G proteins and protein kinases in the same striatal nerve terminals. *J. Neurochem.* 67:374–81

Gulyás AI, Hájos N, Freund TF. 1996. Interneurons containing calretinin are specialized to control other interneurons in the rat hippocampus. *J. Neurosci.* 16:3397–3411

Gulyás AI, Szabó GG, Ulbert I, Holderith N, Monyer H, et al. 2010. Parvalbumin-containing fast-spiking basket cells generate the field potential oscillations induced by cholinergic receptor activation in the hippocampus. *J. Neurosci.* 30:15134–45

Haas KF, Macdonald RL. 1999. GABAA receptor subunit gamma2 and delta subtypes confer unique kinetic properties on recombinant GABAA receptor currents in mouse fibroblasts. *J. Physiol.* 514:27–45

Hafting T, Fyhn M, Molden S, Moser M-B, Moser EI. 2005. Microstructure of a spatial map in the entorhinal cortex. *Nature*. 436:801–6

Hájos N, Katona I, Naiem SS, Mackie K, Ledent C, et al. 2000.

Cannabinoids inhibit hippocampal GABAergic transmission and network oscillations. *Eur. J. Neurosci.* 12:3239–49

Halasy K, Buhl EH, Lörinczi Z, Tamás G, Somogyi P. 1996. Synaptic target selectivity and input of GABAergic basket and bistratified interneurons in the CA1 area of the rat hippocampus. *Hippocampus*. 6:306–29

Hamann M, Rossi DJ, Attwell D. 2002. Tonic and spillover inhibition of granule cells control information flow through cerebellar cortex. *Neuron*. 33:625–33

Hamil NE, Cock HR, Walker MC. 2012. Acute down-regulation of adenosine A(1) receptor activity in status epilepticus. *Epilepsia*. 53:177–88

Hamill OP, Marty A, Neher E, Sakmann B, Sigworth FJ. 1981. Improved patch-clamp techniques for high-resolution current recording from cells and cell-free membrane patches. *Pflügers Arch. Eur. J. Physiol.* 391:85–100

Harz H, Hegemann P. 1991. Rhodopsin-regulated calcium currents in Chlamydomonas. *Nature*. 351:489–91

Hasselmo ME, Schnell E, Barkai E. 1995. Dynamics of learning and recall at excitatory recurrent synapses and cholinergic modulation in rat hippocampal region CA3. *J. Neurosci.* 15:5249–62

Hayashi T. 1958. Inhibition and excitation due to gamma-aminobutyric acid in the central nervous system. *Nature*. 182:1076–77

Haydon PG, Carmignoto G. 2006. Astrocyte control of synaptic transmission and neurovascular coupling. *Physiol. Rev.* 86:1009–31

Hefft S, Jonas P. 2005. Asynchronous GABA release generates long-lasting inhibition at a hippocampal interneuron-principal neuron synapse. *Nat. Neurosci.* 8:1319–28

Hetherington PA, Austin KB, Shapiro ML. 1994. Ipsilateral associational pathway in the dentate gyrus: An excitatory feedback system that supports N-methyl-D-aspartate - Dependent long-term potentiation. *Hippocampus*. 4:422–38

Hill DR. 1985. GABAB receptor modulation of adenylate cyclase activity in rat brain slices. *Br. J. Pharmacol.* 84:249–57

Hill DR, Bowery NG. 1981. 3H-baclofen and 3H-GABA bind to bicuculline-insensitive GABA B sites in rat brain. *Nature*. 290:149–52

Hines RM, Davies PA, Moss SJ, Maguire J. 2012. Functional regulation of GABAA receptors in nervous system pathologies. *Curr. Opin. Neurobiol.* 22:552–58

Hodgkin AL, Huxley AF. 1939. Action potentials recorded from inside a nerve fibre. *Nature*. 144:710–11

Hodgkin AL, Huxley AF. 1947. Potassium leakage from an active nerve fibre. *J. Physiol.* 106:341–67

Hodgkin AL, Huxley AF. 1952a. A quantitative description of membrane current and its application to conduction and excitation in nerve. *Bull. Math. Biol.* 117:25–71

Hodgkin AL, Huxley AF. 1952b. Currents carried by sodium and potassium ions through the membrane of the giant axon of Loligo. *J. Physiol.* 116:449–72

Hodgkin AL, Huxley AF. 1952c. The components of membrane conductance in the giant axon of Loligo. *J. Physiol.* 116:473–96

Hodgkin AL, Huxley AF. 1952d. The dual effect of membrane potential on sodium conductance in the giant axon of Loligo. *J. Physiol.* 116:497–506

Hodgkin AL, Huxley AF, Katz B. 1952. Measurement of current-voltage relations in the membrane of the giant axon of Loligo. *J. Physiol.* 116:424–48

Holt GR, Koch C. 1997. Shunting inhibition does not have a divisive effect on firing rates. *Neural Comput.* 9:1001–13

Hooke R. 1665. *Micrographia: Or Some Physiological Descriptions of Minute Bodies Made by Magnifying Glasses with Observations and Inquiries Thereupon*. London: J. Martyn and J. Allestry Royal Society

Huguenard JR, Alger BE. 1986. Whole-cell voltage-clamp study of the fading of GABA-activated currents in acutely dissociated hippocampal neurons. *J. Neurophysiol.* 56:1–18

Ilie A, Raimondo J V, Akerman CJ. 2012. Adenosine release during seizures attenuates GABAA receptor-mediated depolarization. *J. Neurosci.* 32:5321–32

Ishizuka N, Weber J, Amaral DG. 1990. Organization of intrahippocampal projections originating from CA3 pyramidal cells in the rat. *J. Comp. Neurol.* 295:580–623

Iversen LL, Neal MJ. 1968. The uptake of [3H]GABA by slices of rat cerebral cortex. *J. Neurochem.* 15:1141–49

Izumi Y, Zorumski CF. 2008. Direct cortical inputs erase long-term potentiation at Schaffer collateral synapses. *J. Neurosci.* 28:9557–63

Jackson J, Beevor C. 1890. Case of tumor of the right temporosphenoidal lobe bearing on the localization of the sense of smell and on the interpretation of a particular variety of epilepsy. *Brain*. 12:346–57

Jackson MB, Scharfman HE. 1996. Positive feedback from hilar mossy cells to granule cells in the dentate gyrus revealed by voltage-sensitive dye and microelectrode recording. *J. Neurophysiol.* 76:601–16

Jacobson KA, Gao Z-G. 2006. Adenosine receptors as therapeutic targets. *Nat. Rev. Drug Discov.* 5:247–64

Jeong H-J, Jang I-S, Nabekura J, Akaike N. 2003. Adenosine A1

receptor-mediated presynaptic inhibition of GABAergic transmission in immature rat hippocampal CA1 neurons. *J. Neurophysiol.* 89:1214–22

Jin S, Fredholm BB. 1997. Adenosine A2A receptor stimulation increases release of acetylcholine from rat hippocampus but not striatum, and does not affect catecholamine release. *Naunyn. Schmiedebergs. Arch. Pharmacol.* 355:48–56

Jinno S, Kosaka T. 2002. Patterns of expression of calcium binding proteins and neuronal nitric oxide synthase in different populations of hippocampal GABAergic neurons in mice. *J. Comp. Neurol.* 449:1–25

Jockers R, Linder ME, Hohenegger M, Nanoff C, Bertin B, et al. 1994. Species difference in the G protein selectivity of the human and bovine A1-adenosine receptor. *J. Biol. Chem.* 269:32077–84

Johnston GA, Curtis DR, Beart PM, Game CJ, McCulloch RM, Twitchin B. 1975. Cis- and trans-4-aminocrotonic acid as GABA analogues of restricted conformation. *J. Neurochem.* 24:157–60

Jonas P. 2004. Interneuron Diversity series: Fast in, fast out – temporal and spatial signal processing in hippocampal interneurons. *Trends Neurosci.* 27:30–40

Jones MW, McHugh TJ. 2011. Updating hippocampal representations: CA2 joins the circuit. *Trends Neurosci.* 34:526–35

Jones PA, Smith RA, Stone TW. 1998. Protection against hippocampal kainate excitotoxicity by intracerebral administration of an adenosine A2A receptor antagonist. *Brain Res.* 800:328–35

Jones M V, Westbrook GL. 1995. Desensitized states prolong GABAA channel responses to brief agonist pulses. *Neuron*. 15:181–91

Jonzon B, Fredholm BB. 1985. Release of purines, noradrenaline, and GABA from rat hippocampal slices by field stimulation. *J. Neurochem.* 44:217–24

Jung R, Kornmüller A. 1938. Eine methodik der Ableitung lokalisierter Potentialschwankungen aus subcorticalen Hirngebieten. *Arch Psychiatr Nervenkr*. 109:1–30

Kaczmarek LK, Levitan IB. 1987. What is Neuromodulation? In *Neuromodulation*, eds. LK Kaczmarek, IB Levitan, pp. 3–17. Oxford: Oxford University Press, Inc.

Kaila K. 1994. Ionic basis of GABAA receptor channel function in the nervous system. *Prog. Neurobiol.* 42:489–537

Kaila K, Lamsa K, Smirnov S, Taira T, Voipio J. 1997. Long-lasting GABA-mediated depolarization evoked by high-frequency stimulation in pyramidal neurons of rat hippocampal slice is attributable to a network-driven, bicarbonate-dependent K+ transient. *J. Neurosci.* 17:7662–72

Kaila K, Voipio J. 1987. Postsynaptic fall in intracellular pH induced by GABA-activated bicarbonate conductance. *Nature*. 330:163–65

Kamiya H. 1991. Some pharmacological differences between hippocampal excitatory and inhibitory synapses in transmitter release: an in vitro study. *Synapse*. 8:229–35

Kandel ER, Schwartz JH, Jessell TM, Siegelbaum SA, Hudspeth AJ, eds. 2013. *Principles of Neural Science*. New York: McGraw-Hill. Fifth ed.

Kaneda M, Farrant M, Cull-Candy SG. 1995. Whole-cell and single-channel currents activated by GABA and glycine in granule cells of the rat cerebellum. *J. Physiol.* 485:419–35

Kano M, Konnerth A. 1992. Potentiation of GABA-mediated currents by cAMP-dependent protein kinase. *Neuroreport*. 3:563–66

Kano M, Ohno-shosaku T, Hashimotodani Y, Uchigashima M. 2009. Endocannabinoid-Mediated Control of Synaptic Transmission. , pp. 309–80

Kano M, Rexhausen U, Dreessen J, Konnerth A. 1992. Synaptic excitation produces a long-lasting rebound potentiation of inhibitory synaptic signals in cerebellar Purkinje cells. *Nature*. 356:601–4

Kasugai Y, Swinny JD, Roberts JDB, Dalezios Y, Fukazawa Y, et al. 2010. Quantitative localisation of synaptic and extrasynaptic GABAA receptor subunits on hippocampal pyramidal cells by freeze-fracture replica immunolabelling. *Eur. J. Neurosci.* 32:1868–88

Katona I, Sperlágh B, Sík A, Käfalvi A, Vizi ES, et al. 1999. Presynaptically located CB1 cannabinoid receptors regulate GABA release from axon terminals of specific hippocampal interneurons. *J. Neurosci.* 19:4544–58

Kennedy RT, Thompson JE, Vickroy TW. 2002. In vivo monitoring of amino acids by direct sampling of brain extracellular fluid at ultralow flow rates and capillary electrophoresis. *J. Neurosci. Methods*. 114:39–49

Kerr DI, Ong J. 1995. GABAB receptors. *Pharmacol. Ther.* 67:187–246

Khan GM, Smolders I, Ebinger G, Michotte Y. 2001. 2-chloro-N(6)-cyclopentyladenosine-elicited attenuation of evoked glutamate release is not sufficient to give complete protection against pilocarpine-induced seizures in rats. *Neuropharmacology*. 40:657–67

Khazipov R, Congar P, Ben-Ari Y. 1995. Hippocampal CA1 lacunosum-moleculare interneurons: comparison of effects of anoxia on excitatory and inhibitory postsynaptic currents. *J. Neurophysiol.* 74:2138–49

Kimelberg HK, Goderie SK, Higman S, Pang S, Waniewski RA.

1990. Swelling-induced release of glutamate, aspartate, and taurine from astrocyte cultures. *J. Neurosci.* 10:1583–91

King AE, Ackley MA, Cass CE, Young JD, Baldwin SA. 2006. Nucleoside transporters: from scavengers to novel therapeutic targets. *Trends Pharmacol. Sci.* 27:416–25

Kirmse K, Dvorzhak A, Grantyn R, Kirischuk S. 2008. Developmental downregulation of excitatory GABAergic transmission in neocortical layer I via presynaptic adenosine A1 receptors. *Cereb. Cortex*. 18:424–32

Klausberger T, Marton LF, O'Neill J, Huck JHJ, Dalezios Y, et al. 2005. Complementary roles of cholecystokinin- and parvalbumin-expressing GABAergic neurons in hippocampal network oscillations. *J. Neurosci.* 25:9782–93

Klausberger T, Somogyi P. 2008. Neuronal diversity and temporal dynamics: the unity of hippocampal circuit operations. *Science*. 321:53–57

Klishin A, Lozovaya N, Krishtal O. 1995a. A1 adenosine receptors differentially regulate the N-methyl-D-aspartate and non-N-methyl-D-aspartate receptor-mediated components of hippocampal excitatory postsynaptic current in a Ca2+/Mg(2+)-dependent manner. *Neuroscience*. 65:947–53

Klishin A, Tsintsadze T, Lozovaya N, Krishtal O. 1995b. Latent N-methyl-D-aspartate receptors in the recurrent excitatory pathway between hippocampal CA1 pyramidal neurons: Ca(2+)-dependent activation by blocking A1 adenosine receptors. *Proc. Natl. Acad. Sci. U. S. A.* 92:12431–35

Kofuji P, Wang JB, Moss SJ, Huganir RL, Burt DR. 1991. Generation of two forms of the gamma-aminobutyric acidA receptor gamma 2-subunit in mice by alternative splicing. *J. Neurochem.* 56:713–15

Kohl MM, Shipton OA, Deacon RM, Rawlins JNP, Deisseroth K,

Paulsen O. 2011. Corrigendum: Hemisphere-specific optogenetic stimulation reveals left-right asymmetry of hippocampal plasticity. *Nat. Neurosci.* 14:1617–1617

Köhling R, Vreugdenhil M, Bracci E, Jefferys JG. 2000. Ictal epileptiform activity is facilitated by hippocampal GABAA receptor-mediated oscillations. *J. Neurosci.* 20:6820–29

Koizumi S, Fujishita K, Tsuda M, Shigemoto-Mogami Y, Inoue K. 2003. Dynamic inhibition of excitatory synaptic transmission by astrocyte-derived ATP in hippocampal cultures. *Proc. Natl. Acad. Sci. U. S. A.* 100:11023–28

Kong W, Engel K, Wang J. 2004. Mammalian nucleoside transporters. *Curr. Drug Metab.* 5:63–84

Korn SJ, Giacchino JL, Chamberlin NL, Dingledine R. 1987. Epileptiform burst activity induced by potassium in the hippocampus and its regulation by GABA-mediated inhibition. *J. Neurophysiol.* 57:325–40

Krames ES, Peckham PH, Rezai AR, eds. 2009. *Neuromodulation*. London: Academic Press, Elsevier Ltd.

Kraushaar U, Jonas P. 2000. Efficacy and stability of quantal GABA release at a hippocampal interneuron-principal neuron synapse. *J. Neurosci.* 20:5594–5607

Krnjević K, Schwartz S. 1967. The action of gamma-aminobutyric acid on cortical neurones. *Exp. brain Res.* 3:320–36

Kroll K, Decking UK, Dreikorn K, Schrader J. 1993. Rapid turnover of the AMP-adenosine metabolic cycle in the guinea pig heart. *Circ. Res.* 73:846–56

Kuffler SW. 1960. Excitation and inhibition in single nerve cells. *Harvey Lect.* 54:176–218

Kullmann DM, Ruiz A, Rusakov DM, Scott R, Semyanov A, Walker MC. 2005. Presynaptic, extrasynaptic and axonal GABA A receptors in the CNS: Where and why? *Prog.*

Biophys. Mol. Biol. 87:33–46

Küst BM, Biber K, Van Calker D, Gebicke-Haerter PJ. 1999. Regulation of K+ channel mRNA expression by stimulation of adenosine A(2a)-receptors in cultured rat microglia. *Glia*. 25:120–30

Lacaille JC, Mueller AL, Kunkel DD, Schwartzkroin PA. 1987. Local circuit interactions between oriens/alveus interneurons and CA1 pyramidal cells in hippocampal slices: electrophysiology and morphology. *J. Neurosci.* 7:1979–93

Lambert NA, Teyler TJ. 1991. Adenosine depresses excitatory but not fast inhibitory synaptic transmission in area CA1 of the rat hippocampus. *Neurosci. Lett.* 122:50–52

Lamsa K, Heeroma JH, Kullmann DM. 2005. Hebbian LTP in feed-forward inhibitory interneurons and the temporal fidelity of input discrimination. *Nat. Neurosci.* 8:916–24

Lamsa KP, Heeroma JH, Somogyi P, Rusakov DA, Kullmann DM. 2007. Anti-Hebbian long-term potentiation in the hippocampal feedback inhibitory circuit. *Science*. 315:1262–66

Langley JN. 1905. On the reaction of cells and of nerve-endings to certain poisons, chiefly as regards the reaction of striated muscle to nicotine and to curari. *J. Physiol.* 33:374–413

Lasztoczi B, Tukker JJ, Somogyi P, Klausberger T, Lasztóczi B, et al. 2011. Terminal Field and Firing Selectivity of Cholecystokinin-Expressing Interneurons in the Hippocampal CA3 Area. *J. Neurosci.* 31:18073–93

Lawrence JJ. 2008. Cholinergic control of GABA release: emerging parallels between neocortex and hippocampus. *Trends Neurosci.* 31:317–27

Lawrence JJ, Statland JM, Grinspan ZM, McBain CJ. 2006. Cell type-specific dependence of muscarinic signalling in mouse hippocampal stratum oriens interneurones. *J. Physiol.*

570:595–610

Lazarus M, Huang ZL, Lu J, Urade Y, Chen JF. 2012. How do the basal ganglia regulate sleep-wake behavior? *Trends Neurosci.* 35:723–32

Le Duigou C, Simonnet J, Teleñczuk MT, Fricker D, Miles R. 2014. Recurrent synapses and circuits in the CA3 region of the hippocampus: an associative network. *Front. Cell. Neurosci.* 7:262

Lee S, Yoon B-E, Berglund K, Oh S-J, Park H, et al. 2010a. Channel-mediated tonic GABA release from glia. *Science*. 330:790–96

Lee S-H, Földy C, Soltesz I. 2010b. Distinct endocannabinoid control of GABA release at perisomatic and dendritic synapses in the hippocampus. *J. Neurosci.* 30:7993–8000

Lee SY, Földy C, Szabadics J, Soltesz I. 2011. Cell-type-specific CCK2 receptor signaling underlies the cholecystokinin-mediated selective excitation of hippocampal parvalbumin-positive fast-spiking basket cells. *J. Neurosci.* 31:10993–2

Lerma J, Herranz AS, Herreras O, Abraira V, Martín del Río R. 1986. In vivo determination of extracellular concentration of amino acids in the rat hippocampus. A method based on brain dialysis and computerized analysis. *Brain Res.* 384:145–55

Letzkus JJ, Wolff SBE, Meyer EMM, Tovote P, Courtin J, et al. 2011. A disinhibitory microcircuit for associative fear learning in the auditory cortex. *Nature*. 480:331–35

Li H, Henry JL. 1998. Adenosine A2 receptor mediation of pre- and postsynaptic excitatory effects of adenosine in rat hippocampus in vitro. *Eur. J. Pharmacol.* 347:173–82

Li H, Henry JL. 2000. Adenosine receptor blockade reveals N-methyl-D-aspartate receptor- and voltage-sensitive dendritic spikes in rat hippocampal CA1 pyramidal cells in vitro.

Neuroscience. 100:21–31

Li XG, Somogyi P, Ylinen A, Buzsáki G. 1994. The hippocampal CA3 network: an in vivo intracellular labeling study. *J. Comp. Neurol.* 339:181–208

Li XX, Nomura T, Aihara H, Nishizaki T. 2001. Adenosine enhances glial glutamate efflux via A2a adenosine receptors. *Life Sci.* 68:1343–50

Lisman JE. 1999. Relating hippocampal circuitry to function: recall of memory sequences by reciprocal dentate-CA3 interactions. *Neuron*. 22:233–42

Liu QY, Schaffner AE, Chang YH, Maric D, Barker JL. 2000. Persistent activation of GABA(A) receptor/Cl(-) channels by astrocyte-derived GABA in cultured embryonic rat hippocampal neurons. *J. Neurophysiol.* 84:1392–1403

Lloyd HG, Fredholm BB. 1995. Involvement of adenosine deaminase and adenosine kinase in regulating extracellular adenosine concentration in rat hippocampal slices. *Neurochem. Int.* 26:387–95

Lloyd HG, Lindström K, Fredholm BB. 1993. Intracellular formation and release of adenosine from rat hippocampal slices evoked by electrical stimulation or energy depletion. *Neurochem. Int.* 23:173–85

Loewi O. 1921. Uber humorale Ubertragbarkeit der Herznervenwirkung. *Pflügers Arch.* 189:239–42

Londos C, Cooper DM, Wolff J. 1980. Subclasses of external adenosine receptors. *Proc. Natl. Acad. Sci. U. S. A.* 77:2551–54

Lopes L V, Cunha RA, Ribeiro JA. 1999. Cross talk between A(1) and A(2A) adenosine receptors in the hippocampus and cortex of young adult and old rats. *J. Neurophysiol.* 82:3196–3203

Lopes L V, Sebastião AM, Ribeiro JA. 2011. Adenosine and related drugs in brain diseases: present and future in clinical trials. *Curr. Top. Med. Chem.* 11:1087–1101

Lorente de Nó R. 1934. Studies on the structure of the cerebral cortex. Continuation of the study of the ammonic system. *J Psychol Neurol*. 46:113–77

Lovatt D, Xu Q, Liu W, Takano T, Smith NA, et al. 2012. From the Cover: Neuronal adenosine release, and not astrocytic ATP release, mediates feedback inhibition of excitatory activity. *Proc. Natl. Acad. Sci.* 109:6265–70

Lovett-Barron M, Turi GF, Kaifosh P, Lee PH, Bolze F, et al. 2012. Regulation of neuronal input transformations by tunable dendritic inhibition. *Nat. Neurosci.* 15:423–30

Maccaferri G, Roberts JD, Szucs P, Cottingham CA, Somogyi P. 2000. Cell surface domain specific postsynaptic currents evoked by identified GABAergic neurones in rat hippocampus in vitro. *J. Physiol.* 524:91–116

Macdonald RL, Olsen RW. 1994. GABAA receptor channels. *Annu. Rev. Neurosci.* 17:569–602

MacDonald RL, Skerritt JH, Werz MA. 1986. Adenosine agonists reduce voltage-dependent calcium conductance of mouse sensory neurones in cell culture. *J. Physiol.* 370:75–90

Macek TA, Schaffhauser H, Conn PJ. 1998. Protein kinase C and A3 adenosine receptor activation inhibit presynaptic metabotropic glutamate receptor (mGluR) function and uncouple mGluRs from GTP-binding proteins. *J. Neurosci.* 18:6138–46

Maconochie DJ, Zempel JM, Steinbach JH. 1994. How quickly can GABAA receptors open? *Neuron*. 12:61–71

Maex R, De Schutter E. 1998. Synchronization of golgi and granule cell firing in a detailed network model of the cerebellar granule cell layer. *J. Neurophysiol.* 80:2521–37

Magnus CJ, Lee PH, Atasoy D, Su HH, Looger LL, Sternson SM. 2011. Chemical and genetic engineering of selective ion channel-ligand interactions. *Science*. 333:1292–96

Mahan LC, McVittie LD, Smyk-Randall EM, Nakata H, Monsma FJ, et al. 1991. Cloning and expression of an A1 adenosine receptor from rat brain. *Mol. Pharmacol.* 40:1–7

Mann EO, Paulsen O. 2007. Role of GABAergic inhibition in hippocampal network oscillations. *Trends Neurosci.* 30:343–49

Marichich ES, Nasello AG. 1973. Epilepsy and adenosinetriphosphate (ATP): effect of electrical stimulation and high potassium perfusion on hippocampal ATP contents. *Brain Res.* 57:409–16

Marmont G. 1949. Studies on the axon membrane; a new method. *J. Cell. Physiol.* 34:351–82

Martin DL, Olsen RW, eds. 2000. *GABA in the Nervous System: The View at 50 Years*. Pliladelphia: Lippicott Williams and Wilkins

Martín ED, Fernández M, Perea G, Pascual O, Haydon PG, et al. 2007. Adenosine released by astrocytes contributes to hypoxia-induced modulation of synaptic transmission. *Glia*. 55:36–45

Mastakov MY, Baer K, Xu R, Fitzsimons H, During MJ. 2001. Combined injection of rAAV with mannitol enhances gene expression in the rat brain. *Mol. Ther.* 3:225–32

Matos M, Augusto E, Agostinho P, Cunha RA, Chen J-F. 2013. Antagonistic interaction between adenosine A2A receptors and Na+/K+-ATPase-α2 controlling glutamate uptake in astrocytes. *J. Neurosci.* 33:18492–502

Matsuno-Yagi A, Mukohata Y. 1977. Two possible roles of bacteriorhodopsin; a comparative study of strains of Halobacterium halobium differing in pigmentation. *Biochem.*

Biophys. Res. Commun. 78:237–43

Mátyás F, Freund TF, Gulyás AI. 2004. Convergence of excitatory and inhibitory inputs onto CCK-containing basket cells in the CA1 area of the rat hippocampus. *Eur. J. Neurosci.* 19:1243–56

Mayeaux DJ, Johnston RE. 2004. Discrimination of social odors and their locations: role of lateral entorhinal area. *Physiol. Behav.* 82:653–62

Mayfield RD, Suzuki F, Zahniser NR. 1993. Adenosine A2a receptor modulation of electrically evoked endogenous GABA release from slices of rat globus pallidus. *J. Neurochem.* 60:2334–37

McBain CJ, DiChiara TJ, Kauer JA. 1994. Activation of metabotropic glutamate receptors differentially affects two classes of hippocampal interneurons and potentiates excitatory synaptic transmission. *J. Neurosci.* 14:4433–45

McBain CJ, Fisahn A. 2001. Interneurons unbound. *Nat. Rev. Neurosci.* 2:11–23

McCartney MR, Deeb TZ, Henderson TN, Hales TG. 2007. Tonically active GABAA receptors in hippocampal pyramidal neurons exhibit constitutive GABA-independent gating. *Mol. Pharmacol.* 71:539–48

McCormick DA. 1989. GABA as an inhibitory neurotransmitter in human cerebral cortex. *J. Neurophysiol.* 62:1018–27

McKernan RM, Whiting PJ. 1996. Which GABAA-receptor subtypes really occur in the brain? *Trends Neurosci.* 19:139–43

McLaughlin BJ, Barber R, Saito K, Roberts E, Wu JY. 1975. Immunocytochemical localization of glutamate decarboxylase in rat spinal cord. *J. Comp. Neurol.* 164:305–21

Mehta AK, Ticku MK. 1999. An update on GABAA receptors. *Brain Res Rev*. 29:196–217

Meyerhof W, Müller-Brechlin R, Richter D. 1991. Molecular cloning of a novel putative G-protein coupled receptor expressed during rat spermiogenesis. *FEBS Lett.* 284:155–60

Michelson HB, Wong RK. 1991. Excitatory synaptic responses mediated by GABAA receptors in the hippocampus. *Science*. 253:1420–23

Miles R, Tóth K, Gulyás AI, Hájos N, Freund TF. 1996. Differences between somatic and dendritic inhibition in the hippocampus. *Neuron*. 16:815–23

Mitchell SJ, Silver RA. 2003. Shunting inhibition modulates neuronal gain during synaptic excitation. *Neuron*. 38:433–45

Mody I, De Koninck Y, Otis TS, Soltesz I. 1994. Bridging the cleft at GABA synapses in the brain. *Trends Neurosci.* 17:517–25

Mody I, Pearce RA. 2004. Diversity of inhibitory neurotransmission through GABA(A) receptors. *Trends Neurosci.* 27:569–75

Mogul DJ, Adams ME, Fox AP. 1993. Differential activation of adenosine receptors decreases N-type but potentiates P-type Ca2+ current in hippocampal CA3 neurons. *Neuron*. 10:327–34

Montero JM, Fes JB. 1982. Purification and characterization of bovine brain 5'-nucleotidase. *J. Neurochem.* 39:982–89

Moos WH, Szotek DS, Bruns RF. 1985. N6-cycloalkyladenosines. Potent, A1-selective adenosine agonists. *J. Med. Chem.* 28:1383–84

Moschovos C, Kostopoulos G, Papatheodoropoulos C. 2012. Endogenous adenosine induces NMDA receptor-independent persistent epileptiform discharges in dorsal and

ventral hippocampus via activation of A2 receptors. *Epilepsy Res.* 100:157–67

Moss SJ, Gorrie GH, Amato A, Smart TG. 1995. Modulation of GABAA receptors by tyrosine phosphorylation. *Nature*. 377:344–48

Moss SJ, Smart TG, Blackstone CD, Huganir RL. 1992. Functional modulation of GABAA receptors by cAMP-dependent protein phosphorylation. *Science*. 257:661–65

Mozrzymas JW, Zarnowska ED, Pytel M, Mercik K. 2003. Modulation of GABA(A) receptors by hydrogen ions reveals synaptic GABA transient and a crucial role of the desensitization process. *J. Neurosci.* 23:7981–92

Müller T. 2013. Suitability of the adenosine antagonist istradefylline for the treatment of Parkinson's disease: pharmacokinetic and clinical considerations. *Expert Opin. Drug Metab. Toxicol.* 9:1015–24

Naber PA, Caballero-Bleda M, Jorritsma-Byham B, Witter MP. 1997. Parallel input to the hippocampal memory system through peri- and postrhinal cortices. *Neuroreport*. 8:2617–21

Nagel G, Ollig D, Fuhrmann M, Kateriya S, Musti AM, et al. 2002. Channelrhodopsin-1: a light-gated proton channel in green algae. *Science*. 296:2395–98

Nakashiba T, Young JZ, McHugh TJ, Buhl DL, Tonegawa S. 2008. Transgenic inhibition of synaptic transmission reveals role of CA3 output in hippocampal learning. *Science*. 319:1260–64

Nakazawa K, Quirk MC, Chitwood RA, Watanabe M, Yeckel MF, et al. 2002. Requirement for hippocampal CA3 NMDA receptors in associative memory recall. *Science*. 297:211–18

Nanoff C, Mitterauer T, Roka F, Hohenegger M, Freissmuth M. 1995. Species differences in A1 adenosine receptor/G protein coupling: identification of a membrane protein that

stabilizes the association of the receptor/G protein complex. *Mol. Pharmacol.* 48:806–17

Naylor DE, Liu H, Wasterlain CG. 2005. Trafficking of GABA(A) receptors, loss of inhibition, and a mechanism for pharmacoresistance in status epilepticus. *J. Neurosci.* 25:7724–33

Neher E, Sakmann B. 1976. Single-channel currents recorded from membrane of denervated frog muscle fibres. *Nature*. 260:799–802

Nehlig A. 2010. Is caffeine a cognitive enhancer? *J. Alzheimer's Dis.* 20:S85–94

Neu A, Földy C, Soltesz I. 2007. Postsynaptic origin of CB1-dependent tonic inhibition of GABA release at cholecystokinin-positive basket cell to pyramidal cell synapses in the CA1 region of the rat hippocampus. *J. Physiol.* 578:233–47

Newberry NR, Nicoll RA. 1985. Comparison of the action of baclofen with gamma-aminobutyric acid on rat hippocampal pyramidal cells in vitro. *J. Physiol.* 360:161–85

Newby AC. 1985. The role of adenosine kinase in regulating adenosine concentration. *Biochem. J.* 226:343–44

Newman EA. 2003. Glial cell inhibition of neurons by release of ATP. *J. Neurosci.* 23:1659–66

Nishizaki T, Nagai K, Nomura T, Tada H, Kanno T, et al. 2002. A new neuromodulatory pathway with a glial contribution mediated via A2a adenosine receptors. *Glia*. 39:133–47

Nissen W, Szabo A, Somogyi J, Somogyi P, Lamsa KP. 2010. Cell type-specific long-term plasticity at glutamatergic synapses onto hippocampal interneurons expressing either parvalbumin or CB1 cannabinoid receptor. *J. Neurosci.* 30:1337–47

Nugent FS, Penick EC, Kauer JA. 2007. Opioids block long-term potentiation of inhibitory synapses. *Nature*. 446:1086–90

Nusser Z, Cull-Candy S, Farrant M. 1997. Differences in synaptic GABA(A) receptor number underlie variation in GABA mini amplitude. *Neuron*. 19:697–709

Nusser Z, Naylor D, Mody I. 2001. Synapse-specific contribution of the variation of transmitter concentration to the decay of inhibitory postsynaptic currents. *Biophys. J.* 80:1251–61

Nusser Z, Sieghart W, Mody I. 1999. Differential regulation of synaptic GABAA receptors by cAMP-dependent protein kinase in mouse cerebellar and olfactory bulb neurones. *J. Physiol.* 521:421–35

Nusser Z, Sieghart W, Somogyi P. 1998. Segregation of different GABAA receptors to synaptic and extrasynaptic membranes of cerebellar granule cells. *J. Neurosci.* 18:1693–1703

O'Keefe J, Conway DH. 1978. Hippocampal place units in the freely moving rat: why they fire where they fire. *Exp. brain Res.* 31:573–90

O'Keefe J, Dostrovsky J. 1971. The hippocampus as a spatial map. Preliminary evidence from unit activity in the freely-moving rat. *Brain Res.* 34:171–75

O'Regan MH, Simpson RE, Perkins LM, Phillis JW. 1992. Adenosine receptor agonists inhibit the release of gamma-aminobutyric acid (GABA) from the ischemic rat cerebral cortex. *Brain Res.* 582:22–26

Ochiishi T, Chen L, Yukawa A, Saitoh Y, Sekino Y, et al. 1999. Cellular localization of adenosine A1 receptors in rat forebrain: immunohistochemical analysis using adenosine A1 receptor-specific monoclonal antibody. *J. Comp. Neurol.* 411:301–16

Oesterhelt D, Stoeckenius W. 1971. Rhodopsin-like protein from the purple membrane of Halobacterium halobium. *Nat. New*

Biol. 233:149–52

Ogden D. 1994. *Microelectrode Techniques - The Plymouth Workshop Handbook*. Mill Hill, London: National Institute for Medical Research

Okada Y, Sakurai T, Mori M. 1992. Excitatory effect of adenosine on neurotransmission is due to increase of transmitter release in the hippocampal slices. *Neurosci. Lett.* 142:233–36

Oke OO, Magony A, Anver H, Ward PD, Jiruska P, et al. 2010. High-frequency gamma oscillations coexist with low-frequency gamma oscillations in the rat visual cortex in vitro. *Eur. J. Neurosci.* 31:1435–45

Olah ME, Stiles GL. 1995. Adenosine receptor subtypes: characterization and therapeutic regulation. *Annu. Rev. Pharmacol. Toxicol.* 35:581–606

Olsen RW, Sieghart W. 2008. International Union of Pharmacology. LXX. Subtypes of gamma-aminobutyric acid(A) receptors: classification on the basis of subunit composition, pharmacology, and function. Update. *Pharmacol. Rev.* 60:243–60

Olsen RW, Tobin a J. 1990. Molecular biology of GABAA receptors. *FASEB J.* 4:1469–80

Othman T, Yan H, Rivkees SA. 2003. Oligodendrocytes Express Functional A1 Adenosine Receptors That Stimulate Cellular Migration. *Glia*. 44:166–72

Otis TS, Staley KJ, Mody I. 1991. Perpetual inhibitory activity in mammalian brain slices generated by spontaneous GABA release. *Brain Res.* 545:142–50

Owens DF, Boyce LH, Davis MB, Kriegstein AR. 1996. Excitatory GABA responses in embryonic and neonatal cortical slices demonstrated by gramicidin perforated-patch recordings and calcium imaging. *J. Neurosci.* 16:6414–23

Owens DF, Liu X, Kriegstein AR. 1999. Changing properties of GABA(A) receptor-mediated signaling during early neocortical development. *J. Neurophysiol.* 82:570–83

Pak MA, Haas HL, Decking UK, Schrader J. 1994. Inhibition of adenosine kinase increases endogenous adenosine and depresses neuronal activity in hippocampal slices. *Neuropharmacology*. 33:1049–53

Palmer JL, Abeles RH. 1979. The mechanism of action of S-adenosylhomocysteinase. *J. Biol. Chem.* 254:1217–26

Papez JW. 1995. A proposed mechanism of emotion. *J. Neuropsychiatry Clin. Neurosci.* 7:103–12

Park J, Gupta RS. 2008. Adenosine kinase and ribokinase--the RK family of proteins. *Cell. Mol. Life Sci.* 65:2875–96

Pascual O, Casper KB, Kubera C, Zhang J, Revilla-Sanchez R, et al. 2005. Astrocytic purinergic signaling coordinates synaptic networks. *Science*. 310:113–16

Patenaude C, Massicotte G, Lacaille JC. 2005. Cell-type specific GABA synaptic transmission and activity-dependent plasticity in rat hippocampal stratum radiatum interneurons. *Eur. J. Neurosci.* 22:179–88

Pavlov I, Savtchenko LP, Kullmann DM, Semyanov A, Walker MC. 2009. Outwardly rectifying tonically active GABAA receptors in pyramidal cells modulate neuronal offset, not gain. *J. Neurosci.* 29:15341–50

Pavlov I, Walker MC. 2013. Tonic GABAA receptor-mediated signalling in temporal lobe epilepsy. *Neuropharmacology*. 69:55–61

Payne JA, Rivera C, Voipio J, Kaila K. 2003. Cation-chloride co-transporters in neuronal communication, development and trauma. *Trends Neurosci.* 26:199–206

Pearce RA. 1993. Physiological evidence for two distinct GABAA

responses in rat hippocampus. *Neuron*. 10:189–200

Pedata F, Pazzagli M, Tilli S, Pepeu G. 1990. Regional differences in the electrically stimulated release of endogenous and radioactive adenosine and purine derivatives from rat brain slices. *Naunyn. Schmiedebergs. Arch. Pharmacol.* 342:447–53

Penfield W, Erickson T. 1941. *Epilepsy and Cerebral Localization: A Study of the Mechanism, Treatment, and Prevention of Epileptic Seizures*. Springfiel ed.

Peng Z, Huang CS, Stell BM, Mody I, Houser CR. 2004. Altered expression of the delta subunit of the GABAA receptor in a mouse model of temporal lobe epilepsy. *J. Neurosci.* 24:8629–39

Perea G, Sur M, Araque A. 2014. Neuron-glia networks: integral gear of brain function. *Front. Cell. Neurosci.* 8:1–8

Perez Y, Morin F, Lacaille JC. 2001. A hebbian form of long-term potentiation dependent on mGluR1a in hippocampal inhibitory interneurons. *Proc. Natl. Acad. Sci. U. S. A.* 98:9401–6

Perreault P, Avoli M. 1988. A depolarizing inhibitory postsynaptic potential activated by synaptically released gamma-aminobutyric acid under physiological conditions in rat hippocampal pyramidal cells. *Can. J. Physiol. Pharmacol.* 66:1100–1102

Perreault P, Avoli M. 1992. 4-aminopyridine-induced epileptiform activity and a GABA-mediated long-lasting depolarization in the rat hippocampus. *J. Neurosci.* 12:104–15

Phillis JW. 1998. Inhibitory action of CGS 21680 on cerebral cortical neurons is antagonized by bicuculline and picrotoxin - Is GABA involved? *Brain Res.* 807:193–98

Phillis JW, Kostopoulos GK, Limacher JJ. 1974. Depression of corticospinal cells by various purines and pyrimidines. *Can.*

J. Physiol. Pharmacol. 52:1226–29

Phillis JW, Wu PH. 1981. The role of adenosine and its nucleotides in central synaptic transmission. *Prog. Neurobiol.* 16:187–239

Piccolino M. 1998. Animal electricity and the birth of electrophysiology: the legacy of Luigi Galvani. *Brain Res. Bull.* 46:381–407

Pietersen AN, Lancaster DM, Patel N, Hamilton JB, Vreugdenhil M. 2009. Modulation of gamma oscillations by endogenous adenosine through A1 and A2A receptors in the mouse hippocampus. *Neuropharmacology*. 56:481–92

Pikkarainen M, Rönkkö S, Savander V, Insausti R, Pitkänen A. 1999. Projections from the lateral, basal, and accessory basal nuclei of the amygdala to the hippocampal formation in rat. *J. Comp. Neurol.* 403:229–60

Pinto-Duarte A, Coelho JE, Cunha RA, Ribeiro JA, Sebastião AM. 2005. Adenosine A2A receptors control the extracellular levels of adenosine through modulation of nucleoside transporters activity in the rat hippocampus. *J. Neurochem.* 93:595–604

Piomelli D. 2003. The molecular logic of endocannabinoid signalling. *Nat. Rev. Neurosci.* 4:873–84

Poisbeau P, Cheney MC, Browning MD, Mody I. 1999. Modulation of synaptic GABAA receptor function by PKA and PKC in adult hippocampal neurons. *J. Neurosci.* 19:674–83

Ponce A, Bueno E, Kentros C, Vega-Saenz de Miera E, Chow A, et al. 1996. G-protein-gated inward rectifier K+ channel proteins (GIRK1) are present in the soma and dendrites as well as in nerve terminals of specific neurons in the brain. *J. Neurosci.* 16:1990–2001

Pouille F, Scanziani M. 2001. Enforcement of temporal fidelity in

pyramidal cells by somatic feed-forward inhibition. *Science*. 293:1159–63

Pouille F, Scanziani M. 2004. Routing of spike series by dynamic circuits in the hippocampus. *Nature*. 429:717–23

Proctor WR, Dunwiddie T V. 1987. Pre- and postsynaptic actions of adenosine in the in vitro rat hippocampus. *Brain Res.* 426:187–90

Qian H, Dowling JE. 1993. Novel GABA responses from rod-driven retinal horizontal cells. *Nature*. 361:162–64

Ralevic V, Burnstock G. 1998. Receptors for purines and pyrimidines. *Pharmacol. Rev.* 50:413–92

Ramón y Cajal S. 1911. *Histologie Du Système Nerveux de l'Homme et Des Vertébrés*. Paris: A. Maloine

Rebola N, Canas PM, Oliveira CR, Cunha RA. 2005a. Different synaptic and subsynaptic localization of adenosine A2A receptors in the hippocampus and striatum of the rat. *Neuroscience*. 132:893–903

Rebola N, Lujan R, Cunha RA, Mulle C. 2008. Adenosine A2A receptors are essential for long-term potentiation of NMDA-EPSCs at hippocampal mossy fiber synapses. *Neuron*. 57:121–34

Rebola N, Pinheiro PC, Oliveira CR, Malva JO, Cunha RA. 2003. Subcellular localization of adenosine A(1) receptors in nerve terminals and synapses of the rat hippocampus. *Brain Res.* 987:49–58

Rebola N, Porciúncula LO, Lopes L V, Oliveira CR, Soares-da-Silva P, Cunha RA. 2005b. Long-term effect of convulsive behavior on the density of adenosine A1 and A 2A receptors in the rat cerebral cortex. *Epilepsia*. 46 Suppl 5:159–65

Rebola N, Rodrigues RJ, Lopes L V, Richardson PJ, Oliveira CR, Cunha RA. 2005c. Adenosine A1 and A2A receptors are co-

expressed in pyramidal neurons and co-localized in glutamatergic nerve terminals of the rat hippocampus. *Neuroscience*. 133:79–83

Rebola N, Simões AP, Canas PM, Tomé AR, Andrade GM, et al. 2011. Adenosine A2A receptors control neuroinflammation and consequent hippocampal neuronal dysfunction. *J. Neurochem.* 117:100–111

Reppert SM, Weaver DR, Stehle JH, Rivkees SA. 1991. Molecular cloning and characterization of a rat A1-adenosine receptor that is widely expressed in brain and spinal cord. *Mol. Endocrinol.* 5:1037–48

Ribak CE, Vaughn JE, Saito K, Barber R, Roberts E. 1976. Immunocytochemical localization of glutamate decarboxylase in rat substantia nigra. *Brain Res.* 116:287–98

Ribak CE, Vaughn JE, Saito K, Barber R, Roberts E. 1977. Glutamate decarboxylase localization in neurons of the olfactory bulb. *Brain Res.* 126:1–18

Ribeiro JA. 1995. Purinergic inhibition of neurotransmitter release in the central nervous system. *Pharmacol. Toxicol.* 77:299–305

Ribeiro JA, Sebastião AM. 1986. Adenosine receptors and calcium: basis for proposing a third (A3) adenosine receptor. *Prog. Neurobiol.* 26:179–209

Ribeiro JA, Sebastião AM. 2010. Modulation and metamodulation of synapses by adenosine. *Acta Physiol. (Oxf).* 199:161–69

Richardson PJ, Brown SJ. 1987. ATP release from affinity-purified rat cholinergic nerve terminals. *J. Neurochem.* 48:622–30

Richardson PJ, Brown SJ, Bailyes EM, Luzio JP. 1987. Ectoenzymes control adenosine modulation of immunoisolated cholinergic synapses. *Nature*. 327:232–34

Rivera C, Voipio J, Kaila K. 2005. Two developmental switches in GABAergic signalling: the K+-Cl- cotransporter KCC2 and carbonic anhydrase CAVII. *J. Physiol.* 562:27–36

Rivera C, Voipio J, Payne JA, Ruusuvuori E, Lahtinen H, et al. 1999. The K+/Cl- co-transporter KCC2 renders GABA hyperpolarizing during neuronal maturation. *Nature*. 397:251–55

Rivkees SA, Price SL, Zhou FC. 1995. Immunohistochemical detection of A1 adenosine receptors in rat brain with emphasis on localization in the hippocampal formation, cerebral cortex, cerebellum, and basal ganglia. *Brain Res.* 677:193–203

Robello M, Amico C, Cupello A. 1993. Regulation of GABAA receptor in cerebellar granule cells in culture: differential involvement of kinase activities. *Neuroscience*. 53:131–38

Roberts E. 1986. GABA: The road to neurotransmitter status. In *Benzodiazepine/GABA Receptors and Chloride Channels: Structural and Functional Properties*, eds. RW Olsen, JC Venter, pp. 1–39. New York: Alan R. Liss, Inc.

Roberts E, Frankel S. 1950. gamma-Aminobutyric acid in brain: its formation from glutamic acid. *J. Biol. Chem.* 187:55–63

Roberts E, Kuriyama K. 1968. Biochemical-physiological correlations in studies of the gamma-aminobutyric acid system. *Brain Res.* 8:1–35

Rolls ET. 2007. An attractor network in the hippocampus: theory and neurophysiology. *Learn. Mem.* 14:714–31

Roos A, Boron WF. 1981. Intracellular pH. *Physiol. Rev.* 61:296–434

Rosenberg PA, Dichter MA. 1989. Extracellular cAMP accumulation and degradation in rat cerebral cortex in dissociated cell culture. *J. Neurosci.* 9:2654–63

Roseti C, Martinello K, Fucile S, Piccari V, Mascia A, et al. 2008. Adenosine receptor antagonists alter the stability of human epileptic GABAA receptors. *Proc. Natl. Acad. Sci. U. S. A.* 105:15118–23

Roseti C, Palma E, Martinello K, Fucile S, Morace R, et al. 2009. Blockage of A2A and A3 adenosine receptors decreases the desensitization of human GABA(A) receptors microtransplanted to Xenopus oocytes. *Proc. Natl. Acad. Sci. U. S. A.* 106:15927–31

Rossi DJ, Hamann M, Attwell D. 2003. Multiple modes of GABAergic inhibition of rat cerebellar granule cells. *J. Physiol.* 548:97–110

Rothman JS, Cathala L, Steuber V, Silver RA. 2009. Synaptic depression enables neuronal gain control. *Nature*. 457:1015–18

Ruiz A, Campanac E, Scott RS, Rusakov DA, Kullmann DM. 2010. Presynaptic GABAA receptors enhance transmission and LTP induction at hippocampal mossy fiber synapses. *Nat. Neurosci.* 13:431–38

Sagratella S, Frank C, Benedetti M, Scotti de Carolis A. 1987. Modulatory action of purinergic drugs on high potassium-induced epileptiform bursting in rat hippocampal slices. *Pharmacol. Res. Commun.* 19:819–26

Saito K, Barber R, Wu J, Matsuda T, Roberts E, Vaughn JE. 1974. Immunohistochemical localization of glutamate decarboxylase in rat cerebellum. *Proc. Natl. Acad. Sci. U. S. A.* 71:269–73

Salin PA, Prince DA. 1996. Spontaneous GABAA receptor-mediated inhibitory currents in adult rat somatosensory cortex. *J. Neurophysiol.* 75:1573–88

Sargolini F, Fyhn M, Hafting T, McNaughton BL, Witter MP, et al. 2006. Conjunctive representation of position, direction, and

velocity in entorhinal cortex. *Science*. 312:758–62

Sattin A, Rall TW. 1970. The effect of adenosine and adenine nucleotides on the cyclic adenosine 3', 5'-phosphate content of guinea pig cerebral cortex slices. *Mol. Pharmacol.* 6:13–23

Scanziani M, Capogna M, Gähwiler BH, Thompson SM. 1992. Presynaptic inhibition of miniature excitatory synaptic currents by baclofen and adenosine in the hippocampus. *Neuron*. 9:919–27

Schaffer K. 1892. Beitrag zur histologie der ammonshornformation. *Arch Mikroskop Anat.* 39:611–32

Scharfman HE, Schwartzkroin PA. 1988. Electrophysiology of morphologically identified mossy cells of the dentate hilus recorded in guinea pig hippocampal slices. *J. Neurosci.* 8:3812–21

Schiffmann SN, Libert F, Vassart G, Vanderhaeghen JJ. 1991. Distribution of adenosine A2 receptor mRNA in the human brain. *Neurosci. Lett.* 130:177–81

Schofield PR, Darlison MG, Fujita N, Burt DR, Stephenson FA, et al. 1987. Sequence and functional expression of the GABA A receptor shows a ligand-gated receptor super-family. *Nature*. 328:221–27

Schrader J, Schütz W, Bardenheuer H. 1981. Role of S-adenosylhomocysteine hydrolase in adenosine metabolism in mammalian heart. *Biochem. J.* 196:65–70

Schubert P. 1988. Physiological modulation by adenosine: selective blockade of A1-receptors with DPCPX enhances stimulus train-evoked neuronal Ca influx in rat hippocampal slices. *Brain Res.* 458:162–65

Schubert P, Heinemann U, Kolb R. 1986. Differential effect of adenosine on pre- and postsynaptic calcium fluxes. *Brain Res.* 376:382–86

Schubert P, Mager R. 1991. The critical input frequency for NMDA receptor-mediated neuronal Ca2+ influx depends on endogenous adenosine. *Int J Purine Pyrimid Res*. 2:11–16

Schubert P, Pintor J, Miras-Portugal MT. 1995. Inhibitory action of adenosine and adenine dinucleotides on synaptic transmission in the central nervous system. In *Adenosine and Adenine Nucleotides: From Molecular Biology to Integrative Physiology*, eds. L Belardinelli, A Pelleg. New York: Springer Science

Schulte G, Fredholm BB. 2000. Human adenosine A(1), A(2A), A(2B), and A(3) receptors expressed in Chinese hamster ovary cells all mediate the phosphorylation of extracellular-regulated kinase 1/2. *Mol. Pharmacol.* 58:477–82

Schulz SB, Klaft Z-JJ, Rösler AR, Heinemann U, Gerevich Z. 2012. Purinergic P2X, P2Y and adenosine receptors differentially modulate hippocampal gamma oscillations. *Neuropharmacology*. 62:914–24

Scimemi A, Semyanov A, Sperk G, Kullmann DM, Walker MC. 2005. Multiple and plastic receptors mediate tonic GABAA receptor currents in the hippocampus. *J. Neurosci.* 25:10016–24

Seamon KB, Padgett W, Daly JW. 1981. Forskolin: unique diterpene activator of adenylate cyclase in membranes and in intact cells. *Proc. Natl. Acad. Sci. U. S. A.* 78:3363–67

Sebastião AM, Macedo MP, Ribeiro JA. 2000. Tonic activation of A(2A) adenosine receptors unmasks, and of A(1) receptors prevents, a facilitatory action of calcitonin gene-related peptide in the rat hippocampus. *Br. J. Pharmacol.* 129:374–80

Sebastião AM, Ribeiro JA. 1992. Evidence for the presence of excitatory A2 adenosine receptors in the rat hippocampus. *Neurosci. Lett.* 138:41–44

Sebastião AM, Ribeiro JA. 2000. Fine-tuning neuromodulation by adenosine. *Trends Pharmacol. Sci.* 21:341–46

Sebastião AM, Ribeiro JA. 2009. Adenosine receptors and the central nervous system. *Handb. Exp. Pharmacol.* 193:471–534

Sebastião AM, Stone TW, Ribeiro JA. 1990. The inhibitory adenosine receptor at the neuromuscular junction and hippocampus of the rat: antagonism by 1,3,8-substituted xanthines. *Br. J. Pharmacol.* 101:453–59

Segal M. 1982. Intracellular analysis of a postsynaptic action of adenosine in the rat hippocampus. *Eur. J. Pharmacol.* 79:193–99

Sekino Y, Ito K, Miyakawa H, Kato H, Kuroda Y. 1991. Adenosine (A2) antagonist inhibits induction of long-term potentiation of evoked synaptic potentials but not of the population spike in hippocampal CA1 neurons. *Biochem. Biophys. Res. Commun.* 181:1010–14

Selden NR, Everitt BJ, Jarrard LE, Robbins TW. 1991. Complementary roles for the amygdala and hippocampus in aversive conditioning to explicit and contextual cues. *Neuroscience*. 42:335–50

Semyanov A, Walker MC, Kullmann DM. 2003. GABA uptake regulates cortical excitability via cell type-specific tonic inhibition. *Nat. Neurosci.* 6:484–90

Semyanov A, Walker MC, Kullmann DM, Silver RA. 2004. Tonically active GABA A receptors: modulating gain and maintaining the tone. *Trends Neurosci.* 27:262–69

Shinohara M, Saitoh M, Nishizawa D, Ikeda K, Hirose S, et al. 2013. ADORA2A polymorphism predisposes children to encephalopathy with febrile status epilepticus. *Neurology*. 80:1571–76

Shinohara Y, Hirase H, Watanabe M, Itakura M, Takahashi M,

Shigemoto R. 2008. Left-right asymmetry of the hippocampal synapses with differential subunit allocation of glutamate receptors. *Proc. Natl. Acad. Sci. U. S. A.* 105:19498–503

Shook BC, Jackson PF. 2011. Adenosine A2A receptor antagonists and Parkinson's disease. *ACS Chem. Neurosci.* 2:555–67

Soltesz I, Roberts JD, Takagi H, Richards JG, Mohler H, Somogyi P. 1990. Synaptic and Nonsynaptic Localization of Benzodiazepine/GABAA Receptor/Cl- Channel Complex Using Monoclonal Antibodies in the Dorsal Lateral Geniculate Nucleus of the Cat. *Eur. J. Neurosci.* 2:414–29

Somogyi P, Klausberger T. 2005. Defined types of cortical interneurone structure space and spike timing in the hippocampus. *J. Physiol.* 562:9–26

Somogyi P, Nunzi MG, Gorio A, Smith AD. 1983. A new type of specific interneuron in the monkey hippocampus forming synapses exclusively with the axon initial segments of pyramidal cells. *Brain Res.* 259:137–42

Somogyi P, Takagi H, Richards JG, Mohler H. 1989. Subcellular localization of benzodiazepine/GABAA receptors in the cerebellum of rat, cat, and monkey using monoclonal antibodies. *J. Neurosci.* 9:2197–2209

Somogyi P, Tamás G, Lujan R, Buhl EH. 1998. Salient features of synaptic organisation in the cerebral cortex. *Brain Res. Rev.* 26:113–35

Sousa VC, Assaife-Lopes N, Ribeiro JA, Pratt JA, Brett RR, Sebastião AM. 2011. Regulation of hippocampal cannabinoid CB1 receptor actions by adenosine A1 receptors and chronic caffeine administration: implications for the effects of Δ9-tetrahydrocannabinol on spatial memory. *Neuropsychopharmacology*. 36:472–87

Spruston N, Schiller Y, Stuart G, Sakmann B. 1995. Activity-dependent action potential invasion and calcium influx into hippocampal CA1 dendrites. *Science*. 268:297–300

Staley KJ, Soldo BL, Proctor WR. 1995. Ionic mechanisms of neuronal excitation by inhibitory GABAA receptors. *Science*. 269:977–81

Stark C. 2007. Chapter 12: Functional Role of the Human Hippocampus. In *The Hippocampus Book*, eds. P Andersen, R Morris, D Amaral, T Bliss, J O'Keefe, pp. 549–79. New York: Oxford University Press, Inc.

Stell BM, Brickley SG, Tang CY, Farrant M, Mody I. 2003. Neuroactive steroids reduce neuronal excitability by selectively enhancing tonic inhibition mediated by delta subunit-containing GABAA receptors. *Proc. Natl. Acad. Sci. U. S. A.* 100:14439–44

Steward O. 1976. Topographic organization of the projections from the entorhinal area to the hippocampal formation of the rat. *J. Comp. Neurol.* 167:285–314

Stone TW. 1985. Some unresolved problems. In *Purines: Pharmacology and Physiological Roles*, ed. TW Stone, pp. 245–51. London: The Macmillan Press

Storm-Mathisen J, Leknes AK, Bore AT, Vaaland JL, Edminson P, et al. 1983. First visualization of glutamate and GABA in neurones by immunocytochemistry. *Nature*. 301:517–20

Stuart GJ, Dodt HU, Sakmann B. 1993. Patch-clamp recordings from the soma and dendrites of neurons in brain slices using infrared video microscopy. *Pflugers Arch.* 423:511–18

Sun C, Sieghart W, Kapur J. 2004. Distribution of alpha1, alpha4, gamma2, and delta subunits of GABAA receptors in hippocampal granule cells. *Brain Res.* 1029:207–16

Svenningsson P, Le Moine C, Kull B, Sunahara R, Bloch B, Fredholm BB. 1997. Cellular expression of adenosine A2A

receptor messenger RNA in the rat central nervous system with special reference to dopamine innervated areas. *Neuroscience*. 80:1171–85

Swanson LW, Wyss JM, Cowan WM. 1978. An autoradiographic study of the organization of intrahippocampal association pathways in the rat. *J. Comp. Neurol.* 181:681–715

Swanson TH, Drazba JA, Rivkees SA. 1995. Adenosine A1 receptors are located predominantly on axons in the rat hippocampal formation. *J. Comp. Neurol.* 363:517–31

Szentágothai J. 1975. The “module-concept” in cerebral cortex architecture. *Brain Res.* 95:475–96

Szentágothai J, Arbib MA. 1974. Conceptual models of neural organization. *Neurosci. Res. Program Bull.* 12:305–510

Takahashi RN, Pamplona FA, Prediger RDS. 2008. Adenosine receptor antagonists for cognitive dysfunction: a review of animal studies. *Front. Biosci.* 13:2614–32

Terrian DM, Hernandez PG, Rea MA, Peters RI. 1989. ATP release, adenosine formation, and modulation of dynorphin and glutamic acid release by adenosine analogues in rat hippocampal mossy fiber synaptosomes. *J. Neurochem.* 53:1390–99

Thompson SM, Deisz RA, Prince DA. 1988. Relative contributions of passive equilibrium and active transport to the distribution of chloride in mammalian cortical neurons. *J. Neurophysiol.* 60:105–24

Thompson SM, Gähwiler BH. 1989a. Activity-dependent disinhibition. II. Effects of extracellular potassium, furosemide, and membrane potential on ECl- in hippocampal CA3 neurons. *J. Neurophysiol.* 61:512–23

Thompson SM, Gähwiler BH. 1989b. Activity-dependent disinhibition. I. Repetitive stimulation reduces IPSP driving force and conductance in the hippocampus in vitro. *J.*

Neurophysiol. 61:501–11

Thompson SM, Haas HL, Gähwiler BH. 1992. Comparison of the actions of adenosine at pre- and postsynaptic receptors in the rat hippocampus in vitro. *J. Physiol.* 451:347–63

Tossman U, Jonsson G, Ungerstedt U. 1986. Regional distribution and extracellular levels of amino acids in rat central nervous system. *Acta Physiol. Scand.* 127:533–45

Tóth K, Freund TF, Miles R. 1997. Disinhibition of rat hippocampal pyramidal cells by GABAergic afferents from the septum. *J. Physiol.* 500:463–74

Traub RD, Kopell N, Bibbig A, Buhl EH, LeBeau FE, Whittington MA. 2001. Gap junctions between interneuron dendrites can enhance synchrony of gamma oscillations in distributed networks. *J. Neurosci.* 21:9478–86

Traub RD, Whittington MA, Colling SB, Buzsáki G, Jefferys JG. 1996. Analysis of gamma rhythms in the rat hippocampus in vitro and in vivo. *J. Physiol.* 493:471–84

Trussell LO, Jackson MB. 1985. Adenosine-activated potassium conductance in cultured striatal neurons. *Proc. Natl. Acad. Sci. U. S. A.* 82:4857–61

Tukker JJ, Fuentealba P, Hartwich K, Somogyi P, Klausberger T. 2007. Cell type-specific tuning of hippocampal interneuron firing during gamma oscillations in vivo. *J. Neurosci.* 27:8184–89

Udenfriend S. 1950. Identification of gamma-aminobutyric acid in brain by the isotope derivative method. *J. Biol. Chem.* 187:65–69

Unwin N. 1989. The structure of ion channels in membranes of excitable cells. *Neuron*. 3:665–76

van Aerde KI, Qi G, Feldmeyer D. 2013. Cell Type-Specific Effects of Adenosine on Cortical Neurons. *Cereb. Cortex*.

[Epub ahead of print]

van Calker D, Müller M, Hamprecht B. 1979. Adenosine regulates via two different types of receptors, the accumulation of cyclic AMP in cultured brain cells. *J. Neurochem.* 33:999–1005

van Strien NM, Cappaert NLM, Witter MP. 2009. The anatomy of memory: an interactive overview of the parahippocampal-hippocampal network. *Nat. Rev. Neurosci.* 10:272–82

Vida I, Halasy K, Szinyei C, Somogyi P, Buhl EH. 1998. Unitary IPSPs evoked by interneurons at the stratum radiatum-stratum lacunosum-moleculare border in the CA1 area of the rat hippocampus in vitro. *J. Physiol.* 506:755–73

von Euler US. 1946. A Specific Sympathomimetic Ergone in Adrenergic Nerve Fibres (Sympathin) and its Relations to Adrenaline and Nor-Adrenaline. *Acta Physiol. Scand.* 12:73–97

von Euler US. 1948. Identification of the sympathomimetic ergone in adrenergic nerves of cattle (sympathin N) with laevo-noadrenaline. *Acta Physiol. Scand.* 16:63–74

Wall MJ, Usowicz MM. 1997. Development of action potential-dependent and independent spontaneous GABAA receptor-mediated currents in granule cells of postnatal rat cerebellum. *Eur. J. Neurosci.* 9:533–48

Wang CM, Chang YY, Kuo JS, Sun SH. 2002. Activation of P2x7 receptors induced [3H]GABA release from the RBA-2 type-2 astrocyte cell line through a Cl-/HCO3 - - dependent mechanism. *Glia*. 37:8–18

Wang H, Bedford FK, Brandon NJ, Moss SJ, Olsen RW. 1999. GABA(A)-receptor-associated protein links GABA(A) receptors and the cytoskeleton. *Nature*. 397:69–72

Wang XJ, Buzsáki G. 1996. Gamma oscillation by synaptic inhibition in a hippocampal interneuronal network model. *J.*

Neurosci. 16:6402–13

Wang YF, Gao XB, van den Pol AN. 2001. Membrane properties underlying patterns of GABA-dependent action potentials in developing mouse hypothalamic neurons. *J. Neurophysiol.* 86:1252–65

Wei CJ, Augusto E, Gomes CA, Singer P, Wang Y, et al. 2014. Regulation of fear responses by striatal and extrastriatal adenosine A 2A receptors in forebrain. *Biol. Psychiatry*. 75:855–63

Wei CJ, Li W, Chen JF. 2011. Normal and abnormal functions of adenosine receptors in the central nervous system revealed by genetic knockout studies. *Biochim. Biophys. Acta - Biomembr.* 1808:1358–79

Wei W, Zhang N, Peng Z, Houser CR, Mody I. 2003. Perisynaptic localization of delta subunit-containing GABA(A) receptors and their activation by GABA spillover in the mouse dentate gyrus. *J. Neurosci.* 23:10650–61

White TD, MacDonald WF. 1990. Neural release of ATP and adenosine. *Ann. N. Y. Acad. Sci.* 603:287–98; discussion 298–99

Whiting P, McKernan RM, Iversen LL. 1990. Another mechanism for creating diversity in gamma-aminobutyrate type A receptors: RNA splicing directs expression of two forms of gamma 2 phosphorylation site. *Proc. Natl. Acad. Sci. U. S. A.* 87:9966–70

Whittington MA, Traub RD, Jefferys JG. 1995. Synchronized oscillations in interneuron networks driven by metabotropic glutamate receptor activation. *Nature*. 373:612–15

Wieraszko A, Goldsmith G, Seyfried TN. 1989. Stimulation-dependent release of adenosine triphosphate from hippocampal slices. *Brain Res.* 485:244–50

Wlodarczyk AI, Sylantyev S, Herd MB, Kersanté F, Lambert JJ,

et al. 2013. GABA-independent GABAA receptor openings maintain tonic currents. *J. Neurosci.* 33:3905–14

Wu LG, Saggau P. 1994. Adenosine inhibits evoked synaptic transmission primarily by reducing presynaptic calcium influx in area CA1 of hippocampus. *Neuron*. 12:1139–48

Wulff P, Ponomarenko AA, Bartos M, Korotkova TM, Fuchs EC, et al. 2009. Hippocampal theta rhythm and its coupling with gamma oscillations require fast inhibition onto parvalbumin-positive interneurons. *Proc. Natl. Acad. Sci. U. S. A.* 106:3561–66

Xiao D, Bastia E, Xu Y-H, Benn CL, Cha J-HJ, et al. 2006. Forebrain adenosine A2A receptors contribute to L-3,4-dihydroxyphenylalanine-induced dyskinesia in hemiparkinsonian mice. *J. Neurosci.* 26:13548–55

Yawo H, Chuhma N. 1993. Preferential inhibition of omega-conotoxin-sensitive presynaptic Ca2+ channels by adenosine autoreceptors. *Nature*. 365:256–58

Yizhar O, Fenno L, Davidson TJ, Mogri M, Deisseroth K. 2011. Optogenetics in neural systems. *Neuron*. 71:9–34

Yoon KW, Rothman SM. 1991. Adenosine inhibits excitatory but not inhibitory synaptic transmission in the hippocampus. *J. Neurosci.* 11:1375–80

Yoshioka K, Hosoda R, Kuroda Y, Nakata H. 2002. Hetero-oligomerization of adenosine A1 receptors with P2Y1 receptors in rat brains. *FEBS Lett.* 531:299–303

Zeraati M, Mirnajafi-Zadeh J, Fathollahi Y, Namvar S, Rezvani ME. 2006. Adenosine A1 and A2A receptors of hippocampal CA1 region have opposite effects on piriform cortex kindled seizures in rats. *Seizure*. 15:41–48

Zhang L, McBain CJ. 1995. Voltage-gated potassium currents in stratum oriens-alveus inhibitory neurones of the rat CA1 hippocampus. *J. Physiol.* 488:647–60

Zhang N, Wei W, Mody I, Houser CR. 2007. Altered localization of GABA(A) receptor subunits on dentate granule cell dendrites influences tonic and phasic inhibition in a mouse model of epilepsy. *J. Neurosci.* 27:7520–31

Zhou QY, Li C, Olah ME, Johnson RA, Stiles GL, Civelli O. 1992. Molecular cloning and characterization of an adenosine receptor: the A3 adenosine receptor. *Proc. Natl. Acad. Sci. U. S. A.* 89:7432–36

Zhu PJ, Krnjević K. 1994. Endogenous adenosine deaminase does not modulate synaptic transmission in rat hippocampal slices under normoxic or hypoxic conditions. *Neuroscience*. 63:489–97

Zimmermann H, Grondal EJM, Keller F. 1986. Hydrolysis of ATP and formation of adenosine at the surface of cholinergic nerve endings. In *Cellular Biology of Ectoenzumes*, eds. GW Kreutzberg, M Reddington, H Zimmermann, pp. 35–48. Berlin: Springer-Verlag

Zimmermann H, Zebisch M, Sträter N. 2012. Cellular function and molecular structure of ecto-nucleotidases. *Purinergic Signal.* 8:437–502

10 Papers

- **Rombo DM**, Dias RB, Duarte ST, Ribeiro JA, Lamsa KP, Sebastião AM (2014). Adenosine A1 receptors suppress tonic GABAA receptor currents in hippocampal pyramidal cells and in a defined subpopulation of interneurons. *Cerebral Cortex*. (Epub ahead of print).

- **Rombo DM**, Newton K, Nissen W, Badurek S, Horn J, Minichiello L, Jefferys J, Sebastiao AM, Lamsa K (2015). Synaptic mechanims of adenosine A2A receptor mediated hyperexcitability in the hippocampus. *Hippocampus* 25, 566-80.

Cerebral Cortex Advance Access published December 1, 2014

OXFORD

Cerebral Cortex, 2014, 1–15

doi: 10.1093/cercor/bhu288
Original Article

ORIGINAL ARTICLE

Adenosine A_1 Receptor Suppresses Tonic $GABA_A$ Receptor Currents in Hippocampal Pyramidal Cells and in a Defined Subpopulation of Interneurons

Diogo M. Rombo[1,2], Raquel B. Dias[1,2], Sofia T. Duarte[1,2,3], Joaquim A. Ribeiro[1,2], Karri P. Lamsa[4], and Ana M. Sebastião[1,2]

[1]Instituto de Farmacologia e Neurociências, Faculdade de Medicina, Universidade de Lisboa, Lisboa, Portugal, [2]Unidade de Neurociências, Instituto de Medicina Molecular, Universidade de Lisboa, Lisboa, Portugal, [3]Neuropaediatrics Department, Hospital D. Estefânia, Centro Hospitalar Lisboa Central, Lisboa, Portugal, and [4]Medical Research Council Anatomical Neuropharmacology Unit, Department of Pharmacology, Oxford University, Oxford, UK

Address correspondence to Ana M. Sebastião, Instituto de Farmacologia e Neurociências, Faculdade de Medicina, Universidade de Lisboa, Avenida Professor Egas Moniz, Edifício Egas Moniz, 1649-028 Lisboa, Portugal. Email: anaseb@medicina.ulisboa.pt

Abstract

Adenosine is an endogenous neuromodulator that decreases excitability of hippocampal circuits activating membrane-bound metabotropic A_1 receptor (A_1R). The presynaptic inhibitory action of adenosine A_1R in glutamatergic synapses is well documented, but its influence on inhibitory GABAergic transmission is poorly known. We report that $GABA_A$ receptor ($GABA_AR$)-mediated tonic, but not phasic, transmission is suppressed by A_1R in hippocampal neurons. Adenosine A_1R activation strongly inhibits $GABA_AR$ agonist (muscimol)-evoked currents in *Cornu Ammonis* 1 (CA1) pyramidal neurons and in a specific subpopulation of interneurons expressing axonal cannabinoid receptor type 1. In addition, A_1R suppresses tonic $GABA_AR$ currents measured in the presence of elevated ambient GABA as well as in naïve slices. The inhibition of GABAergic currents involves both protein kinase A (PKA) and protein kinase C (PKC) signaling pathways and decreases $GABA_AR$ δ-subunit expression. On the contrary, no A_1R-mediated modulation was detected in phasic inhibitory postsynaptic currents evoked either by afferent electrical stimulation or by spontaneous quantal release. The results show that A_1R modulates extrasynaptic rather than synaptic $GABA_AR$-mediated signaling, and that this modulation selectively occurs in hippocampal pyramidal neurons and in a specific subpopulation of inhibitory interneurons. We conclude that modulation of tonic $GABA_AR$ signaling by adenosine A_1R in specific neuron types may regulate neuronal gain and excitability in the hippocampus.

Key words: disinhibition, GABAergic interneurons, network excitability, neuromodulation, tonic and phasic inhibition

Introduction

GABA-releasing hippocampal interneurons regulate excitability of postsynaptic neurons via phasic and tonic $GABA_A$ receptor ($GABA_AR$)-mediated signaling (McBain and Fisahn 2001; Klausberger and Somogyi 2008). GABAergic phasic transmission shows fast and precisely timed current kinetics generated by synaptic $GABA_AR$. Tonic inhibition is generated by sustained or persistent activity of mainly extrasynaptic (Brickley et al. 1996; Salin and Prince 1996; Semyanov et al. 2003) high-affinity and slowly desensitizing $GABA_AR$ (Nusser et al. 1998; Haas and Macdonald 1999; Bianchi and Macdonald 2003; Caraiscos et al. 2004). In the hippocampus, tonic $GABA_AR$-mediated currents

have been characterized in pyramidal cells (Bai et al. 2001) and in inhibitory interneurons (Semyanov et al. 2003). Tonic and phasic $GABA_AR$-mediated inhibition also exhibit distinct pharmacological properties (Semyanov et al. 2004; Farrant and Nusser 2005; Mann and Paulsen 2007), and hence these can be selectively modulated (see Farrant and Nusser 2005).

Adenosine, acting through high-affinity A_1 receptor (A_1R), is a well-characterized endogenous modulator of neuronal activity in the brain (Sebastião and Ribeiro 2009). Adenosine A_1R modulates excitatory glutamatergic synapses at both the pre- and postsynaptic site (Boison 2012; Dias et al. 2013). On the contrary, phasic GABAergic transmission in pyramidal cells is not modulated by A_1R (Burke and Nadler 1988; Kamiya 1991; Lambert and Teyler 1991; Yoon and Rothman 1991; Cunha and Ribeiro 2000). However, in pyramidal cells, immunohistochemical studies show intense labeling of A_1R not only in dendritic glutamatergic synapses, but also in the perisomatic region where synapses are mainly GABAergic and inhibitory (Kasugai et al. 2010). Adenosine A_1Rs are also expressed postsynaptically in GABAergic interneurons (Rivkees et al. 1995; Ochiishi et al. 1999). Although phasic $GABA_AR$ currents are unaffected by A_1R activity, it is unknown whether tonic inhibitory currents (tonic-ICs) in pyramidal cells are modulated by the receptor. In addition, how adenosine A_1R acts on disinhibitory signaling, that is, GABAergic transmission in inhibitory interneurons has not been studied.

We report that activation of adenosine A_1R suppresses tonic, but not phasic $GABA_A$ currents in hippocampal pyramidal cells. In addition, similar suppression is present in a subpopulation of CA1 area inhibitory interneurons, with axonal cannabinoid receptor type 1 (CB1R). The results demonstrate that the A_1R has a highly selective influence on GABAergic neurons. The target-specific modulation of tonic $GABA_AR$ conductance through A_1R has implications in normal brain function as well as for the use of adenosine in antiepileptic therapies (Boison 2012; Duguid et al. 2012).

Materials and Methods

Hippocampal Slices

The procedures were identical to those previously used and described elsewhere (Dias et al. 2012). Three- to 5-week-old male Wistar rats (Harlan, Italy) were anesthetized with halothane (Sigma-Aldrich, St Louis, MO, USA) and sacrificed by decapitation in accordance with Portuguese law on animal care and the European Community guidelines (86/609/EEC). The brain was quickly removed and hemisected, and the hippocampus used to obtain transverse slices (300 µm thickness) cut on a Vibratome (Leica VT 1000S; Leica Microsystems, Germany) in ice-cold dissecting solution containing (in mM): 110 sucrose, 2.5 KCl, 0.5 $CaCl_2$, 7 $MgCl_2$, 25 $NaHCO_3$, 1.25 NaH_2PO_4, 7 glucose, pH 7.4, bubbled with 95% O_2/ 5% CO_2. Slices were first incubated for 30 min at 35 °C in artificial cerebrospinal fluid (aCSF) that contained (in mM): 124 NaCl, 3 KCl, 1.25 NaH_2PO_4, 26 $NaHCO_3$, 1 $MgSO_4$, 2 $CaCl_2$, 10 glucose, pH 7.4 (gassed with 95% O_2/5% CO_2), and used for experiment after recovering in a submerged storage chamber at room temperature (22–24 °C) for at least 60 min.

Individual slices were clamped with a grid in a recording chamber and continuously superfused by a gravitational superfusion system at 2–3 mL/min with aCSF at room temperature.

Chemicals

Unless otherwise stated, drugs were added via the superfusion solution and their final concentration diluted from concentrated stocks.

N^6-cyclopentyladenosine (CPA), 1,3-dipropyl-8-cyclopentylxanthine (DPCPX), and 1-[2-[tris(4-methoxyphenyl)methoxy] ethyl]-(*S*)-3-piperidinecarboxylic acid (SNAP5114) were obtained from Tocris Bioscience (Bristol, UK) and dissolved as 5, 5, and 100 mM stock solutions, respectively, in DMSO (maximal final concentration in aCSF was 0.036% v/v of DMSO and did not affected muscimol-evoked postsynaptic currents (muscimol-PSCs); change to 104.0 ± 2.3% of the baseline, $n = 6$, $P = 0.140$). 6-Cyano-7-nitroquinoxaline-2,3-dione (CNQX), DL-2-amino-5-phosphonopentanoic acid (DL-AP5), 2-(3-carboxypropyl)-3-amino-6-(4 methoxyphenyl)pyridazinium bromide (gabazine, SR-95531), tetrodotoxin citrate (TTX), and 1-(4,4-diphenyl-3-butenyl)-3-piperidinecarboxylic acid hydrochloride (SFK89976A) were obtained from Abcam Biochemicals (Cambridge, UK) and dissolved in water as 10, 50, 10, 1, and 100 mM, respectively. Muscimol was obtained from Sigma-Aldrich and dissolved as a 10-mM stock solution in NaOH (10 mM).

Electrophysiology

Visually guided whole-cell voltage-clamp recordings ($V_h = -70$ mV) were performed from CA1 neurons using a Carl Zeiss Axioskop 2FS upright microscope (Jena, Germany) equipped with a differential interference contrast-infrared (DIC-IR) CCD video camera (VX44, Till Photonics, Gräfelfing, Germany) and screen and recorded with an EPC-7 electrical amplifier (List Biologic, Campbell, CA, USA). Patch pipettes (4–9 MΩ) were pulled from borosilicate glass capillaries (1.5 mm outer diameter, 0.86 mm inner diameter, Harvard Apparatus, Holliston, MA, USA) with PC-10 Puller (Narishige Group, London, UK).

Whole-cell recordings of muscimol-PSCs were performed with an intracellular filling solution containing (in mM): 125 K-gluconate, 11 KCl, 0.1 $CaCl_2$, 2 $MgCl_2$, 1 EGTA, 10 HEPES, 2 MgATP, 0.3 NaGTP, 10 phosphocreatine, pH 7.3, adjusted with KOH (1 M), 280–290 mOsm; biocytin (Tocris Bioscience; 0.4%) was added in some experiments for post hoc analyses. Muscimol-PSCs were evoked through a micropipette (2–4 MΩ) containing muscimol ($GABA_AR$ agonist; 30 µM in aCSF) coupled to a pressure application system (Picopump PV820, World Precision Instruments, Stevenage, UK) and positioned close to the soma of the recorded cell. Single pulses of 10–15 ms and 6–8 psi were applied every 2 min.

Inhibitory postsynaptic currents (IPSCs), miniature IPSCs (mIPSCs), and tonic-ICs were recorded with a pipette solution containing (in mM): 125 CsCl, 8 NaCl, 1 $CaCl_2$, 10 EGTA, 10 HEPES, 10 glucose, 5 MgATP, 0.4 NaGTP, pH 7.2, adjusted with CsOH (50 wt% in H_2O), 280–290 mOsm; biocytin (0.4%) was added in some recordings for post hoc structural analyses. IPSCs were evoked as described elsewhere (Chevaleyre et al. 2007) with some alterations. Briefly, stimuli (0.067 Hz, 1–15 µA) were delivered via monopolar stimulation with a patch-type pipette filled with aCSF and positioned in *Stratum radiatum*, *S. oriens*, or *S. pyramidale*, 80–120 µm from the recorded cell. Recordings were performed in the continuous presence of *N*-methyl-D-aspartate (NMDA) and α-amino-3-hydroxy-5-methyl-4-isoxazolepropionic acid (AMPA)/kainate (KA) receptor antagonists (50 µM DL-AP5 and 10 µM CNQX, respectively).

The mIPSCs were recorded in the presence of NMDA (50 µM DL-AP5) and AMPA/KA (10 µM CNQX) receptor antagonists, as well as TTX (0.5 µM). The events were analyzed off-line using spontaneous event detection parameters of the Mini Analysis software (Synaptosoft, GA, USA).

For tonic-ICs, SFK89976A (GABA transporter (GAT)-1 inhibitor; 20 µM) and SNAP5114 (GAT-3 inhibitor; 20 µM) were added to the

aCSF. GABA (5 μM) also added where mentioned. SR95531 (gabazine, a $GABA_AR$ inhibitor; 100 μM) was fast applied using a DAD-12 Superfusion System (ALA Scientific Instruments, Farmingdale, NY, USA). The tonic current measurements were performed as described in Glykys and Mody (2007a). Briefly, the digitized recording acquired at 10 kHz (0.1 ms) was binned to 5 ms. Binned data were loaded with Prism Version 5.00 for Windows (GraphPad Software, La Jolla, CA, USA) and an all-point histogram was plotted for every 200 points (every 1 s) and smoothed by Savitzky–Golay algorithm to obtain the peak value. A Gaussian was fitted to the part of the distribution from a point 3 pA to the left of the peak value to the rightmost (most positive) value of the histogram distribution. The mean of the fitted Gaussian was considered to be the mean holding current. This process was repeated for the entire recording. For statistical purposes, the 20- to 30-s period before applying gabazine (in control or CPA conditions) was compared with the 10- to 15-s period in the presence of gabazine (100 μM) under the same drug conditions. For a given neuron, we obtained the magnitude of the tonic current by subtracting the tonic current before perfusing gabazine from that recorded in the presence of gabazine. Slices were incubated for 50 min at room temperature with CPA (30 nM) for test conditions and with DMSO (0.0006%, v/v; same concentration of solvent as in test conditions) for control conditions.

In all recordings, data were low-pass filtered using a 3- and 10-kHz three-pole Bessel filter of an EPC-7 amplifier, digitized at 5 kHz (for muscimol-PSC and IPSCs) or 10 kHz (for mIPSCs and tonic-IC) using a Digidata 1322A board, and registered by the Clampex software version 10.2 (Molecular Devices, Sunnyvale, CA, USA). Series resistance was not compensated during voltage-clamp recordings, but was regularly monitored throughout each experiment with a −5 mV, 50 ms pulse, and cells with >20% change in series resistance were excluded from the data. All membrane potential values given in this study were corrected for liquid junction potential.

Morphologic and Immunohistochemical Analysis

The procedures were identical to those described previously by Oren et al. (2009), with some alterations. Briefly, interneurons were filled with biocytin (0.4%) during whole-cell recordings (at least 30 min). Slices were fixed overnight at 4 °C in 4% paraformaldehyde in 0.1 M sodium phosphate buffer (PB), pH 7.42. During fixation, slices were kept between 2 mixed cellulose ester membrane filter papers (Millipore, Durham, UK) to minimize deformation. Next day, slices were washed thoroughly in 0.1 M PB and stored in PB with 0.05% sodium azide at 4 °C. The permeabilization was made by 3 washes of 10 min each in 50 mM Tris-buffered saline (TBS) with 0.3% Triton X-100 (TBS-X). Slices were mounted in gelatin, re-sectioned to 60–70 μm thick, and neurons were visualized streptavidin conjugated with AlexaFluor 488 (diluted 1 : 1000, Invitrogen, Eugene, OR, USA) or Cy3 (diluted 1 : 2000, Jackson ImmunoResearch Laboratories, Inc., USA) in TBS-X (5 h of incubation) and mounted in Vectashield (Vector Laboratories, Peterborough, UK) under coverslips. Visualized cells were studied under an epifluorescence microscope [see Oren et al. (2009)] and illustrations made from collapsed z-stack images obtained with a laser scanning confocal microscope (Zeiss LSM 510 META, Jena, Germany) and reconstructed with the ImageJ software (v1.43u, NIH, MD, USA; NeuronJ plugin).

Postsynaptic pyramidal cells were identified by their characterized structure with mushroom-like spiny spines on dendrites, and CB1R-positve cells by co-localization of positive CB1R reaction signal in the Biocytin/Streptavidin reaction-visualized axon (Katona et al. 1999; Pawelzik et al. 2002). Basket cells were identified by their characteristic axon arborization inside *S. pyramidale* [see Nissen et al. (2010)].

Free-floating 60- to 70-μm-thick sections were washed in 50 mM TBS-TX, blocked in 20% normal horse serum (NHS, Vector Laboratories) in TBS-TX, and incubated in primary antibody (CB1R Guinea pig antibody, diluted 1 : 1000, Frontier Science Co., Ltd, Japan) at 4 °C for 48 h. Fluorochrome-conjugated secondary antibodies [indocarbocyanine (Cy3) or indodicarbocyanine (Cy5); Jackson ImmunoResearch Laboratories, Inc., USA] were applied overnight at 4 °C. After another wash in TBS-TX, sections were mounted in Vectashield (Vector Laboratories) under coverslips. Immunoreactivity was evaluated at ×40 objective using a laser scanning confocal microscope (Zeiss LSM 510 META, Jena, Germany) with the LSM software. Micrographs were adjusted for brightness and contrast only. Immunoreactivity was declared negative when fluorescence was not detected in relevant parts of the cell in an area where similar parts of unfilled cells were immunopositive.

Immunoblot Assay

Hippocampal slices were prepared as described for electrophysiological recordings and incubated with CPA as described for tonic-ICs. After the incubation period, the tissue (12–14 slices per condition) was stored at −80 °C. Samples were sonicated in 1% NP-40 lysis buffer containing (in mM): 50 Tris–HCl (pH 7.5), 150 NaCl, 5 ethylenediamine tetra-acetic acid (EDTA), 2 dithiothreitol (DTT), SDS 0.1%, and protease inhibitors (Roche). The lysate was incubated on ice and then the supernatant was collected following centrifugation at 16000 × g for 10 min at 4 °C. Protein concentrations were determined using a commercial Bradford assay (Sigma, MO, USA). Total protein (100 μg) was loaded onto a 10% SDS polyacrylamide gel, subjected to gel electrophoresis, transferred to a PVDF membrane (GE Healthcare), blocked in 10% nonfat milk, and probed with an antibody specific for the $GABA_AR$ δ subunit (1 : 500, PhosphoSolutions 868-GDN). After washing (3 × 5 min in TBST [10 mM Tris, 150 mM NaCl, and 0.05% Tween 20 in H_2O]), blots were then incubated with secondary antibodies conjugated with horseradish peroxidase and bands were visualized with a commercial enhanced chemiluminescence detection method (ECL) kit (PerkinElmer Life Sciences, MA, USA). Values were normalized to glyceraldehyde-3-phosphate dehydrogenase (GAPDH) loading control, and the relative intensities were normalized to the control sample. Densitometry of the bands was performed using the ImageJ processing software (NIH, MD, USA).

Statistical Analysis

Data are expressed as the mean ± SEM of n cells from different slices (electrophysiological recordings) or n measurements from independent experiments (immunoblot assay). Statistical significance was either assessed by two-tailed Student's t-test, when comparing 2 groups, or by performing one-way ANOVA followed by Bonferroni's post hoc test for comparison between multiple experimental groups. A P-value of <0.05 was considered to account for significant differences. Analyses were conducted with the GraphPad Software.

Results

Adenosine A_1R Inhibits Agonist-Evoked $GABA_AR$-Mediated Currents in CA1 Pyramidal Cells

To investigate whether activation of adenosine A_1R influences $GABA_AR$-mediated responses in the postsynaptic neuron, we

performed whole-cell patch-clamp recordings ($V_h = -70$ mV). In a first set of experiments, a selective $GABA_AR$ agonist, muscimol (30 µM), was pressure applied close to the soma of the recorded CA1 pyramidal cell (Fig. 1*A*) eliciting postsynaptic currents (muscimol-PSCs) that were blocked by $GABA_AR$ antagonist gabazine (10 µM; Fig. 1*B*).

We found that the adenosine A_1R agonist CPA (30 nM, Moos et al. 1985) decreased muscimol-PSCs and the suppression reached a steady state within 40 min from wash-in of CPA (Fig. 1*B*). The amplitude of muscimol-PSCs was significantly reduced in 14 of 16 cells tested (effect showing a Gaussian distribution, Shapiro–Wilk test, $n = 16$), indicating consistency in pyramidal cells (average decrease to 62.1 ± 4.5% of the baseline, $n = 16$, $P < 0.001$, *t*-test; Fig. 1*B*,*C*). During CPA wash out, the suppression persisted for at least 40 min (Fig. 1*B*,*C*). Data from all tested pyramidal cells are plotted throughout the paper.

In a next set of experiments, we applied a high-affinity A_1R antagonist, DPCPX (100 nM, Sebastião et al. 1990), to revert the suppressive effect of CPA on GABAergic currents. This restored muscimol-PSCs in all cells (average to 96.2 ± 3.7% of the original baseline, $n = 7$, $P < 0.001$, *t*-test; Fig. 1*D*,*E*), demonstrating that the CPA effect on $GABA_AR$ currents is reversible. A lower concentration of CPA (10 nM) was also capable of decreasing amplitude of muscimol-PSCs significantly in 12 of 17 cells (Fig. 1*G*). In addition, CPA (30 nM) failed to change muscimol-PSCs when washed in the presence of A_1R antagonist DPCPX (100 nM; 103.7 ± 1.4% of the baseline, $n = 6$, $P = 0.17$, *t*-test; Fig. 1*G*). Interestingly, we found a significant increase in muscimol-PSCs following wash-in of

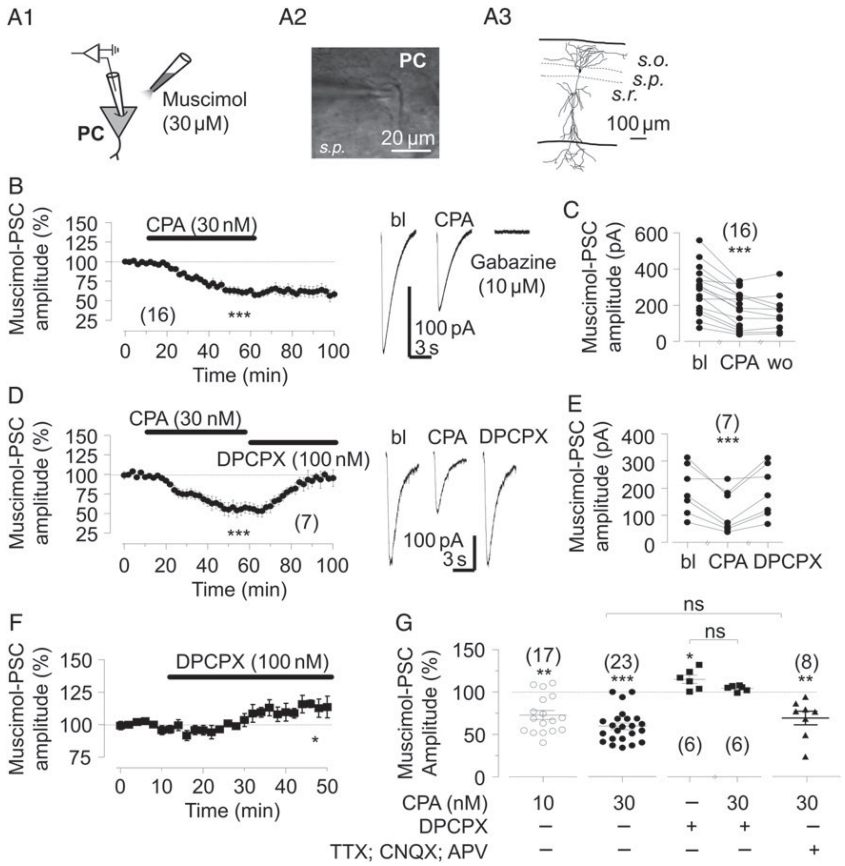

Figure 1. Adenosine A_1R suppresses local agonist-evoked $GABA_A$ currents in pyramidal cells. (*A*1) Schematic representation of the experimental design to evoke postsynaptic $GABA_A$ currents by local application of a $GABA_AR$ agonist, muscimol (30 µM, muscimol-PSC) on the soma of a voltage-clamped pyramidal cell. (*A*2) Differential interference contrast-infrared (DIC-IR) image. (*A*3) Illustration of a recorded pyramidal cell. (*B*) Left: A_1R agonist, CPA (30 nM) reduces the agonist-evoked $GABA_AR$ current amplitude (baseline-normalized mean ± SEM, $n = 16$); right: Representative PSCs from one cell in baseline (bl), in the presence of CPA and after application of gabazine (10 µM); each trace is the average of 5 consecutive responses. (*C*) Muscimol-PSC amplitude (pA) of all cells in *B*, in baseline (bl), following wash-in of CPA and after 30 min washout of CPA (wo). Values from each cell are connected with line. (*D*) Left: Wash-in of A_1R antagonist DPCPX (100 nM), fully restored CPA-inhibited muscimol-PSCs to the baseline level (baseline-normalized mean ± SEM, $n = 7$); right: Representative PSCs from one cell in the baseline (bl), in the presence on CPA and following further application of DPCPX; each trace is the average of 5 consecutive responses. (*E*) Muscimol-PSC amplitudes (in pA) of all cells in *D*, in baseline (bl), in the presence of CPA and following DPCPX application. Values from each cell are connected with line. (*F*) DPCPX (100 nM) had a facilitatory effect on muscimol-PSCs (baseline-normalized mean ± SEM, $n = 7$). (*G*) Plot showing baseline-normalized PSC amplitude in different conditions in all studied cells; from left: Effect of CPA (10 nM) after baseline; effect of CPA (30 nM) after baseline; effect of DPCPX (100 nM) after baseline; full prevention of CPA effect on PSC amplitude in the presence of DPCPX; CPA-induced suppression of $GABA_AR$ currents in the presence of glutamate blockers (CNQX, 10 µM; APV, 50 µM), and TTX (0.5 µM; mean ± SEM, baseline-normalized). In all panels, the number of experiments is shown in brackets; ns: not statistically significant; *$P < 0.05$; **$P < 0.01$; ***$P < 0.001$ (Student's *t*-test); PC: pyramidal cell; *s.r.*: *Stratum radiatum*; *s.p.*: *Stratum pyramidale*; *s.o.*: *Stratum oriens*.

DPCPX in naïve slices to 115.3 ± 4.9% of the baseline ($n = 6$, $P < 0.05$, *t*-test; Fig. 1*F*,*G*), which suggests tonically activated A_1R and suppression of $GABA_A$R-mediated currents in standard physiological conditions.

To confirm that the observed inhibitory action of adenosine A_1R on $GABA_A$R currents was not caused via an indirect effect on glutamatergic transmission or axonal GABAergic excitation (Alle and Geiger 2007; Ruiz et al. 2010), we reproduced the experiments in the continuous presence of NMDA and AMPA/KA receptor antagonists (50 μM DL-AP5 and 10 μM CNQX, respectively), and TTX (0.5 μM) to block action potential firing. Indeed, in these conditions, there was a similar suppression of muscimol-PSC by CPA (30 nM) as observed above (decrease in amplitude to 69.5 ± 8.0% of the baseline, $n = 8$, $P < 0.001$, *t*-test; Fig. 1*G*). Although previous studies have reported that GABAergic synapses may not be directly modulated by A_1R (Lambert and Teyler 1991), our results show suppression of agonist-evoked postsynaptic $GABA_A$R-mediated currents in pyramidal cells.

Phasic $GABA_A$R-Mediated Currents Are Not Affected by Adenosine A_1R in CA1 Pyramidal Cells

We next explored whether adenosine A_1R modulates $GABA_A$R-mediated IPSCs evoked by electrical afferent fiber stimulation. We stimulated in *S. radiatum* or *S. oriens* and recorded monosynaptic IPSCs in pyramidal cells in the presence of CNQX (10 μM) and DL-AP5 (50 μM). The IPSCs were fully blocked with gabazine (10 μM) at the end of experiment (Fig. 2*A*). We found that, in contrast to muscimol-PSCs, synaptic $GABA_A$R IPSCs were not significantly modulated by CPA (30 nM) (89.3 ± 6.4% of the baseline, $n = 9$, $P = 0.14$, *t*-test; Fig. 2*A*,*B*). We also studied in separate experiments GABAergic mIPSCs in the presence of CNQX (10 μM), DL-AP5 (50 μM), and TTX (0.5 μM). Wash-in of CPA (30 nM for at least 50 min) failed to change either mIPSC frequency (99.4 ± 2.2% of the baseline, $n = 13$, $P = 0.80$, *t*-test; Fig. 2*C*, *D*) or amplitude (100.1 ± 1.2% of the baseline, $n = 13$, $P = 0.96$, *t*-test; Fig. 2*C*,*E*), confirming a lack of modulation of synaptic IPSCs by A_1R.

Adenosine A_1R Suppresses Tonic GABAergic Currents in CA1 Pyramidal Cells

Next, we hypothesized that A_1R modulation could be selective to extrasynaptic $GABA_A$R and studied adenosine A_1R agonist effects on tonic-ICs in pyramidal cells. Glutamate receptor blockers (CNQX, 10 μM and DL-AP5, 50 μM) and TTX (0.5 μM) were added to the superfusion solution. In addition, to avoid any interference of adenosine receptors upon GAT activity (Cristóvão-Ferreira et al. 2009, 2013), which could indirectly affect tonic-ICs, the GABA transporters blockers, SFK89976A (20 μM; GAT-1 inhibitor) and SNAP5114 (20 μM; GAT-3 inhibitor), were also added to the superfusion solution. Tonic-IC was measured comparing the holding current before and in the presence of gabazine (100 μM; Fig. 3*A*,*B*; see Materials and Methods). Consistent with previous reports (Semyanov et al. 2003), pyramidal cells did not express measurable tonic $GABA_A$R-mediated conductance (−3.1 ± 1.1 pA, $n = 4$), unless the extracellular concentration of GABA was enhanced (Glykys and Mody 2007a) to increase the signal-to-noise ratio. Therefore, in the remaining experiments aiming to evaluate tonic-ICs in pyramidal cells, GABA (5 μM) was added to the superfusion solution. Under such conditions, tonic-ICs were easily visualized (Fig. 3). Interestingly, in the presence of CPA (30 nM, incubated for at least 50 min), tonic-ICs were significantly lower than in control slices (−119.7 ± 12.5 pA, $n = 8$, for control compared with −57.7 ± 14.8 pA, $n = 7$, for CPA, $P < 0.01$, *t*-test; Fig. 3*B*–*D*). These results, taken together with the absence of effect of CPA on afferent-evoked IPSCs and mIPSCs, allow to conclude that adenosine A_1R in pyramidal neurons selectively suppress tonic-ICs, known to be mediated by extra- and perisynaptically localized $GABA_A$R (Glykys and Mody 2007b).

Adenosine A_1R-Mediated Effect on $GABA_A$ Currents Is PKA/PKC-Dependent

Adenosine A_1R is Gi/o coupled (Freissmuth et al. 1991; Jockers et al. 1994; Nanoff et al. 1995) and involves signaling cascades that require PKA and in some cases, PKC (Akbar et al. 1994; Cascalheira and Sebastião 1998). $GABA_A$R-mediated currents are affected by activity of both PKA (Kano and Konnerth 1992; Kano et al. 1992; Moss et al. 1992; Robello et al. 1993; Nusser et al. 1999; Poisbeau et al. 1999) and PKC signaling pathways (Poisbeau et al. 1999; Brandon, Jovanovic, Smart, et al. 2002; Bright and Smart 2013). We tested whether activity of those kinases could be involved in A_1R suppression of tonic $GABA_A$R currents (Fig. 4*A*). The PKC or the PKA blockers (GF109203x, 1 μM, or Rp-cAMPs, 100 μM, respectively) were added intracellularly through the whole-cell patch-pipette filling solution. In either situation (intracellular inhibition of PKA or PKC), the effect of CPA (30 nM) on muscimol-PSC was blocked. Amplitude of muscimol-PSCs in the presence of CPA and GF109203x was 97.1 ± 4.3% ($n = 6$, $P = 0.53$, *t*-test; Fig. 4*B*,*C*) and in the presence of CPA and Rp-cAMPs 101.0 ± 4.0% ($n = 6$, $P = 0.80$, *t*-test; Fig. 4*B*,*C*) of the pre-CPA values. These results show the involvement of both kinases in A_1R modulation of GABAergic currents. We then asked if we could uncover a sequence of kinase activation cascade. We measured muscimol-PSC modulation when one of the signaling pathways was activated in the presence of a blocker of the other pathway. First, the adenylate cyclase (AC) activator, forskolin (5 μM, Seamon et al. 1981), was bath applied to activate cAMP/PKA signaling. Forskolin increased the amplitude of muscimol-PSC to 117.5 ± 4.4% of the baseline ($n = 4$, $P = 0.029$, *t*-test; Fig. 4*D*,*F*). The effect was similar to the blockade of A_1R in naïve slices with DCPCX (see Fig. 1*G*). Loading the patch pipette with the PKC inhibitor, GF109203x (1 μM), completely prevented forskolin effect on muscimol-PCSs (96.0 ± 4.1% of the baseline, $n = 5$, $P = 0.38$, *t*-test; Fig. 4*D*,*F*). These results suggest that PKA signaling is upstream of PKC in the $GABA_A$R current suppression cascade. To further test this idea, we washed-in an activator of PKC (phorbol 12,13 didecanoate, PDD, 250 nM). This suppressed muscimol-PSCs to 54.4 ± 4.8% of the baseline ($n = 4$, $P = 0.002$, *t*-test; Fig. 4*E*,*F*), akin to the generated by A_1R activation with CPA (see Fig. 1*B*,*C*). Adding a PKA inhibitor, Rp-cAMPs to the pipette filling solution, failed to prevent the suppression of muscimol-PSCs by PDD (60.5 ± 8.6% of the baseline; $n = 3$, $P = 0.04$, *t*-test; Fig. 4*E*,*F*). Altogether these results show that PKC is downstream to PKA activation in the $GABA_A$R current suppression cascade.

Knowing that $GABA_A$Rs are substrate for kinases and that PKC activity decreases extrasynaptic $GABA_A$R expression (Bright and Smart 2013), we decided to evaluate whether A_1R actions on tonic inhibition could be associated with decreased expression of $GABA_A$R. We performed immunoblot assays against the δ-subunit of $GABA_A$R, a subunit present exclusively in extra- and perisynaptic $GABA_A$Rs in the hippocampus (Nusser et al. 1998; Wei et al. 2003; Sun et al. 2004; Glykys et al. 2007), therefore most relevant for tonic-ICs. We found that, in slices that had been incubated with CPA (30 nM, for at least 50 min), $GABA_A$R δ-subunit immunoreactivity was significantly decreased to 68.5 ± 9.5%

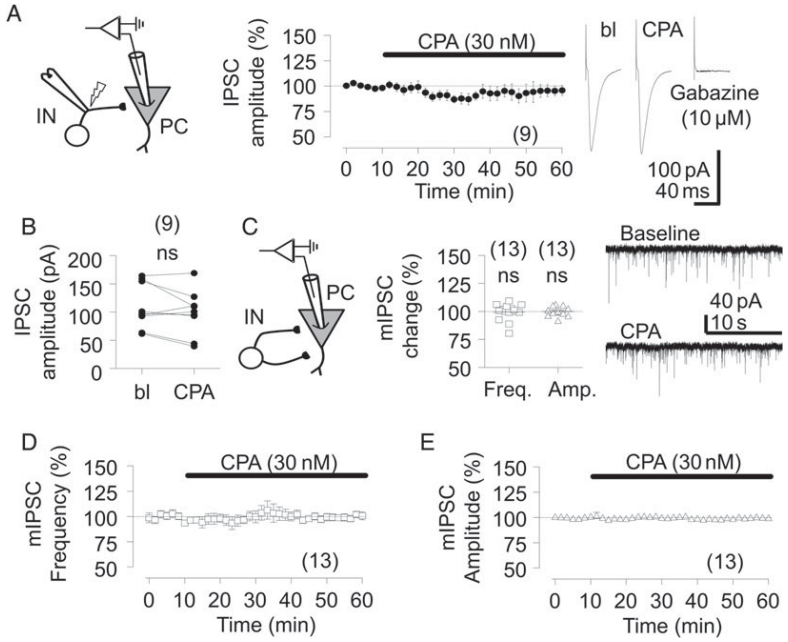

Figure 2. Synaptic $GABA_AR$ currents evoked by electrical afferent stimulation or spontaneous quantal release are not affected by A_1R. (*A*) Left: Schematic representation of the experimental design for IPSC recordings in pyramidal cells; middle: IPSCs evoked in CA1 pyramidal cells by electrical stimulation of inhibitory afferents are not modulated by CPA (30 nM; baseline-normalized mean ± SEM, $n = 9$); right: Representative IPSCs in baseline (bl) after wash-in of CPA and after gabazine (10 µM); each trace is the average of 10 consecutive responses. (*B*) IPSC amplitude (pA) in all cells during baseline (bl) and following wash-in of CPA; values from each cell are connected with line. (*C*) Left: Experimental design for mIPSC recordings in pyramidal cells; middle: mIPSC frequency and amplitude in individual cells (baseline-normalized; 100%: 9.6 ± 1.7 Hz and 11.8 ± 1.6 pA); right: Sample traces from one cell in baseline and following wash-in of CPA. (*D* and *E*) CPA has no significant effect on either miniature frequency (*D*) or amplitude (*E*) of mIPSCs (baseline-normalized mean ± SEM, $n = 13$). In all panels, the number of experiments is shown in brackets; ns: not statistically significant (Student's *t*-test); PC: pyramidal cell; IN: interneuron.

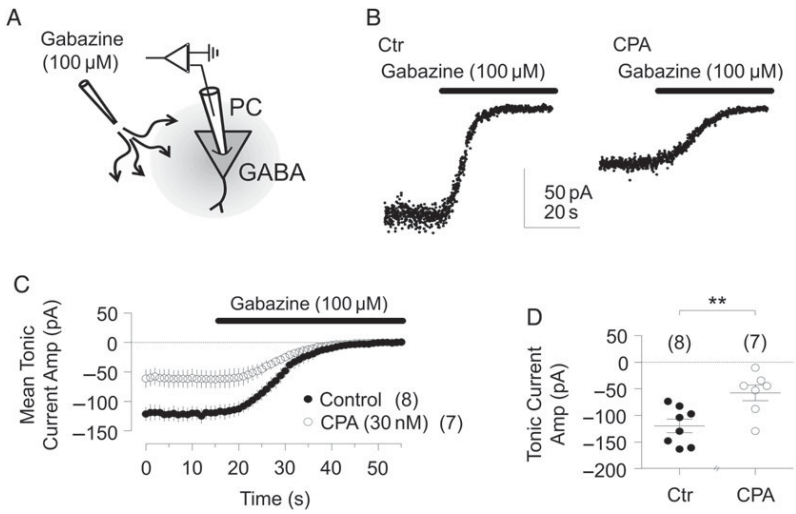

Figure 3. Tonic $GABA_AR$ currents in pyramidal cells are inhibited by adenosine A_1R activation. (*A*) Schematic representation of the experimental design used to access tonic currents; tonic $GABA_A$ inhibition (amplified by adding 5 µM ambient GABA; see Glykys and Mody 2007a) was revealed by application of gabazine (100 µM); the difference between the holding current in the absence and presence of gabazine being used as tonic current measurement (see Materials and Methods). (*B*) Tonic current (plotted at 5 ms intervals) recorded from an individual pyramidal cell in a control slice (left) and in a CPA (30 nM)-incubated slice (right). (*C*) Averaged tonic current (mean ± SEM, pA) recorded from pyramidal cells in control slices (filled circles, $n = 8$) and in slices where CPA (30 nM) was added at least 50 min prior gabazine (open circles; $n = 7$); note that tonic $GABA_A$ currents were quantitatively smaller in the presence of CPA. (*D*) Plot showing tonic $GABA_A$ current in all studied cells in control slices and in slices incubated with CPA. In all panels, the number of experiments is shown in brackets; $^{**}P < 0.01$ (Student's *t*-test); PC: pyramidal cell.

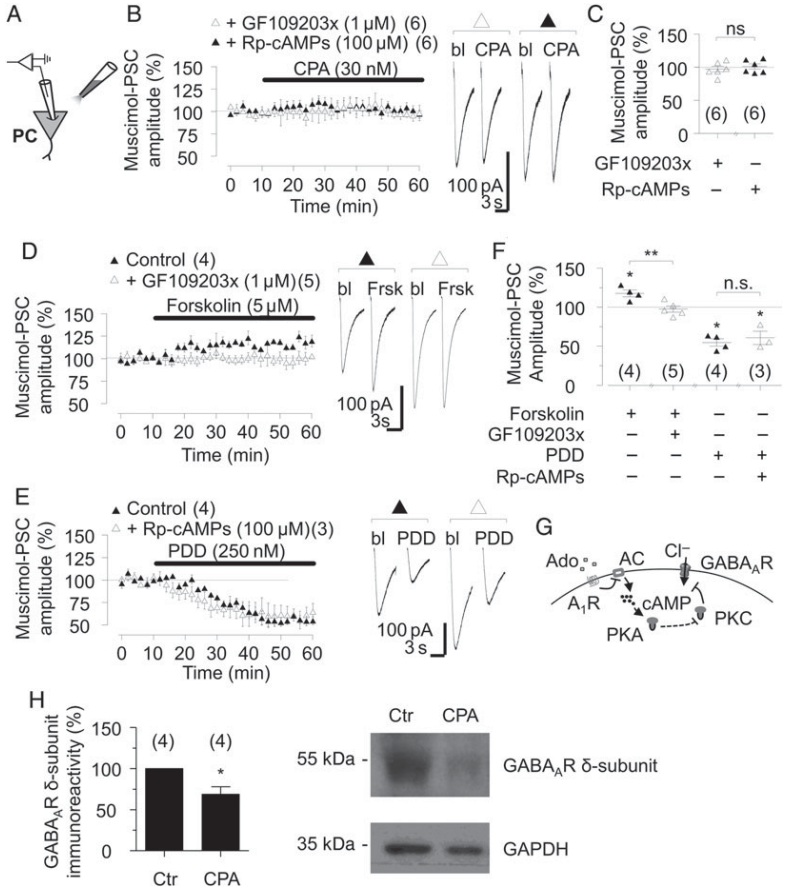

Figure 4. A_1R-mediated modulation of GABAergic responses involves both PKA and PKC signaling cascades and sustained A_1R activation results in decreased expression of $GABA_AR$ δ-subunit. (*A*) Schematic experimental design. (*B*) Left: Either a PKC inhibitor (GF109203x, 1 μM) or a PKA blocker (Rp-cAMPs, 100 μM) in pipette filling solution prevents suppression of GABAergic currents by CPA (30 nM; baseline-normalised mean ± SEM; $n = 6$ for both conditions). Right: Representative muscimol-PSCs in the presence of GF109203x (open triangle) or Rp-cAMPs (filled triangle) in baseline (bl) and following application of CPA. (*C*) Baseline-normalized muscimol-PSCs in all studied cells in the presence of either GF109203x or Rp-cAMP. (*D*) Left: Plot showing that intracellular application of GF109203x completely prevented the facilitatory effect of Forskolin (5 μM) on muscimol-PSCs (baseline-normalized mean ± SEM; $n = 4$–5 as indicated). Right: Representative muscimol-PSCs in one pyramidal cell in baseline (bl) and after Forskolin application (Frsk), in the absence (filled triangle) or presence (open triangle) of GF109203x. (*E*) Left: Plot showing that intracellular Rp-cAMPs failed to prevent a PKC activator PDD (250 nM)-elicited suppression of muscimol-PSCs (baseline-normalized mean ± SEM; $n = 3$–4 as indicated). Right: Representative muscimol-PSCs in baseline (bl) and after PPD perfusion, in the absence (filled triangle) or presence (open triangle) of intracellular Rp-cAMPs. (*F*) Baseline-normalized muscimol-PSC in all studied pyramidal cells shown in *D* and *E*. From left: Application of Forskolin after baseline; intracellular GF109203x with forskolin application of PDD after baseline; and intracellular Rp-cAMPs with forskolin. (*G*) Schematic diagram of suggested postsynaptic cascade of PKC and PKA action underlying A_1R-mediated inhibition of $GABA_AR$ currents. (*H*) Left: Plot showing control-normalized $GABA_AR$ δ-subunit immunoreactivity after incubation of hippocampal slices in the absence (control: Ctr) or presence of CPA (30 nM) for at least 50 min (see Materials and Methods for details). Right: Representative western blot obtained from control slices (left lane) and from slices treated with CPA (30 nM) for at least 50 min (right lane). GAPDH was used as a loading control (bottom lanes). In all panels, the number of experiments is shown in brackets; the representative PSCs correspond to the average of 5 consecutive responses; ns: not statistically significant; $^*P < 0.05$; $^{**}P < 0.01$ (Student's *t*-test); PC: pyramidal cell.

when compared with the control slices ($n = 4$, $P = 0.04$, paired *t*-test; Fig. 4*H*).

Taken together, these results demonstrate that A_1R actions upon GABAergic currents involve postsynaptic signaling requiring both PKA and PKC pathways and suggest that A_1R activation leads to inhibition of PKA signaling, releasing PKC activity which then suppresses $GABA_AR$ currents (Fig. 4G). Results from immunoblot assays fit this idea, suggesting that A_1R-mediated decrease in tonic inhibition is associated with decreased expression of extrasynaptic $GABA_AR$ δ-subunit.

Adenosine A_1R Suppresses Tonic $GABA_AR$ Currents in a Specific Subpopulation of Hippocampal Interneurons

Next, we investigated A_1R effects on $GABA_AR$ responses in hippocampal interneurons (Fig. 5*D*). We recorded muscimol-PSCs in CA1 area interneurons whose soma was located in *S. radiatum* or *S. oriens*. The interneuron population showed nonparametric distribution in response to CPA (30 nM; Shapiro–Wilk test, $n = 17$; Fig. 5A), and in fact we found 2 different populations of cells. A subset of interneurons showed a significant and robust

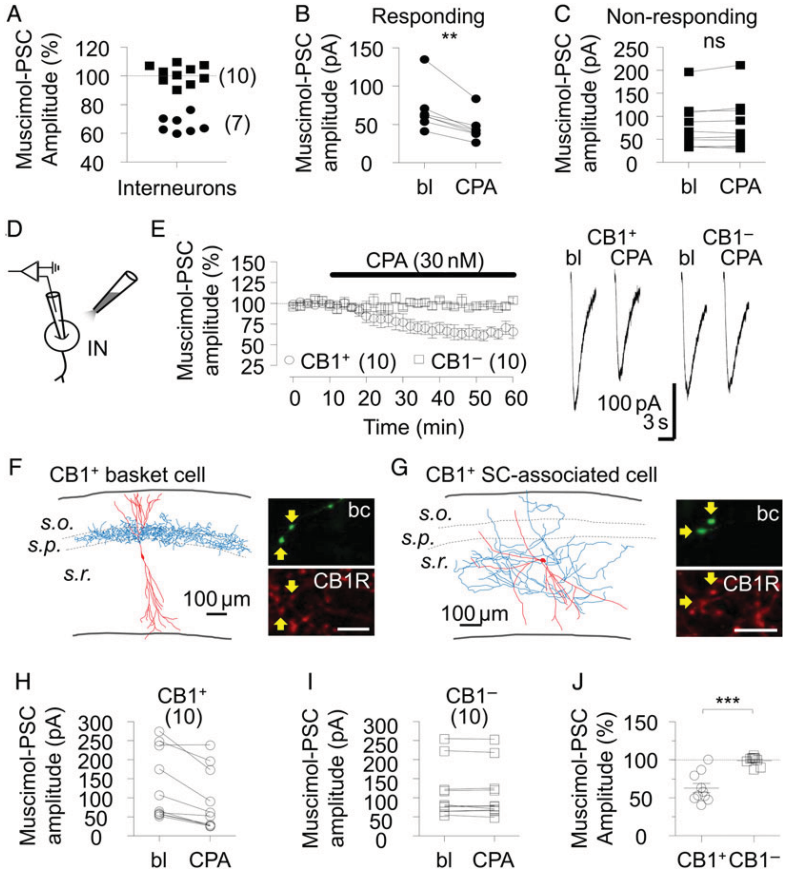

Figure 5. A_1R activation suppresses muscimol-evoked $GABA_A$ currents in interneurons expressing CB1R. (*A*) Circles: A_1R activation with CPA (30 nM) significantly depressed baseline-normalized muscimol-PSCs in 7 interneurons. Squares: 10 interneurons where CPA (30 nM) that failed to show an effect (baseline-normalized, *t*-test). (*B* and *C*) Muscimol-PSC amplitudes (in pA) of studied interneurons before (bl) and after CPA superfusion, where data from cells with significant suppression are shown in *B* and data from cells with no effect of CPA are shown in *C*; values from each cell are connected with line. (*D*) Schematic representation of the experimental design to record muscimol-PSCs from interneurons in all experiments illustrated in this figure. (*E*) CPA (30 nM) suppresses muscimol-PSCs in GABAergic interneurons expressing axonal CB1R ($CB1R^+$), but not in CB1-immunonegative interneurons ($CB1R^-$). Left: Baseline-normalized muscimol-PSCs (mean ± SEM) recorded for $CB1R^+$ ($n = 10$) and for $CB1R^-$ ($n = 10$) neurons. Right: Representative traces of muscimol-PSCs from one $CB1R^+$ and one $CB1R^-$ interneuron in baseline (bl) and in CPA. (*F* and *G*) Left: Reconstructed studied $CB1R^+$ basket cell (*E*) and Schaffer collateral (SC)-associated cell (*F*) (soma and dendrites in red; axon in blue); right: Confocal images showing positive axonal immunoreaction for CB1R (red, Cy3; scale bar corresponds to 5 µm) in Biocytin/Alexa-Streptavidin reaction-visualized axon (green, bc). Arrows show co-localization. (*H* and *I*) Muscimol-PSCs (in pA) of all $CB1R^+$ (H) and $CB1R^-$ interneurons (*I*) in baseline (bl) and in the presence of CPA; values from each cell are connected with line. (*J*) Baseline-normalized muscimol-PSCs recorded in the presence of CPA from $CB1R^+$ and $CB1R^-$ individual cells. In all panels, the number of experiments is shown in brackets; the representative current traces correspond to 5 consecutive responses; ns: not statistically significant; $^{**}P < 0.01$; $^{***}P < 0.001$ (Student's *t*-test); IN: interneuron; *s.r.*: *Stratum radiatum*; *s.p.*: *Stratum pyramidale*; *s.o.*: *Stratum oriens*.

suppression of muscimol-PSCs following CPA application (average reduction to 66.3 ± 2.2% of the baseline, $n = 7$, $P < 0.001$, *t*-test; Fig. 5*B*) similar to that observed in pyramidal cells (see Fig. 1*C*,*D*). In the remaining tested interneurons, muscimol-PSC was unchanged by CPA (amplitude 101.2 ± 2.0% of the baseline, $n = 10$, $P = 0.58$, *t*-test; Fig. 5*C*).

Aiming to identify the characteristics of the CPA responsive interneurons, we discovered that the A_1R effect on $GABA_AR$ currents correlated with the expression of a specific marker, axonal CB1R, in the studied cells. Recorded interneurons were filled with biocytin and visualized with streptavidin-fluorophore. All successfully visualized cells were tested in immunohistochemical reaction for axonal CB1R expression (Katona et al. 1999; Klausberger et al. 2005; Nissen et al. 2010). Importantly, we found that 9 of 10 cells responding to CPA in muscimol-PSCs were immunopositive for CB1R (CB1R-positive). In CB1R-positive interneurons, average muscimol-PSC inhibition by CPA was to 58.8 ± 5.0% of baseline responses ($n = 10$, $P < 0.001$, *t*-test; Fig. 5*E*,*H*,*J*). Analyses on the laminar distribution of CB1R-positive interneuron axon revealed basket cells ($n = 4$; Fig. 5*F*) and dendritic targeting Schaffer collateral-associated cells (Fig. 5*G*), indicating that $GABA_AR$ current modulation by A_1R occurs in various types of CB1R-positive interneurons (Somogyi and Klausberger 2005; Lee et al. 2010). Interestingly, the A_1R agonist (CPA, 30 nM) failed to significantly suppress muscimol-PSCs in any CB1R immunonegative (CB1R-negative) interneuron. Indeed, muscimol-PSCs in CB1R-negative interneurons were 99.0 ± 1.4% of the baseline ($n = 10$, $P = 0.60$, *t*-test; Fig. 5*E*,*I*,*J*) in

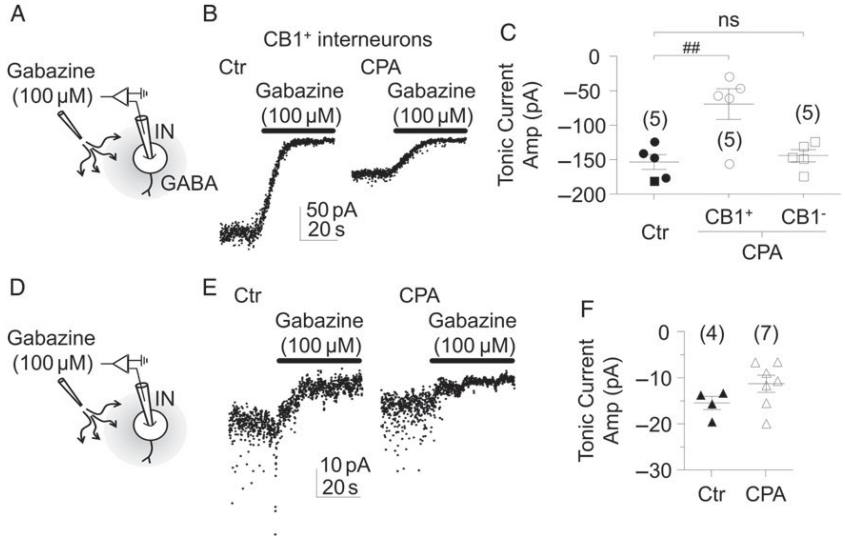

Figure 6. Tonic $GABA_AR$ currents in CB1R-immunoposivite interneurons are inhibited by adenosine A_1R activation. (*A*) Schematic representation of experimental design used to access tonic currents; ambient GABA [5 µM, see Glykys and Mody (2007a)] was added to aCSF and tonic-IC was revealed by application of gabazine (100 µM). (*B*) Representative tonic current (plotted at 5 ms intervals) recorded from a CB1R-positive interneuron in a control slice (left) and in a CPA (30 nM)-incubated slice (right). (*C*) Averaged tonic current (mean ± SEM, pA) recorded from interneurons (circles correspond to $CB1R^+$ interneurons; squares correspond to $CB1R^-$ interneurons) in control slices (filled symbols) and in slices where CPA (30 nM) was added at least 50 min prior gabazine (open symbols). (*D*) Schematic representation of the experimental design used to access endogenous tonic currents; no GABA was added to aCSF, tonic-IC was revealed by application of gabazine (100 µM). (*E*) Representative tonic current (plotted at 5 ms intervals) recorded from interneurons in control (left) and in a CPA (30 nM)-incubated slices (right). (*F*) Averaged tonic current (mean ± SEM, pA) recorded from interneurons in control slices (filled triangles, $n = 4$) and in slices where CPA (30 nM) was added at least 50 min prior gabazine (open triangles, $n = 7$). In all panels, the number of experiments is shown in brackets; $^{\#\#}P < 0.01$ (one-way ANOVA followed by Bonferroni's multiple comparison test); IN: interneuron.

the presence of CPA. This population of CB1R-negative neurons included 3 basket cells.

To directly assess A_1R-mediated actions on tonic inhibitory responses, we recorded tonic-IC in immuhistochemical-identified CB1R-positive and CB1R-negative interneurons. In the first set of experiments, to allow better comparison with results from pyramidal cells, GABA (5 µM) was added to the aCSF together with GABA transport blockers (SFK89976A, 20 µM and SNAP5114, 20 µM), glutamate receptor antagonists (CNQX, 10 µM and DL-AP5, 50 µM), and TTX (0.5 µM). In these experiments, averaged tonic-ICs recorded from interneurons in control slices were −153.3 ± 10.8 pA ($n = 5$). In slices incubated with CPA (30 nM for at least 50 min), tonic-ICs were significantly lower than control in 4 of 5 CB1R-positive interneurons (−47.9 ± 7.0 pA, $n = 4$, $P < 0.001$, *t*-test; Fig. 6*A–C*), but not in CB1R-negative interneurons (−144.1 ± 8.7 pA, $n = 5$, CB1R-negative in CPA, $P = 0.53$, *t*-test; Fig. 6*A*,*C*).

We then evaluated if adenosine A_1R could also affect tonic transmission in the presence of endogenous concentrations of GABA and recorded tonic-ICs in interneurons without supplying the aCSF with GABA. Contrary to what was observed for pyramidal cells, naïve interneurons showed a significant tonic-IC (−15.4 ± 1.4 pA, $n = 4$, Fig. 6*D–F*). Upon incubation with CPA, tonic-IC was clearly smaller in 5 of 7 anatomically identified interneurons (−8.8 ± 1.0 pA, $n = 5$, in CPA, $P < 0.05$, *t*-test; Fig. 6*D–F*).

Finally, we tested whether, similar to that observed in pyramidal cells, A_1R modulation of inhibitory currents in interneurons was restricted to extrasynaptic $GABA_AR$-mediated currents. We recorded electrical stimulation-evoked IPSCs in the CA1 area interneurons. Cells were visualized post hoc and tested for axonal CB1R immunoreaction. Similar to the results obtained with pyramidal cells, A_1R activation failed to significantly modulate IPSCs in either CB1R-positive (84.0 ± 5.7% of the baseline, $n = 3$, $P = 0.10$, *t*-test; Fig. 7*A–C*) or CB1R-negative (96.1 ± 3.6% of the baseline, $n = 11$, $P = 0.3$, *t*-test; Fig. 7*A–D*) interneurons, indicating a lack of modulation of phasic interneuron inhibition by A_1R.

Taken together, the above results show A_1R modulation of tonic $GABA_AR$ currents in a specific subpopulation of GABAergic interneurons expressing axonal CB1Rs.

Discussion

The results show that adenosine A_1R selectively modulates tonic $GABA_AR$ currents generated by extrasynaptic receptors, but has no effect on phasic synaptic $GABA_AR$ currents. The modulation is consistent with CA1 pyramidal cells, but present only in a specific population of postsynaptic CA1 GABAergic inhibitory interneurons with axonal CB1R. A_1R-mediated modulation requires intracellular PKA/PKC signaling. Sustained A_1R activity results in a decreased expression of $GABA_AR$ δ-subunit, a key component of extrasynaptic receptors mediating tonic $GABA_AR$ currents [see Farrant and Nusser (2005)].

Adenosine has a broad spectrum of modulatory actions in the brain. Through A_1R, it acts as an anticonvulsant agent with neuroprotective effects (Sebastião and Ribeiro 2009; Boison 2012). These actions are partly based on suppression of glutamatergic transmission either by presynaptically reducing calcium influx (Scanziani et al. 1992; Yawo and Chuhma 1993) and neurotransmitter release (Schubert et al. 1986; Proctor and Dunwiddie 1987; Barrie and Nicholls 1993) or postsynaptically facilitating potassium currents (Gerber et al. 1989; Thompson et al. 1992) and inhibiting ionotropic glutamatergic receptors (de Mendonça et al.

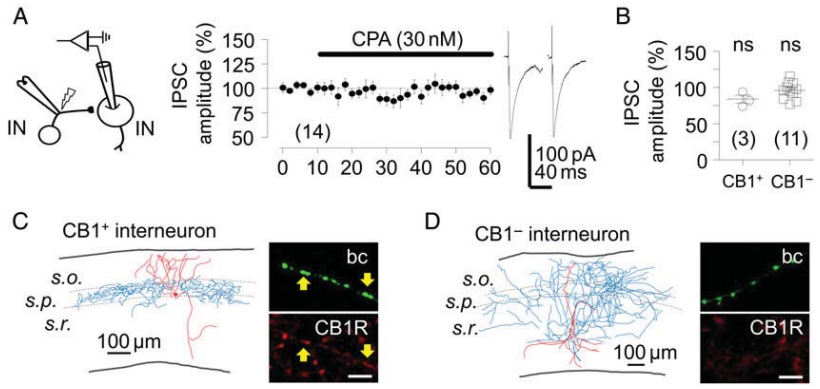

Figure 7. Phasic synaptic IPSCs in interneurons are not suppressed by adenosine A_1R. (*A*) Left: Schematic experimental design to record IPSCs from interneurons; middle: Time course plot showing that synaptic IPSCs evoked by electrical stimulation were not altered by CPA; right: Representative IPSC recorded from one CB1R$^+$ interneuron in baseline (bl) and in the presence of CPA; each trace corresponds to the average of 10 consecutive responses. (*B*) Baseline-normalized IPSCs recorded in the presence of CPA from all individual cells studied and tested for CB1R immunoreactivity; note that IPSCs were not affected by CPA, either in CB1R$^+$ or CB1R$^-$ interneurons. (*C* and *D*) Left: Reconstructed studied CB1R$^+$ (*C*) and CB1R$^-$ (*D*) interneurons (soma and dendrites in red; axons in blue); right: Confocal images of positive (*C*) and negative (*D*) CB1R immunoreaction (red, Cy3, scale bar corresponds to 5 µm) in Biocytin/Alexa-Sterptavidin reaction (green, bc). Arrows point at co-staining. In all panels, the number of experiments is shown in brackets; ns: not statistically significant (Student's t-test); IN: interneuron; *s.r.*: *Stratum radiatum*; *s.p.*: *Stratum pyramidale*; *s.o.*: *Stratum oriens*.

1995; Li and Henry 2000). Thus, the effect of adenosine via A_1R on glutamatergic transmission is well known. A role of adenosine in regulation of inhibitory GABAergic transmission has received much less attention and is much less investigated. This is surprising because already in early 90s, it was demonstrated that adenosine strongly modulates dysynaptic inhibition in the hippocampus, although it has no direct effect on GABAergic synapses to pyramidal cells (Kamiya 1991; Lambert and Teyler 1991; Yoon and Rothman 1991; Thompson et al. 1992).

During the past 2 decades, tonic $GABA_A$R-mediated inhibition has been described in neurons in the hippocampus and in many other brain areas [for review see Semyanov et al. (2004); Farrant and Nusser (2005); Glykys and Mody (2007b)]. Tonic $GABA_A$R-mediated membrane conductance plays a role in regulation of synaptic integration, input to output signal transformation, and firing rate of individual neurons and ultimately overall excitability of the hippocampus (Hamann et al. 2002; Mitchell and Silver 2003; Semyanov et al. 2003; Bright et al. 2007; Rothman et al. 2009). Deregulation of tonic inhibition has also been implicated in pathophysiological conditions including schizophrenia (Damgaard et al. 2011; Gill et al. 2011; Hines et al. 2012), stroke (Clarkson et al. 2010), and epilepsy (Dibbens et al. 2004; Peng et al. 2004; Naylor et al. 2005; Scimemi et al. 2005; Feng et al. 2006; Zhang et al. 2007). This makes tonic GABAergic responses an important target to modulation via endogenous or exogenous drugs. Indeed, neuroactive steroids, ethanol, and some anticonvulsant drugs act on extrasynaptic $GABA_A$R and modulate tonic GABAergic conductance (Stell et al. 2003; Cope et al. 2005; Ferando and Mody 2012). Interestingly, $GABA_A$R responsible for tonic currents and postsynaptic adenosine A_1R mainly locate in extra- and perisynaptic areas (Rivkees et al. 1995; Swanson et al. 1995; Ochiishi et al. 1999; Glykys and Mody 2007a), which makes them potential candidates to interact. This idea is further supported by A_1R coupling to Gi/o signaling pathways since $GABA_A$R is strongly modulated by PKA- and PKC-mediated phosphorylation (Kano and Konnerth 1992; Kano et al. 1992; Moss et al. 1992; Robello et al. 1993; Nusser et al. 1999; Poisbeau et al. 1999; Brandon, Jovanovic, Smart, et al. 2002; Bright and Smart 2013). We evaluated this possibility by recording afferent-evoked synaptic IPSCs and agonist-evoked $GABA_A$R currents in hippocampal neurons. These 2 ways to generate postsynaptic GABAergic currents allowed us to discriminate responses mediated by synaptic and extrasynaptic $GABA_A$R. Local application of muscimol (a selective $GABA_A$R agonist) through a micropipette positioned close to the recorded cell soma predominantly activates extrasynaptic $GABA_A$R, which are prominent in the perisomatic postsynaptic area (Kasugai et al. 2010). Accordingly, the resulting muscimol-PSC exhibited slow current kinetics characteristic of extrasynaptic $GABA_A$R-mediated responses (Pearce 1993; Banks et al. 1998; Banks and Pearce 2000). As we here report, in all studied pyramidal cells and in a subpopulation of interneurons, the muscimol-evoked $GABA_A$R currents were inhibited by the A_1R agonist. In contrast, the A_1R agonist failed to change phasic synaptic $GABA_A$R currents generated either by quantal release or by afferent stimulation [see also Kamiya (1991); Lambert and Teyler (1991); Yoon and Rothman (1991); Thompson et al. 1992]. Such selective modulation of tonic $GABA_A$R signaling might be important in controlling neuronal synchronization (Maex and De Schutter 1998; Glykys and Mody 2007b). Our data on the facilitation of muscimol-PSCs by the A_1R antagonist in naïve slices demonstrate that endogenous adenosine can tonically suppress extrasynaptic $GABA_A$R conductance. Because adenosine is paracrinally released from neurons and astrocytes (Boison 2006; Haydon and Carmignoto 2006), changes in ambient levels of endogenous adenosine are likely to occur and, therefore, tune peri- and extrasynaptic $GABA_A$R activity. Interestingly, when compared with glutamatergic neurons, interneurons are easily disconnected by hypoxia due to A_1R activation (Khazipov et al. 1995), an indication that adenosine release onto GABAergic neurons is higher.

Many signaling mechanisms are involved in the modulation of $GABA_A$R that are relevant to both phasic and tonic inhibition. Various protein kinases phosphorylate serine residues of $GABA_A$R subunits (Brandon, Jovanovic, and Moss 2002), including PKA and PKC phosphorylation mechanism (Moss et al. 1995; Brandon et al. 2001; Brandon, Jovanovic, Smart, et al. 2002). Adenosine A_1Rs are coupled to Gi/o proteins (Freissmuth et al. 1991; Jockers et al. 1994; Nanoff et al. 1995), but also affect phospholipase C and phosphoinositol-3-kinase activity (Akbar et al. 1994; Dickenson and Hill 1998; Schulte and Fredholm 2000; Cascalheira and

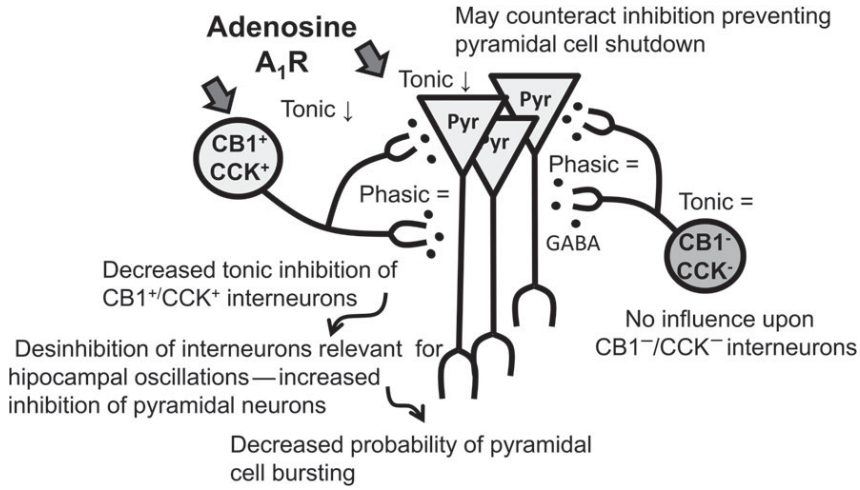

Figure 8. Schematic representation of the A_1R-mediated actions upon GABAergic transmission into CA1 hippocampal pyramidal cells and interneurons.

Sebastião 1998; Cascalheira et al. 2002). We found that PKA and PKC signaling cascades were responsible for A_1R-mediated inhibition of tonic $GABA_A$ currents. The results also indicated that A_1R-mediated inhibition of AC activity relieves a negative regulation of PKA over PKC. Disinhibition of PKC then promotes suppression of tonic $GABA_A$ currents in hippocampal neurons (see Fig. 4G). PKC-mediated phosphorylation of extrasynaptic $GABA_AR$ in the hippocampus causes a decrease in their expression level and function (Bright and Smart 2013). Accordingly, we detected that, upon incubation with an A_1R agonist, there is a decrease in the expression of a marker of extrasynaptic $GABA_AR$.

All tested pyramidal cells were sensitive to A_1R-mediated modulation of tonic GABAergic currents, somehow contrasting what occurs in pyramidal neurons from the somatosensory cortex, which are heterogeneous for the sensitivity to postsynaptic A_1R-mediated modulation (van Aerde et al. 2013). Among the interneurons, we show that those that exhibit modulation of tonic $GABA_A$ currents by A_1R are also immunopositive for CB1R, whereas CB1R-negative interneurons are insensitive to A_1R activation. Similar to the pyramidal neurons, A_1R-mediated suppression of GABAergic responses in interneurons was significant only for tonic $GABA_A$ currents. In the hippocampus, axonal expression of CB1R strongly correlates with expression of cholecystokinin (CCK) in interneurons (Katona et al. 1999). The modulation of tonic $GABA_AR$ allows regulation of excitability and signaling through these interneurons (Mitchell and Silver 2003). In fact, low concentration of picrotoxin (1 μM), aimed to predominantly inhibit tonic currents in interneurons, increases spontaneous output from GABAergic cells to pyramidal cells, seen as the increased frequency of spontaneous IPSCs (Semyanov et al. 2003). Discharge of interneurons expressing CCK is coupled to coordinated oscillatory activities in hippocampus in vivo (Klausberger and Somogyi 2008). Firing of hippocampal CCK-positive inhibitory neurons is coupled to synchronous network oscillations in theta (4–8 Hz) and gamma (30–80 Hz) rhythms, which occur during cognitive processes in the hippocampus (Klausberger et al. 2005; Tukker et al. 2007; Lasztóczi et al. 2011). Controlling excitability and discharge by robust tonic $GABA_AR$ conductance in these neurons (Pietersen et al. 2009; Oke et al. 2010; Schulz et al. 2012) could allow adenosine A_1R modulation of hippocampal rhythm generation and information processing associated with coordinated rhythmic activities.

Adenosine A_1R actions decrease hippocampal excitability, and hence adenosine is a suitable endogenous anticonvulsant compound (Boison 2012; Dias et al. 2013). Most documented actions of A_1R as an anticonvulsant substance rely on its ability to refrain glutamatergic transmission (Khan et al. 2001; Boison 2012). Here, we demonstrate a direct suppression of tonic GABAergic inhibition by A_1R in inhibitory interneurons, therefore highlighting another target for A_1R-mediated neuromodulation and excitability control. The resulting reduction in the disinhibition of interneurons caused by A_1R-mediated suppression of tonic GABAergic inhibition can increase inhibitory GABAergic output to the hippocampal principal cell population. In parallel, adenosine A_1R also reduce tonic GABAergic inhibition in pyramidal cells. However, in low ambient GABA levels, tonic $GABA_AR$ inhibition is likely to be more pronounced in interneurons than in pyramidal cells (Bai et al. 2001; Semyanov et al. 2003). Therefore, the net effect of A_1R-mediated modulation of tonic $GABA_AR$ on hippocampal pyramidal cell excitability may depend on ambient GABA concentrations as well as other conditions that control extrasynaptic $GABA_AR$ activation levels in the 2 cell populations (Scimemi et al. 2005; Wlodarczyk et al. 2013). (see Fig. 8).

Ambient GABA and adenosine levels are dynamic in the brain and both are increased during episodes of epileptiform activity (Chin et al. 1995; Berman et al. 2000; Pavlov and Walker 2013). Decreasing tonic $GABA_AR$ conductance in pyramidal cells during high ambient GABA levels should increase pyramidal cell excitability. However, during epileptiform discharges when ambient GABA concentrations reach peak, $GABA_AR$ currents can turn to depolarizing and excitatory (Köhling et al. 2000; Cohen et al. 2002; Ellender et al. 2014). This means that A_1R-mediated suppression of tonic $GABA_AR$ conductance in pyramidal cells can also have an antiepileptic effect (Ilie et al. 2012). In contrast, adenosine A_{2A} and A_3 receptors may promote excitability in epileptic tissues by exacerbating use-dependent run-down of phasic $GABA_A$ currents (Roseti et al. 2009). These opposite actions of adenosine receptors are particularly relevant when planning adenosine-mediated therapies in pathological conditions such as epilepsy.

In conclusion, we here propose that adenosine A_1Rs, by changing the inhibitory tonus of neurons without affecting phasic inhibitory synaptic transmission, can homeostatically regulate inhibition and control neuronal gain without disrupting fidelity of synaptic GABAergic inhibition (Pouille and Scanziani 2001; Lamsa et al. 2005). Its selectivity to specific interneuron populations may confer to adenosine an important modulatory action on hippocampal network oscillations that are the critical bases for hippocampal-dependent behavior and cognitive processes.

Funding

This work was supported by Fundação para a Ciência e Tecnologia (FCT), Portugal fellowships (to D.M.R.—SFRH/BD/60386/2009 and R.B.D.—SFRH/BPD/89057/2012), and project grant (PTDC/SAU-NMC/110838/2009 to D.M.R., R.B.D., J.A.R., and A.M.S. and EXPL/bim-mec/0009/2013 to D.M.R., R.B.D., S.T.D., J.A.R., and A.M.S.); Faculdade de Medicina, Universidade de Lisboa (to D.M.R., R.B.D., J.A.R., and A.M.S.); the Medical Research Council UK (to K.P.L.); the John Fell OUP Research Fund (to K.P.L.), and the Department of Pharmacology University of Oxford (to K.P.L.). S.T.D. integrates the Portuguese Program for Advanced Medical Education, sponsored by Fundação Calouste Gulbenkian and FCT (SFRH/BDINT/51548/2011).

Notes

We acknowledge Dr Wiebke Nissen and Kathryn Newton from the Department of Pharmacology, University of Oxford, for all support with the immunohistochemistry of interneurons. *Conflict of Interest*: None declared.

References

Akbar M, Okajima F, Tomura H, Shimegi S, Kondo Y. 1994. A single species of A_1 adenosine receptor expressed in Chinese hamster ovary cells not only inhibits cAMP accumulation but also stimulates phospholipase C and arachidonate release. Mol Pharmacol. 45:1036–1042.

Alle H, Geiger JRP. 2007. GABAergic spill-over transmission onto hippocampal mossy fiber boutons. J Neurosci. 27:942–950.

Bai D, Zhu G, Pennefather P, Jackson MF, MacDonald JF, Orser BA. 2001. Distinct functional and pharmacological properties of tonic and quantal inhibitory postsynaptic currents mediated by gamma-aminobutyric acid(A) receptors in hippocampal neurons. Mol Pharmacol. 59:814–824.

Banks MI, Li TB, Pearce RA. 1998. The synaptic basis of $GABA_{A,slow}$. J Neurosci. 18:1305–1317.

Banks MI, Pearce RA. 2000. Kinetic differences between synaptic and extrasynaptic GABA(A) receptors in CA1 pyramidal cells. J Neurosci. 20:937–948.

Barrie AP, Nicholls DG. 1993. Adenosine A_1 receptor inhibition of glutamate exocytosis and protein kinase C-mediated decoupling. J Neurochem. 60:1081–1086.

Berman RF, Fredholm BB, Aden U, O'Connor WT. 2000. Evidence for increased dorsal hippocampal adenosine release and metabolism during pharmacologically induced seizures in rats. Brain Res. 872:44–53.

Bianchi MT, Macdonald RL. 2003. Neurosteroids shift partial agonist activation of GABA(A) receptor channels from low- to high-efficacy gating patterns. J Neurosci. 23:10934–10943.

Boison D. 2012. Adenosine dysfunction in epilepsy. Glia. 60:1234–1243.

Boison D. 2006. Adenosine kinase, epilepsy and stroke: mechanisms and therapies. Trends Pharmacol Sci. 27:652–658.

Brandon NJ, Delmas P, Hill J, Smart TG, Moss SJ. 2001. Constitutive tyrosine phosphorylation of the GABA(A) receptor gamma 2 subunit in rat brain. Neuropharmacology. 41:745–752.

Brandon N, Jovanovic J, Moss S. 2002. Multiple roles of protein kinases in the modulation of gamma-aminobutyric acid(A) receptor function and cell surface expression. Pharmacol Ther. 94:113–122.

Brandon NJ, Jovanovic JN, Smart TG, Moss SJ. 2002. Receptor for activated C kinase-1 facilitates protein kinase C-dependent phosphorylation and functional modulation of GABA(A) receptors with the activation of G-protein-coupled receptors. J Neurosci. 22:6353–6361.

Brickley SG, Cull-Candy SG, Farrant M. 1996. Development of a tonic form of synaptic inhibition in rat cerebellar granule cells resulting from persistent activation of $GABA_A$ receptors. J Physiol. 497:753–759.

Bright DP, Aller MI, Brickley SG. 2007. Synaptic release generates a tonic GABA(A) receptor-mediated conductance that modulates burst precision in thalamic relay neurons. J Neurosci. 27:2560–2569.

Bright DP, Smart TG. 2013. Protein kinase C regulates tonic GABA (A) receptor-mediated inhibition in the hippocampus and thalamus. Eur J Neurosci. 38:3408–3423.

Burke SP, Nadler JV. 1988. Regulation of glutamate and aspartate release from slices of the hippocampal CA1 area: effects of adenosine and baclofen. J Neurochem. 51:1541–1551.

Caraiscos VB, Elliott EM, You-Ten KE, Cheng VY, Belelli D, Newell JG, Jackson MF, Lambert JJ, Rosahl TW, Wafford KA, et al. 2004. Tonic inhibition in mouse hippocampal CA1 pyramidal neurons is mediated by alpha5 subunit-containing gamma-aminobutyric acid type A receptors. Proc Natl Acad Sci USA. 101:3662–3667.

Cascalheira JF, Sebastião AM. 1998. Adenosine A_1 receptor activation inhibits basal accumulation of inositol phosphates in rat hippocampus. Pharmacol Toxicol. 82:189–192.

Cascalheira JF, Sebastião AM, Ribeiro JA. 2002. Pertussis toxin-sensitive G proteins mediate the inhibition of basal phosphoinositide metabolism caused by adenosine A_1 receptors in rat hippocampal slices. Neurochem Res. 27:1707–1711.

Chevaleyre V, Heifets BD, Kaeser PS, Südhof TC, Purpura DP, Castillo PE. 2007. Endocannabinoid-mediated long-term plasticity requires cAMP/PKA signaling and RIM1alpha. Neuron. 54:801–812.

Chin JH, Wiesner JB, Fujitaki J. 1995. Increase in adenosine metabolites in human cerebrospinal fluid after status epilepticus. J Neurol Neurosurg Psychiatry. 58:513–514.

Clarkson AN, Huang BS, Macisaac SE, Mody I, Carmichael ST. 2010. Reducing excessive GABA-mediated tonic inhibition promotes functional recovery after stroke. Nature. 468:305–309.

Cohen I, Navarro V, Clemenceau S, Baulac M, Miles R. 2002. On the origin of interictal activity in human temporal lobe epilepsy in vitro. Science. 298:1418–1421.

Cope DW, Hughes SW, Crunelli V. 2005. $GABA_A$ receptor-mediated tonic inhibition in thalamic neurons. J Neurosci. 25:11553–11563.

Cristóvão-Ferreira S, Navarro G, Brugarolas M, Pérez-Capote K, Vaz SH, Fattorini G, Conti F, Lluis C, Ribeiro JA, McCormick PJ, et al. 2013. A1R-A2AR heteromers coupled to Gs and G i/0 proteins modulate GABA transport into astrocytes. Purinergic Signal. 9:433–449.

Cristóvão-Ferreira S, Vaz SH, Ribeiro JA, Sebastião AM. 2009. Adenosine A2A receptors enhance GABA transport into

nerve terminals by restraining PKC inhibition of GAT-1. J Neurochem. 109:336–347.

Cunha RA, Ribeiro JA. 2000. Purinergic modulation of [(3)H] GABA release from rat hippocampal nerve terminals. Neuropharmacology. 39:1156–1167.

Damgaard T, Plath N, Neill JC, Hansen SL. 2011. Extrasynaptic $GABA_A$ receptor activation reverses recognition memory deficits in an animal model of schizophrenia. Psychopharmacology (Berl). 214:403–413.

De Mendonça A, Sebastião AM, Ribeiro JA. 1995. Inhibition of NMDA receptor-mediated currents in isolated rat hippocampal neurones by adenosine A_1 receptor activation. Neuroreport. 6:1097–1100.

Dias RB, Ribeiro JA, Sebastião AM. 2012. Enhancement of AMPA currents and GluR1 membrane expression through PKA-coupled adenosine A(2A) receptors. Hippocampus. 22:276–291.

Dias RB, Rombo DM, Ribeiro JA, Henley JM, Sebastião AM. 2013. Adenosine: setting the stage for plasticity. Trends Neurosci. 36:248–257.

Dibbens LM, Feng H-J, Richards MC, Harkin La, Hodgson BL, Scott D, Jenkins M, Petrou S, Sutherland GR, Scheffer IE, et al. 2004. GABRD encoding a protein for extra- or peri-synaptic $GABA_A$ receptors is a susceptibility locus for generalized epilepsies. Hum Mol Genet. 13:1315–1319.

Dickenson JM, Hill SJ. 1998. Involvement of G-protein betagamma subunits in coupling the adenosine A_1 receptor to phospholipase C in transfected CHO cells. Eur J Pharmacol. 355:85–93.

Duguid I, Branco T, London M, Chadderton P, Häusser M. 2012. Tonic inhibition enhances fidelity of sensory information transmission in the cerebellar cortex. J Neurosci. 32:11132–11143.

Ellender TJ, Raimondo JV, Irkle A, Lamsa K, Akerman CJ. 2014. Excitatory effects of parvalbumin-expressing interneurons maintain hippocampal epileptiform activity via synchronous afterdischarges. J Neurosci. 34:15208–15222.

Farrant M, Nusser Z. 2005. Variations on an inhibitory theme: phasic and tonic activation of GABA(A) receptors. Nat Rev Neurosci. 6:215–229.

Feng H-J, Kang J-Q, Song L, Dibbens L, Mulley J, Macdonald RL. 2006. Delta subunit susceptibility variants E177A and R220H associated with complex epilepsy alter channel gating and surface expression of alpha4beta2delta $GABA_A$ receptors. J Neurosci. 26:1499–1506.

Ferando I, Mody I. 2012. $GABA_A$ receptor modulation by neurosteroids in models of temporal lobe epilepsies. Epilepsia. 53 (Suppl 9):89–101.

Freissmuth M, Schütz W, Linder ME. 1991. Interactions of the bovine brain A_1-adenosine receptor with recombinant G protein alpha-subunits. Selectivity for rGi alpha-3. J Biol Chem. 266:17778–17783.

Gerber U, Greene RW, Haas HL, Stevens DR. 1989. Characterization of inhibition mediated by adenosine in the hippocampus of the rat in vitro. J Physiol. 417:567–578.

Gill KM, Lodge DJ, Cook JM, Aras S, Grace AA. 2011. A novel α5GABA(A)R-positive allosteric modulator reverses hyperactivation of the dopamine system in the MAM model of schizophrenia. Neuropsychopharmacology. 36:1903–1911.

Glykys J, Mody I. 2007b. Activation of GABAA receptors: views from outside the synaptic cleft. Neuron. 56:763–770.

Glykys J, Mody I. 2007a. The main source of ambient GABA responsible for tonic inhibition in the mouse hippocampus. J Physiol. 582:1163–1178.

Glykys J, Peng Z, Chandra D, Homanics GE, Houser CR, Mody I. 2007. A new naturally occurring GABA(A) receptor subunit partnership with high sensitivity to ethanol. Nat Neurosci. 10:40–48.

Haas KF, Macdonald RL. 1999. $GABA_A$ receptor subunit gamma2 and delta subtypes confer unique kinetic properties on recombinant $GABA_A$ receptor currents in mouse fibroblasts. J Physiol. 514:27–45.

Hamann M, Rossi DJ, Attwell D. 2002. Tonic and spillover inhibition of granule cells control information flow through cerebellar cortex. Neuron. 33:625–633.

Haydon PG, Carmignoto G. 2006. Astrocyte control of synaptic transmission and neurovascular coupling. Physiol Rev. 86: 1009–1031.

Hines RM, Davies PA, Moss SJ, Maguire J. 2012. Functional regulation of $GABA_A$ receptors in nervous system pathologies. Curr Opin Neurobiol. 22:552–558.

Ilie A, Raimondo JV, Akerman CJ. 2012. Adenosine release during seizures attenuates $GABA_A$ receptor-mediated depolarization. J Neurosci. 32:5321–5332.

Jockers R, Linder ME, Hohenegger M, Nanoff C, Bertin B, Strosberg AD, Marullo S, Freissmuth M. 1994. Species difference in the G protein selectivity of the human and bovine A_1-adenosine receptor. J Biol Chem. 269:32077–32084.

Kamiya H. 1991. Some pharmacological differences between hippocampal excitatory and inhibitory synapses in transmitter release: an in vitro study. Synapse. 8:229–235.

Kano M, Konnerth A. 1992. Potentiation of GABA-mediated currents by cAMP-dependent protein kinase. Neuroreport. 3:563–566.

Kano M, Rexhausen U, Dreessen J, Konnerth A. 1992. Synaptic excitation produces a long-lasting rebound potentiation of inhibitory synaptic signals in cerebellar Purkinje cells. Nature. 356:601–604.

Kasugai Y, Swinny JD, Roberts JDB, Dalezios Y, Fukazawa Y, Sieghart W, Shigemoto R, Somogyi P. 2010. Quantitative localisation of synaptic and extrasynaptic $GABA_A$ receptor subunits on hippocampal pyramidal cells by freeze-fracture replica immunolabelling. Eur J Neurosci. 32:1868–1888.

Katona I, Sperlágh B, Sík A, Käfalvi A, Vizi ES, Mackie K, Freund TF. 1999. Presynaptically located CB1 cannabinoid receptors regulate GABA release from axon terminals of specific hippocampal interneurons. J Neurosci. 19:4544–4558.

Khan GM, Smolders I, Ebinger G, Michotte Y. 2001. 2-chloro-*N*(6)-cyclopentyladenosine-elicited attenuation of evoked glutamate release is not sufficient to give complete protection against pilocarpine-induced seizures in rats. Neuropharmacology. 40:657–667.

Khazipov R, Congar P, Ben-Ari Y. 1995. Hippocampal CA1 lacunosum-moleculare interneurons: comparison of effects of anoxia on excitatory and inhibitory postsynaptic currents. J Neurophysiol. 74:2138–2149.

Klausberger T, Marton LF, O'Neill J, Huck JHJ, Dalezios Y, Fuentealba P, Suen WY, Papp E, Kaneko T, Watanabe M, et al. 2005. Complementary roles of cholecystokinin- and parvalbumin-expressing GABAergic neurons in hippocampal network oscillations. J Neurosci. 25:9782–9793.

Klausberger T, Somogyi P. 2008. Neuronal diversity and temporal dynamics: the unity of hippocampal circuit operations. Science. 321:53–57.

Köhling R, Vreugdenhil M, Bracci E, Jefferys JG. 2000. Ictal epileptiform activity is facilitated by hippocampal $GABA_A$ receptor-mediated oscillations. J Neurosci. 20:6820–6829.

Lambert NA, Teyler TJ. 1991. Adenosine depresses excitatory but not fast inhibitory synaptic transmission in area CA1 of the rat hippocampus. Neurosci Lett. 122:50–52.
Lamsa K, Heeroma JH, Kullmann DM. 2005. Hebbian LTP in feed-forward inhibitory interneurons and the temporal fidelity of input discrimination. Nat Neurosci. 8:916–924.
Lasztóczi B, Tukker JJ, Somogyi P, Klausberger T. 2011. Terminal field and firing selectivity of cholecystokinin-expressing interneurons in the hippocampal CA3 area. J Neurosci. 31:18073–18093.
Lee S-H, Földy C, Soltesz I. 2010. Distinct endocannabinoid control of GABA release at perisomatic and dendritic synapses in the hippocampus. J Neurosci. 30:7993–8000.
Li H, Henry JL. 2000. Adenosine receptor blockade reveals N-methyl-D-aspartate receptor- and voltage-sensitive dendritic spikes in rat hippocampal CA1 pyramidal cells in vitro. Neuroscience. 100:21–31.
Maex R, De Schutter E. 1998. Synchronization of golgi and granule cell firing in a detailed network model of the cerebellar granule cell layer. J Neurophysiol. 80:2521–2537.
Mann EO, Paulsen O. 2007. Role of GABAergic inhibition in hippocampal network oscillations. Trends Neurosci. 30:343–349.
McBain CJ, Fisahn A. 2001. Interneurons unbound. Nat Rev Neurosci. 2:11–23.
Mitchell SJ, Silver RA. 2003. Shunting inhibition modulates neuronal gain during synaptic excitation. Neuron. 38:433–445.
Moos WH, Szotek DS, Bruns RF. 1985. N^6-cycloalkyladenosines. Potent, A_1-selective adenosine agonists. J Med Chem. 28:1383–1384.
Moss SJ, Gorrie GH, Amato A, Smart TG. 1995. Modulation of $GABA_A$ receptors by tyrosine phosphorylation. Nature. 377:344–348.
Moss SJ, Smart TG, Blackstone CD, Huganir RL. 1992. Functional modulation of $GABA_A$ receptors by cAMP-dependent protein phosphorylation. Science. 257:661–665.
Nanoff C, Mitterauer T, Roka F, Hohenegger M, Freissmuth M. 1995. Species differences in A_1 adenosine receptor/G protein coupling: identification of a membrane protein that stabilizes the association of the receptor/G protein complex. Mol Pharmacol. 48:806–817.
Naylor DE, Liu H, Wasterlain CG. 2005. Trafficking of GABA(A) receptors, loss of inhibition, and a mechanism for pharmacoresistance in status epilepticus. J Neurosci. 25:7724–7733.
Nissen W, Szabo A, Somogyi J, Somogyi P, Lamsa KP. 2010. Cell type-specific long-term plasticity at glutamatergic synapses onto hippocampal interneurons expressing either parvalbumin or CB1 cannabinoid receptor. J Neurosci. 30:1337–1347.
Nusser Z, Sieghart W, Mody I. 1999. Differential regulation of synaptic $GABA_A$ receptors by cAMP-dependent protein kinase in mouse cerebellar and olfactory bulb neurones. J Physiol. 521:421–435.
Nusser Z, Sieghart W, Somogyi P. 1998. Segregation of different $GABA_A$ receptors to synaptic and extrasynaptic membranes of cerebellar granule cells. J Neurosci. 18:1693–1703.
Ochiishi T, Chen L, Yukawa A, Saitoh Y, Sekino Y, Arai T, Nakata H, Miyamoto H. 1999. Cellular localization of adenosine A_1 receptors in rat forebrain: immunohistochemical analysis using adenosine A_1 receptor-specific monoclonal antibody. J Comp Neurol. 411:301–316.
Oke OO, Magony A, Anver H, Ward PD, Jiruska P, Jefferys JGR, Vreugdenhil M. 2010. High-frequency gamma oscillations coexist with low-frequency gamma oscillations in the rat visual cortex in vitro. Eur J Neurosci. 31:1435–1445.
Oren I, Nissen W, Kullmann DM, Somogyi P, Lamsa KP. 2009. Role of ionotropic glutamate receptors in long-term potentiation in rat hippocampal CA1 oriens-lacunosum moleculare interneurons. J Neurosci. 29:939–950.
Pavlov I, Walker MC. 2013. Tonic GABA(A) receptor-mediated signalling in temporal lobe epilepsy. Neuropharmacology. 69:55–61.
Pawelzik H, Hughes DI, Thomson AM. 2002. Physiological and morphological diversity of immunocytochemically defined parvalbumin- and cholecystokinin-positive interneurones in CA1 of the adult rat hippocampus. J Comp Neurol. 443:346–367.
Pearce RA. 1993. Physiological evidence for two distinct $GABA_A$ responses in rat hippocampus. Neuron. 10:189–200.
Peng Z, Huang CS, Stell BM, Mody I, Houser CR. 2004. Altered expression of the delta subunit of the $GABA_A$ receptor in a mouse model of temporal lobe epilepsy. J Neurosci. 24:8629–8639.
Pietersen AN, Lancaster DM, Patel N, Hamilton JB, Vreugdenhil M. 2009. Modulation of gamma oscillations by endogenous adenosine through A1 and A2A receptors in the mouse hippocampus. Neuropharmacology. 56:481–492.
Poisbeau P, Cheney MC, Browning MD, Mody I. 1999. Modulation of synaptic $GABA_A$ receptor function by PKA and PKC in adult hippocampal neurons. J Neurosci. 19:674–683.
Pouille F, Scanziani M. 2001. Enforcement of temporal fidelity in pyramidal cells by somatic feed-forward inhibition. Science. 293:1159–1163.
Proctor WR, Dunwiddie TV. 1987. Pre- and postsynaptic actions of adenosine in the in vitro rat hippocampus. Brain Res. 426:187–190.
Rivkees SA, Price SL, Zhou FC. 1995. Immunohistochemical detection of A_1 adenosine receptors in rat brain with emphasis on localization in the hippocampal formation, cerebral cortex, cerebellum, and basal ganglia. Brain Res. 677:193–203.
Robello M, Amico C, Cupello A. 1993. Regulation of $GABA_A$ receptor in cerebellar granule cells in culture: differential involvement of kinase activities. Neuroscience. 53:131–138.
Roseti C, Palma E, Martinello K, Fucile S, Morace R, Esposito V, Cantore G, Arcella A, Giangaspero F, Aronica E, et al. 2009. Blockage of A2A and A3 adenosine receptors decreases the desensitization of human GABA(A) receptors microtransplanted to Xenopus oocytes. Proc Natl Acad Sci USA. 106:15927–15931.
Rothman JS, Cathala L, Steuber V, Silver RA. 2009. Synaptic depression enables neuronal gain control. Nature. 457:1015–1018.
Ruiz A, Campanac E, Scott RS, Rusakov DA, Kullmann DM. 2010. Presynaptic $GABA_A$ receptors enhance transmission and LTP induction at hippocampal mossy fiber synapses. Nat Neurosci. 13:431–438.
Salin PA, Prince DA. 1996. Spontaneous $GABA_A$ receptor-mediated inhibitory currents in adult rat somatosensory cortex. J Neurophysiol. 75:1573–1588.
Scanziani M, Capogna M, Gähwiler BH, Thompson SM. 1992. Presynaptic inhibition of miniature excitatory synaptic currents by baclofen and adenosine in the hippocampus. Neuron. 9:919–927.
Schubert P, Heinemann U, Kolb R. 1986. Differential effect of adenosine on pre- and postsynaptic calcium fluxes. Brain Res. 376:382–386.
Schulte G, Fredholm BB. 2000. Human adenosine A(1), A(2A), A(2B), and A(3) receptors expressed in Chinese hamster ovary cells all mediate the phosphorylation of extracellular-regulated kinase 1/2. Mol Pharmacol. 58:477–482.

Schulz SB, Klaft Z-J, Rösler AR, Heinemann U, Gerevich Z. 2012. Purinergic P2X, P2Y and adenosine receptors differentially modulate hippocampal gamma oscillations. Neuropharmacology. 62:914–924.

Scimemi A, Semyanov A, Sperk G, Kullmann DM, Walker MC. 2005. Multiple and plastic receptors mediate tonic $GABA_A$ receptor currents in the hippocampus. J Neurosci. 25: 10016–10024.

Seamon KB, Padgett W, Daly JW. 1981. Forskolin: unique diterpene activator of adenylate cyclase in membranes and in intact cells. Proc Natl Acad Sci USA. 78:3363–3367.

Sebastião AM, Ribeiro JA. 2009. Adenosine receptors and the central nervous system. Handb Exp Pharmacol. 193: 471–534.

Sebastião AM, Stone TW, Ribeiro JA. 1990. The inhibitory adenosine receptor at the neuromuscular junction and hippocampus of the rat: antagonism by 1,3,8-substituted xanthines. Br J Pharmacol. 101:453–459.

Semyanov A, Walker MC, Kullmann DM. 2003. GABA uptake regulates cortical excitability via cell type-specific tonic inhibition. Nat Neurosci. 6:484–490.

Semyanov A, Walker MC, Kullmann DM, Silver RA. 2004. Tonically active $GABA_A$ receptors: modulating gain and maintaining the tone. Trends Neurosci. 27:262–269.

Somogyi P, Klausberger T. 2005. Defined types of cortical interneurone structure space and spike timing in the hippocampus. J Physiol. 562:9–26.

Stell BM, Brickley SG, Tang CY, Farrant M, Mody I. 2003. Neuroactive steroids reduce neuronal excitability by selectively enhancing tonic inhibition mediated by delta subunit-containing $GABA_A$ receptors. Proc Natl Acad Sci USA. 100:14439–14444.

Sun C, Sieghart W, Kapur J. 2004. Distribution of alpha1, alpha4, gamma2, and delta subunits of $GABA_A$ receptors in hippocampal granule cells. Brain Res. 1029:207–216.

Swanson TH, Drazba JA, Rivkees SA. 1995. Adenosine A_1 receptors are located predominantly on axons in the rat hippocampal formation. J Comp Neurol. 363:517–531.

Thompson SM, Haas HL, Gähwiler BH. 1992. Comparison of the actions of adenosine at pre- and postsynaptic receptors in the rat hippocampus in vitro. J Physiol. 451:347–363.

Tukker JJ, Fuentealba P, Hartwich K, Somogyi P, Klausberger T. 2007. Cell type-specific tuning of hippocampal interneuron firing during gamma oscillations in vivo. J Neurosci. 27:8184–8189.

Van Aerde KI, Qi G, Feldmeyer D. 2013. Cell type-specific effects of adenosine on cortical neurons. Cereb Cortex. [Epub ahead of print].

Wei W, Zhang N, Peng Z, Houser CR, Mody I. 2003. Perisynaptic localization of delta subunit-containing GABA(A) receptors and their activation by GABA spillover in the mouse dentate gyrus. J Neurosci. 23:10650–10661.

Wlodarczyk AI, Sylantyev S, Herd MB, Kersanté F, Lambert JJ, Rusakov DA, Linthorst ACE, Semyanov A, Belelli D, Pavlov I, et al. 2013. GABA-independent $GABA_A$ receptor openings maintain tonic currents. J Neurosci. 33:3905–3914.

Yawo H, Chuhma N. 1993. Preferential inhibition of omega-conotoxin-sensitive presynaptic Ca^{2+} channels by adenosine autoreceptors. Nature. 365:256–258.

Yoon KW, Rothman SM. 1991. Adenosine inhibits excitatory but not inhibitory synaptic transmission in the hippocampus. J Neurosci. 11:1375–1380.

Zhang N, Wei W, Mody I, Houser CR. 2007. Altered localization of GABA(A) receptor subunits on dentate granule cell dendrites influences tonic and phasic inhibition in a mouse model of epilepsy. J Neurosci. 27:7520–7531.

HIPPOCAMPUS 25:566–580 (2015)

Synaptic Mechanisms of Adenosine A_{2A} Receptor-Mediated Hyperexcitability in the Hippocampus

Diogo M. Rombo,[1,2,3] Kathryn Newton,[4] Wiebke Nissen,[3] Sylvia Badurek,[5] Jacqueline M. Horn,[3,5] Liliana Minichiello,[3,5] John G.R. Jefferys,[3,6] Ana M. Sebastiao,[1,2] and Karri P. Lamsa[3,4]*

ABSTRACT: Adenosine inhibits excitatory neurons widely in the brain through adenosine A_1 receptor, but activation of adenosine A_{2A} receptor (A_{2A}R) has an opposite effect promoting discharge in neuronal networks. In the hippocampus A_{2A}R expression level is low, and the receptor's effect on identified neuronal circuits is unknown. Using optogenetic afferent stimulation and whole-cell recording from identified postsynaptic neurons we show that A_{2A}R facilitates excitatory glutamatergic Schaffer collateral synapses to CA1 pyramidal cells, but not to GABAergic inhibitory interneurons. In addition, A_{2A}R enhances GABAergic inhibitory transmission between CA1 area interneurons leading to disinhibition of pyramidal cells. Adenosine A_{2A}R has no direct modulatory effect on GABAergic synapses to pyramidal cells. As a result adenosine A_{2A}R activation alters the synaptic excitation - inhibition balance in the CA1 area resulting in increased pyramidal cell discharge to glutamatergic Schaffer collateral stimulation. In line with this, we show that A_{2A}R promotes synchronous pyramidal cell firing in hyperexcitable conditions where extracellular potassium is elevated or following high-frequency electrical stimulation. Our results revealed selective synapse- and cell type specific adenosine A_{2A}R effects in hippocampal CA1 area. The uncovered mechanisms help our understanding of A_{2A}R's facilitatory effect on cortical network activity. © 2014 The Authors Hippocampus Published by Wiley Periodicals, Inc.

KEY WORDS: antiepileptic; basket cell; cholecystokinin; disinhibition; parvalbumin; synchrony

[1] **Institute of Pharmacology and Neurosciences, Faculty of Medicine, University of Lisbon, Portugal;** [2] **Unit of Neurosciences, Institute of Molecular Medicine, University of Lisbon, Portugal;** [3] **Department of Pharmacology, Oxford University, Oxford, United Kingdom;** [4] **Medical Research Council Anatomical Neuropharmacology Unit at the Department of Pharmacology, Oxford University, Oxford, United Kingdom;** [5] **Centre for Neuroregeneration, University of Edinburgh, Edinburgh, United Kingdom;** [6] **School of Clinical and Experimental Medicine, College of Medical and Dental Sciences, University of Birmingham, Birmingham, United Kingdom**

Grant sponsor: Epilepsy Reseacrh UK; Grant number: P1102; Grant sponsor: Fundação para a Ciência e Tecnologia, Portugal; Grant number: PTDC/SAU-NMC/110838/2009; SFRH/BD/60386/2009; Grant sponsor: European Union; Grant number: EU FP6 MEMORIES; 037831; EU FP6 StemStroke, 037526; Grant sponsor: Network of European Neuroscience Programmes fellowship; Grant sponsor: Medical Research Council UK, the John Fell OUP Research Fund, the Department of Pharmacology, Faculty of Medicine University of Lisbon.

*Correspondence to: Karri Lamsa, Mansfield Road, Department of Pharmacology, Oxford University, OX1 3QT Oxford, UK. E-mail: karri.lamsa@pharm.ox.ac.uk

Accepted for publication 12 November 2014.
DOI 10.1002/hipo.22392
Published online 17 November 2014 in Wiley Online Library (wileyonlinelibrary.com).

INTRODUCTION

Adenosine is well known for its inhibitory effect on neocortical and hippocampal glutamatergic principal cells via the A_1 receptor (A_1R) (Dias et al., 2013). In addition, the high affinity adenosine A_{2A} receptor (A_{2A}R) is expressed in the brain, and although present at low levels in the neocortex and hippocampus (Schiffmann et al., 1991; Dixon et al., 1996) its activation in pathological conditions promotes epileptiform activity and facilitates excitotoxic neuronal death (Jones et al., 1998; Etherington and Frenguelli, 2004; Zeraati et al., 2006; El Yacoubi et al., 2009). However, evidence for A_{2A}R-mediated facilitation of cortical excitatory neuron discharge is largely based on results in epilepsy and neuronal trauma models, and function of A_{2A}R under physiological conditions in the cortex is less well known. Facilitatory effect of A_{2A}R on excitatory neurons in healthy brain is well characterized in basal ganglia where it is involved in controlling arousal and motor responses (Rebola et al., 2005a; Ciruela et al., 2006; Shook and Jackson, 2011; Wei et al., 2011; Lazarus et al., 2012). Adenosine A_{2A}R-mediated modulation of neuronal activity has also been reported in the hippocampus and neocortex where the receptor activation facilitates excitatory input from the CA3 area to CA1 enhancing glutamatergic synapses directly or by altering glutamate transport (Cunha et al., 1994; Rebola et al., 2005c; Dias et al., 2012; Matos et al., 2013). In physiological conditions adenosine A_{2A}Rs are involved in synaptic long-term plasticity in hippocampal glutamatergic mossy fibers (Rebola et al., 2008; Chamberlain et al., 2013), and a recent study demonstrated that deletion of A_{2A}R selectively in the hippocampus compromizes contextual memory formation (Wei et al., 2013).

The paucity of apparent adenosine A_{2A}R expression in the hippocampus hints that the receptor may be localized to specific neuron subpopulations or subtypes of synapses (Schiffmann and Vanderhaeghen, 1991; Dixon et al., 1996). Although reported facilitatory effects on glutamatergic transmission between pyramidal cells could explain, at least partly, why A_{2A}R activation promotes cortical pyramidal cell discharge (Jones et al., 1998; Zeraati et al., 2006; El

Yacoubi et al., 2008; El Yacoubi et al., 2009; Moschovos et al., 2012), it is unknown if modulation of GABAergic inhibitory interneurons contributes to $A_{2A}R$-mediated effects on hippocampal function. Adenosine $A_{2A}R$ expression level increases in posttraumatic and epileptic neocortex and hippocampus (Dixon et al., 1996; Rebola et al., 2005b), and this may emphasize a role of the receptor in the activity modulation in pathological conditions. Knowledge of the action of $A_{2A}R$ on identified hippocampal synaptic circuits is crucial for understanding adenosine function in physiological conditions in the cortex and the therapeutic potential of high affinity adenosine receptors in pathological conditions such as epilepsy.

MATERIALS AND METHODS

Animals

Mice were anaesthetized with Na-pentobarbitone and decapitated in accordance with the United Kingdom Animals (Scientific Procedures) Act (1986), and the European Community guidelines (86/609/EEC). Experiments were conducted on 4-8 week old heterozygous *PV-Cre* mice (The Jackson Laboratory B6;129P2-Pvalbtm1(cre)Arbr/J), *BAC-CCK-Cre*$^{tg/+}$ (Geibel et al., 2014) and *CaMKII-Cre* mice$^{tg/+}$ (B6.Cg-Tg(Camk2a-cre)T29-1Stl/J) and their wild type littermates. Homozygous *PV-Cre* mice were crossed with homozygous *Ai9* mice (*Ai9*$^{tm/tm}$) (B6.Cg-Gt(ROSA)26Sortm9(CAG-tdTomato)Hze/J) to produce tdTomato fluorophore expression specifically in PV+ cells.

Slice Preparations

The brain was removed and placed in 4°C solution (in mM): 75 sucrose, 87 NaCl, 2.5 KCl, 0.5 $CaCl_2$, 7 $MgCl_2$, 1.0 NaH_2PO_4, 25 $NaHCO_3$, 25 glucose (pH 7.4). For experiments in submerge chamber (Figs. 1–6) coronal slices (250 μm) were cut from both hemispheres using a vibratome (Microm HM650V, Carl Zeiss). For Figure 7 experiments in interface chamber slices were 400 μm thick. In either configurations slices were kept submerged in 32°C cutting solution for 20 min, then stored in interface chamber at 20–25°C for at least 60 min in recording solution (in mM): 119 NaCl, 2.5 KCl, 2.5 $CaCl_2$, 1.3 $MgSO_4$, 1.25 NaH_2PO_4, 25 $NaHCO_3$, and 11 glucose (pH 7.4). For data in Figure 2, slices were stored and experiments performed in the continuous presence of KN-62 (3 μM) and MCPG (200 μM) to prevent long-term plasticity with repetitive glutamatergic fiber burst stimulation (Perez et al., 2001; Lamsa et al., 2007; Campanac et al., 2013). A surgical cut was made between CA1 and CA3 areas. Slices in a submerged recording chamber (Luigs and Neumann) mounted on the stage of BX51WI microscope (Olympus), were visualized using a 20× immersion objective (2–4 zoom) with epifluorescence for YFP and tdTomato and with DIC-IR optics in combination with a CCD camera (Till-Photonics). Slices were superfused with recording solution at 5 mL/min and oxygenated with 95% O_2 /5% CO_2.

Electrophysiology

Whole cell and field potential recording electrodes (5–9 MΩ) were pulled (P-97, Sutter Instrument Co.) from borosilicate glass capillaries (GC150F-10, Harvard Apparatus). Intracellular solution for experiments in Figure 2 was (in mM): 145 Cs-Methansulfonate, 20 HEPES, 10 CsOH, 8 NaCl, 0.2 CsOH-EGTA, 2 ATP-Mg, 0.3 GTP-Na (295 mOsm, pH 7.2); in Figure 3 (in mM), 145 K-gluconate, 10 KOH, 0.2 KOH-EGTA were used instead; in figs 4, Cs-Methanosulphonate was replaced with CsCl. QX-314 (5 mM) and Neurobiotin (0.2–0.5%, Vector Laboratories) were included in all intracellular filling solutions. Field potential electrodes were filled with saline. Ratio of baseline fEPSP slope values and popspike amplitudes evoked with different intensities were fitted with regression line in each experiment baseline. The fEPSP slope–popspike relation was considered linear when regression fitting index was > 0.8 (0.89 ± 0.03, $n = 11$, mean ± s.e.m, Sigma Plot). fEPSP slope values recorded following wash-in of CGS21680 were fitted in the baseline condition regression line. Then, measured popspike amplitude in CGS21680 and popspike estimate given to same fEPSP value in baseline linear slope–popspike relation were compared. This gave Δ popspike/fEPSP used in Figure 1E. Because lowest intensity often failed to elicit stable popspike in baseline, intensities from 75 μs till 150 μs stimulus duration were used to determine linear relation of fEPSP slope and popspike amplitude in baseline conditions with regression line. The fEPSP values in the presence of agonist, which were potentiated out of the baseline fEPSP slope range, were excluded in analyses because no linear relation between fEPSP slope and popspike could be confirmed.

Data in Figures 1–6 were recorded with a Multiclamp 700B amplifier (Molecular Devices), low-pass filtered (4 kHz), digitized (10 kHz), and acquired by Clampex software (Molecular Devices). Field potential recordings in interface chamber (data for Fig. 7) were performed with an AC preamplifier and AC/DC amplifiers Neurolog NL104 and NL106 (0.3 Hz high-pass filtering) (Digitimer Ltd.). The signal was digitized by a Power 1401 plus (Cambridge Electronic Design). Additionally, a Humbug 50/60 Hz (Digitimer Ltd.) was used to remove noise locked to the electrical mains supply. Data were stored for off-line analysis using Signal5 software (Cambridge Electronic Design) at 10 kHz acquisition rate. In Figure 7 experiments a single-pulse electrical stimuli was delivered (every 20 s), and elicited fEPSPs (100 ms from stimulation) were excluded from spontaneous activity analysis.

Access resistance (<20 MΩ) was not compensated. Whole-cell recordings with >25% change were rejected. Liquid-junction potential was not corrected. Single, paired-pulse and HFS electrical stimuli (50–250 μA) were applied with concentric bipolar electrodes (CBAPC75PL1, FHC) connected to stimulus isolator boxes and triggered via computer. In Figure

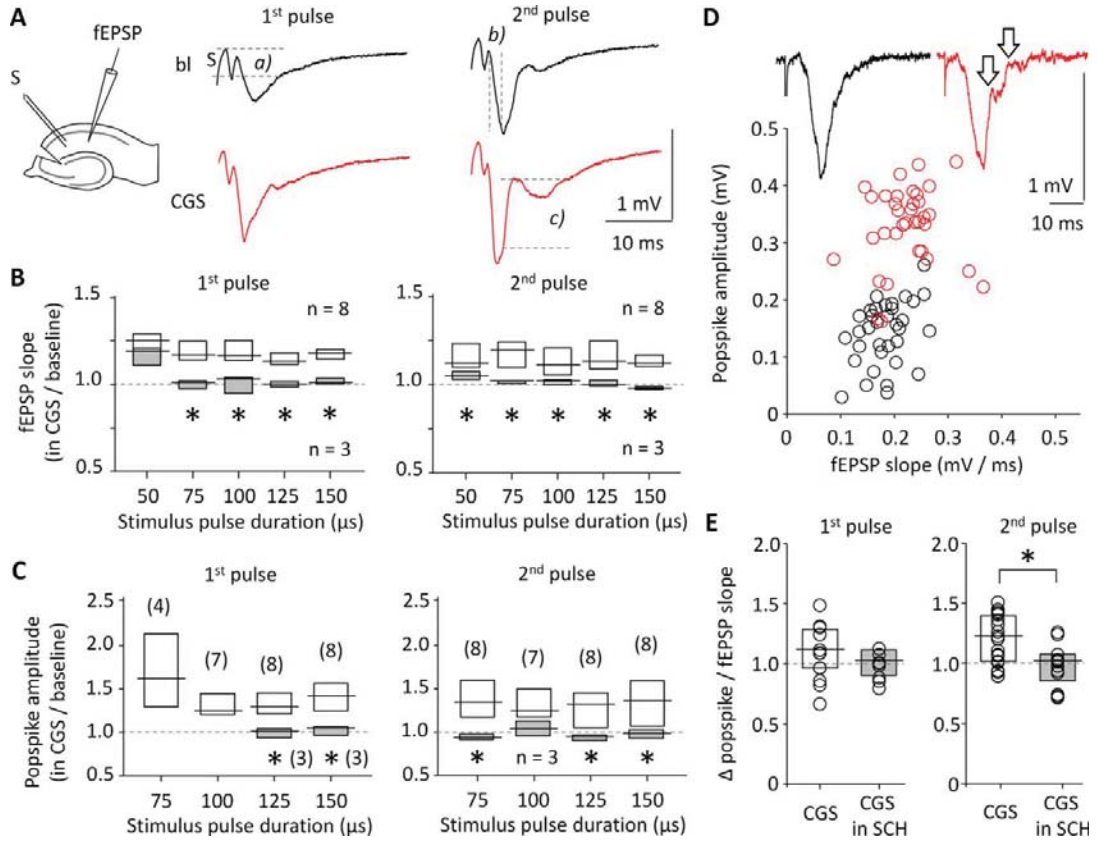

FIGURE 1. Activation of adenosine A_{2A} receptor facilitates glutamatergic transmission in hippocampal Schaffer collaterals and amplifies CA1 pyramidal cell input-output function. A-C: A selective agonist CGS21680 (30 nM) increases fEPSP slope and population spike amplitude evoked by stimulation of Schaffer collaterals. A: Schematic shows experimental design. Paired-pulse (50 ms interval) electrical stimulation (S) was delivered in the CA1 area. The CA3 area was removed by surgical cut to avoid recurrent excitation. Averaged field potential traces (10) evoked with mid-strength stimulation (100 µs pulse duration) in baseline (bl, black) and following application of GCS21680 (30 nM) (CGS, red). (a) shows prespike volley amplitude (between horizontal dotted lines), (b) fEPSP slope was measured between dotted vertical lines, and (c) popspike amplitude between horizontal lines. Stimulation artifact (S) is truncated. B: Increase of fEPSP slope by CGS21680 (30 nM). fEPSPs were elicited in every experiment with five stimulation intensities gradually increasing stimulus pulse duration from 50 to 150 µs. Open boxes show median (with 25% and 75% quartiles) of baseline-normalized fEPSP slope in 8 experiments following wash-in of CGS21680. Solid boxes show CGS21680 wash-in results in presence of the A_{2A}R antagonist SCH58261 (100 nM) ($n = 3$). Significant difference between open and solid boxes is indicated by asterisk (*$P < 0.05$, Mann-Whitney test). C: Increase of popspike amplitude by CGS21680 (30 nM) in experiments shown in B. When popspike data are not available in all experiments n is indicated in parenthesis. Asterisks show difference between the open and solid boxes (*$P < 0.05$, Mann-Whitney test). D, E: GCS21680 increases popspike amplitude - fEPSP slope ratio. D: Relation of popspike amplitude and fEPSP slope in one experiment in baseline (black trace and symbols) and following wash-in of CGS21680 (red). fEPSPs were evoked with various intensities using stimulation pulse duration from 75 to 125 µs. Inset: Averaged (10) field potential responses in baseline (black) and following wash-in of CGS21680 (red). Popspikes appearing in the fEPSP following wash-in of CGS21680 are indicated by arrows. (Data in the plot show first popspike amplitude when more than one popspike is elicited in CGS21680.) E: Effect of CGS21680 on popspike amplitude - fEPSP slope relation in all experiments. In baseline conditions popspike – fEPSP slope relation was determined in each experiment (see Materials and Methods). Plot shows a relation of popspike amplitude associated with similar size fEPSP slope in CGS21680 and baseline. This is indicated as Δ popspike/fEPSP slope. Open boxes represent median of means of individual experiments (circles). fEPSPs upon 2nd stimulation of paired-pulse generated significantly higher popspikes than similar magnitude fEPSPs in baseline ($P < 0.05$, Mann-Whitney test). For 1st stimulation pulse response, there was no significant difference between baseline and CGS21680. Solid boxes correspond to control experiments where CGS21680 was applied in the presence of A_{2A}R blocker SCH58261 (30 nM). Antagonist blocks the agonist-induced increase in Δ popspike/fEPSP slope (*$P < 0.05$, Mann-Whitney test). [Color figure can be viewed in the online issue, which is available at wileyonlinelibrary.com.]

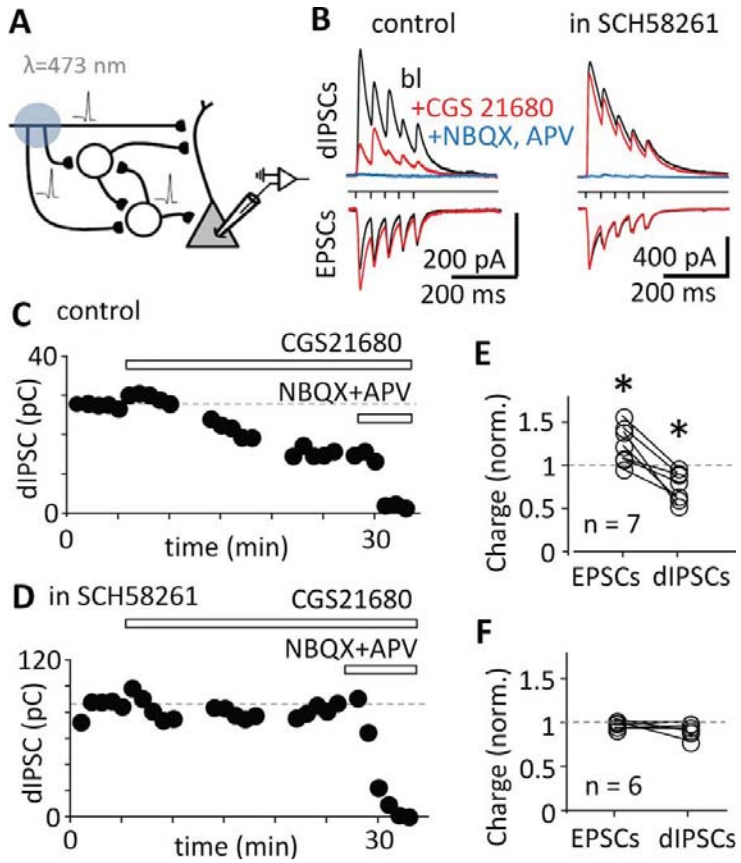

FIGURE 2. Adenosine A_{2A} receptor facilitates excitatory Schaffer collateral synapses and suppresses feed-forward GABAergic inhibitory input to CA1 pyramidal cells. A: Experimental design; optogenetic fixed-spot laser stimulation (blue dot) of Schaffer collateral fibers in the CA1 area, and recording in a postsynaptic pyramidal cell (gray). ChR2 is expressed in glutamatergic cells in *Cre*-dependent manner. GABAergic interneuron somata in the schematic are shown white. Action potentials indicate activation of axons between neurons. B: $A_{2A}R$ agonist CGS21680 (30 nM) suppresses disynaptic feed-forward GABAergic IPSCs (dIPSCs) and enhances glutamatergic EPSCs evoked by a train (5 pulses 20 Hz) of stimuli. Left: Averaged traces (5) from two sample experiments illustrate the effect of CGS21680 (red) on EPSCs and dIPSC following a baseline (black). Right: The effects of CGS21680 are blocked in the presence of $A_{2A}R$ antagonist SCH58261 (100 nM). The dIPSCs are fully abolished with glutamate receptor blockers NBQX (25 μM) and DL-APV (100 μM) (blue). Stimulus train in shown in the middle between traces. C,D: Time course of the effect of CGS21680 (horizontal bar) on dISPCs charge in control (C) and in the presence of antagonist (D). The dIPSCs were recorded at EPSC reversal potential and blocked by NBQX and DL-APV at the end. Gaps in IPSC data during agonist wash-in show time points when EPSCs were recorded at IPSC reversal potential (see E,F). E,F: Baseline-normalized effect of CGS21680 on EPSC and disynaptic IPSC charge in all experiments. Values from each cell are connected with line. E: EPSCs are significantly enhanced and dIPSCs suppressed by CGS21680 (*$P < 0.05$, *t*-test). F: The effect is blocked in presence of antagonist SCH58261 (100 nM). [Color figure can be viewed in the online issue, which is available at wileyonlinelibrary.com.]

6, stimulation with S2 electrode was suspended after baseline during SCH58261 wash-in and resumed after 10 min. Data were analyzed offline using Clampfit 10.2 software (Molecular Devices) or Spike2 software (Cambridge Electronic Design). Recorded signals were low-pass filtered on-line at 6 kHz and off-line in Figure 7 experiments as reported in results using Spike2 software. Drugs were purchased from Abcam, Ascent Scientific, Sigma-Aldrich, and Tocris Bioscience. Drugs were diluted (1 : 1,000) in ddH_2O, DMSO or ethanol, and applied via superfusion.

Statistics

All data presented were tested for normal distribution (Shapiro-Wilk test, Sigma Plot), and when passed *t*-test or single way ANOVA and Tukey's post hoc test was used to confirm

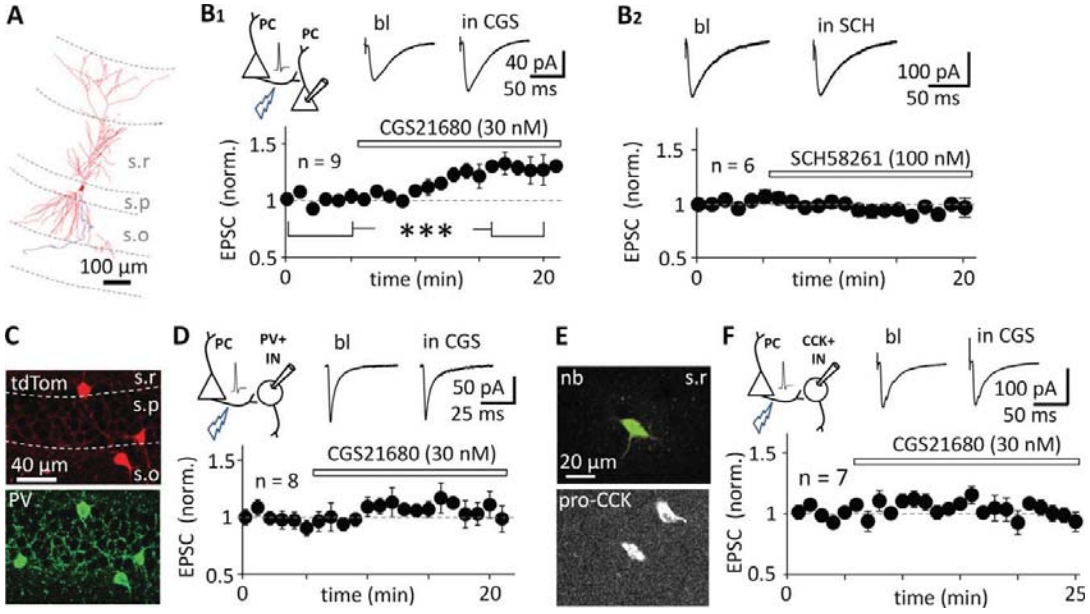

FIGURE 3. Adenosine $A_{2A}R$ facilitates glutamatergic synapses to pyramidal cells, but not to two major feed-forward GABAergic inhibitory interneuron populations expressing either PV or CCK. Electrical stimulation of Schaffer collaterals in the presence of GABA receptors blockers (PiTX, 100 µM) and CGP55845, 1 µM). Timing of bath-applied $A_{2A}R$ agonist and antagonist is indicated by horizontal bars. A,B: Facilitation of EPSCs by CGS21680 in identified pyramidal cells. A: Illustration of one recorded, neurobiotin-filled and visualized pyramidal cell (soma and dendrites red; axon blue). (s.r., stratum radiatum, s.p., stratum pyramidale, s.o., stratum oriens). B1: Bath-applied $A_{2A}R$ agonist CGS21680 (30 nM) facilitates glutamatergic EPSC amplitude (mean ± sem, baseline-normalized, $^{***}P < 0.001$, *t*-test). Insets; experimental design. Averaged EPSCs (10) from one cell in baseline (bl) and following CGS21680 application (at 15–20 min time point). B2: Adenosine $A_{2A}R$ antagonist SCH58261 (100 nM) has no effect on EPSC amplitude in the experimental conditions (*t*-test). Plot (mean ± sem) and averaged EPSCs as in B1. C–F: The $A_{2A}R$ agonist fails to modulate EPSCs in interneurons. C: PV+ interneurons were identified by *Cre*-dependent fluorophore (tdTomato, tdTom) expression. Confocal images showing tdTom (above) and immunoreaction for PV (below, visualized with Alexa-488) in the CA1 area in a fixed slice. D: EPSCs in PV+ cells were not altered by CGS21680 (mean ± sem). Insets: experimental design and averaged EPSCs (10) from one postsynaptic PV+ cell. E: Postsynaptic CCK+ interneurons were identified by positive immunoreaction for pro-CCK in *post hoc* analysis. Confocal images from one postsynaptic neurobiotin-filled (nb, Alexa-488) and pro-CCK+ (Cy5) interneuron. F: Adenosine $A_{2A}R$ agonist CGS21680 does not change EPSCs in CCK+ GABAergic interneurons (mean ± sem). Insets: experimental design and averaged EPSCs (10) in one pro-CCK+ interneuron. [Color figure can be viewed in the online issue, which is available at wileyonlinelibrary.com.]

significance, and data were shown as mean ± sem. Otherwise Mann-Whitney was used instead and data shown as median and quartiles.

Stereotaxic Injections

An adeno-associated virus serotype 2 or 5 construct *(AAV2/5:ChR2-eYFP)* was stereotaxically injected into dorsal hippocampus of heterozygous *PV-Cre*, *CCK-Cre*, and *CaMK*II-*Cre* mice (CA1-CA3 area) via 33-gauge needle attached to a Microlitre Syringe (Hamilton). Craniotomy was made for mice anesthetized with 2–4% isoflurane. In each hemisphere, 800 nL of virus suspension was delivered at 80 nL/min by a Micro Syringe Pump Controller (World Precision Instruments). Following suturing of the wound, mice were allowed to recover for 14–21 days after injections.

Optogenetics

ChR2 was activated by a fixed-spot 20 or 80 µm diameter laser light spot (pulse 3 ms, max. 100 mW, Rapp OptoElectronics) via the microscope objective (diameter measured under objective). All experiments with 20 Hz 5-pulse stimulation were performed in the presence of blockers for high-frequency stimulation-elicited long-term plasticity. Paired-pulse ratios are presented as 2nd versus 1st IPSC amplitude. Compound IPSC and EPSC charge was measured in 500 ms window from current onset.

Cell Visualization, Anatomical Analysis, and Immunohistochemistry

Processes and analyses are described in Oren et al. (2009). Briefly, slices were fixed overnight at 4°C, washed in 0.1 M

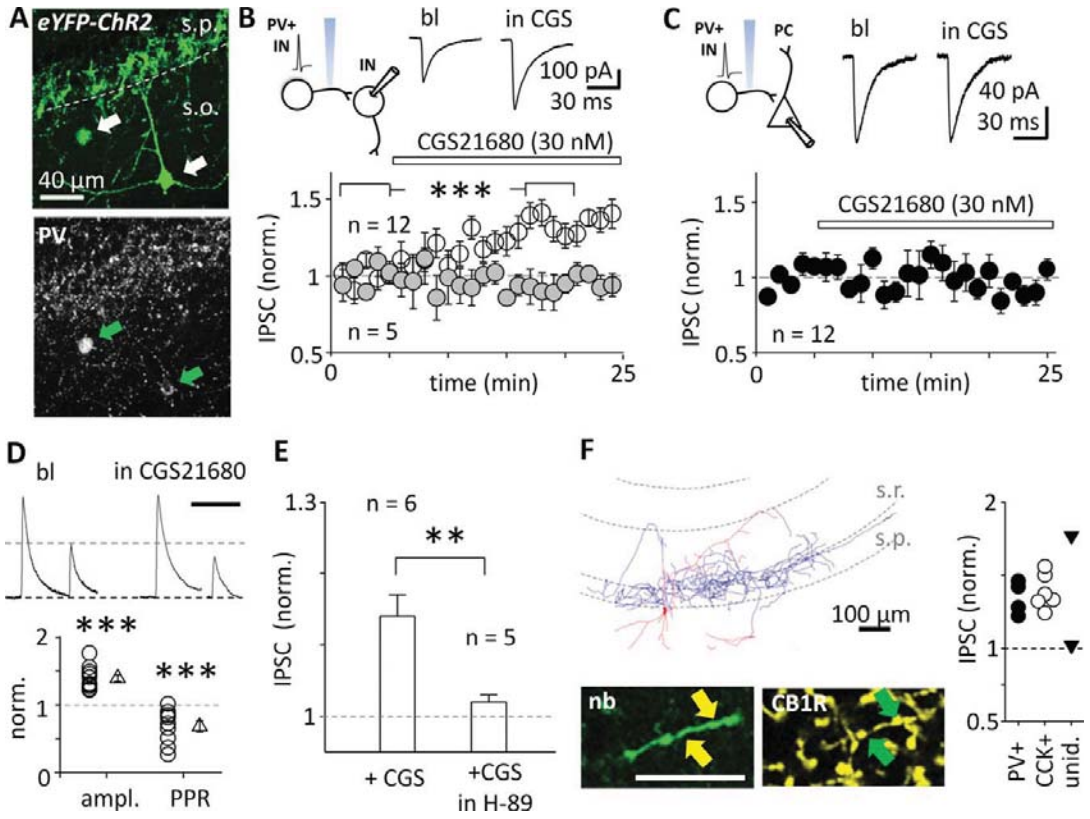

FIGURE 4. **$A_{2A}R$ selectively facilitates GABAergic synapses between feed-forward interneurons, but has no direct effect on GABAergic inhibitory synapses to pyramidal cells. A–C: $A_{2A}R$ agonist facilitates IPSCs elicited from GABAergic PV+ cells to various inhibitory interneurons, but not to pyramidal cells. A: Optogenetic stimulation of GABAergic synapses from PV+ interneurons. ChR2 is expressed in *Cre*-dependent manner. Confocal images show eYFP-ChR2 (*above*) in PV+ cells (*below*, Cy5). Arrows point to positive somata (fixed slice). B: Plot shows that CGS21680 (30 nM) facilitates IPSC amplitude in postsynaptic interneurons (open symbols; mean ± sem of baseline-normalized IPSCs, $^{***}P < 0.001$, *t*-test). Facilitation by CGS21680 is blocked in the presence of $A_{2A}R$ antagonist (SCH58261, 100 nM; gray symbols, *t*-test). *Insets*: Schematic of experimental design. Averaged IPSCs (10) in baseline and after 15 min in CGS21680. C: CGS21680 fails to modulate IPSCs from PV+ GABAergic synapses to identified pyramidal cells (mean ± sem, *t*-test). *Insets*: Schematic shows experimental design. Averaged IPSCs (10) in baseline and after 15 min in CGS21680. D: The CGS21680-induced IPSC facilitation in interneurons is associated with reduced paired-pulse ratio (PPR). A plot shows baseline-normalized IPSC amplitude (for 1st IPSC) and PPR (2nd vs. 1st IPSC amplitude) following wash-in of CGS21680 Circles, mean in individual experiments; triangles mean ± sem of the means ($^{***}P < 0.001$, *t*-test). Averaged IPSCs (10) shown on the top, scale 50 ms. Traces are scaled by 1st IPSC amplitude and dotted line indicates 2nd IPSC peak in baseline. E: Facilitation of IPSCs by CGS21680 in interneurons involves protein kinase A (PKA). Histogram shows baseline-normalized IPSC amplitude following CGS21680 application in control (mean ± sem, $n = 6$), and in the presence of a PKA inhibitor H-89 (1 µM, $n = 5$) ($^{**}P < 0.01$, *t*-test). IPSCs were elicited by electrical stimulation of GABAergic fibers (glutamate receptors blocked with NBQX 25 µM and DL-APV, 100 µM). F: IPSC facilitation by CGS21680 occurs in various different postsynaptic interneuron types. Illustration of a basket cell (*above*; collapsed *z*-stack epifluorescence image from one 60 µm-thick section, soma and dendrites red, axon blue) with positive axonal immunoreaction for CB1R (*below;* confocal images of CB1R at Cy3 and a neurobiotin-filled axon in Alexa488, pointed by arrows). s.r. and s.p = *stratum radiatum* and *pyramidale*, scale 20 µm. Histogram shows baseline-normalized IPSC in CGS21680 in all recorded interneurons ($n = 12$). Analyses revealed four putatively PV+ cells (two O-LM cells and two CB1R- basket cells) and six putative CCK+ cells immunopositive for axonal CB1R. Two interneurons remained unidentified. [Color figure can be viewed in the online issue, which is available at wileyonlinelibrary.com.]**

phosphate buffer (PB), embedded in 20% gelatine, and sectioned (60–70 µm) with a vibratome (Leica Microsystems) in 0.1 M PB. Then, washed in 50 mM Tris-buffered saline (TBS, pH 7.4) with 0.3% Triton X-100 (TBS-Tx), incubated overnight with streptavidin conjugated to either AlexaFluor-488 or Cy3, washed in 50 mM TBS-Tx, mounted in Vectashield

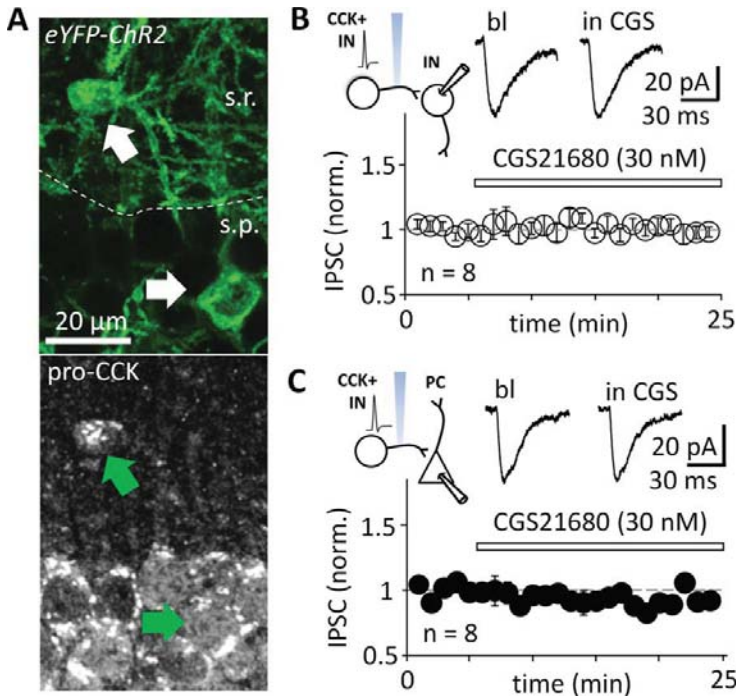

FIGURE 5. Facilitation of efferent GABAergic synapses by CGS21680 is specific to PV+ cells. The IPSCs elicited from CCK+ interneurons are not modulated by the $A_{2A}R$ agonist. A: Optogenetic stimulation of axons from CCK-expressing GABAergic cells. Confocal images of AAV-transduced *Cre*-dependent eYFP-ChR2 (*above*) in proCCK+ neurons (*below*; at Cy5). Fluorophore-positive somata are pointed with arrows (fixed slice). IPSCs evoked from CCK+ cells are not modulated by CGS21680 (30 nM) either in postsynaptic interneurons (B) nor in pyramidal cells (C) (mean ± sem, *t*-test). All recordings were in the presence of NBQX (25 µM) and DL-APV (100 µM). *Insets*; schematic shows experimental design. Averaged IPSCs (10) from sample recordings. [Color figure can be viewed in the online issue, which is available at wileyonlinelibrary.com.]

(Vector Laboratories) and examined with an epifluorescent microscope (DM5000 B, Leica Microsystems) using appropriate filter sets (L5 or Y3) and a CCD camera (ORCA-ER, Hamamatsu). Pyramidal cells were identified by mushroom spines on dendrites, basket cells and oriens-lacunosum molecular (O-LM) cells by their axon arborisation inside *stratum pyramidale* or *lacunosum moleculare*, respectively (Oren et al., 2009; Nissen et al., 2010). Digital micrographs were constructed from z-stack images recorded with epifluorescence microscope, collapsed, and analyzed with Image-J software (Somogyi et al., 2012).

Free-floating sections were washed in 50 mM TBS-Tx, blocked in 20% normal horse serum (NHS, Vector Laboratories) in TBS-Tx, and incubated in primary antibodies at 4°C for 48 h. Fluorochrome-conjugated secondary antibodies were applied overnight at 4°C. After another wash-in TBS-Tx, sections were mounted in Vectashield under coverslips. Immunoreactivity was evaluated at 40× magnification with 2× zoom using confocal laser-scanning microscopy (LSM710, Carl Zeiss) with Zen2008 software. Details of primary and secondary antibodies are reported in Nissen et al. (2010).

RESULTS

Adenosine $A_{2A}R$ Facilitates Glutamatergic Schaffer Collateral Synapses and Amplifies CA1 Pyramidal Cell Input–Output Transformation

We studied effect of $A_{2A}R$ activation on hippocampal Schaffer collateral synapses in the CA1 area using paired-pulse microelectrode stimulation (50 ms interval, delivered every 15 s) and field potential recording in mouse hippocampal slices. Wash-in of selective $A_{2A}R$ agonist CGS21680 (30 nM) after a baseline (at least 10 min) enhanced stimulus-evoked field EPSP (fEPSP) slope and increased population spike (popspike) amplitude ($P < 0.05$), but did not alter prespike volley (Mann-Whitney test) (Figs. 1A–C). Stimulus-evoked fEPSP and popspike details are shown in Figures 1B,C. Baseline-normalized prespike volley in CGS21680 was 1.02 ± 0.02 for 1st stimulation pulse and 1.01 ± 0.03 for 2nd ($n = 11$) (Sebastiao and Ribeiro, 1992). Facilitatory effects of CGS21680 on fEPSP slope and popspike amplitude were fully blocked in

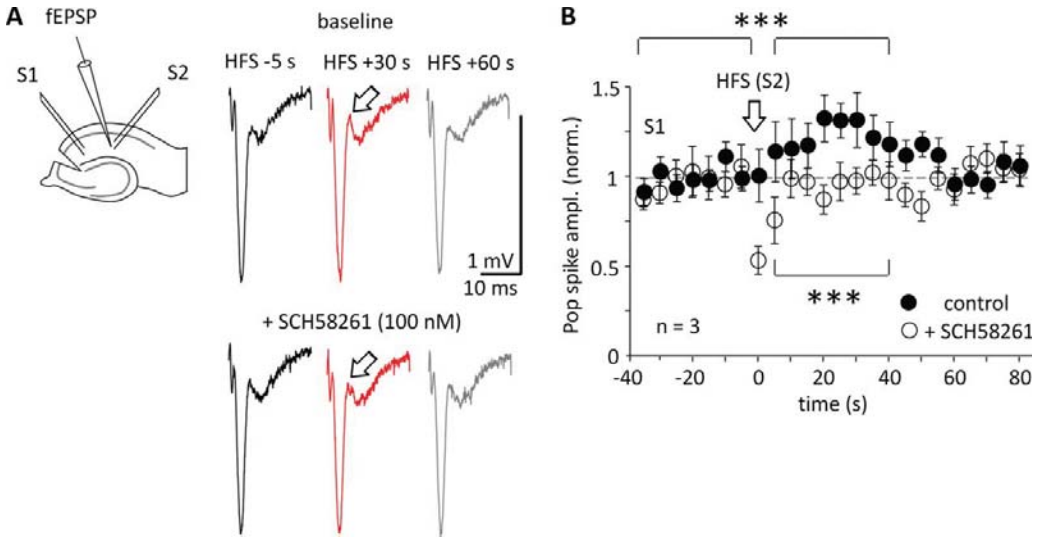

FIGURE 6. Facilitation of hippocampal pyramidal cell discharge through A_{2A} receptors activated by high-frequency electrical stimulation. A: Transient facilitation of Schaffer collateral stimulation (S1) -evoked popspike following high-frequency stimulation with another electrode (S2) in the vicinity of recording site. *Left*: A schematic shows experimental design in the CA1 area. Paired-pulse (50 ms interval) electrical stimulation of Schaffer collaterals (S1) was delivered every 5 s, and high-frequency local stimulation (HFS, 50 Hz with 100 pulses) applied with electrode S2 every 2 min. The S2 electrode was positioned ~100 μm from field potential (fEPSP) recording. *Right*: Averaged (5) traces from one experiment show facilitation of fEPSP-associated popspike (pointed with arrow) following S2 HFS. Wash-in of $A_{2A}R$ antagonist SCH58261 (100 nM, 10 min) abolished facilitation in the same experiment. Traces at different time points in relation to HFS are shown in distinct colors. Arrow points to increased popspike 30 s after HFS in baseline conditions, and below shows same response following wash-in of SCH58261 (10 min). Popspikes was elicited in 2nd pulse of paired-pulse stimulation. B: Mean ± sem of baseline-normalized popspike amplitude in three experiments. Solid symbols indicate baseline conditions (before SCH58261 wash-in) and open circles following 10 min wash-in of SCH58261 (100 nM) (*$P < 0.001$, Single-way ANOVA and Tukey's *post hoc* test, $n = 3$). In each experiment 5 cycles were recorded at each time point. Timing of HFS is indicated by arrow (delivered immediately before abscissa 0-time point). [Color figure can be viewed in the online issue, which is available at wileyonlinelibrary.com.]**

experiments with continuous presence of the $A_{2A}R$ antagonist SCH58261 (100 nM) (Mann-Whitney test) (Figs. 1B,C). Effect of CGS21680 on field potential responses was studied in each experiment with five stimulation intensities. In all experiments stimulation intensity was adjusted to generate a popspike with mid-range intensity in baseline conditions (popspike amplitude 0.25 ± 0.06 mV for 1st pulse, and 0.59 ± 0.17 mV for 2nd pulse, $n = 11$, mean ± sem. This corresponded to fEPSP slope of 0.32 ± 0.06 mV/ms and 0.57 ± 0.11 mV/ms, respectively).

We discovered that following wash-in of CGS21680 (30 nM), popspike amplitude–fEPSP slope ratio also changed. In the presence of CGS21680, fEPSPs were associated with higher amplitude popspikes than during baseline (Fig. 1D). We used linear regression to fit fEPSP slope and popspike amplitude values (evoked with various stimulus intensities) in baseline conditions in each experiment (see Material and Methods). Following wash-in of CGS21680 (30 nM), fEPSPs upon 2nd stimulation of the paired-pulse generated significantly higher amplitude popspikes than similar magnitude fEPSPs during baseline ($P < 0.05$, Mann-Whitney test) (Fig. 1E). Popspike amplitude–fEPSP slope relation details are shown in Figures 1D and E. The results show that $A_{2A}R$ facilitates glutamatergic synapses in the hippocampus, and in addition increases CA1 pyramidal cells' output in response to Schaffer collateral excitation.

Adenosine $A_{2A}R$ Increases Glutamatergic Excitation and Suppresses GABAergic Feed-Forward Inhibition to CA1 Pyramidal Cells

Next, we investigated how $A_{2A}R$ activation modulates monosynaptic excitatory and disynaptic inhibitory currents in the CA1 hippocampal pyramidal cells. We selectively stimulated Schaffer collaterals delivering 473 nm laser light-pulses (3 ms, 5 pulses at 50-ms interval, delivered every 30 s) to CA1 *stratum radiatum* in slices expressing channelrhodopsin 2 (ChR2) in glutamatergic neurons (Fig. 2A). Slices were prepared from hippocampi of heterozygous *CaMKII-Cre* (*CaMKII-Cre*$^{tg/+}$) mice transduced with AAV2/5-ChR2-eYFP to express ChR2 in a *Cre*-dependent manner in CA1-CA3 pyramidal cells (see Materials and Methods). Postsynaptic cells were voltage-

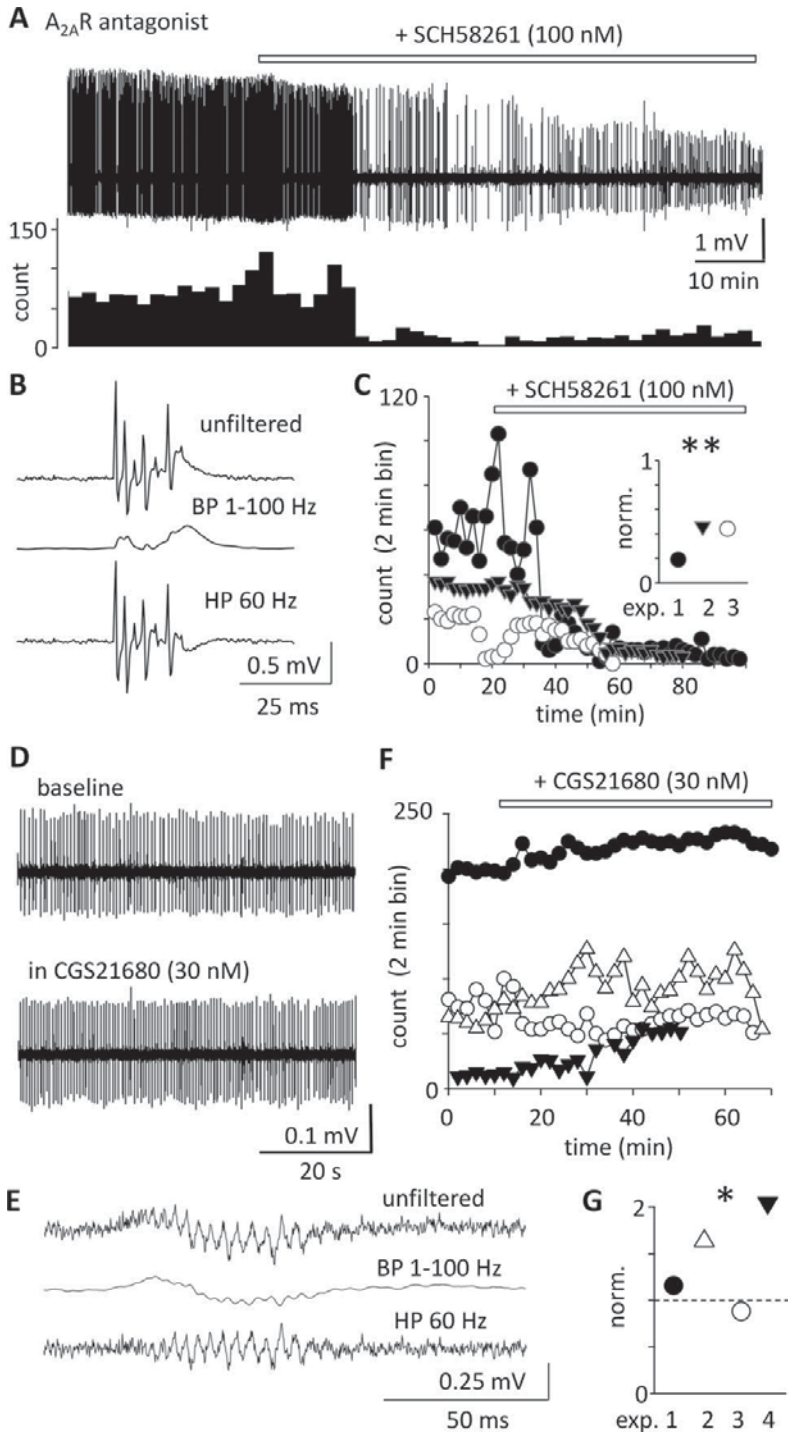
A
A2AR antagonist
+ SCH58261 (100 nM)
150
count
0
1 mV
10 min
B
unfiltered
BP 1-100 Hz
HP 60 Hz
0.5 mV
25 ms
C
+ SCH58261 (100 nM)
120
count (2 min bin)
0
0 20 40 60 80
time (min)
**
norm.
1
0
exp. 1 2 3
D
baseline
in CGS21680 (30 nM)
0.1 mV
20 s
F
+ CGS21680 (30 nM)
250
count (2 min bin)
0
0 20 40 60
time (min)
E
unfiltered
BP 1-100 Hz
HP 60 Hz
0.25 mV
50 ms
G
*
2
norm.
0
exp. 1 2 3 4

FIGURE 7.

clamped sequentially at −70 mV and at a reversal potential of EPSCs (11 ± 1 mV, $n = 7$ cells) to record glutamatergic EPSCs and disynaptic GABAergic IPSCs, respectively (Fig. 2B). Wash-in of $A_{2A}R$ agonist CGS21680 (30 nM) potentiated glutamatergic EPSCs and simultaneously suppressed disynaptic GABAergic IPSCs in CA1 pyramidal cells (Figs. 2B,C,E). Charge of baseline-normalized EPSCs increased to 1.25 ± 0.08 ($P < 0.05$, $n = 7$ cells, t-test), and disynaptic IPSCs decreased to 0.77 ± 0.07 ($P < 0.05$, $n = 7$ cells, t-test). Baseline EPSC and IPSC were 25.3 ± 4.7 pC and 55.2 ± 12.6 pC, respectively. When we repeated experiments in the presence of the $A_{2A}R$ antagonist SCH58261 (100 nM, applied at least 30 min prior to agonist wash-in), $A_{2A}R$ agonist effect was fully blocked and neither EPSCs nor IPSCs were altered (Figs. 2D–F). Baseline-normalized EPSCs and IPSCs were 0.98 ± 0.02 and 0.94 ± 0.03, respectively ($n = 6$, t-test). During baseline, mean ± sem of EPSCs was 48.0 ± 8.5 pC and IPSCs was 70.1 ± 7.6 pC).

Because pyramidal cells in the CA1 area can express low levels of CCK and *Cre*, light-evoked ChR2 currents could mask synaptic EPSCs in these experiments (Geibel et al., 2014). We therefore washed in glutamate receptor blockers NBQX (25 μM) and *DL*-APV (100 μM) at the end to measure ChR2-contribution to light stimulation-evoked excitatory currents. In all tested cells glutamatergic current was predominant (78 ± 8% of total charge, $n = 7$ cells) showing that the facilitatory effect of $A_{2A}R$ agonist on excitatory currents is caused by increased glutamatergic EPSCs.

The results show that $A_{2A}R$ activation modulates Schaffer collateral-driven synaptic input from CA3 area to CA1 pyramidal cells in two ways; facilitating monosynaptic glutamatergic excitation and suppressing network-driven disynaptic GABAergic inhibition simultaneously. These changes can at least partially explain our above findings on $A_{2A}R$-mediated facilitation of Schaffer collateral fEPSP (see Figs. 1A,B) and popspike upon Schaffer collateral paired pulse stimulation (see Figs. 1C), and the observed facilitation in CA1 pyramidal cells input–output transformation (see Figs. 1D,E).

Adenosine $A_{2A}R$ Facilitates Glutamatergic Schaffer Collateral Synapses Selectively to Pyramidal Cells

We repeated Schaffer collateral electrical stimulation experiments (see Fig. 1) and recorded intracellularly from either postsynaptic CA1 pyramidal cells or interneurons. Bath-applied adenosine $A_{2A}R$ agonist CGS21680 (30 nM) facilitated glutamatergic EPSC amplitude to 1.30 ± 0.04 from baseline (10–15 min following application, $P < 0.001$, $n = 9$, t-test) in synapses onto identified CA1 pyramidal cells (see Material and Methods). Wash-in of $A_{2A}R$ antagonist SCH58261 (100 nM) after baseline failed to change EPSCs, and baseline-normalized EPSC amplitude in SCH58261 was 0.94 ± 0.04 ($n = 6$, t-test) indicating that $A_{2A}R$s are not activated by endogenous adenosine under the experimental conditions (Figs. 3A,B). Next, we studied EPSCs in two major interneuron populations involved in feed-forward inhibition in area CA1; GABAergic cells expressing either parvalbumin (PV+) or cholecystokinin (CCK+) with axonal cannabinoid receptor Type 1 (CB1R) (Katona et al., 1999; Glickfeld and Scanziani, 2006; Nissen et al., 2010; Armstrong and Soltesz, 2012). EPSCs in PV+ and CCK+ interneurons were not altered by $A_{2A}R$ agonist (t-test), and baseline-normalized EPSC amplitudes in CGS21680 (30 nM) were 1.05 ± 0.05 ($n = 8$) and 1.04 ± 0.02 ($n = 7$) accordingly (Figs. 3C–F). Thus, activation of $A_{2A}R$ facilitates excitatory Schaffer collateral synapses in target-specific manner. Mean ± sem of EPSCs during baseline was 79.6 ± 8.1 pA in pyramidal cells ($n = 9$) and 77.8 ± 15.8 pA in the interneurons ($n = 15$). GABA receptors were blocked with PiTX (100 μM) and CGP55845 (1 μM), and cells were filled with neurobiotin for *post hoc* anatomical and immunohistochemical studies (Figs. 3A,E).

FIGURE 7. Modulation of spontaneous epileptiform pyramidal cell discharge by $A_{2A}R$ antagonist and agonist in hyperexcitable conditions with elevated extracellular potassium. A–C: Adenosine $A_{2A}R$ blocker SCH58261 (100 nM) suppresses spontaneous epileptiform discharges in hippocampal slices exposed to elevated (8–9 mM) extracellular potassium. Spontaneous interictal-like synchronous bursting activity was recorded with field potential electrode in CA3 area. A: A sample trace from one experiment showing inhibition of spontaneous epileptiform burst activity by SCH58261 (unfiltered trace). Timing for wash-in of $A_{2A}R$ antagonist SCH58261 (100 nM) is indicated by horizontal bar. Histogram below shows occurrence of spontaneous epileptiform bursts in 2 min bins. For burst occurrence analysis data were band-pass filtered (1–100 Hz) to avoid detection of occasional single unitary extracellular spikes. B: Epileptiform population bursts are characterized by 1–100 Hz band-pass filtered (BP 1–100 Hz) field potential deflection associated with extracellular spikes (high-pass filtered at 60 Hz, HP 60 Hz). An unfiltered epoch shown on top with filtering below as indicated. C: Plot shows suppression in occurrence of spontaneous epileptiform events by SCH58261 in the three of three experiments. Occurrence of events is shown in 2 min bins. Horizontal bar indicates wash-in of the antagonist. Inset plot shows baseline-normalized effect of the antagonist on burst occurrence (indicated with same symbols as in main plot). Inhibitory effect of SCH58261 was highly significant ($P < 0.01$, t-test, at 20–30 min after drug application). D–F: Wash-in of $A_{2A}R$ agonist CGS21680 (30 nM) is associated with increased spontaneous occurrence of epileptiform bursts. D: Traces from one experiment illustrate spontaneous burst activity in baseline and following agonist application (20–30 min wash-in). E: Illustration of one burst event from same experiment. Unfiltered (top) and filtered (band-pass 1–100 Hz and high-pass 60 Hz) traces of the same event are illustrated as indicated. F: Plot shows effect of $A_{2A}R$ agonist (CGS21680, 30 nM) on occurrence of spontaneous epileptiform bursts in four experiments (2 min bin). Wash-in of the antagonist is indicated by horizontal bar. G: Baseline-normalized burst occurrence in the presence of agonist in the four experiments above (indicated with same symbols). Burst occurrence is variably modulated, but significantly increased in pool of four experiments (*$P < 0.05$, t-test, at 20–30 min time point following agonist application.**

Adenosine $A_{2A}R$ Enhances GABAergic Inhibition in the CA1 Area Selectively Between Interneurons

The results above do not explain why feed-forward IPSCs were strongly suppressed by $A_{2A}R$ activation in experiments shown in Figure 2. To explore this, we investigated whether GABAergic synapses from interneurons to pyramidal cells are modulated by $A_{2A}R$ agonist, or if GABAergic synapses between interneurons are altered. We utilized *Cre*-dependent ChR2 expression to optogenetically activate GABAergic synapses from either PV- or CCK–expressing CA1 interneurons. Slices were prepared from heterozygous PV-*Cre* (Fig. 4) and *BAC*-CCK-$Cre^{fg/+}$ mice (Fig. 5) transduced with AAV:ChR2-eYFP (see Materials and Methods) (Geibel et al., 2014). We first stimulated ChR2-expressing PV+ GABAergic interneuron axons with paired-pulse laser light pulses (3 ms, 50 ms interval) in the CA1 area, and found that wash-in of the agonist CGS21680 (30 nM) increased IPSC amplitude in postsynaptic interneurons to 1.35 ± 0.04 of baseline ($P < 0.001$, $n = 12$, *t*-test) (Figs. 4A,B). The facilitation was significant in 11 of 12 anatomically verified interneurons, and was fully blocked when studied in the presence of the $A_{2A}R$ antagonist SCH58261 (100 nM) ($n = 5$, *t*-test) (Fig. 4B). However, CGS21680 (30 nM) failed to directly modulate GABAergic synapses from PV+ cells to postsynaptic pyramidal cells (*t*-test) (Fig. 4C). Baseline-normalized IPSC amplitude in postsynaptic pyramidal cells was 0.93 ± 0.04 in the presence of CGS21680 (30 nM) ($n = 12$).

The IPSC facilitation by CGS21680 (30 nM) in interneurons was associated with a decrease in the paired-pulse ratio to 0.67 ± 0.08 from baseline ($P < 0.001$, $n = 10$, *t*-test), suggesting presynaptic modulation of transmission by $A_{2A}R$ in GABAergic fibers (Fig. 4D). In addition, facilitation of IPSC by CGS21680 was blocked in the presence of a PKA inhibitor H-89 dihydrochloride hydrate (1 μM) (baseline-normalized IPSC amplitude was to 1.02 ± 0.01, $n = 5$) (Fig. 4E). In PKA-inhibitor studies, IPSCs were elicited with afferent electrical stimulation in the presence of glutamate receptor blockers (NBQX, 25 μM and *DL*-APV, 100 μM) and in control experiments IPSC increased to 1.14 ± 0.03 from baseline by CGS21680 (30 nM) ($P < 0.01$, 15 min wash-in, $n = 6$, *t*-test). Wash-in of $A_{2A}R$ antagonist SCH58261 after baseline (100 nM) failed to change IPSCs (amplitude 0.99 ± 0.11 of baseline, $n = 6$, *t*-test).

The results on IPSCs in postsynaptic pyramidal cells and interneurons show that $A_{2A}R$-mediated modulation of inhibitory synapses from PV+ GABAergic fibers depends on the postsynaptic cell type. Postsynaptic neurons were filled with neurobiotin during recording for *post hoc* analysis of the cells (see Materials and Methods). This confirmed that $A_{2A}R$-mediated facilitation of IPSCs occurs in various postsynaptic interneuron types including oriens-lacunosum moleculare (O-LM) cells ($n = 2$), and basket cells with negative ($n = 2$) or positive ($n = 6$) axonal immunoreaction for CB1R (Fig. 4F) (Glickfeld and Scanziani, 2006; Lawrence et al., 2006; Klausberger and Somogyi, 2008). Two interneurons, of which one showed IPSC facilitation by $A_{2A}R$, remained unidentified (Fig. 4F).

Conversely, IPSCs elicited from CCK+ GABAergic fibers (Fig. 5A) were not modulated by $A_{2A}R$. Exposure to CGS21680 (30 nM) failed to alter IPSCs either in postsynaptic interneurons ($n = 8$) or pyramidal cells ($n = 5$) (*t*-test, baseline IPSCs = 94.0 ± 25.2 pA and 52.7 ± 9.9 pA, respectively) (Figs. 5B,C). Inhibitory PSCs were elicited by paired-pulse optical stimulation in slices from *BAC*-CCK-$Cre^{fg/+}$ mice transfected with AAV:ChR2-eYFP. Ionotropic glutamate receptors were blocked with NBQX (25 μM) and *DL*-APV (100 μM), because in addition to GABAergic neurons also CCK-containing glutamatergic fibers in the CA1 area may express *Cre* (Geibel et al., 2014). We also confirmed that optogenetically evoked IPSCs in the slices were elicited from CCK+ interneuron axons demonstrating suppression of the IPSCs by CBR1 agonist WIN55,212-2 (5 μM) to 0.62 ± 0.03 of baseline ($P < 0.001$, $n = 6$, *t*-test) with a characteristic increase in paired-pulse ratio (to 1.49 ± 0.18 from baseline, $P < 0.05$, $n = 5$, *t*-test) (Katona et al., 1999; Glickfeld and Scanziani, 2006; Nissen et al., 2010).

Endogenous Adenosine Promotes Synchronous Pyramidal Cell Discharge Via $A_{2A}Rs$ in Hippocampal Slices

We next studied whether endogenous adenosine released by high-frequency electrical stimulation is sufficient to modulate hippocampal pyramidal cell discharge through adenosine $A_{2A}R$ (Chamberlain et al., 2013). We utilized experimental design used above in Figure 1 to electrically stimulate Schaffer collaterals with paired pulses (50 ms interval), while recording field potential in the CA1 area. In addition, we applied high-frequency stimulation (HFS, 50 Hz 100 pulse) with a second stimulation electrode positioned in the vicinity of recording electrode aiming to elicit local release of adenosine (Fig. 6A) (Chamberlain et al., 2013). Schaffer collaterals were stimulated every 5 s and HFS delivered with second electrode every 2 min. To uncover adenosine $A_{2A}R$-mediated modulation the experiments were performed in continuous presence of blockers for CB1R (AM-251 2 μM), $GABA_B$ receptor (CGP55485, 1 μM), adenosine A_1R (DPCPX, 200 nM) as well as with *DL*-APV (100 μM). We analyzed same fEPSP parameters as in Figure 1 and found that HFS was followed by significant increase of pop-spike amplitude in Schaffer collateral –mediated field potential response. Popspike were elicited by 2nd stimulation pulse of the paired-pulse and they were significantly increased from baseline up to 40 s following the HFS. Importantly, the facilitation was blocked after wash-in of SCH58261 (100 nM) ($P < 0.001$, ANOVA, Tukey's HSD test, Fig. 6B). Although HFS transiently also modulated fEPSP slope in the experiments, application of the $A_{2A}R$ blocker failed to cause any change in the effect on slope. Neither did HFS or SCH58261 affect prespike volley (ANOVA, Tukey's HSD test, data not

shown). The HFS and $A_{2A}R$ antagonists effects on popspike are shown in detail in Figure 6.

Finally, we investigated whether $A_{2A}R$ activation by endogenous adenosine modulates spontaneous epileptiform discharge of hippocampal pyramidal cells in hyperexcitable conditions. Spontaneous inter-ictal like pyramidal cell population bursts were generated exposing slices to elevated (8–9 mM) extracellular potassium ($[K_o]$) in perfusion solution (Korn et al., 1987; Sagratella et al., 1987). Field potential was recorded in the CA3 area in an interface chamber. Following stable baseline (at least 10 min), either $A_{2A}R$ blocker SCH58261 (100 nM) or agonist CGS21680 (30 nM) was washed in. Epileptiform activity was quantified analyzing the occurrence of spontaneous inter-ictal like events characterized by a low frequency content field potential deflection associated with a barrage of extracellular spikes. Recordings were band-pass (1–100 Hz) filtered offline to uncover low-frequency deflections and analyze event occurrence (Figs. 7A,B). Amplitude threshold was set to 0.25 mV, and event detection was visually verified. Parallel high-pass filtering (>60 Hz) of recordings uncovered extracellular spikes associated with the events. Occurrence of inter-ictal like events in baseline conditions was 32.7 ± 11.7 events/min, ranging from 6.3 to 97.4 events/min ($n = 7$). The adenosine $A_{2A}R$ blocker SCH58261 strongly inhibited the occurrence spontaneous population bursts to $36 \pm 9\%$ ($P < 0.01$, $n = 3$, t-test) of baseline in 20–30 min following drug application. The activity-suppressing effect of antagonist persisted and in 40–50 min from drug application the burst occurrence dropped to $16 \pm 5\%$ of baseline level ($P < 0.001$, $n = 3$, t-test) (Fig. 7C). Adenosine $A_{2A}R$ agonist CGS21680 (100 nM) increased spontaneous epileptiform burst occurrence (Figs. 7D–G) from baseline to $140 \pm 16\%$ ($P < 0.05$, $n = 4$, t-test) in 20–30 min following drug application. Increase of burst occurrence was significant in three of four experiments, but varied in magnitude (Figs. 7F,G). Samples of band-pass and high-pass -filtered events are illustrated in Figures 7B,E. Modulation of spontaneous activity with $A_{2A}R$ drugs suggests the receptors are tonically activated in slices with elevated $[K_o]$, possibly because of increased ambient adenosine levels (Marichich and Nasello, 1973; Etherington and Frenguelli, 2004; Dias et al., 2013).

DISCUSSION

Adenosine has a well-established role as an endogenous neuronal inhibitor in the brain. Adenosine's suppressive effect on excitatory glutamatergic transmission via A_1R is well characterized, but its effect via other adenosine receptor types is not as well known (Dunwiddie and Masino, 2001; Sebastiao and Ribeiro, 2009). In the hippocampus and neocortex the high-affinity $A_{2A}R$ is expressed in low quantities (Dixon et al., 1996), but elevated levels of extracellular adenosine activate these receptors to facilitate neuronal discharge (Etherington and Frenguelli, 2004; Zeraati et al., 2006; El Yacoubi et al., 2008; El Yacoubi et al., 2009). It has been proposed that excitatory effects of adenosine in the cortex may mainly occur in pathological conditions, because $A_{2A}R$ expression levels increase in those circumstances in parallel with desensitization and down-regulation of A_1R (Rebola et al., 2005b; D'Alimonte et al., 2009; Hamil et al., 2012; Moschovos et al., 2012). In addition evidence for $A_{2A}R$-mediated modulation of activity in the hippocampus in physiological conditions is emerging (Cunha and Ribeiro, 2000; Rebola et al., 2005a; Rebola et al., 2008; Dias et al., 2012; Chamberlain et al., 2013; Dias et al., 2013; Wei et al., 2013), but $A_{2A}R$ effect on identified neuronal circuits in this area is still poorly understood.

We identified here two sites of synaptic modulation by which $A_{2A}R$ acts to shift the balance between synaptic excitation and inhibition in mouse hippocampus to facilitate principal cell discharge. Adenosine $A_{2A}R$ activation directly enhances excitatory glutamatergic Schaffer collateral synapses to CA1 pyramidal cells, and simultaneously suppresses feed-forward GABAergic inhibition to the same neurons. This at least partially explains the facilitatory effects of $A_{2A}R$ agonist on Schaffer collateral field potential responses in the CA1 area with increased fEPSP slope and popspike amplitude (Sebastiao and Ribeiro, 1992) (also shown here in Figs. 1–6). Our results also demonstrate that adenosine $A_{2A}R$ is unlikely to modulate glutamatergic Schaffer collateral axon excitability, for example through axonal receptors (Kullmann et al., 2005), because the agonist did not have effect on extracellular prespike volley. Together our findings provide a simple mechanistic explanation how $A_{2A}R$ activity increases excitability in the hippocampal CA3-CA1 circuitry modulating identified excitatory and inhibitory synapses. Although modulatory effects of $A_{2A}R$ are not restricted to synapses, but in addition can include alterations in intrinsic properties of neurons (Rebola et al., 2011) as well as glial glutamate transport (Matos et al., 2013), the synaptic modulatory action can at least partly explain proconvulsive effect of $A_{2A}R$ reported previously (Jones et al., 1998; Zeraati et al., 2006; El Yacoubi et al., 2008; El Yacoubi et al., 2009) and also demonstrated here.

Facilitation of epileptiform activity through low $A_{2A}R$ expression level in the hippocampus (Dixon et al., 1996) can be explained by synergistic action of the synaptic modulatory actions shown here. Increased Schaffer collateral excitation of pyramidal cells, but not feed-forward interneurons increases CA1 pyramidal firing to glutamatergic input from the CA3 area (Pouille and Scanziani, 2001; Lamsa et al., 2005; Xu et al., 2006; Pavlov et al., 2011; Lovett-Barron et al., 2012). We studied two major subpopulations of CA1 area GABAergic interneurons, either expressing PV or CCK, which both contribute to CA3-CA1 feed-forward inhibition controlling CA1 area pyramidal cell firing and their input-output transformation (Cobb et al., 1995; Buhl et al., 1996; Glickfeld and Scanziani, 2006; Klausberger and Somogyi, 2008; Lovett-Barron et al., 2012). Inhibitory transmission through these interneurons to CA1 pyramidal cells was not enhanced by $A_{2A}R$. Instead $A_{2A}R$ activation suppressed feed-forward GABAergic inhibition in pyramidal cells through a mechanism, which is likely to

include disinhibition. Facilitation of inhibitory synapses between CA1 interneurons has been demonstrated to effectively suppress network activity-driven GABAergic inhibition in the CA1 area pyramidal cells (Chamberland and Topolnik, 2012; Lovett-Barron et al., 2012). This promotes synaptically-driven pyramidal cell discharge and increases their input-output transformation (Toth et al., 1997; Letzkus et al., 2011; Lovett-Barron et al., 2012; Xu et al., 2013). We report that $A_{2A}R$-mediated facilitation of IPSCs was present in various postsynaptic CA1 area interneuron types, including O-LM cells specialized to inhibit distal dendrites of pyramidal cells, and basket cells that directly control pyramidal cell action potential firing via perisomatic inhibitory synapses (Zhang and McBain, 1995; Glickfeld and Scanziani, 2006; Klausberger and Somogyi, 2008). Through modulation of the GABAergic circuits $A_{2A}Rs$ can control co-ordinated rhythmic neuronal activities in the hippocampus (Cobb et al., 1995; Klausberger et al., 2005; Wulff et al., 2009). Interestingly, the $A_{2A}R$-mediated facilitation of GABAergic efferents was specific to PV-expressing interneurons, and was not detected in CCK+ GABAergic interneuron fibers (Armstrong and Soltesz, 2012).

Importantly, we showed that $A_{2A}R$-mediated facilitation of CA1 pyramidal cell activity also occurs through endogenous adenosine. High-frequency electrical stimulation experiment demonstrated that CA1 area pyramidal cell input–output transformation to Schaffer collateral stimulation is similarly facilitated via endogenous and agonist-induced $A_{2A}R$ activity. Although high-frequency stimulation-evoked $A_{2A}R$ activation failed to significantly change synaptic Schaffer collateral responses in the experiments, this can be explained by higher sensitivity of the network-driven input–output function than a monosynaptic pathway to synaptic modulations (Lovett-Barron et al., 2012).

Our results on spontaneous activity modulation by $A_{2A}R$ antagonist and agonist in hyperexcitable conditions confirm the previously reported findings that $A_{2A}R$ controls spontaneous epileptiform pyramidal cell discharge in the hippocampus (Sebastiao and Ribeiro, 2009). In addition, the results indicate that in slices with elevated extracellular potassium adenosine $A_{2A}Rs$ are tonically active promoting synchronous discharge in the hippocampus. This was evidenced by robust effect with $A_{2A}R$ antagonist suppressing the spontaneous interictal like events in the CA3 area. Variability and occasionally a lack of $A_{2A}R$ agonist effect to promote synchronous discharge in these conditions could also be explained by vigorous tonic $A_{2A}R$ activity in baseline conditions (Dias et al., 2013). Given that ambient adenosine levels elevate in epileptic tissue and $A_{2A}R$ expression increases whereas A_1R levels go down, $A_{2A}R$ blockers might provide an effective supplementary treatment in specific forms of epilepsy (Sebastiao and Ribeiro, 2009; Gomes et al., 2011). Adenosine's therapeutic effect via A_1R might benefit from inhibition of $A_{2A}Rs$. A seizure promoting role of $A_{2A}R$ in humans has recently been highlighted (Shinohara et al., 2013), and adenosine $A_{2A}R$ antagonists have already entered clinical trials and are safe to use with relatively mild side effects (Lopes et al., 2011; Shook and Jackson, 2011; Muller, 2013). Our findings here identify specific synaptic targets for $A_{2A}R$-modulation. This helps to understand how these receptors are involved in generation of aberrant hippocampal activity and can point out specific therapeutic targets in cortical microcircuits.

Acknowledgments

The authors acknowledge Prof. Marco Capogna for comments to the manuscript.

REFERENCES

Armstrong C, Soltesz I. 2012. Basket cell dichotomy in microcircuit function. J Physiol 590(Part 4):683–694.

Buhl EH, Szilagyi T, Halasy K, Somogyi P. 1996. Physiological properties of anatomically identified basket and bistratified cells in the CA1 area of the rat hippocampus in vitro. Hippocampus 6:294–305.

Chamberlain SE, Sadowski JH, Teles-Grilo Ruivo LM, Atherton LA, Mellor JR. 2013. Long-term depression of synaptic kainate receptors reduces excitability by relieving inhibition of the slow afterhyperpolarization. J Neurosci 33:9536–9545.

Chamberland S, Topolnik L. 2012. Inhibitory control of hippocampal inhibitory neurons. Front Neurosci 6:165.

Ciruela F, Casado V, Rodrigues RJ, Lujan R, Burgueno J, Canals M, Borycz J, Rebola N, Goldberg SR, Mallol J, et al. 2006. Presynaptic control of striatal glutamatergic neurotransmission by adenosine A1-A2A receptor heteromers. J Neurosci 26:2080–2087.

Cobb SR, Buhl EH, Halasy K, Paulsen O, Somogyi P. 1995. Synchronization of neuronal activity in hippocampus by individual GABAergic interneurons. Nature 378:75–78.

Cunha RA, Ribeiro JA. 2000. Adenosine A2A receptor facilitation of synaptic transmission in the CA1 area of the rat hippocampus requires protein kinase C but not protein kinase A activation. Neurosci Lett 289:127–130.

Cunha RA, Johansson B, van der Ploeg I, Sebastiao AM, Ribeiro JA, Fredholm BB. 1994. Evidence for functionally important adenosine A2a receptors in the rat hippocampus. Brain Res 649(1-2): 208–216.

D'Alimonte I, D'Auro M, Citraro R, Biagioni F, Jiang S, Nargi E, Buccella S, Di Iorio P, Giuliani P, Ballerini P, et al. 2009. Altered distribution and function of A2A adenosine receptors in the brain of WAG/Rij rats with genetic absence epilepsy, before and after appearance of the disease. Eur J Neurosci 30:1023–1035.

Dias RB, Ribeiro JA, Sebastiao AM. 2012. Enhancement of AMPA currents and GluR1 membrane expression through PKA-coupled adenosine A(2A) receptors. Hippocampus 22:276–291.

Dias RB, Rombo DM, Ribeiro JA, Henley JM, Sebastiao AM. 2013. Adenosine: setting the stage for plasticity. Trends Neurosci 36:248–257.

Dixon AK, Gubitz AK, Sirinathsinghji DJ, Richardson PJ, Freeman TC. 1996. Tissue distribution of adenosine receptor mRNAs in the rat. Br J Pharmacol 118:1461–1468.

Dunwiddie TV, Masino SA. 2001. The role and regulation of adenosine in the central nervous system. Annu Rev Neurosci 24:31–55.

El Yacoubi M, Ledent C, Parmentier M, Costentin J, Vaugeois JM. 2008. Evidence for the involvement of the adenosine A(2A) receptor in the lowered susceptibility to pentylenetetrazol-induced seizures produced in mice by long-term treatment with caffeine. Neuropharmacology 55:35–40.

El Yacoubi M, Ledent C, Parmentier M, Costentin J, Vaugeois JM. 2009. Adenosine A2A receptor deficient mice are partially resistant to limbic seizures. Naunyn Schmiedebergs Arch Pharmacol 380: 223–232.

Etherington LA, Frenguelli BG. 2004. Endogenous adenosine modulates epileptiform activity in rat hippocampus in a receptor subtype-dependent manner. Eur J Neurosci 19:2539–2550.

Geibel M, Badurek S, Horn JM, Vatanashevanopakorn C, Koudelka J, Wunderlich CM, Bronneke HS, Wunderlich FT, Minichiello L. 2014. Ablation of TrkB signalling in CCK neurons results in hypercortisolism and obesity. Nat Commun 5:3427.

Glickfeld LL, Scanziani M. 2006. Distinct timing in the activity of cannabinoid-sensitive and cannabinoid-insensitive basket cells. Nat Neurosci 9:807–815.

Gomes CV, Kaster MP, Tome AR, Agostinho PM, Cunha RA. 2011. Adenosine receptors and brain diseases: neuroprotection and neurodegeneration. Biochim Biophys Acta 1808:1380–1399.

Hamil NE, Cock HR, Walker MC. 2012. Acute down-regulation of adenosine A(1) receptor activity in status epilepticus. Epilepsia 53: 177–188.

Jones PA, Smith RA, Stone TW. 1998. Protection against hippocampal kainate excitotoxicity by intracerebral administration of an adenosine A2A receptor antagonist. Brain Res 800:328–335.

Katona I, Sperlagh B, Sik A, Kafalvi A, Vizi ES, Mackie K, Freund TF. 1999. Presynaptically located CB1 cannabinoid receptors regulate GABA release from axon terminals of specific hippocampal interneurons. J Neurosci 19:4544–4558.

Klausberger T, Somogyi P. 2008. Neuronal diversity and temporal dynamics: The unity of hippocampal circuit operations. Science 321:53–57.

Klausberger T, Marton LF, O'Neill J, Huck JH, Dalezios Y, Fuentealba P, Suen WY, Papp E, Kaneko T, Watanabe M, et al. 2005. Complementary roles of cholecystokinin- and parvalbumin-expressing GABAergic neurons in hippocampal network oscillations. J Neurosci 25:9782–9793.

Kullmann DM, Ruiz A, Rusakov DM, Scott R, Semyanov A, Walker MC. 2005. Presynaptic, extrasynaptic and axonal GABAA receptors in the CNS: Where and why? Prog Biophys Mol Biol 87:33–46.

Lamsa K, Heeroma JH, Kullmann DM. 2005. Hebbian LTP in feed-forward inhibitory interneurons and the temporal fidelity of input discrimination. Nat Neurosci 8:916–924.

Lawrence JJ, Statland JM, Grinspan ZM, McBain CJ. 2006. Cell type-specific dependence of muscarinic signalling in mouse hippocampal stratum oriens interneurones. J Physiol 570(Part 3):595–610.

Lazarus M, Huang ZL, Lu J, Urade Y, Chen JF. 2012. How do the basal ganglia regulate sleep-wake behavior? Trends Neurosci 35: 723–732.

Letzkus JJ, Wolff SB, Meyer EM, Tovote P, Courtin J, Herry C, Luthi A. 2011. A disinhibitory microcircuit for associative fear learning in the auditory cortex. Nature 480:331–335.

Lopes LV, Sebastiao AM, Ribeiro JA. 2011. Adenosine and related drugs in brain diseases: Present and future in clinical trials. Curr Top Med Chem 11:1087–1101.

Lovett-Barron M, Turi GF, Kaifosh P, Lee PH, Bolze F, Sun XH, Nicoud JF, Zemelman BV, Sternson SM, Losonczy A. 2012. Regulation of neuronal input transformations by tunable dendritic inhibition. Nat Neurosci 15:423–430, S1-S3.

Marichich ES, Nasello AG. 1973. Epilepsy and adenosinetriphosphate (ATP): Effect of electrical stimulation and high potassium perfusion on hippocampal ATP contents. Brain Res 57:409–416.

Matos M, Augusto E, Agostinho P, Cunha RA, Chen JF. 2013. Antagonistic interaction between adenosine A2A receptors and Na+/K+-ATPase-alpha2 controlling glutamate uptake in astrocytes. J Neurosci 33:18492–18502.

Moschovos C, Kostopoulos G, Papatheodoropoulos C. 2012. Endogenous adenosine induces NMDA receptor-independent persistent epileptiform discharges in dorsal and ventral hippocampus via activation of A2 receptors. Epilepsy Res 100(1-2): 157–167.

Muller T. 2013. Suitability of the adenosine antagonist istradefylline for the treatment of Parkinson's disease: pharmacokinetic and clinical considerations. Expert Opin Drug Metab Toxicol 9:1015–1024.

Nissen W, Szabo A, Somogyi J, Somogyi P, Lamsa KP. 2010. Cell type-specific long-term plasticity at glutamatergic synapses onto hippocampal interneurons expressing either parvalbumin or CB1 cannabinoid receptor. J Neurosci 30:1337–1347.

Pavlov I, Scimemi A, Savtchenko L, Kullmann DM, Walker MC. 2011. I(h)-mediated depolarization enhances the temporal precision of neuronal integration. Nat Commun 2:199.

Pouille F, Scanziani M. 2001. Enforcement of temporal fidelity in pyramidal cells by somatic feed-forward inhibition. Science 293: 1159–1163.

Rebola N, Canas PM, Oliveira CR, Cunha RA. 2005a. Different synaptic and subsynaptic localization of adenosine A2A receptors in the hippocampus and striatum of the rat. Neuroscience 132:893–903.

Rebola N, Porciuncula LO, Lopes LV, Oliveira CR, Soares-da-Silva P, Cunha RA. 2005b. Long-term effect of convulsive behavior on the density of adenosine A1 and A 2A receptors in the rat cerebral cortex. Epilepsia 46 (Suppl 5):159–165.

Rebola N, Rodrigues RJ, Lopes LV, Richardson PJ, Oliveira CR, Cunha RA. 2005c. Adenosine A1 and A2A receptors are co-expressed in pyramidal neurons and co-localized in glutamatergic nerve terminals of the rat hippocampus. Neuroscience 133: 79–83.

Rebola N, Lujan R, Cunha RA, Mulle C. 2008. Adenosine A2A receptors are essential for long-term potentiation of NMDA-EPSCs at hippocampal mossy fiber synapses. Neuron 57:121–134.

Rebola N, Simoes AP, Canas PM, Tome AR, Andrade GM, Barry CE, Agostinho PM, Lynch MA, Cunha RA. 2011. Adenosine A2A receptors control neuroinflammation and consequent hippocampal neuronal dysfunction. J Neurochem 117:100–111.

Schiffmann SN, Vanderhaeghen JJ. 1991. Distribution of cells containing mRNA encoding cholecystokinin in the rat central nervous system. J Comp Neurol 304):219–233.

Schiffmann SN, Libert F, Vassart G, Vanderhaeghen JJ. 1991. Distribution of adenosine A2 receptor mRNA in the human brain. Neurosci Lett 130:177–181.

Sebastiao AM, Ribeiro JA. 1992. Evidence for the presence of excitatory A2 adenosine receptors in the rat hippocampus. Neurosci Lett 138:41–44.

Sebastiao AM, Ribeiro JA. 2009. Tuning and fine-tuning of synapses with adenosine. Curr Neuropharmacol 7:180–194.

Shinohara M, Saitoh M, Nishizawa D, Ikeda K, Hirose S, Takanashi J, Takita J, Kikuchi K, Kubota M, Yamanaka G, et al. 2013. ADORA2A polymorphism predisposes children to encephalopathy with febrile status epilepticus. Neurology 80:1571–1576.

Shook BC, Jackson PF. 2011. Adenosine A(2A) Receptor Antagonists and Parkinson's Disease. ACS Chem Neurosci 2:555–567.

Toth K, Freund TF, Miles R. 1997. Disinhibition of rat hippocampal pyramidal cells by GABAergic afferents from the septum. J Physiol 500 (Part 2):463–474.

Wei CJ, Li W, Chen JF. 2011. Normal and abnormal functions of adenosine receptors in the central nervous system revealed by genetic knockout studies. Biochim Biophys Acta 1808:1358–1379.

Wei CJ, Augusto E, Gomes CA, Singer P, Wang Y, Boison D, Cunha RA, Yee BK, Chen JF. 2013. Regulation of fear responses by

striatal and extrastriatal adenosine A receptors in forebrain. Biol Psychiatry 1;75:855–863.

Wulff P, Ponomarenko AA, Bartos M, Korotkova TM, Fuchs EC, Bahner F, Both M, Tort AB, Kopell NJ, Wisden W, et al. 2009. Hippocampal theta rhythm and its coupling with gamma oscillations require fast inhibition onto parvalbumin-positive interneurons. Proc Natl Acad Sci USA 106:3561–3566.

Xu NL, Ye CQ, Poo MM, Zhang XH. 2006. Coincidence detection of synaptic inputs is facilitated at the distal dendrites after long-term potentiation induction. J Neurosci 26:3002–3009.

Xu H, Jeong HY, Tremblay R, Rudy B. 2013. Neocortical somatostatin-expressing GABAergic interneurons disinhibit the thalamorecipient layer 4. Neuron 77:155–167.

Zeraati M, Mirnajafi-Zadeh J, Fathollahi Y, Namvar S, Rezvani ME. 2006. Adenosine A1 and A2A receptors of hippocampal CA1 region have opposite effects on piriform cortex kindled seizures in rats. Seizure 15:41–48.

Zhang L, McBain CJ. 1995. Voltage-gated potassium currents in stratum oriens-alveus inhibitory neurones of the rat CA1 hippocampus. J Physiol 488 (Part 3):647–660.